universität wien

DISSERTATION / DOCTORAL THESIS

Titel der Dissertation /Title of the Doctoral Thesis

"Applications of Pericyclic Reactions in Diverse Settings: Selenium-catalysed Rearrangements and Immunosuppressive Natural Product Synthesis"

verfasst von / submitted by

Manuel Schupp, BSc MSc

angestrebter akademischer Grad / in partial fulfilment of the requirements for the degree of

Doktor der Naturwissenschaften (Dr. rer. nat.)

Wien, 2023 / Vienna 2023

Studienkennzahl lt. Studienblatt / degree programme code as it appears on the student record sheet:	A 796 605 419
Dissertationsgebiet lt. Studienblatt / field of study as it appears on the student record sheet:	Doktoratsstudium Naturwissenschaften: Chemie
Betreut von / Supervisor:	Univ.-Prof. Dr. Nuno Maulide

The work presented in this doctoral thesis was conducted between January 2020 and December 2023 at the University of Vienna and at CeMM Research Center for Molecular Medicine of the Austrian Academy of Sciences under supervision of Prof. Dr. Nuno Maulide.

Referees:

Prof. Dr. Karl Gademann

Univ.-Prof. Davide Bonifazi, PhD

I hereby confirm that I have written this doctoral thesis on my own and no other sources, tools or assistance than those reported have been used.

_____ _____

Location, Date Signature

Für meine Familie

Acknowledgements

First, I would like to thank my *Doktorvater* Univ.-Prof. Dr. Nuno Maulide for his guidance, trust and support throughout the years. As the first PhD student affiliated with CeMM, I very much appreciate the freedom you gave me in shaping the research, learning about biology and following my curiosity to progress the projects. I will cherish the time I got to spend working with you and the Maulide group, which remains one of the most welcoming and talented group of individuals I have ever encountered, which is a reflection of their leader in my eyes. Last but not least, I am most appreciative of the support you have shown when I needed time away from the lab to be with my freshly formed family and the flexibility in pursuing a PhD while learning how to be a parent.

Second, I am grateful to thank Prof. Dr. Karl Gademann and Univ.-Prof. Davide Bonifazi, PhD for agreeing to review this thesis and for their time doing so.

Third, I would like to thank Dr. Giulia Ianelli, Dr. Paolo Piancetini, Bogdan-Razvan Brutiu, Dr. Saad Shaaban and Dr. Daniel Kaiser for their time and effort proofreading and improving this thesis.

As for every research group, there are a number of people who keep the engine going and who were essential to my time in the Maulide group. I am thankful for the help and support from Martina Drescher, Dr. Daniel Kaiser, Dr. Saad Shaaban, Patricia Emberger, Florian Doubek, Anne Fischer, Elena Macoratti and Omar Abdo on both a personal as well as a professional level. I will especially miss Martina's ability to not only mend lab equipment but also spirits, should that be required.

"Noone works alone in the Maulide group" has really been a quote to live by. I would like to express my gratitude to the colleagues with whom I have shared labs, offices and research projects: Bogdan-Razvan Brutiu, Vincent Porte, Dr. Phillip Grant, Dr. Iakovos Saridakis, Haoqi Zhang, Dr. Thomas Leischner, Miloš

Vavrik, Dr. Giovanni Di Mauro, Ricardo Meyrelles, Dr. Boris Maryasin, Yi Xiao, Dr. Daniel Kaiser, Dr. Miran Lemmerer, Dr. Immo Klose, Roberto Tinelli, Dr. Saad Shaaban, Dr. Hsiang-Yu Chuang, Dr. Martin Berger, Dr. Giulia Ianelli, Dr. Adriano Bauer, Dr. Miryam Pastor Fernandez and Dr. Clemens Farr.

This of course extends to the whole Maulide family and colleagues at Uni Wien, namely: Christian, Alex, Miran, Philipp, Ana S., Ana A., Anthony, Minghao, Sergio, Branca, Nico, Carlos, Ben, David, Jan, Bruna, Ivan, Zhi-Jie, Angela, Irmgard, Uros, Milene, Konstantin, Tommaso, Juliana, Alejandro, Jules, Margaux, Vinicius, Eleonora, Steffi, Laurin and Yury.

At the University of Vienna and at CeMM, I considered myself lucky to have my research supported by highly skilled co-workers in the core facilities, such as the NMR, Xray and HRMS facilities at Uni Wien or the MDP at CeMM and I am grateful for their help.

Moreover, I would like to thank everybody at CeMM for their support. Starting with the directors, Prof. Dr. Giulio Superti-Furga and Anita Ender, and extending my gratitude to all faculty at CeMM for giving a synthetic chemist a chance and an opportunity to learn. I'm especially grateful for my close colleagues, my cohort of PhD students and co-workers: Sören, Laura, Stephan, Katja, Salvo, Florian, Amanda, Sasha, Zsofia, Eugenia, Filip, Anh, Ludovica, Monika, Thomas, Lisa, Johanna, Jakob, Jan, Walther, Anton, Peter, Marc, Memo, Alina and Matthew. CeMM has proven truly special, mostly thanks to having people like you around.

I would like to also include the mentors I had the pleasure of working with along the way: Prof. Dr. Claus Feldmann & Dr. Joachim Heck; Prof. Dr. Hans-Achim Wagenknecht, Dr. Damian Ploschik, Dr. Christoph Bickmann & Dr. David Rombach; Prof. Dr. Andrew G. Myers, Dr. Thomas Lepitre & Dr. Sven Hildebrandt. Thank you for allowing me to hone my skills as a synthetic chemist and preparing me for the future.

On the personal side, I am grateful for all of my friends but especially to those who have supported me throughout the years and who have remained close although I have moved far away and I am equally

grateful to the new friends I have met in Vienna: Kevin, Friedrich, Jan, Thilo, Sören and Bogdan have always provided me with an open ear and mind and with the necessary distraction from stress. Be it playing games, bouldering or a different perspective on science and life, thank you for being there for me.

I am most deeply grateful for my family for providing care, reassurance and perspective. For my parents, Gerd and Beate, for my brother Florian, who are always there if they are needed and for my extended family as well as my in-laws, Rainer, Heidi and Patrick, who have welcomed me into their family with open arms.

Lastly, I want to thank the most important person in my life, my wife Regine. You laid the foundation for our time in Vienna, our future elsewhere and you have given us our son Oliver. I'm grateful to be by your side as we watch him grow and I love you.

Table of contents

Abstract

Within this doctoral thesis, two distinct types of pericyclic reactions, whose application allows for the synthesis of structurally diverse molecules with remarkable efficiency, will be explored.

In the first chapter, a general introduction into pericyclic reactions will be presented, with a firm focus placed on the chemistry enabled by sigmatropic rearrangements of organochalcogen compounds. The synthesis of *para*-aminophenols through a double [2,3]-sigmatropic rearrangement mediated by a selenium-based catalyst will be presented and the mechanism of the transformation will be elucidated *via* combined experimental and computational investigation and more far-reaching applications will be explored.

In the second chapter, the total synthesis of immunosuppressive natural products enabled by a domino reaction process will be introduced. The key step of the successful synthesis occurs through electrocyclic ring opening, another type of pericyclic reaction, and allows for the synthesis of a range of fully synthetic analogues. These analogues are thoroughly probed with regards to their immunosuppressive properties in a range of biological systems and highly-active compounds are evaluated more deeply. The chapter is concluded with the discovery of a surprising byproduct, which results from electrocyclic ring opening and whose occurrence is systematically studied by the synthesis of model system.

Kurzzusammenfassung

In dieser Dissertation werden zwei unterschiedliche Arten der pericyclischen Reaktionen erkundet, deren Anwendungen es erlauben strukturell vielfältige Moleküle mit bemerkenswerter Effizienz zu erschaffen.

Im ersten Kapitel wird eine generelle Einführung in die pericyclischen Reaktionen präsentiert, mit einem Fokus auf der Chemie, welche durch sigmatrope Umlagerungen von Organochalkogenverbindungen ermöglicht wird. Die Synthese von *para*-Aminophenolen mittels zweifacher [2,3]-sigmatroper Umlagerung eines selenhaltigen Katalysators wird vorgestellt und der Mechanismus dieser Reaktion, mittels experimentellen Untersuchungen und computergestützter Berechnungen, sowie weitere Anwendungen werden erkundet.

Im zweiten Kapitel wird die Totalsynthese immunsupprimierender Naturstoffe, die durch einen Domino-Reaktionsprozess ermöglicht wird, vorgestellt. Die Schlüsselreaktion der erfolgreichen Synthese verläuft über eine elektrozyklische Ringöffnung und erlaubt die Synthese einer Reihe an vollsynthetischen Analoga. Jene Verbindungen werden bezüglich ihrer immunsupprimierenden Fähigkeiten in verschiedenen biologischen Systemen untersucht und hochaktive Verbindungen werden tiefergehend analysiert. Abschließend wird ein überraschendes Nebenprodukt, welches der elektrozyklischen Ringöffnung entspringt, eingehend systematisch aufgearbeitet und es werden eine Reihe an Modelsystemen synthetisiert und untersucht.

List of Abbreviations

°C	degrees Celsius
Ac	acetyl
Ad	adamantyl
APC	antigen-presenting cell
app	apparent
Ar	aryl
BDE	bond dissociation energy (at 298.15 K)
Bn	benzyl
Boc	*tert*-butyloxycarbonyl
bp	boiling point
Bpin	boron pinacolato
br	broad
brsm	based on recovered starting material
Bu	butyl
CAC	cell activation cocktail
cat.	catalytic
CD	cluster of differentiation
cf.	*confer* (*latin* for: "compare")
CSA	cyclosporin A
d	doublet
δ	chemical shift
ΔG	Gibbs free energy change
dba	dibenzylideneacetone
DBU	1,8-diazabicyclo[5.4.0]undec-7-ene
DC	dendritic cells
DCE	1,2-dichloroethane
DCM	dichloromethane
DIBAL	diisobutylaluminium hydride
DIPEA	*N*,*N*-diisopropylethylamine; Hünig's base
DMAP	4-dimethylaminopyridine
DMF	dimethylformamide
DNA	desoxyribonucleic acid
DPPA	diphenylphosphoryl azide
dr	diastereomeric ratio
EDCI	1-ethyl-3-(3-dimethylamino-propyl)carbodiimide
EDG	electron-donating group
ee	enantiomeric excess;
e.g.	*exempli gratia* (*latin for*: "for example")
er	enantiomeric ratio
Et	ethyl

et al.	*et alia* (*latin for*: “and others”)
etc.	*et cetera* (*latin for:* “and other things”)
EtOAc	ethyl acetate
eq.	equivalents
EWG	electron-withdrawing group
FMO	frontier molecular orbital
GC-MS	gas chromatography – mass spectrometry
h	hour(s)
HBA	hydrogen bond acceptor
HBD	hydrogen bond donor
HFIP	hexafluoroisopropanol; 1,1,1,3,3,3-hexafluoropropan-2-ol
HMPA	hexamethylphosphoramide
HOBt	1*H*-1,2,3-benzotriazol-1-ol
HOMO	highest occupied molecular orbital
HRMS	high resolution mass spectrometry
HWE	Horner-Wadsworth-Emmons
Hz	Hertz (s^{-1})
i	*ipso*; *iso*
IC_{50}	half maximal inhibitory concentration
i.e.	*id est (latin* for: “that is to say”)
IFN-γ	interferon gamma
IL	interleukin
IR	infrared
K	Kelvin
L	litre(s)
LDA	lithium diisopropylamide
LUMO	lowest unoccupied molecular orbital
m	metre; multiplet
m	*meta*
M	molar, mol*L^{-1}
***m*CPBA**	*meta*-chloroperbenzoic acid
Me	methyl
MeCN	acetonitrile
MFSDA	methyl 2,2-difluoro-2-(fluorosulfonyl)acetate
MHC	major histocompatibility complex
MeOH	methanol
MHz	Megahertz, $1 \cdot 10^6\ s^{-1}$
mm	millimetre(s)
MNBA	2-methyl-6-nitrobenzoic anhydride
MOM	methoxymethyl
MPM	*p*-methoxybenzyl, also abbreviates as PMB
Ms	mesyl, methanesulfonyl

n	normal
NBS	*N*-bromosuccinimide
NFAT	nuclear factor of activated T cells
NHC	*N*-heterocyclic carbene
NIS	*N*-iodosuccinimide
NK	natural killer (cells)
nm	nanometre(s)
NMR	nuclear magnetic resonance
o	*ortho*
p	*para*
p	pentet
PBMC	peripheral blood mononuclear cell
PFA	paraformaldehyde
pH	= -log([H^+])
Ph	phenyl
PMA	phorbol 12-myristate 13-acetate
PMB	*see* MPM
ppm	parts per million
Pr	propyl
py	pyridine
q	quartet
quant.	quantitative
rac	racemic
s	singlet
SAR	structure-activity relationship
SOMO	singly occupied molecular orbital
t	triplet
TBDPS	*tert*-butyldiphenylsilyl
TBS	*tert*-butyldimethylsilyl
TCR	T cell receptor; identical to CD3
TDF	THF-d_8, octadeuterotetrahydrofuran
tert, t	*tertiary*
TES	triethylsilyl
Tf	triflyl, trifluoromethanesulfonyl
TFA	trifluoroacetic acid
THF	tetrahydrofuran
TIPS	tri-*iso*-propylsilyl
TLC	thin layer chromatography
TMS	trimethylsilyl
TNF-α	tumor necrosis factor a
Tol	tolyl
Trt	trityl, triphenylmethyl
Ts	toluenesulfonyl
TsOH	*p*-toluenesulfonic acid
vide infra	*latin for*: “see below”
vide supra	*latin for*: “see above”
xs	excess

1. *Para*-Aminophenols *via* a Se-catalysed Rearrangement

1.1. Introduction

1.1.1. Rearrangements in Organic Chemistry

Organic chemistry is the field within the natural science of chemistry that is concerned with the properties, structure and reactions of carbon-based molecules. Such reactions can occur through either an *intermolecular* process (reacting with a second molecule to elicit change) or an *intramolecular* process, (eliciting change from within a given molecular framework). Often, these processes are interlinked, with an *intermolecular* reaction setting the stage for an *intramolecular* reaction, typically in the form of a rearrangement. For example, cyclohexanone (**1.001**) can be consumed in an *intermolecular* reaction, forming 2-bromocyclohexan-1-one (**1.002**) upon treatment with *N*-bromosuccinimide (NBS) and an acid (Scheme 1.1).[1] Treating the resulting 2-bromocyclohexan-1-one (**1.002**) with a base, such as sodium methoxide, leads to deprotonation of the starting material in an *intermolecular* reaction step, which sets the stage for the *intramolecular* reaction, particularly a Favorskii rearrangement, leading to the methyl ester of cyclopentane carboxylic acid (**1.004**).[2,3]

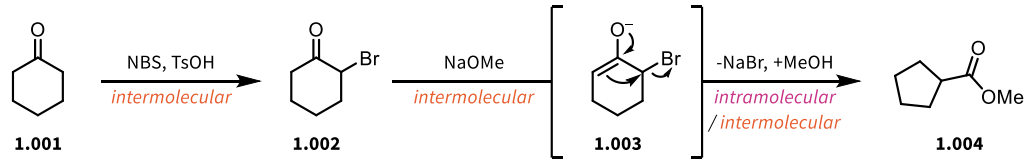

Scheme 1.1: Reaction of cyclohexanone (**1.001**) with NBS under acid catalysis to 2-bromocyclohexan-1-one (**1.002**) in an *intermolecular* reaction. A following *intermolecular* deprotonation generates enolate **1.003**, which then can undergo an *intramolecular* rearrangement, known as the Favorskii rearrangement, to form methyl cyclopentanecarboxylate (**1.004**). The mechanism of the reaction is abbreviated.

Rearrangement reactions are processes in which the carbon skeleton of a molecule changes, leading to a different connectivity within the product compared to its starting material. These processes may involve

leaving groups (such as the bromide in the case of the Favorskii rearrangement) or reactive intermediates, such as in the case of the Masamune-Bergman cyclisation, where a highly reactive diradical species is the immediate product of the rearrangement process.[4,5] Interestingly, it was discovered that this type of rearrangement/cyclisation was at the heart of the mechanism of action of some of the most potent cytotoxic natural products, so-called enediyne antibiotics such as dynemicin A (**1.010**) or neocarzinostatin chromophore (**1.011**) (Scheme 1.2).[6,7]

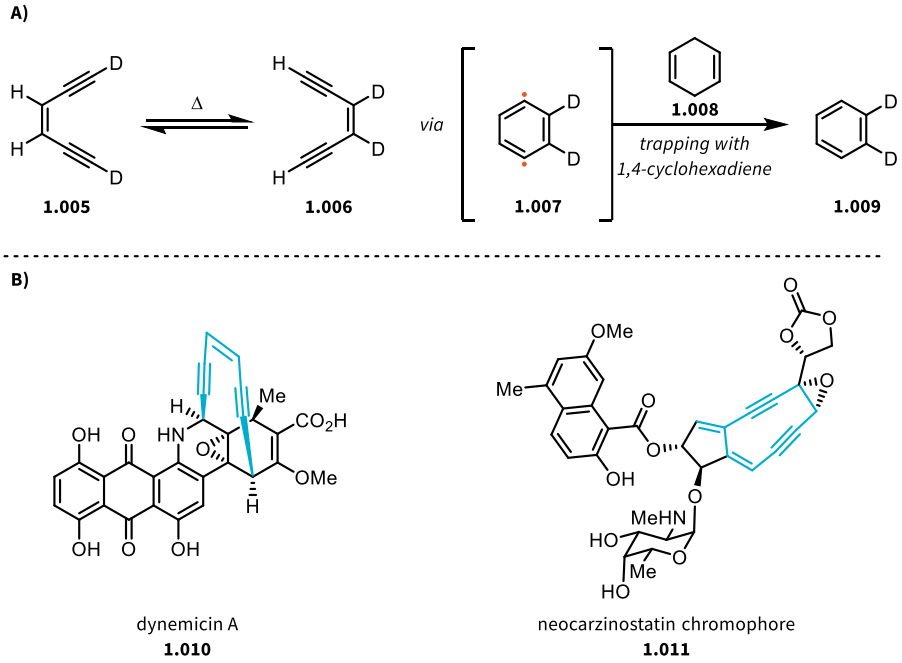

Scheme 1.2: A) Overview reaction of the Masamune-Bergman cyclisation, leading to isomerisation of the bisdeuterated enediyne (**1.005**/**1.006**) *via* a diradical intermediate **1.007**. In the presence of a hydrogen atom donor, such as 1,4-cyclohexadiene (**1.008**), this intermediate can be trapped to ultimately generate benzene-1,2-d_2 (**1.009**). B) Selected examples of natural products bearing enediyne structural motifs (highlighted in blue).

The examples highlighted above illustrate the two major families of rearrangement processes: polar versus apolar rearrangements. In the case of the Favorskii reaction, an anionic intermediate undergoes rearrangement and the charge is ultimately transposed to the leaving group, in this case a bromide anion. Generally, polar rearrangements can involve either cationic or anionic intermediates, depending on the reaction conditions. A range of other polar rearrangements, such as Wagner-Meerwein rearrangements,[8] Seyferth-Gilbert homologations,[9,10] or the Ramberg-Bäcklund rearrangement,[11] all rely on the activation of a starting material by an external reagent to then generate the reactive intermediate capable of undergoing the desired rearrangement process.

In contrast to this, apolar rearrangements feature neutral or zwitterionic intermediates, which are transformed into the products. In addition to the aforementioned Masamune-Bergman cyclisation, the Sommlet-Hauser rearrangement,[12] or the Claisen rearrangement,[13] are to be highlighted as exemplary members of this class of transformations. Both the Sommlet-Hauser and the Claisen rearrangement are sigmatropic rearrangements – concerted reactions that belong to the larger family of pericyclic reactions.

1.1.2. Sigmatropic Rearrangements

Sigmatropic rearrangements are part of a class of reactions called pericyclic reactions. These reactions are defined by the involvement of a cyclic transition state and a concerted progress of the reaction *via* overlap of the molecular orbitals involved in the process. Pericyclic reactions have no isolable or stable intermediates, as the concerted nature of the reaction directly converts starting material into product. As formally reversible processes, pericyclic reactions can progress in both reactional directions, meaning that a driving force has to be applied to enable the full conversion of starting materials to the desired products.[2,14,15] Typically, four types of pericyclic reactions are defined: cycloadditions, group transfer reactions, electrocyclic reactions and sigmatropic rearrangements. While the chemistry enabled by each of these classes of reactions is diverse,[16–18] the work presented within this thesis is mostly concerned with electrocyclic reactions (Chapter 2) and sigmatropic rearrangements.

Sigmatropic rearrangements occur when a group bound by a σ-bond migrates to the other end of a flanking π-system, leading to the transposition of the groups attached *via* the σ-bond to the other end of the π-system.[14] The first example of a sigmatropic rearrangement was disclosed by Ludwig Claisen in 1912 and reports the conversion of, among others, the ether *O*-allyl guaiacol (**1.012**) to its *ortho*-allyl derivative (**1.013**) (Scheme 1.3) in a strictly intramolecular reaction.

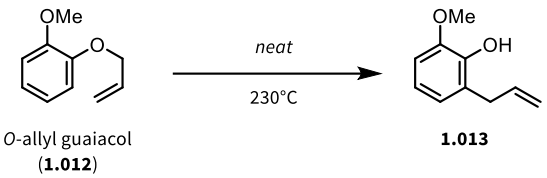

O-allyl guaiacol (**1.012**) **1.013**

Scheme 1.3: First example of a sigmatropic rearrangement, as described by Claisen.

Sigmatropic rearrangements are defined by their order, typically depicted in the form of [i,j], where i and j correspond to the number of atoms in the migrating fragment and in the π-system, respectively.[14] In the aforementioned Claisen report, this would correspond to a [3,3]-sigmatropic rearrangement, as a three atom fragment forms a new σ-bond, which is three atoms removed from the previously cleaved σ-bond, as depicted and highlighted in Scheme 1.4.

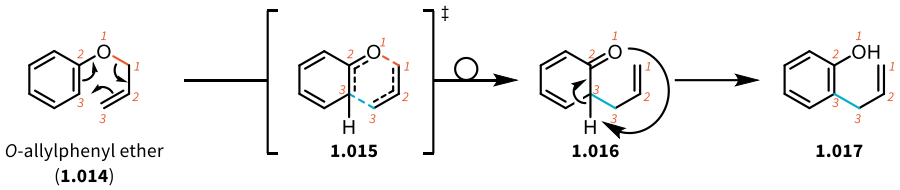

O-allylphenyl ether (**1.014**) **1.015** **1.016** **1.017**

Scheme 1.4: Mechanistic overview on a general [3,3]-sigmatropic (Claisen) rearrangement of *O*-allyl phenol (**1.014**) to *o*-allyl phenol **1.017** *via* transition state **1.015** and a dearomatised intermediate **1.016**. The distance between the cleaved (orange) and newly formed σ-bond (blue) determines the order of the sigmatropic rearrangement.

Generally, sigmatropic rearrangements, like other pericyclic reactions, can be “allowed” or “forbidden” based on the symmetry of the orbitals involved in the rearrangement process.[19,20] These reactions can occur in either a *suprafacial* or *antarafacial* manner, depending on whether the migrating group remains on the same face of the π-system throughout the reaction (*suprafacial*) or if the migrating group changes face to the opposing side during the reaction (*antarafacial*). One additional consideration relates to stereochemically distinct migrating groups, as these may react with either inversion or retention of stereochemistry. All of these aspects, together with the number of electrons involved in the reaction, can determine whether a given sigmatropic rearrangement is allowed or forbidden. The generalised rules for the feasibility of sigmatropic processes based on orbital symmetry, as established by Woodward and Hoffmann, are summarised in Table 1.1.

Table 1.1

Order	Supra/Retention	Supra/Inversion	Antara/Retention	Antara/Inversion
[1,j]; 1 + j = 4n	Forbidden	Allowed	Allowed	Forbidden
[1,j]; 1 + j = 4n + 2	Allowed	Forbidden	Forbidden	Allowed
Order	**Supra/Supra**	**Supra/Antara**	**Antara/Antara**	
[i,j]; i + j = 4n	Forbidden	Allowed	Forbidden	
[i,j]; i + j = 4n + 2	Allowed	Forbidden	Allowed	

Table 1.1: Summary of the general selection rules for sigmatropic rearrangements. i, j and n are natural numbers, where i and j correspond to the aforementioned order of the sigmatropic rearrangement and n to the number of electrons involved in the rearrangement process.

The orbital symmetry prerequisites of a given sigmatropic reaction can be evaluated by considering the interactions between the frontier molecular orbitals (FMO) of the π-system and those of the migrating fragment. The simplest sigmatropic rearrangement, the hypothetical [1,3]-hydrogen shift can be used to illustrate the concept. One can view it as the transfer of the hydrogen 1*s* orbital along the allyl Ψ_2 orbital (HOMO; highest occupied molecular orbital), which treats the system as a hydrogen radical interacting with an allyl radical, as depicted in Scheme 1.5A. However, the [1,3]-hydrogen shift, while theoretically feasible, is not possible, as the necessary antarafacial transfer would require the system to severely distort. This requirement arises from the presence of a node in the allyl Ψ_2 orbital, which leaves the orbital lobes at the terminal carbons with opposing signs. In order to connect to the correct orbital lobe, the hydrogen atom would need to cross the plane of the molecule, while forcing a cyclic transition state (**1.021**). The activation barrier to induce such severe distortion is beyond achievable under experimental conditions and therefore the reaction is deemed impossible. In the case of the [1,5]-hydrogen shift, migration of the hydrogen atom can happen suprafacially, therefore no distortion is required and for larger cases, such as the antarafacial [1,7]-hydrogen shift, distortion is feasible. Similar orbital considerations can be applied to other [i,j]-sigmatropic rearrangements and an overview can be found in Scheme 1.5B.

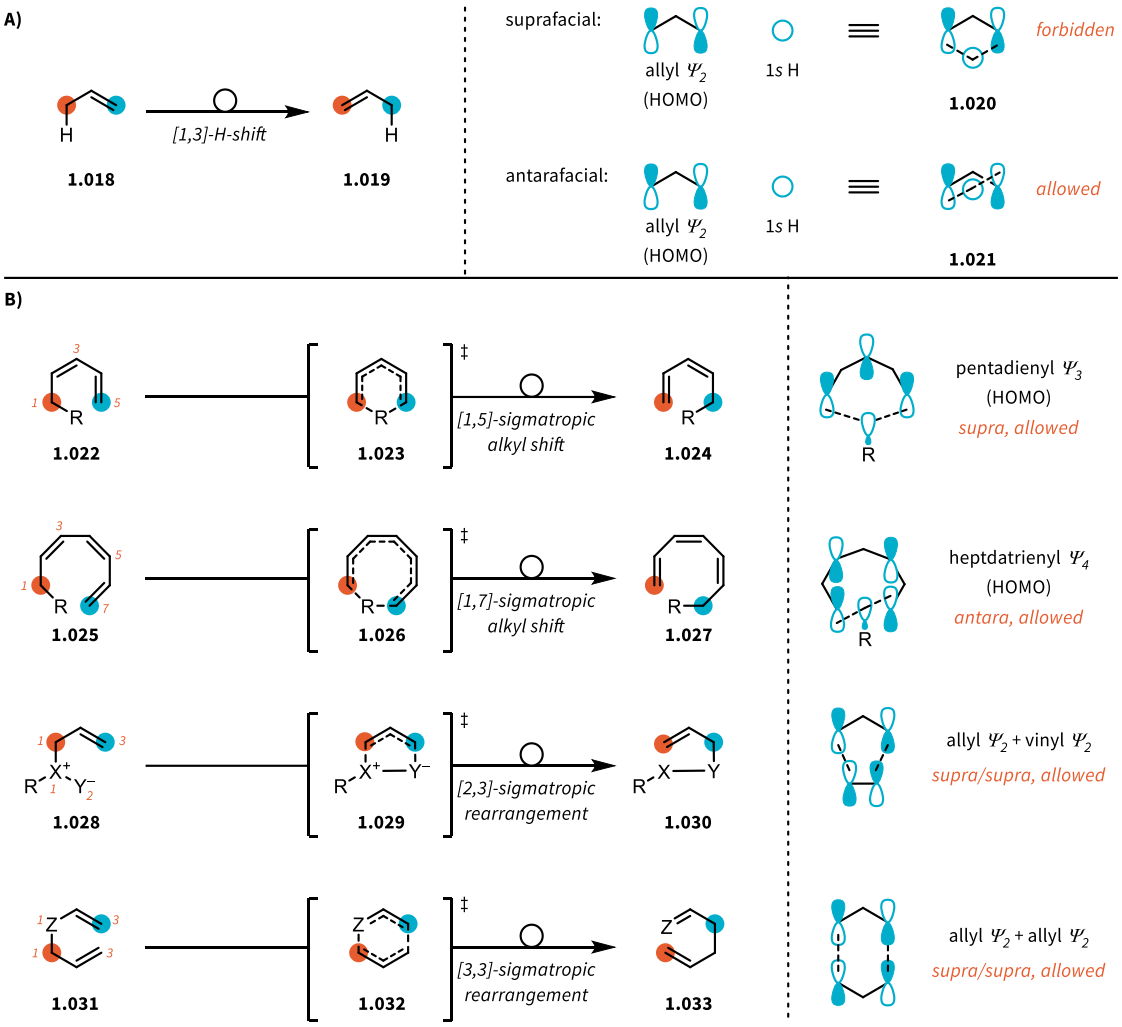

Scheme 1.5: Overview of different types of generalised sigmatropic rearrangements. A) [1,3]-hydrogen shift is allowed for the antarafacial pathway, however since distortion of the orbitals would be required to facilitate this reaction, it is not possible to progress and remains a theoretical reaction under this mechanism. B) Various types of sigmatropic rearrangements, featuring [1,5]- and [1,7]-alkyl shifts as well as [2,3]- and [3,3]-sigmatropic rearrangements. For every reaction type, the orbitals of the TS are visualised on the right side of the scheme.

1.1.3. [3,3]-Sigmatropic Rearrangements

As sigmatropic rearrangements are predictable in their reaction outcome and are often reliably conducted providing the starting material possesses the correct structural elements, they have become a staple in the synthesis of functionally diverse and difficult to access scaffolds.[21–29]

As previously discussed, the first example of a [3,3]-sigmatropic rearrangement was reported by Ludwig Claisen in 1912.[13] Since this seminal discovery, several variations and modification of the eponymous Claisen reaction have been developed, enabling the synthesis of different functionalised products and ultimately finding application in the total synthesis of natural products. If the oxygen atom, which is typically present within the rearranging scaffold is replaced by a carbon, the reaction is then referred to as a Cope rearrangement, a [3,3]-sigmatropic rearrangement of 1,5-dienes (**1.037**, Scheme 1.6).[30] As depicted in Scheme 1.6, the simplest Claisen rearrangement product is driven by the formation of a carbonyl species (**1.036**), whereas the parent Cope rearrangement is in fact degenerate: starting material and product are identical in the absence of substituents (**1.037**/**1.039**).

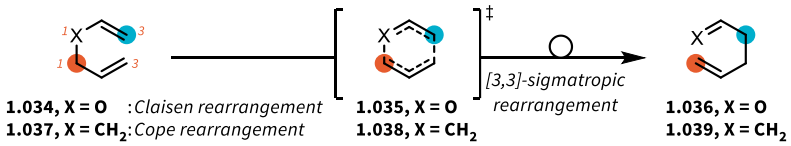

Scheme 1.6: Overview on the Claisen rearrangement for allyl vinyl ethers (**1.034**, X = O) and the Cope rearrangement for 1,5-dienes (**1.037**, X = CH_2).

1.1.3.1. The Claisen Rearrangement and its Variations

The Claisen rearrangement is capable of producing all-carbon quaternary centres with predictable stereochemistry. The scope of accessible products has been greatly expanded since the original discovery.

A recent example was presented by Kawamoto *et al.* in their total synthesis of (−)-lucidumone (**1.045**).[31] The key Claisen rearrangement, which is part of a two-step process (Claisen rearrangement followed by intramolecular aldol addition) that established the core skeleton of the natural product is shown in

Scheme 1.7B. Through this sequence, the sole stereocentre of the starting allylic alcohol (**1.040**) transfers chiral information through the sigmatropic rearrangement and ultimately establishes all stereocentres of (−)-lucidumone (**1.045**) over the course of the total synthesis.

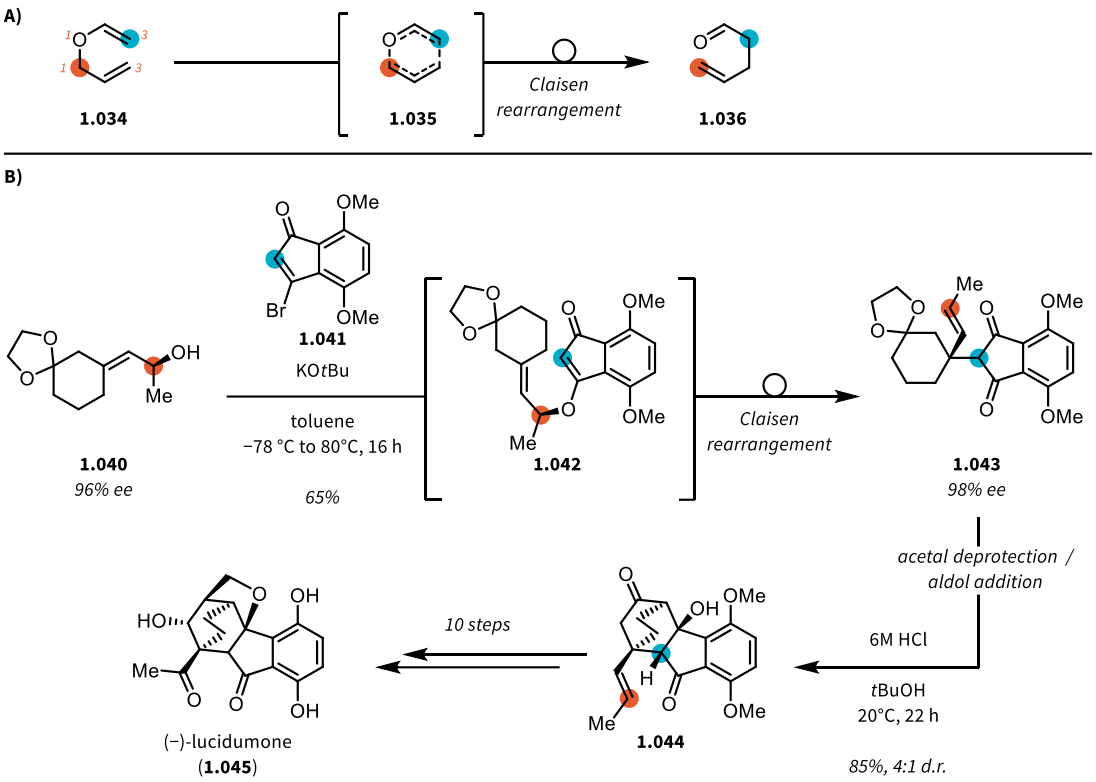

Scheme 1.7: A) General Claisen rearrangement of allyl vinyl ethers to yield γ,δ-unsaturated carbonyls. B) Key Claisen rearrangement in the total synthesis of (−)-lucidumone (**1.045**) from chiral allyl alcohol **1.040**.

Variations to the Claisen rearrangement were introduced to either produce different types of carbonyl products in a single step or to enable less harsh reaction conditions (room temperature or below). Among these variations or modifications are the Carroll-Claisen,[32–35] Eschenmoser-Claisen,[36] Johnson-Claisen,[37] Ireland-Claisen,[38–40] and other reactions,[41] which have been developed and applied to complex synthetic problems in the last century. An overview of different Claisen-type rearrangements is given in Scheme 1.8.

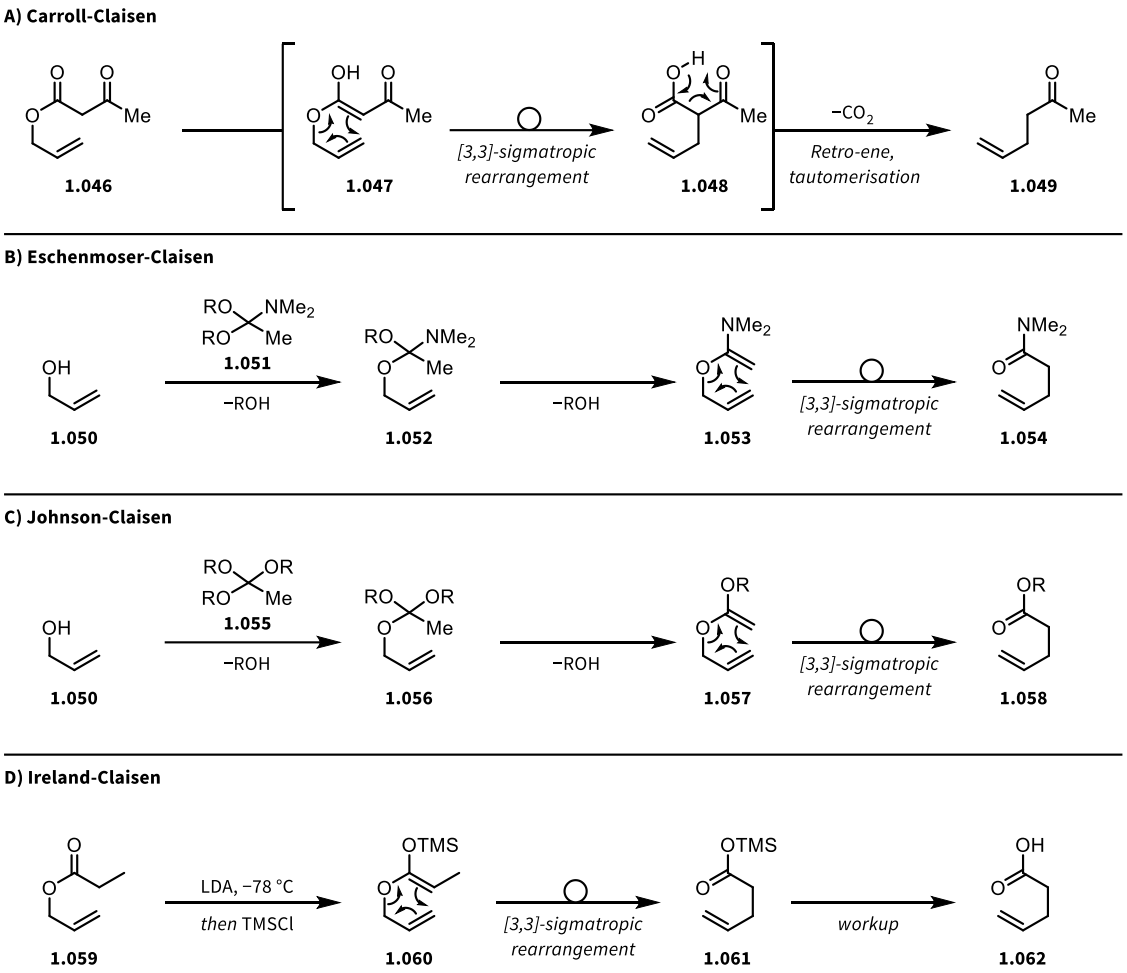

Scheme 1.8: Summary of the most commonly applied variations on the Claisen rearrangement in chronological order of discovery. A) the Carroll-Claisen rearrangement, which converts β-keto allyl esters such as **1.046** to γ,δ-unsaturated ketones (**1.049**) through a [3,3]-sigmatropic rearrangement followed by decarboxylation. B) Eschenmoser-Claisen rearrangement starting from an allylic alcohol **1.050**, which upon reaction with *N*,*N*-dimethylacetamide dialkyl acetal **1.051** and formation of *N*,*O*-ketene acetal **1.053**, produces γ,δ-unsaturated amide **1.054**. C) The Johnson-Claisen reaction, using an ortho ester leading to γ,δ-unsaturated ester **1.058**. D) Ireland-Claisen variation, starting from *O*-allyl alkyl ester **1.059**, which is converted to silyl ketene acetal **1.060** capable of undergoing [3,3]-sigmatropic rearrangement at low temperature to deliver γ,δ-unsaturated acid **1.062** after workup.

The Carroll-Claisen rearrangement was first published in 1940 and was further studied in the 1980's and 1990's.[32–35,42] The starting materials of the reaction are β-keto allyl esters, such as **1.046**, which are prone to tautomerisation to form the corresponding ketene hemiacetal **1.047**, which can undergo [3,3]-sigmatropic rearrangement to deliver the β-keto carboxylic acid intermediate **1.048**. The latter can evolve through extrusion of CO_2 *via* a retro-ene reaction to provide γ,δ-unsaturated ketone **1.049** after an additional tautomerisation step (Scheme 1.8A). This variation of the Claisen rearrangement can also be conducted at lower temperatures with the aid of a Pd-catalyst, which is able to bind to the allyl moiety to convert it into an excellent leaving group,[43] or *via* formation of the doubly-deprotonated form of the acetoacetate starting materials, mediated by LDA.[35]

In the Eschenmoser variation of the Claisen rearrangement, allyl alcohol **1.050** is reacted with a *N*,*N*-dimethylacetamide dialkyl acetal, such as **1.051**, to form a *N*,*O*-ketene acetal (**1.053**), which can undergo [3,3]-sigmatropic rearrangement delivering a γ,δ-unsaturated amide such as **1.054** (Scheme 1.8B). This reaction was first discovered by Meerwein *et al.* as an undesired process in the context of their research and was later formalised by Eschenmoser *et al*.[36,44] Heating of the reaction mixture is typically required to force the transesterification and introduction of the allyl alcohol to form **1.052**.[41]

Closely related to the Eschenmoser-Claisen rearrangement is the Johnson-Claisen rearrangement. In this reaction, the allyl alcohol **1.050** is reacted with an ortho ester, such as **1.055**, to form **1.056** through transesterification. This intermediate then undergoes elimination to form the ketene acetal **1.057**, which proceeds through the [3,3]-sigmatropic rearrangement to yield γ,δ-unsaturated ester **1.058** (Scheme 1.8C).[37,41]

The last variation of the Claisen rearrangement to be highlighted herein is the Ireland-Claisen rearrangement. Here, an allyl ester **1.059** is first deprotonated by LDA and the enolate is captured with TMSCl to form silyl ketene acetal **1.060** (Scheme 1.8D). The latter undergoes [3,3]-sigmatropic rearrangement to form γ,δ-unsaturated acid **1.062** after the hydrolysis of silylcarboxylate **1.061** upon workup. Since the Ireland-Claisen reaction utilises enolates, it is related to the enol ester variation of the Carroll-Claisen process previously mentioned.

1.1.3.2. [3,3]-Sigmatropic Rearrangements involving Chalcogens

Since the Claisen rearrangement relies on the driving force of carbonyl formation from an allyl vinyl ether, interest in the replacement of oxygen by other chalcogens has arisen in order to explore the chemistry of thio- or selenocarbonyls. This has led to the development of the thio- and seleno-Claisen rearrangements, both of which, however, have limited applicability (Scheme 1.9).[45–49]

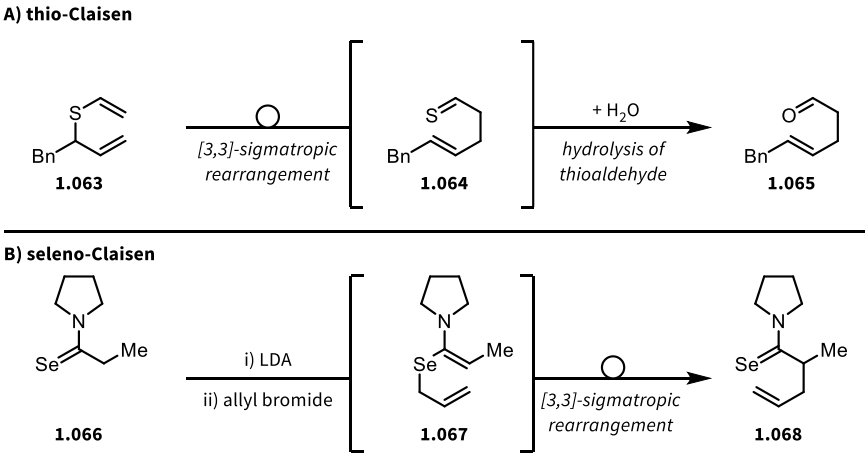

Scheme 1.9: Abbreviated overview on the thio- and seleno-Claisen rearrangements. A) thio-Claisen rearrangement from *S*-allyl vinyl sulfide **1.063** to the thioaldehyde **1.064**. B) seleno-Claisen rearrangement from selenoamide **1.066**, which undergoes Se-allylation before the [3,3]-sigmatropic rearrangement takes place to deliver the γ,δ-unsaturated selenoamide **1.068**.

Given the instability of thioaldehydes towards hydrolysis, the synthesis of γ,δ-unsaturated aldehydes (**1.065**) from *S*-allyl vinyl sulfides such as **1.063** *via* a thio-Claisen rearrangement merely constitutes another approach to compounds similar to **1.065**, should the standard Claisen rearrangement of the corresponding allyl ether fail to deliver the desired product (Scheme 1.9A). It additionally offers the possibility to mask a putative aldehyde as a vinyl sulfide to be revealed at a later point in a synthetic sequence.

Interestingly, the reaction of selenoamide **1.066** with LDA and allyl bromide leads to **1.067**, a species that could be seen as the seleno analogue of the Eschenmoser-Claisen intermediate **1.053** (*cf.* Scheme 1.8). This species can undergo [3,3]-sigmatropic rearrangement to form a γ,δ-unsaturated selenoamide **1.068**, which could theoretically be hydrolysed to the corresponding carboxamide. The benefit of using selenoamides in this process is that the reaction can be carried out at 0°C, whereas Eschenmoser-Claisen rearrangements are typically conducted at elevated temperatures in order to form the required *N*,*O*-ketene acetals.

As previously described, sigmatropic rearrangements have proven powerful in asymmetric synthesis, as stereoinformation is generally faithfully relayed from starting material to product due to the typically organised, cyclic transitions states involved.

Recently, Maulide *et al*. reported processes hinging on the [3,3]-sigmatropic rearrangement of sulfonium intermediates to deliver valuable products, in which the chirality of the starting materials is translated into the products.[27,50] Of particular interest is the synthetic access to 1,4-dicarbonyls, a class of compounds which are highly sought after, but are intrinsically challenging to synthesise due to their inherent polarity mismatch.[26] In this case, chiral vinyl sulfoxides (**1.070**) were reacted with activated ynamides (**1.069**) to form an activated sulfonium intermediate **1.071** (Scheme 1.10). This intermediate undergoes charge-accelerated [3,3]-sigmatropic rearrangement, followed by *in situ* hydrolysis of the thionium intermediate **1.072**, to deliver 1,4-dicarbonyl products (**1.073**) in an enantiospecific reaction. The choice of (*E*)- or (*Z*)-vinyl sulfoxide (**1.070**), paired with the choice of sulfoxide configuration ((S_S)- or (R_s)), allows full control over the reaction's stereochemical outcome. The generation of a similar sulfonium intermediate such as **1.071** through Au-mediated activation of the ynamide was published recently by Voituriez *et al*.[28,29]

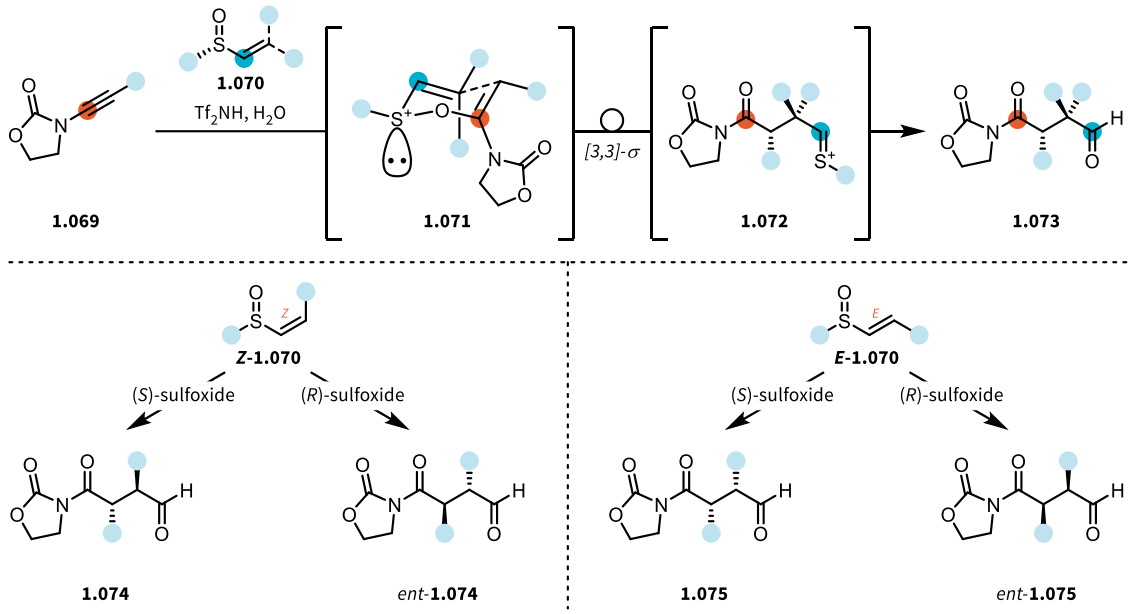

Scheme 1.10: Charge accelerated [3,3]-sigmatropic rearrangement of sulfonium intermediates (**1.071**) derived from Brønsted acid-activated ynamide **1.069** and chiral sulfoxide **1.070**.

1.1.4. [2,3]-Sigmatropic Rearrangements and Chalcogen-mediated Processes

Similarly to the aforementioned [3,3]-sigmatropic rearrangements, [2,3]-sigmatropic rearrangements are concerted reactions involving the reorganisation of six electrons and the realm of [2,3]-sigmatropic rearrangements is typically divided into formally neutral rearrangements and anionic rearrangements.[14] Formally neutral [2,3]-sigmatropic rearrangements involve ylides or oxides (**1.076**, Scheme 1.11A), whereas anionic [2,3]-sigmatropic rearrangements are defined by the rearrangement of an anion (**1.079**, Scheme 1.11B).

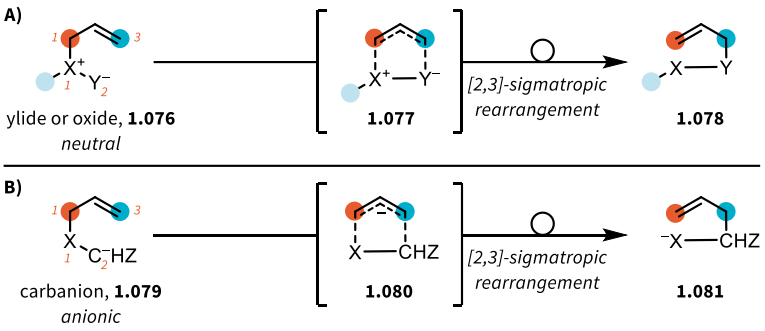

Scheme 1.11: Generalised overview on the two classes of [2,3]-sigmatropic rearrangements, A) formally neutral rearrangements of ylides and oxides (**1.076**) and B) anionic rearrangements of carbanions (**1.079**, Z = electron-withdrawing group).

The propensity for the reaction to proceed hinges on the ability of X to act as a good leaving group while Y begins bond formation to the allylic system. If X and Y bear formal charges, the rearrangement progresses readily, with the most developed examples of [2,3]-sigmatropic rearrangements being centred around the rearrangements of allyl sulfoxides,[51–54] selenoxides,[55,56] ammonium ylides,[57–60] and sulfonium ylides.[57,61,62] In the following chapter some specific [2,3]-sigmatropic rearrangements will be explored, with a focus on rearrangements involving chalcogens.

1.1.4.1. Sommelet-Hauser Rearrangement

The Sommelet-Hauser rearrangement describes the [2,3]-sigmatropic rearrangement of quaternary benzylic ammonium ylides (**1.082**) to yield (*o*-methylbenzyl) amine products (**1.084**, Scheme 1.12). Initially discovered in 1937 by Sommelet,[63] and formalised by Hauser in 1951,[3,12] this process suffers from the harsh reaction conditions necessary for the deprotonation of the ammonium salt to initiate the rearrangement. This hurdle can be overcome by the use of silylated ammonium species ($R'_3SiCH_2NR''_3^+$), which may be converted into the reactive intermediate upon treatment with a fluoride source.[64] Additionally, asymmetric versions of the Sommelet-Hauser rearrangement have been developed, enabling stereoselective synthesis in more structurally complex products.[65]

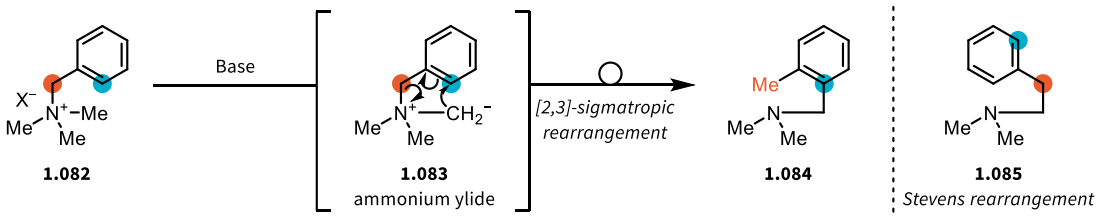

Scheme 1.12: Sommelet-Hauser [2,3]-sigmatropic rearrangement of ammonium salts *via* ammonium ylides to form *o*-methylbenzyl amines.

A commonly encountered side reaction of the Sommelet-Hauser rearrangement is the Stevens rearrangement, a [1,2]-alkyl shift, leading to an α-secondary amine product (**1.085**).

1.1.4.2. Mislow-Evans Rearrangement

One of the most important [2,3]-sigmatropic rearrangements involving chalcogens is the Mislow-Evans rearrangement. Initially observed by Mislow *et al*.,[66,67] this reaction was further developed by Evans *et al*. to exploit is synthetic utility.[51,68] It consists of the rearrangement of an allylic sulfoxide (**1.086**) to a sulfenate allyl ester (**1.088**), which can be cleaved to yield the often desired allylic alcohol product (**1.089**) (Scheme 1.13A). The synthetic utility of this rearrangement again stems from its predictable stereochemical outcome, allowing for chirality transfer in both directions of the rearrangement. For

example, if a chiral allylic alcohol is reacted with an arylsulfenyl species to form the sulfenate ester (**1.091**), the following retro-Mislow-Evans rearrangement yields a chiral sulfoxide (**1.093**), in which the chiral information of the starting material is transferred from carbon to sulfur. In a similar fashion, if chiral allyl sulfoxides are rearranged and the sulfenate allyl ester cleaved by a thiophile, the resulting allylic alcohols carry forward the stereoinformation encoded in the sulfoxide, given that the substitution pattern yields a chiral allyl alcohol.[66,69] The direction into which the equilibrium is shifted, is determined by the stability of the resulting products, with sulfoxides (such as **1.086**) being more stable than sulfenate esters (such as **1.088**), favouring retro-Mislow-Evans rearrangement, while the presence of a thiophile (a species capable of cleaving the sulfenate esters and therefore removing them from the equilibrium) leads to allylic alcohols (such as **1.089**).

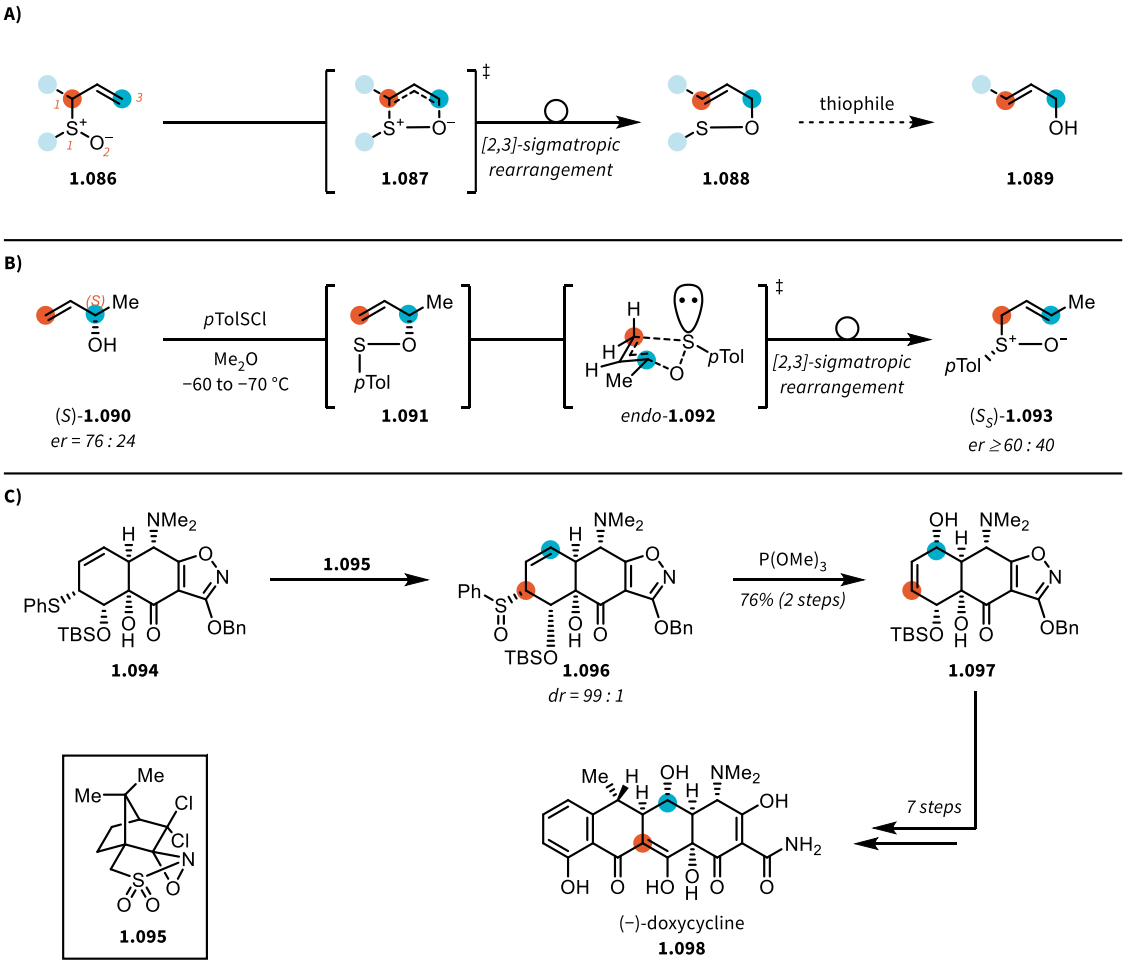

Scheme 1.13: A) General overview of the Mislow-Evans rearrangement starting from an allyl sulfoxide **1.086**, which undergoes [2,3]-sigmatropic rearrangement to form sulfenate allyl ester **1.088**, which can be converted to the allylic alcohol **1.089** through the action of a thiophile. B) Chirality transfer from carbon to sulfur as observed by Mislow *et al*. in a retro-Mislow-Evans rearrangement. C) Application of the Mislow-Evans rearrangement by Myers *et al.* in the total synthesis of (−)-doxycycline (**1.098**), transforming allylic sulfide **1.094** into the enantioenriched allylic sulfoxide **1.096** through diastereoselective oxidation using a chiral oxaziridine reagent (**1.095**).

A synthetic application of this rearrangement can be found in the synthesis of (−)-doxycycline (**1.098**) and analogues reported by Myers *et al.*[70] In the event, a Mislow-Evans rearrangement is used to set a key allylic alcohol stereocentre through the rearrangement of the corresponding allylic sulfoxide **1.096**. to ultimately form **1.097** after the action of the thiophile $P(OMe)_3$, which releases the hydroxyl moiety (Scheme 1.13C). In this case, the [2,3]-sigmatropic rearrangement progresses with sulfur-to-carbon chirality transfer.

1.1.4.3. Seleno-Mislow-Evans Rearrangement

Replacing the sulfoxide of the Mislow-Evans rearrangement with a selenoxide (**1.099**) leads to one of the most widely applied variations of this reaction. Arylselenium species are readily incorporated into the molecular scaffold and, following oxidation to the corresponding selenoxide and given an adjacent allylic group, the [2,3]-sigmatropic rearrangement proceeds, even at cryogenic temperatures. Typically, the selenenic acid esters (**1.101**) are readily hydrolysed, thereby not requiring an additional reagent to release the desired product, in contrast to the sulfur-based Mislow-Evans rearrangement (Scheme 1.14).[54,56,71–73]

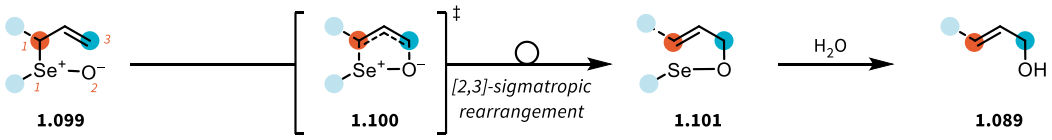

Scheme 1.14: General overview on the seleno-Mislow-Evans rearrangement of allylic selenoxides (**1.099**) to form allylic alcohols (**1.089**) *via* a [2,3]-sigmatropic rearrangement followed by hydrolysis of the allyl selenenate **1.101**.

It is noteworthy that selenoxides are capable of undergoing [2,3]-sigmatropic rearrangement preferentially given the choice between the aforementioned process and a potential *syn* elimination to form an olefin (**1.102**), a process that is well established for organoselenoxide species (Scheme 1.15).[56,74–76]

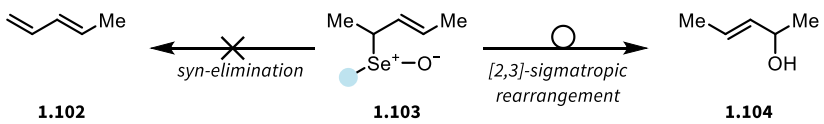

Scheme 1.15: Visualisation of the reactivity of allyl selenoxides (**1.103**) if presented with two possible reaction pathways.

The ease with which both selenoxide [2,3]-sigmatropic rearrangements and *syn*-eliminations proceed, compared to the corresponding sulfur versions of the reactions, is a result of the weaker C–Se bond in comparison to the C–S bond. This property lends itself well to the incorporation into complex synthetic problems, as exemplified by the total synthesis of (−)-13-oxyingenol (**1.109**) by Kigoshi *et al.*, as presented in Scheme 1.16.[77] In the event, mesylate **1.105** was converted to phenyl selenide **1.106** through a nucleophilic substitution process using an *in situ* generated selenide anion. The newly introduced phenyl selanyl moiety was carried forward through eight synthetic transformations, including oxidative conditions, before finally being oxidised, triggering a [2,3]-sigmatropic rearrangement to reveal, after cleavage of the selenate ester, allylic alcohol **1.108**. **1.108** is subsequently deprotected to furnish the natural product (−)-13-oxyingenol (**1.109**).

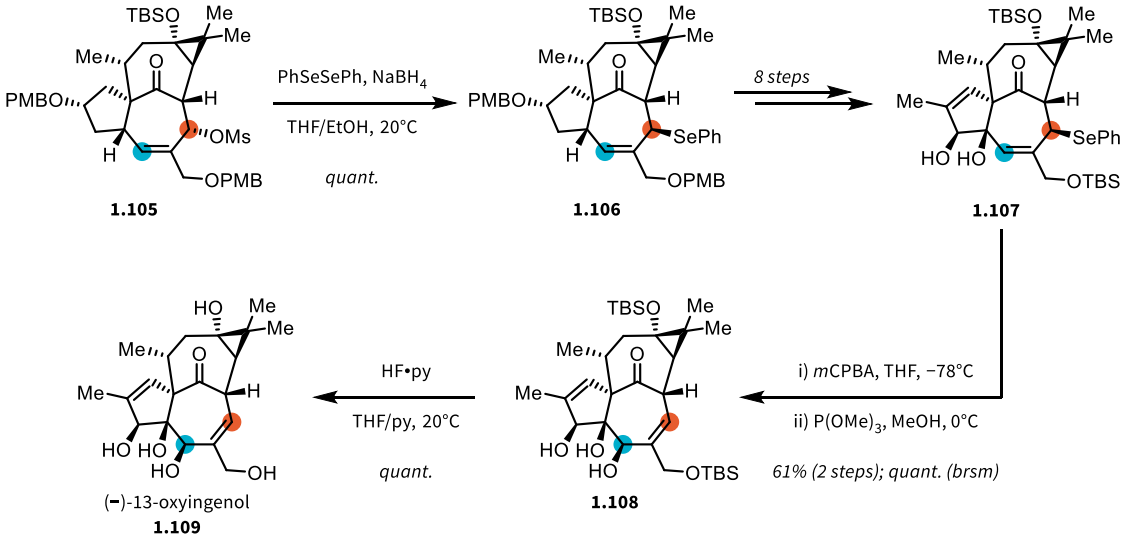

Scheme 1.16: Total synthesis of (−)-13-oxyingenol (**1.109**) through a key late-stage [2,3]-sigmatropic rearrangement.

Much like their sulfur congeners, organoselenides can be enantioselectively oxidised with enantiopure oxidants, such as the previously mentioned variation of Davis' oxaziridine (**1.095**),[78] or under oxidative conditions reminiscent of Sharpless' asymmetric allylic epoxidation.[79]

1.1.4.4. Se-mediated Double [2,3]-Sigmatropic Rearrangement of *N*-aryloxyacetamides

The capabilities of aromatic selenoxides to undergo sigmatropic rearrangements are underdeveloped compared to their allylic counterparts. Naturally, since organoselenide moieties are typically introduced into molecular scaffolds in their phenyl selenide form, the aromatic moiety bound to the selenium atom is looked upon as a mere bystander in the chemistry that is happening on the other side of the C_{Ar}–Se bond. Recently, however, it was established by Zhao *et al*. that organoselenides are capable of undergoing a double [2,3]-sigmatropic rearrangement process on an aromatic scaffold to lead to *p*-aminophenol derivatives (such as **1.111**) as their products.[80] If the *para*-position of the starting material is blocked, the double [2,3]-sigmatropic rearrangement occurs but leads to the formation of dearomatised products such as **1.120**.

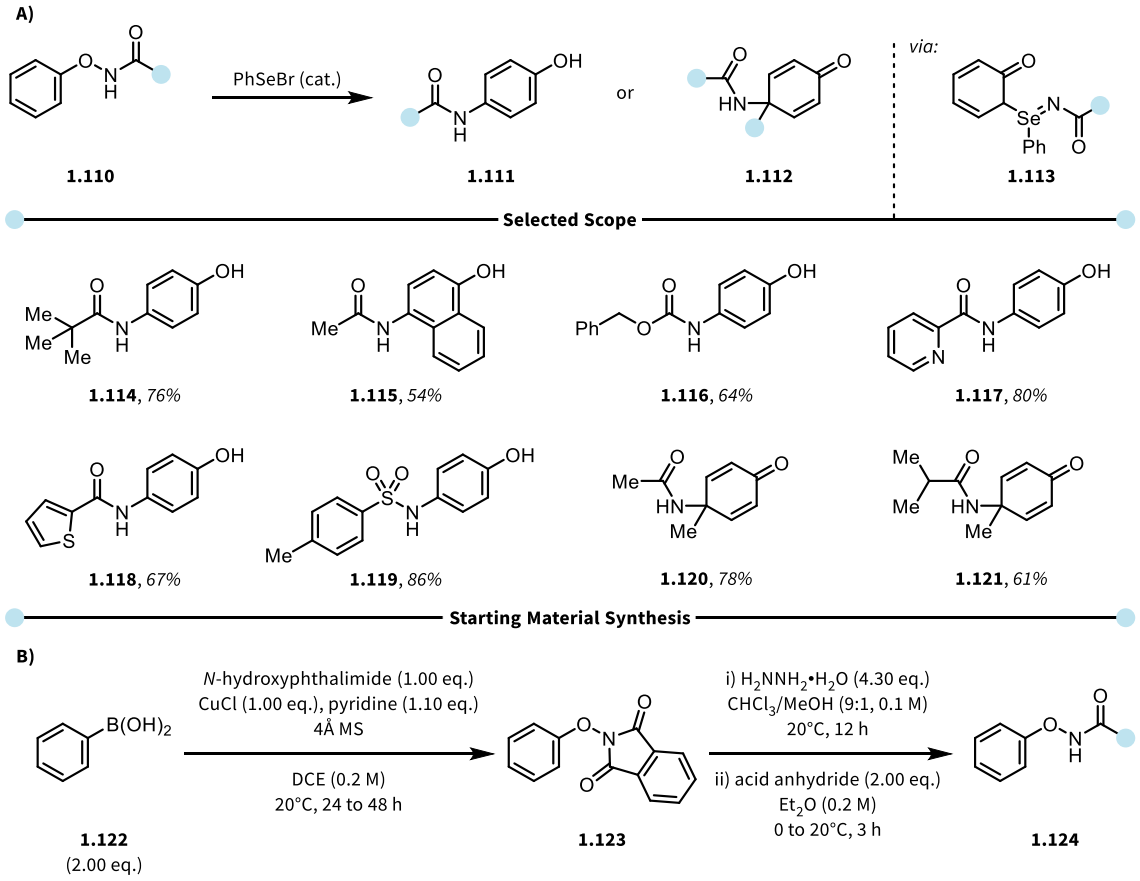

Scheme 1.17: A) Selected scope entries for the synthesis of *p*-aminophenols and 4-oxocyclohexa-2,5-dien-1-yl amides derivatives starting from *N*-aryloxyacetamides (**1.110**) through a double [2,3]-sigmatropic rearrangement process. B) Synthesis of *N*-aryloxyacetamides from arylboronic acid (**1.122**) and *N*-hydroxyphthalimide.

While the developed methodology is mechanistically intriguing, its broad application is hindered by the laborious synthesis of the starting materials, requiring three steps from *N*-hydroxyphthalimide and arylboronic acid **1.122**, with the intermittent use of stoichiometric amounts of a copper reagent. The authors also demonstrate that an analogous process using a sulfur-based reagent (*N*-(phenylthio)-phthalimide) leads to the double [2,3]-sigmatropic rearrangement. However, release of the sulfur species does not occur, thereby requiring stoichiometric use of the sulfur reagent.[80]

1.1.5. Rearrangement Reactions of Hydroxylamines and Hydroxamic Acids

1.1.5.1. Bamberger Rearrangement

The aforementioned double [2,3]-sigmatropic process is far from the only or first synthetic method to access *p*-aminophenols in a selective fashion. One of the first reactions to enable the synthesis of *p*-aminophenol (**1.128**) was discovered by Eugen Bamberger in 1894 in a reaction now known as the Bamberger rearrangement.[81,82] Here, phenylhydroxylamine (**1.125**) is treated with 5% sulfuric acid and heated at reflux, leading to the formation of a nitrenium ion (**1.126**/**1.127**) *via* the loss of water. This nitrenium ion can then be attacked by water in the *p*-position to yield *p*-aminophenol after loss of the catalytic proton (Scheme 1.18).

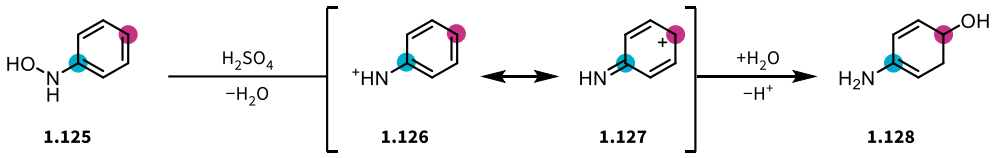

Scheme 1.18: The Bamberger rearrangement with conditions taken from Bamberger's 1894 publication.[81,82]

The Bamberger rearrangement, while of fundamental interest, does not bear synthetic utility in a modern setting. Industrially, *p*-aminophenols are synthesised from readily available phenols through nitration (H_2SO_4/$NaNO_3$) and reduction.[83]

1.1.5.2. *ortho*-Selective Reactions of Hydroxamic Acids

While it has been established that hydroxylamines and hydroxamic acids may undergo unproductive N–O bond cleavage in acidic media, the influence of Lewis acids on hydroxamic acids and esters has not been extensively studied. In 1989, Kikugawa *et al*. reported that phenylhydroxamic acid esters, such as **1.129**, undergo a rearrangement to yield the *o*-methoxy product **1.131** (Scheme 1.19).[84] The *p*-product, which could theoretically also be formed from a hypothetical nitrenium intermediate

1.130 was not observed. This phenomenon is rationalised through the formation of a contact-ion pair between the nitrenium ion and the $AlCl_3$-OMe^- anion (Scheme 1.19), in which the anion can also bind to the carbonyl oxygen. This forces proximity to the *o*-position and therefore enables regioselective *o*-substitution. Interestingly, one side product that was observed during the reaction was *p*-chloroanilide **1.132**, indicating the possibility of the nitrenium ion to be quenched by addition of a chloride anion to the *p*-position before the methoxy moiety can be reintroduced.

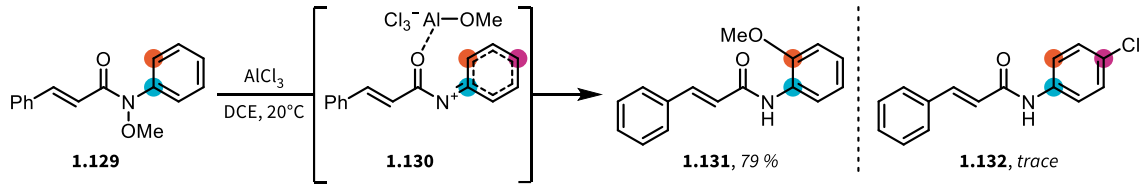

Scheme 1.19: Lewis acid-mediated *o*-selective migration of a methoxy moiety starting from hydroxamic acid ester **1.129** and leading to the product **1.131** through a putative contact ion pair intermediate (**1.130**).

Several years later, the same group reported an analogous process starting from hydroxamic acids (**1.133**) to yield *o*-aminophenols (**1.134**). This process does not rely on the use of Lewis acids to mediate the rearrangement but rather a mixture of CCl_4 and $P(n\text{Bu})_3$, leading to the assumed intermediate **1.135**, which ultimately forms the products (Scheme 1.20).[85]

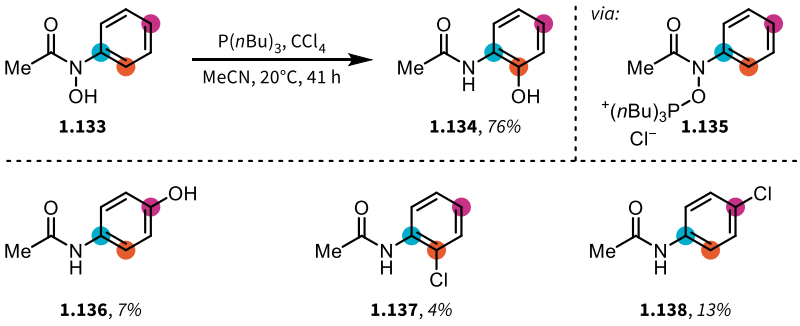

Scheme 1.20: Rearrangement of hydroxamic acid **1.133** to *o*-aminophenol **1.134** through a rearrangement process mediated by $P(n\text{Bu})_3$ and CCl_4. The observed side products are shown below the dashed line.

While this process was not fully studied mechanistically, the formation of trace amounts of *p*-chloroanilide (**1.138**) and *p*-aminophenol (**1.136**) again suggested the intermediacy of a nitrenium ion, presumably as a result of the cleavage of the N–O bond in **1.135**. Interestingly, the phosphine species does not simply react with the starting material to form the stable phosphine oxide, but rather acts as a mediator of the reaction and the final products can be isolated upon aqueous workup of the reaction.

Another interesting approach to the rearrangement of hydroxamic acid ester derivatives was published by Ngai *et al*. in 2014.[86] In this approach, a range of O-CF_3 arylhydroxamic acid esters (**1.139**) were heated to 120°C in nitromethane to induce a thermal rearrangement process (Scheme 1.21). The scope of the reaction is mostly limited to scaffolds bearing electron-withdrawing substituents on the aromatic system, with only a sole example bearing an electron-donating substituent (**1.147**) being includeds.

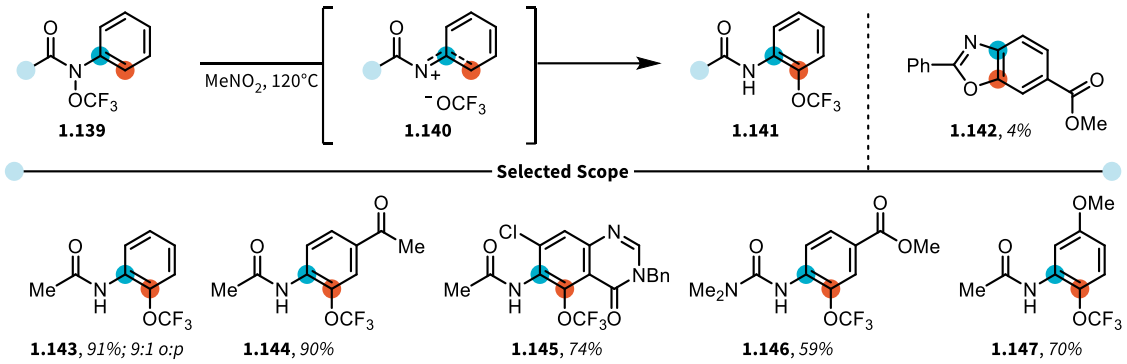

Scheme 1.21: Thermally induced rearrangement of O-CF_3 hydroxamic acid esters such as **1.139** to *o*-OCF_3 products (**1.141**). Selected scope entries are shown (**1.143** – **1.147**) alongside an isolated byproduct, benzoxazole (**1.142**), which is potentially formed through the self-quenching of the putative nitrenium ion (**1.140**).

Mechanistically, the rearrangement process seems to be of polar rather than radical nature, hinting at a heterolytic cleavage of the highly polarised N–O bond. The authors also reported the formation of a benzoxazole side product (**1.142**), which most probably arises from the intermediate nitrenium ion. The high *ortho*-selectivity is again rationalised by invoking the formation of a contact ion pair between the nitrenium ion (**1.140**) and the OCF_3^- anion, although traces of the *p*-OCF_3 product could also be detected.

In 2017, Nakamura *et al.* published two catalytic methods for the rearrangement of hydroxamic acid derivatives to *o*-functionalised products.[87,88]

In a first approach, *O*-carboxyl-*N*-arylhydroxamic acids (**1.148**) underwent a cobalt-catalysed rearrangement to yield *O*-carboxyl-*o*-aminophenols (**1.150**). The process leading to these products could be envisioned to proceed through a [3,3]-sigmatropic rearrangement, as had been established in the past for similar processes.[89] However, ^{18}O-labeling experiments revealed the reaction to proceed through a concerted [1,3]-shift, enabled by the cobalt catalyst (**1.149**, Scheme 1.22A). The reaction works well on electron-neutral or electron-poor aromatic scaffolds, while electron-rich substrates were not prominently featured in the scope of the reaction.

In their second publication, Nakamura *et al*. presented a reaction related to the methodology published by Kikugawa *et al*. for the rearrangement of hydroxamic acid esters (**1.155**) to form *o*-alkoxyaminophenol products (**1.156**).[84,88] This version of the reaction utilised a copper-NHC catalyst to achieve the *o*-selective rearrangement of a number of substrates. The reaction worked well across a range of scaffolds, however diminished yields were observed for electron-poor substrates, such as **1.159**. With regard to mechanism, the authors were able to show that a cross-over of alkoxy moieties between two different substrates did not occur, meaning that the putative intermediates stay in close proximity (as was also postulated by Kikugawa *et al.*).[84]

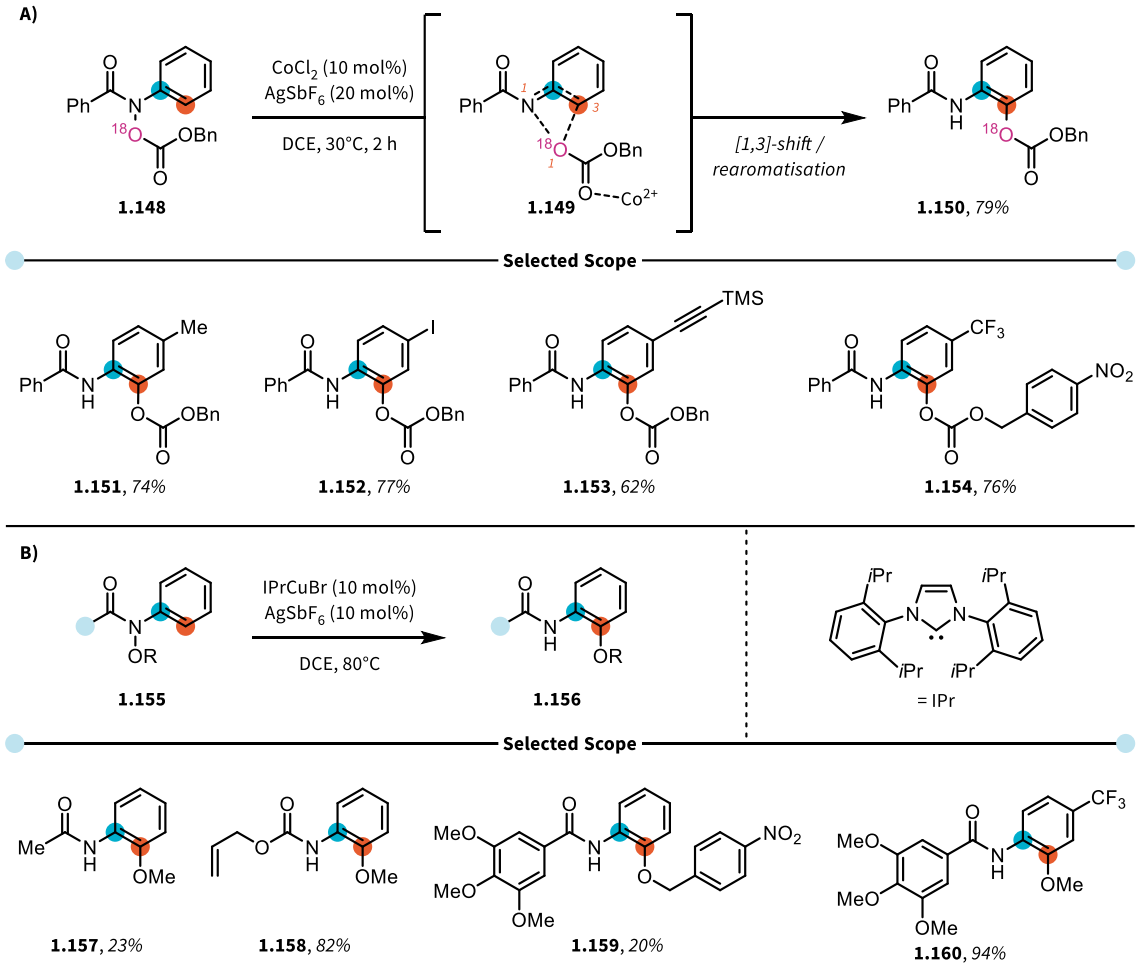

Scheme 1.22: A) [1,3]-Shift catalysed by Co(II) to transform *O*-carboxyl-*N*-arylhydroxamic acid esters (**1.148**) into *N*-acyl-*O*-carboxyl-*o*-aminophenols (**1.150**). Selected scope entries are shown. B) Rearrangement of hydroxamic acid esters (**1.155**) to *o*-alkoxyaminophenol products (**1.156**) through Cu-catalysis using an NHC ligand. Selected scope entries are shown.

1.2. Aims of the Project

The report detailing proposed double [2,3]-sigmatropic rearrangement process of *N*-aryloxy acetamides (**1.110**) to *p*-aminophenols (**1.111**) catalysed by PhSeBr, as described by Zhao *et al.*, did not explore the potential of Se-catalysis to form *p*-aminophenols. While their work demonstrated the feasibility of transposing an amide moiety from the phenolic to the *para*-position of an aromatic system through a sigmatropic rearrangement, the inverse process—where a hydroxamic acid (**1.161**) would undergo transposition of its hydroxy group from the nitrogen to the *para*-position of the aromatic system— was not documented (Scheme 1.23). In this regard, our specific aims of the project included:

a) Establishment of broadly applicable, catalytic and mild conditions for the conversion of hydroxamic acids to *p*-aminophenols and exploration of the scope of the reaction.

b) Application of the developed synthetic method to the synthesis of pharmaceutically relevant products.

c) Determination of the reaction mechanism using a combination of experimental and theoretical approaches.

d) Comparison of the efficiency between PhSeBr- and PhSBr-catalysis.

e) Exploration of a possible extension by employing hydroxamic acid esters or protected hydrazines as starting materials.

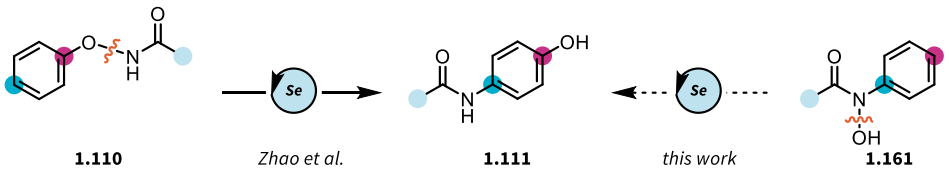

Scheme 1.23: Comparative depiction of the approach of Zhao *et al.* towards *p*-aminophenols (**1.111**) starting from *N*-aryloxy acetamides (**1.110**),[80] and the approach described herein starting from hydroxamic acids (**1.161**).

1.3. Results & Discussion

The results described in this chapter were acquired in collaboration with Dr. Hsiang-Yu Chuang (experimental), Ricardo Meyrelles (theoretical) and Boris Maryasin (theoretical), and have been published as a communication in Angew. Chem. Int. Ed. ***2021****, 60, 13778 – 13782,*[90] *and as a research article in Chem. Eur. J.* ***2023****, doi: 10.1002/chem.202302386.*[91]

1.3.1. Reaction Optimisation

N-phenylbenzhydroxamic acid (**1.162**) was chosen as a model substrate and several reaction parameters were investigated, such as the nature as well as the stoichiometry of the organoselenium source, and the role of the reaction solvent. Highlights of the reaction condition screening are summarised in Table 1.2.

First, it was discovered that the use of PhSeBr in a stoichiometric amount smoothly led to the formation of the desired *p*-aminophenol (**1.163**) with 72% isolated yield (entry 1). Remarkably, the amount of PhSeBr could be reduced to 10 mol% with only a slight decrease in the NMR yield to 66% (entry 2). All following screening reactions for different organoselenium species were carried out at 10 mol% loading and employed PhSeCl (67% NMR yield, entry 3), *N*-(phenylseleno)-phthalimide (40% NMR yield, entry 4), 2-nitrophenyl selenocyanate (Grieco reagent, 35% NMR yield, entry 5),[74] PhSeCl+AgOTf (25% NMR yield, entry 6) and PhSeSePh (no reaction, entry 7). For some reagents, the reaction time had to be extended from three up to 18 hours to ensure full consumption of the starting materials (or the lack thereof – entry 7). The investigation of different solvents at a fixed concentration of 0.2 M revealed that different polar, aprotic solvents are suitable for the reaction, while the use of a polar, protic solvent such as MeOH leads to lower yields. Ultimately, the optimised reaction conditions were found to require 10 mol% of PhSeBr in 1,4-dioxane at 0.2 M concentration. The choice of 1,4-dioxane as the ideal reaction solvent was reinforced during scope development, as this solvent allowed the reaction mixture to be heated to a

higher temperature (boiling point (bp.) of 1,4-dioxane: 101°C) to force conversion of less reactive substrates.

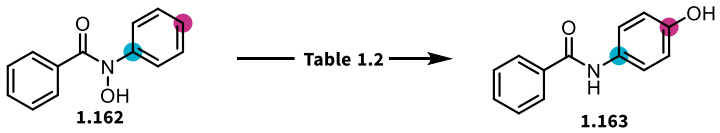

Table 1.2

Entry	Reagent	Solvent	Temperature (°C)	Time	NMR Yield (Isolated)
1	PhSeBr (1.00 eq.)	1,4-dioxane	20°C	1 h	(72%)
2	PhSeBr (10 mol%)	1,4-dioxane	20°C	3 h	66%
3	PhSeCl (10 mol%)	1,4-dioxane	20°C	6 h	67%
4	*N*-(phenylseleno)-phthalimide (10 mol%)	1,4-dioxane	20°C	12 h	40%
5	2-nitrophenyl selenocyanate (10 mol%)	1,4-dioxane	20°C	18 h	35%
6	PhSeCl (10 mol%), AgOTf (10 mol%)	1,4-dioxane	20°C	18 h	25%
7	PhSeSePh (10 mol%)	1,4-dioxane	20°C	18 h	0%
8	PhSeBr (10 mol%)	1,4-dioxane	20°C	3 h	79% (76%)
9	PhSeBr (10 mol%)	MeOH	20°C	3 h	29%
10	PhSeBr (10 mol%)	DCM	20°C	3 h	73%
11	PhSeBr (10 mol%)	MeCN	20°C	3 h	76%
12	PhSeBr (10 mol%)	THF	20°C	3 h	81%

Table 1.2: Optimisation table for the conversion of hydroxamic acid **1.162** into *p*-aminophenol **1.163**. The concentration of the reaction mixture was kept at 0.2 M across all solvents. Yields in brackets refer to isolated material.

The reaction mechanism was proposed to involve a double [2,3]-sigmatropic rearrangement process, initially leading to an intermediate *o*-selenoxide (**1.165**), which then undergoes a second rearrangement to the desired product (**1.163**, Scheme 1.24). Mechanistic details will be discussed in chapter 1.3.4. and experimental as well as computational evidence will be presented.

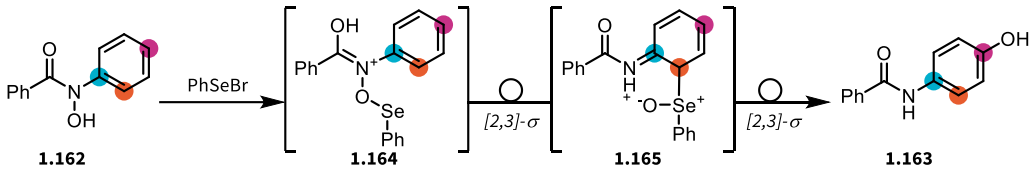

Scheme 1.24: Proposed mechanism of the reaction starting from hydroxamic acid **1.162**, which undergoes double [2,3]-sigmatropic rearrangement to yield *p*-aminophenol **1.163**.

1.3.2. Scope of the Se-catalysed Rearrangement Reaction

After establishing optimised reaction conditions, the focus was placed on developing a broad substrate scope and exploring the limitations of the reaction at hand. Following the logical disconnection of hydroxamic acids, the investigation was split into i) modifications of the acyl moiety (**1.114**, **1.136**, **1.163** – **1.171**) and ii) modifications of the *N*-aryl moieties (**1.115**, **1.172** – **1.182**), as depicted in Scheme 1.25, which also includes some substrates which did not undergo the desired rearrangement (**1.183 – 1.186**).

Sterically hindered substrates such as pivalamide and adamantylamide (yielding **1.114** and **1.166** respectively) underwent the rearrangement smoothly, only requiring heating to 100°C in the case of **1.114**. Hydroxamic acids derived from cyclobutane carboxylic acid (producing **1.167**) and acetic acid (delivering **1.136**) were also able to undergo the rearrangement process, providing the desired products. Subsequently, different aromatic acyl substituents were investigated. Starting with *p*-nitro-benzylphenylhydroxamic acid, which smoothly provided the desired *p*-aminophenol **1.168** in 83% yield, the influence of electron-withdrawing (EWG) and -donating groups (EDG) on the acyl moiety of the hydroxamic acid were investigated. The electron-neutral standard substrate provided the corresponding product **1.163** in 76% isolated yield, while the introduction of an electron-donating methoxy group in the *p*-position led to a reduced yield of 62% of **1.169**. This trend seemed to correlate with the strength of the N–O bond, which is weakened through further polarisation by the presence of an EWG in the benzamide fragment. Interestingly, two substrates bearing double bonds were also found to be tolerated, providing **1.170** and **1.171**, albeit with a slightly diminished yield in the case of **1.171**. This points towards the fact that the electrophilic selenium species is more prone to react with the oxygen, rather than add to the double bond. Some modifications of the acyl moiety were not accepted, such as the introduction of a pyridine (**1.183**) or the use of cyclic hydroxamic acids such as **1.184** and **1.185**, which did not undergo any reaction. These limitations potentially arise from the basicity of the pyridine moiety disturbing the facile protonation/deprotonation steps within the proposed reaction mechanism. The same may be true for cyclic hydroxamic acids, as these structures are less flexible and may therefore be unable to adopt the conformation required by the transition states.

Turning the attention to the *N*-aryl substituent, the introduction of an *N*-naphthyl group was well tolerated, providing **1.115** in 62% yield. Different alkyl substitution patterns on the *N*-aryl moiety were also accepted, in some cases leading to sterically highly encumbered products such as **1.175** and **1.176**. In terms of functional groups, a methoxy group (**1.173**) as well as a methyl ketone (**1.174**) substituent on the aromatic system posed no obstacle to the reaction and various halogen-containing substrates also underwent the desired double sigmatropic rearrangement, providing densely functionalised products (**1.177** – **1.182**). Substrates bearing electron-deficient substituents on the *N*-arene required heating to 100°C, while most other substrates were converted at room temperature. The introduction of a *p*-methyl group on the arene was not possible (**1.186**), as rearomatisation at the end of the catalytic cycle (*vide infra*) is impeded and, again, the introduction of a basic heterocycle, this time in the form of a quinoline (**1.187**) suppressed the reaction.

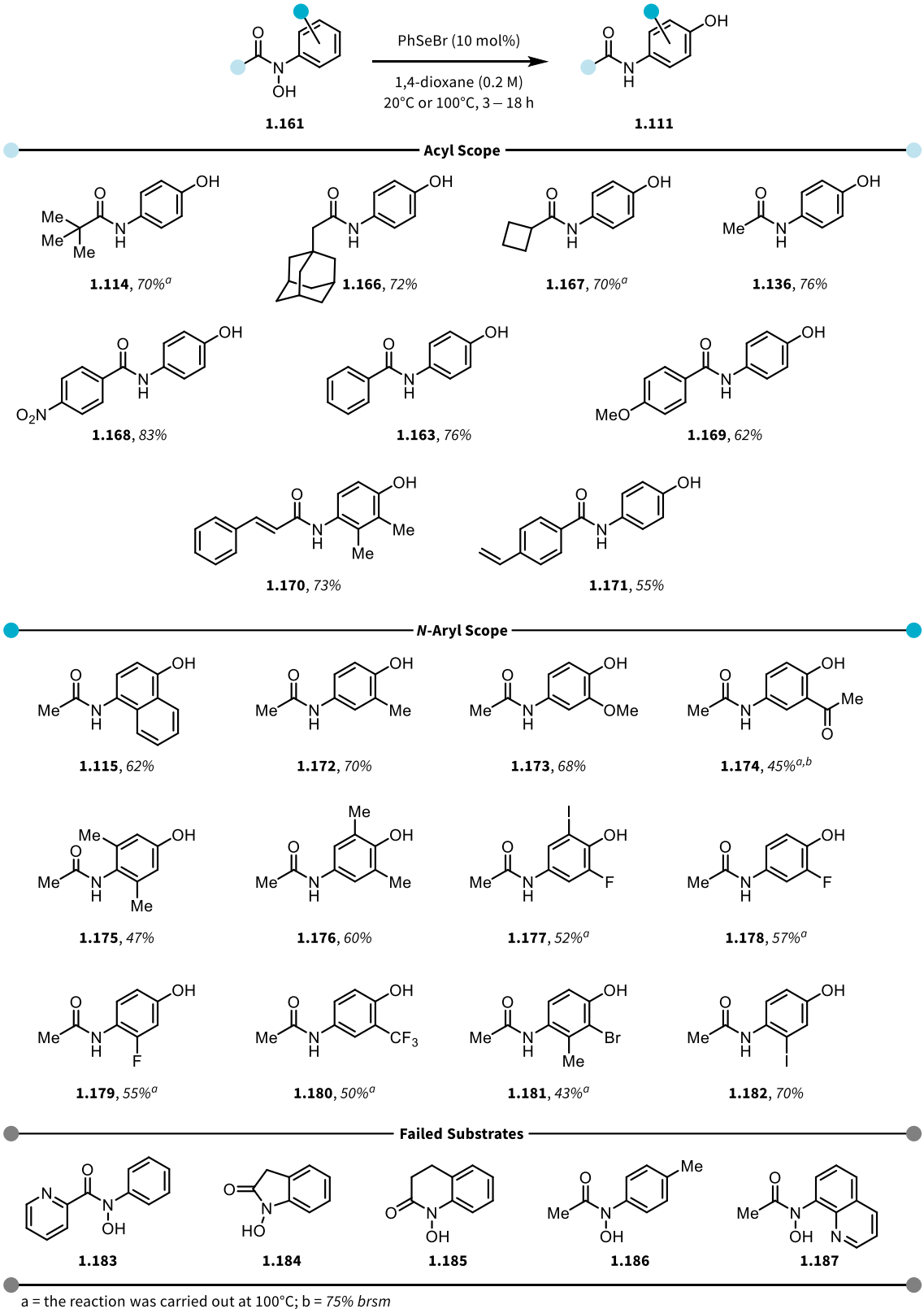

a = the reaction was carried out at 100°C; b = *75% brsm*

Scheme 1.25: Summary of the scope of the Se-catalysed rearrangement leading to *p*-aminoalcohols.

1.3.3. Gram-scale Syntheses and Applications

After having developed a mild and regioselective rearrangement reaction leading to *p*-aminophenols, this method was applied to the synthesis of pharmaceutically relevant molecules, such as paracetamol (**1.136**), practolol (**1.188**) and diloxanide furoate (**1.191**).

Several *p*-aminophenols possess biological activity, which enable their use in medicine as *i.e.*, non-opioid analgesics (painkillers) or beta-adrenergic blocking agents (heart medication, so-called *beta blockers*).[92] Practolol (**1.188**) can be prepared through different routes,[93–95] but in this case, the synthesis of practolol (**1.188**) started from *N*-phenlyacetylhydroxamic acid (**1.133**) which was converted to paracetamol (**1.136**) through the catalytic rearrangement with PhSeBr in 72% yield on a scale of 2.00 g (13.2 mmol, Scheme 1.26), thereby enabling the synthesis of paracetamol in a single step from a simple starting material. Paracetamol (**1.136**) was then mixed with epichlorohydrin and potassium carbonate and heated without any additional solvent to produce a crude epoxide (not shown), which was subsequently opened by *iso*-propylamine to form practolol (**1.188**) in 56% yield over two steps, delivering 1.42 g (5.18 mmol) of the desired beta blocker.

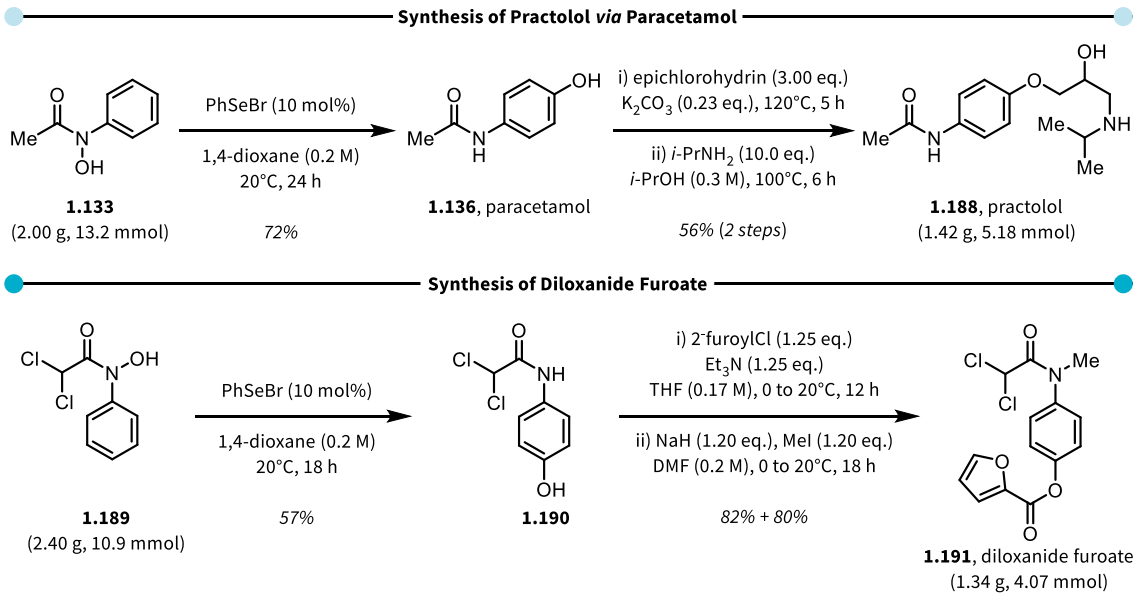

Scheme 1.26: Application of the Se-catalysed sigmatropic rearrangement to the gram-scale synthesis of the pharmaceutically relevant compounds paracetamol (**1.136**), practolol (**1.188**) and diloxanide furoate (**1.191**).

Diloxanide furoate (**1.191**) is a luminal amoebicide, commonly used to treat amoeba infections in the intestine. It is a prodrug to the active metabolite diloxanide, a *p*-aminophenol, after hydrolysis of the furoate ester and it is listed on the WHO list of essential medicines.[96] The use of diloxanide in the form of its furoate as a prodrug has proven beneficial with regards to its metabolic availability, as the furoate is cleaved in the gut to release the active agent. Starting from hydroxamic acid **1.189**, which was synthesised from *N*-phenylhydroxylamine and dichloroacetyl chloride, the desired product **1.190** was isolated in 57% yield after the double [2,3]-sigmatropic rearrangement process. The *p*-aminophenol **1.190** was then esterified with 2-furoyl chloride in 82% yield and subsequently methylated on the nitrogen to provide 1.34 g of diloxanide furoate (**1.191**) (80% yield) in a single run.

1.3.4. Mechanistic Experiments

Thus far, the Se-catalysed conversion of hydroxamic acids to *p*-aminophenols has been described as a double [2,3]-sigmatropic rearrangement process, however no experimental evidence has been provided. This is also the case for the publication by Zhao *et al.*, where the authors propose such a mechanism and underline its feasibility with computational studies, but lack experimental evidence for an *intramolecular* reaction pathway.[80] In theory, an *intramolecular* rearrangement process would lead to the desired products, however, so would an *intermolecular* process, where a selenoxide intermediate could be cleaved from the substrate to form a contact-ion pair, such as **1.192**, before reengaging to form the products.

To give a definitive answer to the question of whether dissociation of an intermediate takes place or whether the reaction is truly *intramolecular*, a cross-over experiment was performed, employing ^{18}O-labeled hydroxamic acid **1.133***, the synthesis of which is described in the experimental procedures (chapter 1.5). The labelled hydroxamic acid **1.133*** was mixed with the unlabelled standard substrate **1.162** in a 1:1 ratio and the mixture was subjected to the reaction conditions (Scheme 1.27).

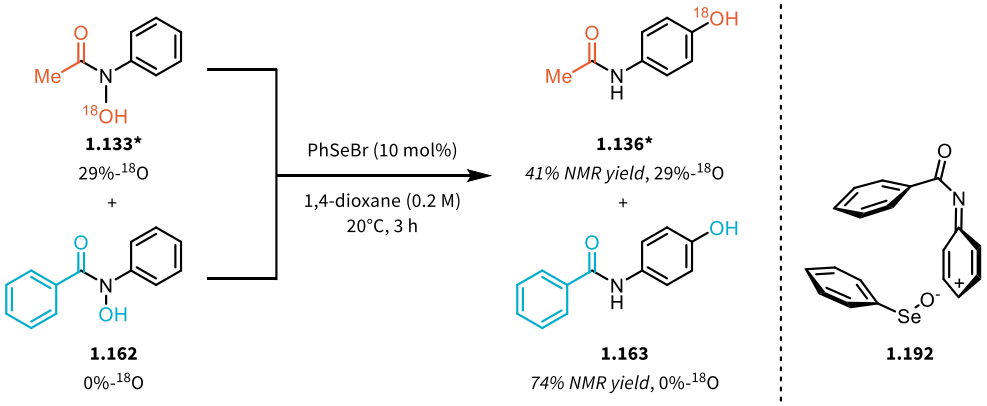

Scheme 1.27: Experimental set-up and results of the ^{18}O-cross-over experiment.

In this scenario, if the reaction involves an intermediate dissociation of a putative selenoxide, it may result in the transfer of an ^{18}O from the labelled intermediate to the unlabelled intermediate, leading to ^{18}O-labelled **1.163**. In the event it was found that no ^{18}O was transferred between the two products and that the ^{18}O-content did not change between the labelled starting material **1.133*** and the labelled product

1.136*. This very strongly suggests an *intramolecular* double [2,3]-sigmatropic rearrangement, where no dissociation of intermediates takes place. In an additional experiment, the unlabelled hydroxamic acid **1.162** was subjected to the reaction conditions in the presence of an excess of ^{18}O-water in order to try and label a putative dissociated intermediate selenoxide, however no incorporation of ^{18}O into the product of the reaction was observed (Scheme 1.28). Interestingly, the reaction worked with a yield identical to that of the reference reaction even in the presence of water.

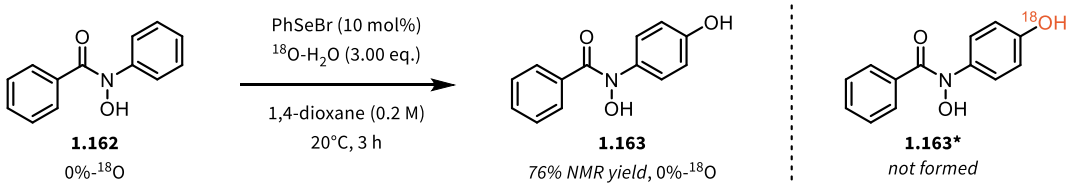

Scheme 1.28: Mechanistic experiment using labelled ^{18}O-H_2O to attempt labelling.

1.3.5. Computational Study of the Reaction Mechanism

In order to provide a reasonable mechanistic explanation for the aforementioned double [2,3]-sigmatropic rearrangement of hydroxamic acids to *p*-aminophenols, a computational study of the mechanism was performed by Ricardo Meyrelles and Dr. Boris Maryasin. The computed mechanism would have to agree with the experimental results, namely that the reaction can be performed with a catalytic amount of PhSeBr at room temperature and that no cross-over between substrates or intermediates takes place (*vide supra*).

The calculations revealed the following: the catalytic reaction begins with hydroxamic acid **1.133**, which undergoes reaction with PhSeBr to form intermediate **I** while releasing a bromide ion. During this process, the proton from the hydroxy group tautomerises to the carbonyl oxygen, a process that moves charge primarily onto the nitrogen atom (Scheme 1.29). Intermediate **I** then undergoes the first [2,3]-sigmatropic rearrangement with a barrier of 9 kcal · mol^{-1}, gaining 7 kcal · mol^{-1} in the process, leading to *o*-selenoxide **II**. Intermediate **II** undergoes low barrier H^+-transfers from the hydroxyl group to the selenoxide and back to the nitrogen to form **III**. This selenoxide-containing intermediate then undergoes the second [2,3]-sigmatropic rearrangement with a small barrier of 4 kcal · mol^{-1}, releasing 2 kcal · mol^{-1} in the process to form intermediate **IV**. Next, a second substrate molecule is engaged in an *intermolecular* proton transfer, restoring aromaticity to form **V** and releasing 28 kcal · mol^{-1} in the process. This last intermediate reacts with the protonated second substrate in the rate-limiting step to turn over the organoselenium species in exchange for a proton, forming product **1.136** and regenerating the catalytically active intermediate **I**. The barrier for this step is 25 kcal · mol^{-1}, while 3 kcal · mol^{-1} are released. This may also serve as an explanation for the empirical finding that some substrates require heating and additional reaction time to fully consume the starting materials and produce the product in sufficient amounts, such as the methyl ketone **1.174** and the fluorinated substrates leading to **1.177**, **1.178** and **1.179**. These substituents on the aromatic system stabilise negative charges on the phenolic oxygen (making the system less prone to protonation), thereby suppressing the turnover of new substrates in the last step of the catalytic cycle.

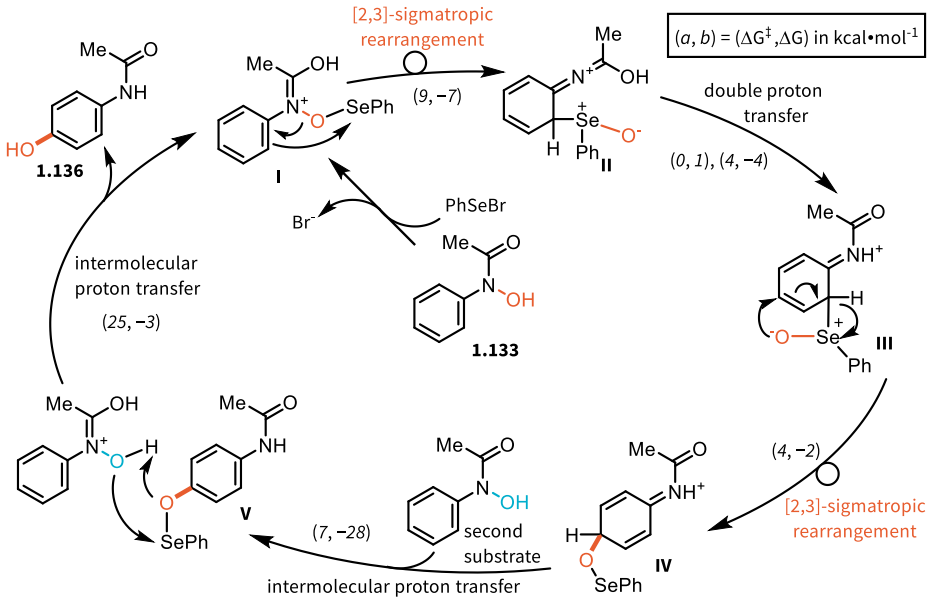

Scheme 1.29: Computed catalytic cycle for the double [2,3]-sigmatropic rearrangement at the PBE0-D3BJ-SMD(THF)/def2-TZVP//PBE0-D3BJ-SMD(THF)/def2-SVP level of theory. The activation energies ($\Delta G^{\ddagger}$) and Gibbs free energies (ΔG) are presented for each individual step in parentheses. Rearrangement reactions are highlighted in orange.

1.3.6. Introduction of a *para*-Substituent into the Hydroxamic Acid

Further experiments were conducted to investigate the potential of displacing substituents at the *para*-position in order to eventually form the *p*-aminophenol product (**1.136**). Moreover, these experiments aimed to determine whether, in cases where displacement was not achievable, an oxidised product such as **1.196** could be formed. To this end, two substrates were synthesised using the established method starting from the corresponding nitrophenols (Scheme 1.30).[86]

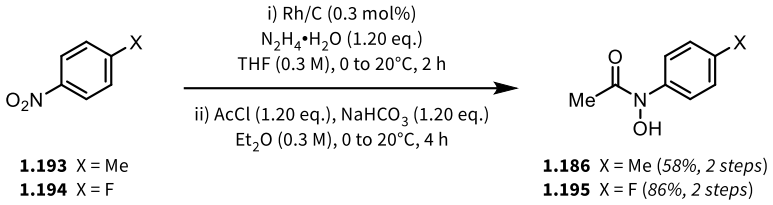

Scheme 1.30: Synthesis of *p*-substituted hydroxamic acids **1.186** (X = Me) and **1.195** (X = F) from the corresponding *p*-nitrophenyl starting materials.

Both thus generated starting materials were subjected to the rearrangement reaction conditions. Tolyl substrate **1.186** formed neither of the hypothetical products, but rather most of the material remained unconsumed, while 10% of the starting material was converted to *p*-Me-acetanilide **1.197** (Scheme 1.31).

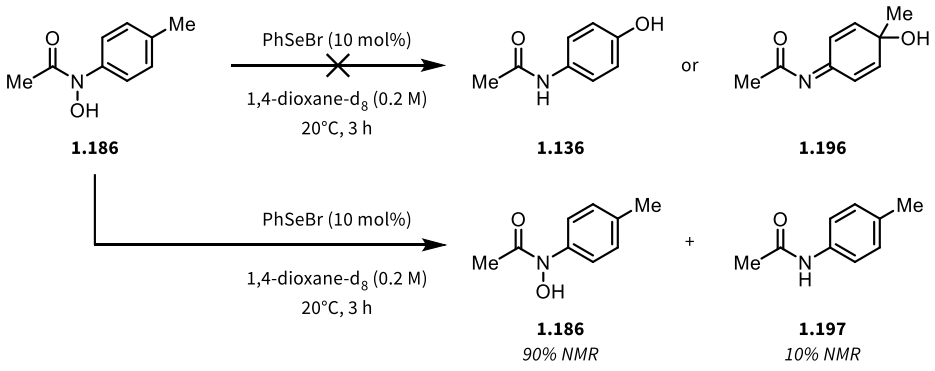

Scheme 1.31: Experimental results employing *p*-tolyl substrate **1.186** in the reaction, leading to recovery of starting material and partial loss of the hydroxy moiety, leading to **1.197**.

In contrast, the *p*-F-phenylhydroxamic acid **1.195** underwent a transformation when subjected to the reaction conditions. However, the results were challenging to interpret, leading to a decision not to pursue these investigations further. When **1.195** was subjected to the optimised reaction conditions, as

well as conducting the reaction at 100°C, a mixture of two products (**1.197** and **1.198**) and unreacted starting material was produced (Scheme 1.32).

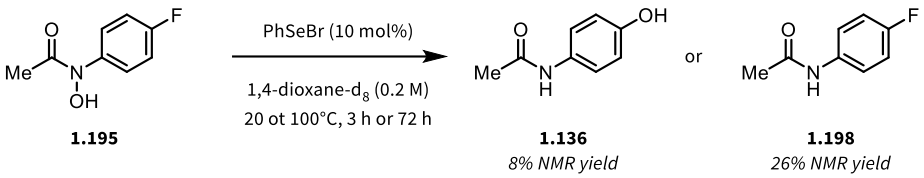

Scheme 1.32: Investigation of *p*-F substituted hydroxamic acid **1.195** at different temperatures. The reaction led to small amounts of the desired rearrangement product (**1.136**) but failed to convert all starting material. Deoxygenation of the hydroxamic acid leading to **1.198** was observed as a side reaction.

The experimental results were followed-up with an NMR investigation to find out why the product was only formed in amounts similar to the catalyst loading. To this end, the reaction was repeated inside an NMR tube and the reaction was monitored by ^{1}H-NMR, ^{19}F- NMR and ^{77}Se-NMR, employing a solvent system of 1,4-dioxane:TDF in a ratio of 10:1 (*vide supra*). This study revealed the formation of PhSeF as a by-product of the reaction, as detected by ^{19}F-NMR (470 MHz, 1,4-dioxane/THF-d_8, δ = −192 ppm; Literature: 376 MHz, MeCN-d_3, δ = −182 ppm).[97] Additionally, when running the reaction at room temperature over three days, an increase in NMR yield of **1.136** to 22% was observed, with the remaining 78% of material being converted to the deoxygenated product **1.198**.

1.3.7. Application of Phenylsulfenyl Bromide as a Reagent

With the clear and mostly complete mechanistic picture on the Se-catalysed double [2,3]-sigmatropic rearrangement in hand, the next task was found in the translation of the reaction to the use of other organochalcogen species, in order to probe whether they may be able to provide similar reactivity. While organotellurides are known to undergo [2,3]-sigmatropic rearrangements,[79] the equivalent PhTeBr was not investigated due to its instability.[98]

The use of phenylsulfenyl bromide in the reaction, freshly prepared from thiophenol and Br_2, provided another interesting result. It was found that the intermediate *o*-sulfoxide does not undergo the second rearrangement, delivering *o*-sulfoxoaniline **1.200** as product of the reaction (Scheme 1.33).[99] The sulfoxide product **1.200** was independently prepared through an alternative route to ensure correct assignment.

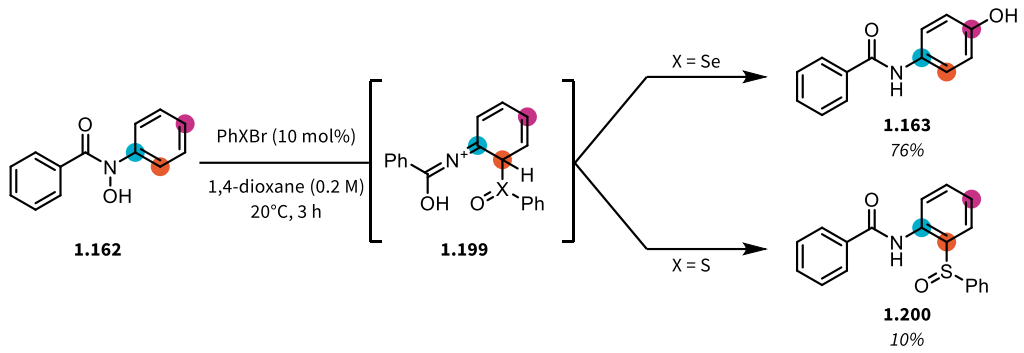

Scheme 1.33: Difference in reactivity between the catalytically active PhSeBr leading to *p*-aminophenol **1.163** and the stoichiometric reagent PhSBr leading to *o*-sulfoxide **1.200**.

With this experimental result, computational investigation of the reaction was commenced. On a surface level, this is well understood, since the C–Se bond is weaker than the C–S bond, enabling the second [2,3]-sigmatropic rearrangement.[56,100,101] It was found that the intermediate **II**/**IIb** is formed through a process with a lower barrier and a lower overall energy in the case of X = S ($\Delta G^{\ddagger}$ = 3.6 kcal·mol^{-1}, ΔG = −15.2 kcal·mol^{-1}, blue pathway to **IIb**), compared to X = Se ($\Delta G^{\ddagger}$ = 8.7 kcal·mol^{-1}, ΔG = -7.1 kcal·mol^{-1}, black pathway to **II**) (Scheme 1.34). However, the proton transfer to arrive at **III**/**IIIb**, a two-step process in the case of PhSeBr, is highly disfavoured in the case of PhSBr, with a barrier of 29.9 kcal·mol^{-1} which is

not readily overcome at room temperature. Intermediate **IIb** is therefore consumed through an alternative pathway, where a second substrate molecule (**1.133**) is recruited to abstract the *o*-proton in order to restore aromaticity to intermediate **VI**, which then tautomerises to the *o*-sulfoxide product **1.200**.

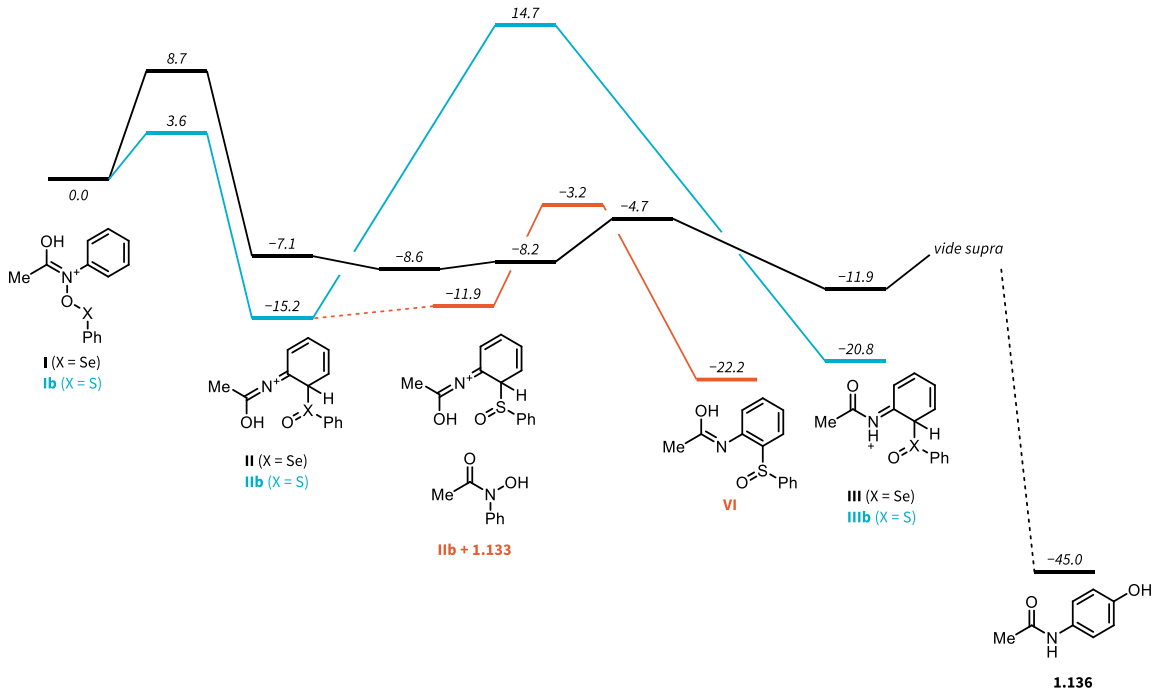

Scheme 1.34: Simplified overview on the computed pathway to *p*-aminophenol *via* Se-catalysis (black), the hypothetical pathway to *p*-aminophenol *via* S-catalysis (blue) and the computed pathway to the *o*-sulfoxide (red). All energies are given in kcal · mol^{-1} at the PBE0-D3/def2-TZVP,SMD(THF)//PBE0-D3/def2-SVP,SMD(THF) level of theory. Comparable intermediates and transition state energies are aligned vertically for the black and blue pathway. Dashed lines indicate a change in the system by introduction or removal of reaction partners.

1.3.8. Translation to Hydroxamic Acid Esters and Hydrazides

As part of the investigation into the double [2,3]-sigmatropic rearrangement of hydroxamic acids, hydroxamic acid methyl esters and hydrazides were tested as potential substrates of the reaction and the results are summarised in Table 1.3. Neither hydroxamic acid methyl ester (X = OMe) nor the hydrazides (X = NH_2 or NHBoc) underwent the desired reaction under any of the tested reaction conditions and no conversion of starting material was observed. The lack of reactivity of the hydroxamic acid methyl ester is readily explained by the necessity of the starting material to bind to the PhSeBr catalyst, which is not possible in the case of the methyl ester.

In the case of the hydrazides, the inability for the starting material to be converted to the desired product could potentially come down to the lower azaphilicity of selenium compared to its high oxophilicity (as estimated from BDE (Se–N) = 370 ± 11 kcal · mol^{-1}; BDE (Se–O) = 465 ± 21 kcal · mol^{-1}),[102] as well as the missing polarisation of the N–N bond in the hydrazides compared to the polarised N–O bond of the hydroxamic acids.

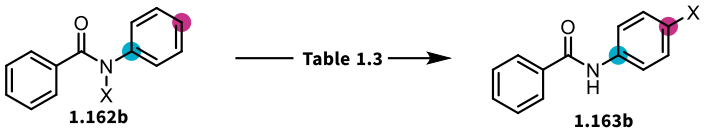

1.162b 1.163b

Table 1.3

Entry	X	Reagent	Solvent	Temperature (°C)	Time	Conversion
1	OMe	PhSeBr (10 mol%)	1,4-dioxane	20°C	3 h	0%
2	OMe	PhSeBr (10 mol%)	1,4-dioxane	100°C	3 h	0%
3	OMe	PhSeBr (1.00 eq.)	1,4-dioxane	20°C	3 h	0%
4	OMe	PhSeBr (10 mol%), HBr (48% in H_2O) (1.00 eq.)	1,4-dioxane	20°C	3 h	0%
5	OMe	PhSeCl (10 mol%), HCl (2 M in Et_2O) (1.00 eq.)	1,4-dioxane	20°C	3 h	0%
6	OMe	PhSeBr (10 mol%)	HFIP	20°C	3 h	0%
7	NH_2	PhSeBr (10 mol%)	1,4-dioxane	20°C	24 h	0%
8	NHBoc	PhSeBr (10 mol%)	1,4-dioxane	20°C	24 h	0%

Table 1.3: Studies towards the conversion of hydroxamic acid esters and hydrazides *via* organoselenium-catalysis to yield products of double [2,3]-sigmatropic rearrangement.

1.4. Conclusions & Outlook

In summary, an organoselenium-catalysed, regioselective double [2,3]-sigmatropic rearrangement reaction of *N*-arylhydroxamic acids for the synthesis of *p*-aminophenols was developed. The reaction was optimised and, ultimately, a 10 mol% loading of PhSeBr and 1,4-dioxane as the solvent proved to be the best conditions. Using a system capable of being heated to high temperatures enabled flexibility towards converting substrates which are less prone to undergo the desired reaction. Several substrates were subjected to the optimised reaction conditions to afford the desired *p*-aminophenols as single regioisomers, leading to a scope of 22 successful examples. The method was additionally applied to the synthesis of pharmaceutically relevant *p*-aminophenols, such as paracetamol (**1.136**), practolol (**1.188**) and diloxanide furoate (**1.191**) on gram-scale without a decrease in yield. The mechanism was supported by ^{18}O-labeling experiments as well as computational methods, supporting an *intramolecular* reaction pathway. Generally, the reaction is robust against the presence of air and water, as the reaction can be set up under ambient atmosphere with no decrease in yield and the presence of water was also found not to have any deleterious effect.

The translation of the selenium-catalysed process to one catalysed by sulfur failed, as the reaction halted after the first [2,3]-sigmatropic rearrangement, leading to *o*-substituted diaryl sulfoxides as the sole products, consuming the catalyst in the process. Extending the scope of the reaction to hydroxamic acid esters or hydrazides was similarly unsuccessful. In the case of the former, replacing the nucleophilic hydroxyl moiety with a methoxy group, void of nucleophilic character, led to unreactive starting materials. In the case of the latter, the lack of polarisation in the N–N bond paired with the decreased azaphilicity of selenium compared to its oxophilicity renders these hydrazides unreactive.

Going forward, the investigation on hydrazides could be intensified, as the *p*-aminoaniline products are of high value for material science. An approach trying to force the double [2,3]-sigmatropic rearrangement of hydrazides in a similar fashion would have to rely on a more azaphilic mediator of the reaction and the polarisation of the N–N bond would need to be increased to ease heterolytic cleavage,

initiating the rearrangement cascade. In the realm of organoselenium compounds, this transformation could potentially occur using high-valent selenium species, such as **1.207**. A related activation process, forming a hypervalent selenium species (**1.204**) has been developed by Michael *et al.* for allylic C–H amination (Scheme 1.35).[103]

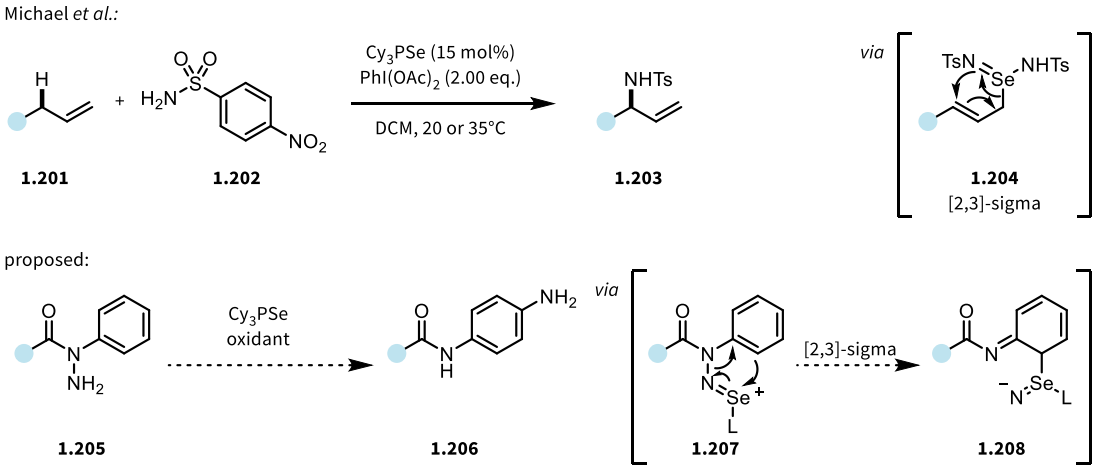

Scheme 1.35: Proposed extension of the work outlined in this chapter on the regioselective double [2,3]-sigmatropic rearrangement towards the utilisation of hydrazides with a hypervalent selenium species, with precedent from Michael *et al.*[103]

1.5. Experimental Procedures and Data

1.5.1. General Information

Unless otherwise stated, all solvents were distilled from appropriate drying agents prior to use or, if purchased in anhydrous form, used as received. Unless otherwise stated, all glassware was flame-dried under low pressure prior to use and all reactions were performed under a positive pressure of Argon. All reagents were used as received from commercial suppliers unless otherwise stated. Reaction progress was monitored by thin layer chromatography (TLC) performed on aluminium plates coated with silica gel F254 with 0.2 mm thickness. Chromatograms were visualised by fluorescence quenching with UV light at 254 nm or by staining using potassium permanganate. Flash column chromatography was performed using silica gel 60 (230-400 mesh, Merck and co.) or prepacked columns (Chromabond silica) using a Biotage Selekt Flash Purification System. Neat infrared spectra were recorded using a Perkin-Elmer Spectrum 100 FT-IR spectrometer. Wavenumbers (ν_{max}) are reported in cm^{-1}. Mass spectra were obtained using a Finnigan MAT 8200 or (70 eV) or an Agilent 5973 (70 eV) spectrometer, using electrospray ionisation (ESI). All ^{1}H-NMR. ^{13}C-NMR, ^{19}F-NMR and ^{77}Se-NMR spectra were recorded using Bruker AV-400, AV-600 or AV-700 spectrometers at 300K. Chemical shifts are given in parts per million (ppm, δ), referenced to the solvent peak of $CDCl_3$, defined at δ = 7.26 ppm (^{1}H-NMR) and δ = 77.16 ppm (^{13}C-NMR), MeOH-d_4, defined at δ = 3.31 ppm (^{1}H-NMR) and δ = 49.00 ppm (^{13}C-NMR), DMSO-d_6, defined at δ = 2.50 (^{1}H-NMR) and δ = 39.52 ppm (^{13}C-NMR), and THF-d_8, defined at δ = 3.62 and 1.79 (^{1}H-NMR) and δ = 68.03 and 26.19 ppm (^{13}C-NMR). Coupling constants are quoted in Hz (*J*). ^{1}H, ^{13}C and ^{19}F NMR splitting patterns are designated as singlet (s), doublet (d), triplet (t), quartet (q) as they appeared in the spectrum. If the appearance of a signal differs from the expected splitting pattern, the observed pattern is designated as apparent (app). Splitting patterns that could not be interpreted or easily visualised are designated as multiplet (m) or broad (br). Room temperature refers to 20°C.

1.5.2. General Procedures

1.5.2.1. Synthesis of Hydroxamic Acids

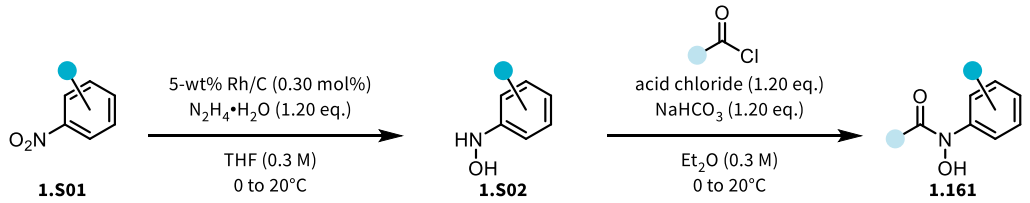

To a solution of nitrobenzene **1.S01** (1.00 eq.) in THF (0.3 M) at 0°C was added 5-wt% Rh/C (0.30 mol% Rh, 0.003 eq.) and hydrazine monohydrate (1.20 eq.). The reaction was allowed to warm to room temperature and stirred until the starting material had been consumed (indicated by TLC analysis, typically < 3 h). The reaction mixture was passed through a short pad of *Celite*®, the filter cake was washed with EtOAc and the solvents were evaporated under reduced pressure to afford the crude hydroxylamine **1.S02**. The crude material was used in the acylation step without further purification.

To a solution of crude hydroxylamine **1.S02** (1.00 eq.) in Et_2O (0.3 M) at 0°C was added $NaHCO_3$ (1.20 eq.) and the corresponding acyl chloride (1.20 eq.). The reaction mixture was allowed to warm to room temperature and stirred until all starting material had been consumed (indicated by TLC analysis, typically between 2 – 12 h). The reaction mixture was passed through a paper filter, which was washed with EtOAc, and the solvents were evaporated under reduced pressure to afford crude hydroxamic acid **1.161**. The crude product was purified by flash column chromatography (SiO_2, heptane/EtOAc) in order to isolate the pure hydroxamic acid **1.161**.

1.5.2.2. Se-catalysed Sigmatropic Rearrangement to *para*-Aminophenols

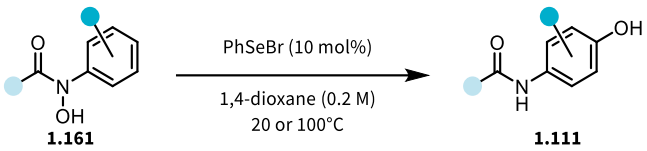

To a solution of arylhydroxamic acid **1.161** (1.00 eq.) in 1,4-dioxane (0.2 M) at room temperature was added PhSeBr (10.0 mol%). The resulting reaction mixture was subsequently stirred at room temperature or at 100°C until all starting material had been consumed (indicated by TLC analysis, typically 3 – 24 h). Afterwards, the solvents were evaporated under reduced pressure and the crude material was purified by flash column chromatography (SiO_2, heptane/EtOAc) to afford the pure *para*-aminophenol **1.111**.

1.5.3. Synthesis and Characterisation of Hydroxamic Acids

Analytical data of hydroxamic acids **1.114sm**,[104] **1.133**,[104] **1.172sm**,[104] **1.173sm**,[104] **1.168sm**,[105] **1.160sm**,[105] **1.115sm**,[106] **1.175sm**,[107] **1.176sm**,[108] **1.178sm**,[86] **1.180sm**,[86] **1.179sm**,[109] **1.182sm**,[109] **1.181sm**[110] were in accordance with the literature.

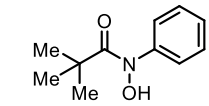
1.114sm

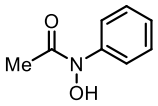
1.133

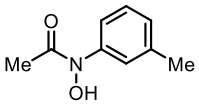
1.172sm

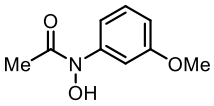
1.173sm

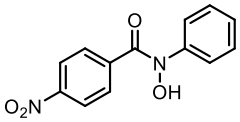
1.168sm

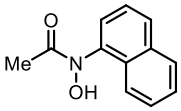
1.115sm

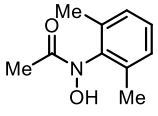
1.175sm

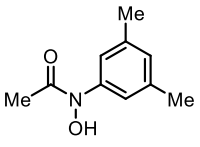
1.176sm

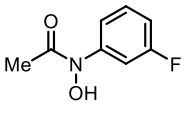
1.178sm

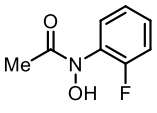
1.179sm

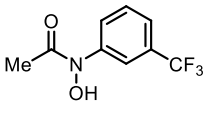
1.180sm

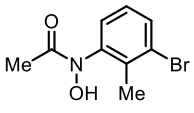
1.181sm

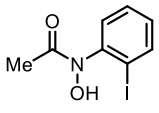
1.182sm

1.5.3.1. 2-((3r,5r,7r)-adamantan-1-yl)-*N*-hydroxy-*N*-phenylacetamide (1.166sm)

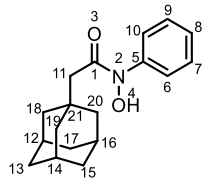

1.166sm

Chemical Formula: $C_{18}H_{23}NO_2$

To a solution of phenylhydroxylamine (200 mg, 1.87 mmol, 1.00 eq.) and 1-adamantaneacetic acid (371 mg, 2.06 mmol, 1.10 eq.) in DCM (0.35 M) at 0°C was added EDCI·HCl (394 mg, 2.06 mmol, 1.10 eq.). The resulting reaction mixture was subsequently allowed to warm to room temperature and was stirred for 12 h. After the starting materials had been consumed, the reaction was diluted with H_2O (5.00 mL) and the layers were separated. The aqueous layer was extracted with DCM (3 x 5.00 mL) and the combined organic layers were dried over anhydrous $MgSO_4$. The solvents were removed *in vacuo* and the crude material was purified by flash column chromatography (SiO_2, heptane/EtOAc) to afford 2-((3r,5r,7r)-adamantan-1-yl)-*N*-hydroxy-*N*-phenylacetamide **1.166sm** (201 mg, 0.710 mmol, 38%) of as an amorphous solid.

^{1}H-NMR (600 MHz, $CDCl_3$): δ 7.26-7.42 (m, 5H, **$H_{6\text{-}10}$**), 2.10 (s, 2H, **H_{11}**) 1.57-1.97 (m, 16H, **$H_{12\text{-}20}$**) ppm.

^{13}C-NMR (125 MHz, $CDCl_3$): δ 177.3 (**C_1**), 129.4 (**C_5**), 125.6 (3C, **$C_{6,8,10}$**), 122.5 (2C, **$C_{7,9}$**), 48.9 (**C_{21}**), 42.6 (**C_{11}**), 36.8 (3C, **$C_{18,19,20}$**), 28.71 (3C, **$C_{12,14,16}$**), 28.69 (3C, **$C_{13,15,17}$**) ppm.

HRMS (ESI^+): exact mass calculated for $[M+H]^+$ ($C_{18}H_{24}NO_2^+$) required *m/z* 286.1802; found *m/z* 286.1802.

FT-IR (neat) ν_{max}: 3100, 2900, 1590, 1250, 1021, 795 cm^{-1}.

1.5.3.2. *N*-hydroxy-*N*-phenylcyclobutanecarboxamide (1.167sm)

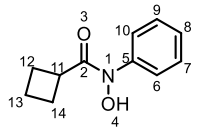

1.167sm
Chemical Formula: $C_{11}H_{13}NO_2$

To a solution of phenylhydroxylamine (218 mg, 2.00 mmol, 1.00 eq.) and cyclobutanecarboxylic acid (220 mg, 2.20 mmol, 1.10 eq.) in DCM (0.35 M) at 0°C was added EDCI·HCl (422 mg, 2.20 mmol, 1.10 eq.). The reaction mixture was subsequently allowed to warm to room temperature and was stirred for 12 h or until all starting material had been consumed. Afterwards, H_2O (5.00 mL) was added and the layers were separated. The aqueous layer was extracted with DCM (3 x 5.00 mL) and the combined organic layers were dried over anhydrous $MgSO_4$. The solvents were removed *in vacuo* and the crude material was purified by column chromatography (SiO_2, heptane/EtOAC) to afford *N*-hydroxy-*N*-phenylcyclobutanecarboxamide **1.167sm** (145 mg, 0.710 mmol, 38%) as a pale yellow oil.

^{1}H-NMR (600 MHz, $CDCl_3$): δ 10.34 (s, 1H, **H_4**), 7.63-7.60 (br. s, 2H, **$H_{6,10}$**), 7.36 (t, *J* = 7.9 Hz, 2H, **$H_{7,9}$**), 7.14 (br. s, 1H, **H_8**), 3.63 (br. s, 1H, **H_{11}**), 2.26-2.20 (m, 2H, **$H_{12,14}$**), 2.15-2.05 (br. s, 2H, **$H_{12,14}$**), 1.95-1.90 (m, 1H, **H_{13}**), 1.80-1.77 (m, 1H, **H_{13}**) ppm.

^{13}C-NMR (125 MHz, $CDCl_3$): δ 173.5 (minor rotamer, **C_2**), 172.9 (major rotamer, **C_2**), 142.0 (**C_x**), 128.4 (3C, **C_{7-9}**), 124.4 (**C_6**), 119.8 (**C_{10}**), 37.6 (**C_{11}**), 24.6 (2C, **$C_{12,14}$**), 17.6 (**C_{13}**) ppm.

HRMS (ESI^+): exact mass calculated for $[M+H]^+$ ($C_{11}H_{14}NO_2^+$) required *m/z* 192.1019; found *m/z* 192.1012.

FT-IR (neat) ν_{max}: 3190, 2984, 1627, 1444, 1392, 1209, 756, 692 cm^{-1}.

1.5.3.3. *N*-hydroxy-*N*-phenyl-4-vinylbenzamide (1.171sm)

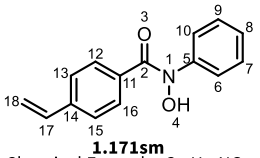

1.171sm
Chemical Formula: $C_{15}H_{13}NO_2$

Following the general procedure for the synthesis of hydroxamic acids (chapter 1.5.2.1.) starting with phenylhydroxylamine (164 mg, 1.50 mmol, 1.00 eq.), 4-vinylbenzoyl chloride (300 mg, 1.80 mmol, 1.20 eq.) and $NaHCO_3$ (151 mg, 1.80 mmol, 1.20 eq.). The reaction mixture was stirred at room temperature for 18 h to yield *N*-hydroxy-*N*-phenyl-4-vinylbenzamide **1.171sm** (137 mg, 0.570 mmol, 38%) as an off-white solid.

^{1}H-NMR (400 MHz, $CDCl_3$): δ 10.7 (s, 1H,), 7.62 (d, *J* = 8.2 Hz, 2H,), 7.53 (dd, *J* = 13.3, 8.1 Hz, 4H,), 7.39 (t, *J* = 7.9 Hz, 2H,), 7.20 (t, *J* = 7.4 Hz, 1H,), 6.77 (dd, *J* = 17.7, 11.0 Hz, 1H,), 5.93 (d, *J* = 17.7 Hz, 1H,), 5.36 (d, *J* = 11.0 Hz, 1H,) ppm.

^{13}C-NMR (100 MHz, $CDCl_3$): δ 167.5 (**C_2**), 138.9 (**C_{11}**), 136.0 (**C_{17}**), 134.7 (**C_5**), 129.7 (**C_{14}**), 128.9 (2C, **$C_{13,15}$**), 128.5 (2C, **$C_{12,16}$**), 126.2 (2C, **$C_{6,10}$**), 125.5 (2C, **$C_{7,9}$**), 122.2 (**C_8**), 116.0 (**C_{18}**) ppm.

HRMS (ESI^+): exact mass calculated for $[M+Na]^+$ ($C_{15}H_{13}NO_2Na^+$) required *m/z* 262.0838; found *m/z* 262.0844.

FT-IR (neat) ν_{max}: 3181, 1677, 1617, 1433, 1404, 1385, 991, 752 cm^{-1}.

1.5.3.4. *N*-(3-acetylphenyl)-*N*-hydroxyacetamide (1.174sm)

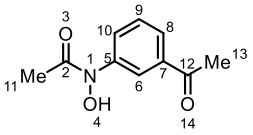

1.174sm
Chemical Formula: $C_{10}H_{11}NO_3$

Following the general procedure for the synthesis of hydroxamic acids (chapter 1.5.2.1.) starting with 3-acetyl phenylhydroxylamine (203 mg, 2.00 mmol, 1.00 eq.), acetyl chloride (0.171 mL, 2.40 mmol, 1.20 eq.) and $NaHCO_3$ (202 mg, 2.40 mmol, 1.20 eq.). The reaction mixture was stirred at room

temperature for 18 h to yield *N*-(3-acetylphenyl)-*N*-hydroxyacetamide**1.174sm** (226 mg, 1.16 mmol, 58%) as a yellow oil.

^{1}H-NMR (600 MHz, DMSO-d_6): δ 10.78 (s, 1H, **H_4**), 8.19 (s, 1H, **H_6**), 7.90 (dd, *J* = 8.1, 1.3 Hz, 1H, **H_8**), 7.75 (d, *J* = 7.7 Hz, 1H, **H_{10}**), 7.52 (t, *J* = 7.9 Hz, 1H, **H_9**), 2.58 (s, 3H, **H_{13}**), 2.24 (s, 3H, **H_{11}**) ppm.

^{13}C-NMR (150 MHz, DMSO-d_6): δ 197.6 (**C_{12}**), 170.3 (**C_2**), 142.0 (**C_5**), 137.0 (**C_7**), 128.9 (2C, **$C_{6,8}$**), 124.5 (**C_9**), 118.9 (**C_{10}**), 26.8 (**C_{13}**), 22.5 (**C_{11}**) ppm.

HRMS (ESI$^+$): exact mass calculated for $[M+H]^+$ ($C_{10}H_{12}NO_3^+$) required *m/z* 194.0812; found *m/z* 194.0812.

FT-IR (neat) ν_{max}: 3171, 2917, 1682, 1372, 1105, 959, 686 cm^{-1}.

1.5.3.5. *N*-(3-fluoro-5-iodophenyl)-*N*-hydroxyacetamide (1.177sm)

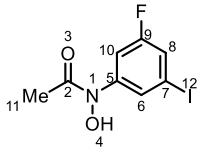

1.177sm
Chemical Formula: $C_8H_7FINO_2$

Following the general procedure for the synthesis of hydroxamic acids (chapter 1.5.2.1.) starting with 3-fluoro-5-iodo phenylhydroxylamine (506 mg, 2.00 mmol, 1.00 eq.), acetyl chloride (0.171 mL, 2.40 mmol, 1.20 eq.) and $NaHCO_3$ (202 mg, 2.40 mmol, 1.20 eq.). The reaction mixture was stirred at room temperature for 18 h to yield *N*-(3-acetylphenyl)-*N*-hydroxyacetamide **1.177sm** (517 mg, 1,74 mmol, 87%) as a yellow solid.

^{1}H-NMR (600 MHz, DMSO-d_6): δ 10.88 (s, 1H, **H_4**), 7.92 (br. s, 1H, **H_6**), 7.54 (dt, *J* = 11.6, 2.2 Hz, 1H, **H_{10}**), 7.40 (ddd, *J* = 7.8, 2.3, 1.4 Hz, 1H, **H_8**), 2.23 (s, 3H, **H_{11}**) ppm.

^{13}C-NMR (150 MHz, DMSO-d_6): δ 170.9 (**C_2**), 161.5 (d, J_{CF} = 246.7 Hz, **C_9**), 143.8 (d, J_{CF} = 11.0 Hz, **C_5**), 123.2 (**C_6**), 119.4 (d, J_{CF} = 23.7 Hz, **C_{10}**), 105.6 (d, J_{CF} = 27.3 Hz, **C_8**), 94.1 (d, J_{CF} = 9.4 Hz, **C_7**), 22.8 (**C_{11}**) ppm.

^{19}FNMR (565 MHz, DMSO-d_6): δ −110.59 (dd, *J* = 11.6, 7.8 Hz).

HRMS (ESI$^+$): exact mass calculated for $[M+H]^+$ ($C_8H_8FINO_2^+$) required *m/z* 295.9578; found *m/z* 295.9569.

FT-IR (neat) ν_{max}: 3161, 2917, 1627, 1424, 1367, 1110, 751, 671 cm^{-1}.

1.5.4. Syntheses of other Starting Materials

1.5.4.1. Synthesis of ^{18}O-Hydroxamic Acid 1.133*

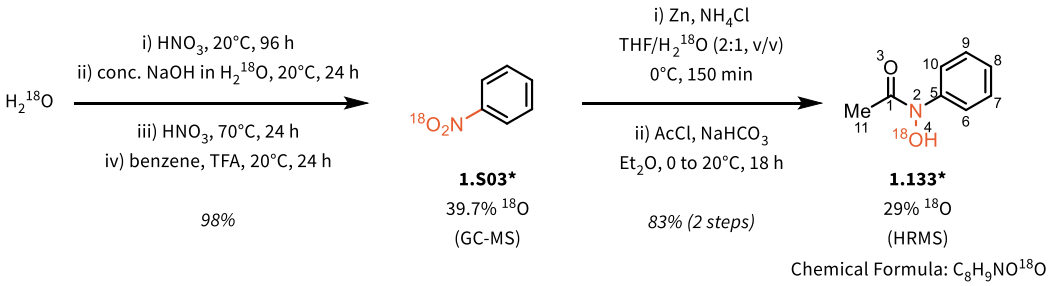

To a 10 mL round-bottom flask equipped with a Teflon-coated magnetic stir bar was added ^{18}O-H_2O (0.300 mL, 15.0 mmol, 9.74 eq.), followed by fuming nitric acid (0.101 mL, 2.40 mmol, 1.56 eq.). The flask was tightly sealed and stirred at room temperature for 4 d. After this reaction time, a solution of NaOH (382 mg, 8.20 mmol, 5.30 eq.) in ^{18}O-H_2O (0.344 mL; c = 24 M) was carefully added and the resulting suspension was stirred for 24 h at room temperature. The ^{18}O-H_2O was distilled off and, following full evaporation, fuming nitric acid (0.016 mL, 0.380 mmol, 0.590 eq.) was once again added. The flask was again tightly sealed and the reaction mixture was heated at 70°C for 24 h while being continuously stirred. Subsequently, the pH of the reaction mixture was controlled to find pH > 7 (required) and the remaining liquids were distilled off to yield crude $NaN^{18}O_3$, which was used in the next step without further purification.

Crude $NaN^{18}O_3$ (8.20 mmol, 5.30 eq.) was dissolved in TFA (7.65 mL, 103 mmol, 66.9 eq.) and benzene (0.14 mL, 1.54 mmol, 1.00 eq.) was added (*Nota bene: the use of HPLC-grade TFA from sealed glass ampoules is recommended, as atmospheric H_2O contaminations in opened bottles of TFA lead to a decrease in ^{18}O-content*). The resulting reaction mixture was stirred at 20°C for 24 h before being quenched by addition of a saturated aqueous solution of NaOH in ^{18}O-H_2O until pH > 10 was reached. The mixture was subsequently extracted with Et_2O (3x10.0 mL) and the combined organic layers were dried over Na_2SO_4. The solvents were removed *in vacuo* to yield ^{18}O-nitrobenzene **1.S03*** (185 mg, 1.50 mmol, 98%; ^{18}O-content = 39.7% by GC-MS) as a yellow oil which was used without further purification.[87]

To a solution of ^{18}O-nitrobenzene (86.2 mg, 0.700 mmol, 1.00 eq.) in THF/^{18}O-H_2O (2.30 mL, 2:1 (v/v), 0.3 M) was added NH_4Cl (150 mg, 2.80 mmol, 4.00 eq.). The resulting mixture was cooled to 0°C before Zn^0

powder (183 mg, 2.80 mmol, 4.00 eq.) was carefully added. The reaction slurry was stirred at 0°C for 150 min before being filtered through a short pad of Celite®, which was washed with EtOAc. The solvents were removed from the filtrate *in vacuo* to yield the crude ^{18}O-phenylhydroxylamine, which was used in the next step without further purification.

To a solution of crude ^{18}O-phenylhydroxylamine (76.4 mg, 0.700 mmol, 1.00 eq.) in Et_2O (0.2 M) at 0°C was added $NaHCO_3$ (70.6 mg, 0.840 mmol, 1.20 eq.). Afterwards, AcCl (59.7 µL, 0.840 mmol, 1.20 eq.) was added dropwise at 0°C and the resulting mixture was allowed to warm to room temperature with stirring over the course of 18 h. After all starting material had been consumed (as indicated by TLC analysis), the solids were removed by filtration through a cotton plug, which was subsequently washed with DCM. The filtrate was concentrated *in vacuo* and the resulting crude material was purified by flash column chromatography (SiO_2, heptane/EtOAc) to afford ^{18}O-labeled hydroxamic acid **1.133*** (83.0 mg, 0.550 mmol, 78%) as a dark orange oil with an ^{18}O-content of 29% (calculated from HRMS [M+H$^+$]) with methylanilidine as an inseparable impurity.

^{1}H-NMR (400 MHz, DMSO-d_6): δ 10.61 (br. s, 1H, **H_4**), 7.62 (d, *J* = 7.8 Hz, 2H, **$H_{6,10}$**), 7.36 (t, *J* = 7.9 Hz, 2H, **$H_{7,9}$**), 7.14 (t, *J* = 7.1 Hz, 1H **H_8**), 2.20 (s, 3H, **H_{11}**) ppm.

^{13}C-NMR (100 MHz, DMSO-d_6): δ 168.3 (**C_1**), 141.7 (**C_5**), 128.4 (**$C_{7,9}$**, 2C), 124.6 (**C_8**), 119.0 (**$C_{6,10}$**, 2C), 22.5 (**C_{11}**) ppm.

HRMS (ESI$^+$): exact mass calculated for [M+H]$^+$ ($C_8H_{10}NO^{18}O^+$) required *m/z* 154.0749; found *m/z* 154.0746.

FT-IR (neat) ν_{max}: 2918, 1643, 1595, 1547, 1308, 1100, 1033, 906, 691 cm^{-1}.

1.5.4.2. Synthesis of Hydroxamic acid ester 1.S04

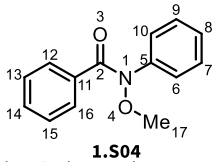

1.S04
Chemical Formula: $C_{14}H_{13}NO_2$

To a solution of *N*-phenylbenzhydroxamic acid (**1.162**) (2.18 g, 1.00 mmol, 1.00 eq.) in DMF (0.5 M) at 20°C was added K_2CO_3 (1.66 g, 1.20 mmol, 1.20 eq.), followed by the dropwise addition of MeI (0.755 mL,

1.20 mmol, 1.20 eq.). The resulting reaction mixture was stirred at 20°C for 20 h or until full conversion was observed (as indicated by TLC analysis). Afterwards, the reaction mixture was diluted with H_2O and EtOAc (equal volume to DMF) and the layers were separated. The aqueous layer was extracted with EtOAc (3 x 20.0 mL) and heptane (3 x 20.0 mL). The combined organic layers were washed with brine (1 x 5.00mL), dried over Na_2SO_4, the solids were filtered off and the solvents were removed *in vacuo* to yield the crude hydroxamic acid ester. The crude product was purified by flash column chromatography (SiO_2, hepantes/EtOAc) to afford the pure *O*-methyl-*N*-phenylbenzhydroxamic acid ester **1.S04** (2.26 g, 9.96 mmol, 99.6%) as a colourless solid.

All spectroscopic data are in accordance with the reported literature.[88]

1.5.4.3. Synthesis of 1-Boc-2-acetyl-2-phenylhydrazide (1.S05)

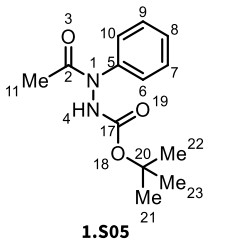

1.S05

Chemical Formula: $C_{13}H_{18}N_2O_3$

To phenylhydrazine (0.985 mL, 10.0 mmol, 1.00 eq.) at 0°C, neat Boc_2O (2.23 g, 10.2 mmol, 1.02 eq.) was carefully added (*lively gas evolution*). The yellow reaction mixture was stirred for 1 h until a white precipitate formed. The reaction mixture was diluted by addition of DCM (10.0 mL) and water (10.0 mL). The layers were separated and the organic layer was washed with brine (1 x 10.0 mL). The organic layer was dried over Na_2SO_4, the solids were filtered off and the solvents were evaporated to afford 1-Boc-2-phenylhydrazine as a white solid which was used without further purification in the next step.

To a solution of 1-Boc-2-phenylhydrazine (2.08 g, 10.0 mmol, 1.00 eq.) in DCM (0.1 M) at room temperature was added $NaHCO_3$ (5.04 g, 60.0 mmol, 6.00 eq.), followed by dropwise addition of acetyl chloride (2.13 mL, 30.0 mmol, 3.00 eq.). The resulting mixture was stirred for 1 h or until all starting material had been consumed (as indicated by TLC analysis). Afterwards, the reaction was diluted with DCM (100 mL) and water (100 mL). The layers were separated and the organic layer was washed with brine (40.0 mL).

The organic layer was dried over Na_2SO_4, the solids were filtered off and the solvents were removed *in vacuo* to afford the product 1-Boc-2-acetyl-2-phenylhydrazide **1.S05** (2.17 g, 8.68 mmol, 87%) as a white solid in pure form.

All spectroscopic data are in accordance with the reported literature.[111]

^{1}H-NMR (600 MHz, DMSO-d_6): δ 7.36 (br. s, 5H, $\mathbf{H_{6\text{-}10}}$), 7.19 (br. s, $\mathbf{H_{NH4}}$), 2.13-2.08 (m, 3H, $\mathbf{H_{11}}$), 1.43 (s, 9H, $\mathbf{H_{21\text{-}23}}$) ppm.

^{13}C-NMR (150 MHz, DMSO-d_6): δ 171.7 ($\mathbf{C_{17}}$), 154.6 ($\mathbf{C_2}$), 141.7 ($\mathbf{C_5}$), 128.5 (2C, $\mathbf{C_{6,10}}$), 125.7 ($\mathbf{C_7}$), 123.8 ($\mathbf{C_8}$), 123.3 ($\mathbf{C_9}$), 80.6 ($\mathbf{C_{20}}$), 28.0 (3C, $\mathbf{C_{21\text{-}23}}$), 21.7 ($\mathbf{C_{11}}$) ppm.

HRMS (ESI^+): exact mass calculated for $[M+Na]^+$ ($C_{13}H_{18}N_2O_3Na^+$) required *m/z* 273.1215; found *m/z* 273.1209.

1.5.4.4. Synthesis of *N*-phenylacetohydrazide (1.S06)

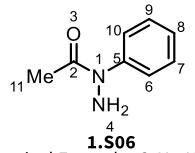

1.S06

Chemical Formula: $C_8H_{10}N_2O$

To a solution of 1-Boc-2-acetyl-2-phenylhydrazide (50.1 mg, 0.200 mmol, 1.00 eq.) in DCM (0.05 M) at 0°C was added TFA (0.297 mL, 4.00 mmol, 20.0 eq). After the reaction was stirred for 30 minutes at 0°C, the temperature was increased to 4°C and stirring at the indicated temperature was continued for 18 h. The reaction mixture was then poured into an ice-cold saturated aqueous solution of $NaHCO_3$ (4.00 mL) and the resulting mixture was stirred for five minutes. The pH was adjusted to >9 by addition of an aqueous solution of NaOH. The aqueous layer was extracted with DCM (3 x 5.00 mL) and the combined organic layers were washed with brine (1 x 5.00 mL). The organic layers were dried over Na_2SO_4, the solids were filtered off and the solvents were evaporated to afford the crude product, which was subsequently purified by flash column chromatography (SiO_2, DCM/MeOH) to afford *N*-phenylacetohydrazide **1.S06** (21.7 mg, 0.144 mmol, 72%) as a viscous brown oil.

All spectroscopic data are in accordance with the reported literature.[111]

1.5.5. Synthesis and Characterisation of *para*-Aminophenols

1.5.5.1. *N*-(4-hydroxyphenyl)benzamide (1.163)

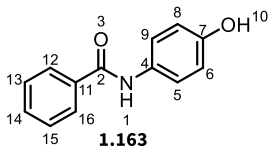

1.163

Chemical Formula: $C_{13}H_{11}NO_2$

Synthesised according to the general procedure described in chapter 1.5.2.2 starting from *N*-phenyl-benzhydroxamic acid **1.162** (50.0 mg, 0.230 mmol, 1.00 eq.) at 20°C for 3 h to afford *N*-(4-hydroxyphenyl)benzamide **1.163** (37.0 mg, 0.175 mmol, 76%) as a white solid.

^{1}H-NMR (600 MHz, DMSO-d_6): δ 10.01 (br. s, 1H, $\mathbf{H_{10}}$), 9.26 (br. s, 1H, $\mathbf{H_1}$), 7.92 (d, *J* = 7.8 Hz, 2H, $\mathbf{H_{6,8}}$), 7.57-7.49 (m, 5H, $\mathbf{H_{12\text{-}16}}$), 6.73 (d, *J* = 8.7 Hz, 2H, $\mathbf{H_{5,9}}$) ppm.

^{13}C-NMR (150 MHz, DMSO-d_6): δ 165.0 ($\mathbf{C_2}$), 153.7 ($\mathbf{C_7}$), 135.2 ($\mathbf{C_{11}}$), 131.3 ($\mathbf{C_4}$), 130.7 ($\mathbf{C_{14}}$), 128.4 (2C, $\mathbf{C_{13,15}}$), 127.5 (2C, $\mathbf{C_{12,16}}$), 122.3 (2C, $\mathbf{C_{5,9}}$), 115.0 (2C, $\mathbf{C_{6,8}}$) ppm.

HRMS (ESI$^+$): exact mass calculated for $[M+H]^+$ ($C_{13}H_{12}NO_2^+$) required *m/z* 214.0863; found *m/z* 214.0867.

FT-IR (neat) ν_{max}: 3169, 2191, 1631, 1507, 1384, 1098, 818 cm^{-1}.

1.5.5.2. *N*-(4-hydroxyphenyl)pivalamide (1.114)

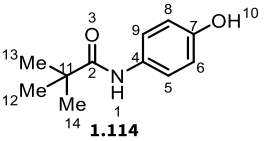

1.114

Chemical Formula: $C_{11}H_{15}NO_2$

Synthesised according to the general procedure described in chapter 1.5.2.2 starting from *N*-hydroxy-*N*-phenylpivalamide **1.114sm** (61.0 mg, 0.310 mmol, 1.00 eq.) at 100°C for 8 h to afford *N*-(4-hydroxyphenyl)pivalamide **1.114** (42.0 mg, 0.217 mmol, 70%) as a white solid.

^{1}H-NMR (600 MHz, DMSO-d_6): δ 9.11 (br. s, 1H, $\mathbf{H_{10}}$), 8.92 (br. s, 1H, $\mathbf{H_1}$), 7.36-7.34 (m, 2H, $\mathbf{H_{6,8}}$), 6.68-6.65 (m, 2H, $\mathbf{H_{5,9}}$), 1.19 (s, 9H, $\mathbf{H_{12\text{-}14}}$) ppm.

^{13}C-NMR (150 MHz, DMSO-d_6): δ 175.9 ($\mathbf{C_2}$), 153.3 ($\mathbf{C_7}$), 130.8 ($\mathbf{C_4}$), 122.3 (2C, $\mathbf{C_{5,9}}$), 114.7 (2C, $\mathbf{C_{6,8}}$), 38.9 ($\mathbf{C_{11}}$), 27.4 (3C, $\mathbf{C_{12\text{-}14}}$) ppm.

HRMS (ESI$^+$): exact mass calculated for $[M+H]^+$ ($C_{11}H_{16}NO_2^+$) required *m/z* 194.1176; found *m/z* 194.1176.

FT-IR (neat) ν_{max}: 3299, 1666, 1614, 1594, 1554, 1489, 1371, 1300, 1264, 783, 692 cm^{-1}.

1.5.5.3. 2-(adamant-1-yl)-*N*-(4-hydroxyphenyl)acetamide (1.166)

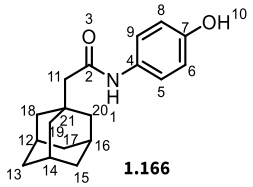

1.166

Chemical Formula: $C_{18}H_{23}NO_2$

Synthesised according to the general procedure described in chapter 1.5.2.2 starting from *N*-hydroxy-*N*-phenyl-adamant-2-ylamide **1.166sm** (60.0 mg, 0.220 mmol, 1.00 eq.) at 60°C for 7 h to afford 2-(adamant-1-yl)-*N*-(4-hydroxyphenyl)acetamide **1.166** (43.0 mg, 0.158 mmol, 72%) as a white solid.

^{1}H-NMR (600 MHz, DMSO-d_6): δ 9.46 (br. s, 1H, **H_{10}**), 9.12 (s, 1H, **H_1**), 7.34 (d, *J* = 12.0 Hz, 2H, **$H_{6,8}$**), 6.66 (d, *J* = 6.0 Hz, 2H, **$H_{5,9}$**), 1.98 (s, 2H, **H_{11}**), 1.91 (br. s, 3H, **$H_{12,14,16}$**), 1.67-1.57 (m, 12H, **$H_{13,15,17,18,19,20}$**) ppm.

^{13}C-NMR (150 MHz, DMSO-d_6): δ 168.4 (**C_2**), 153.1 (**C_7**), 131.0 (**C_4**), 121.0 (2C, **$C_{5,9}$**), 115.0 (2C, **$C_{6,8}$**), 66.4 (**C_{21}**), 50.8 (**C_{11}**), 42.1 (3C, **$C_{12,14,16}$**), 36.5 (3C, **$C_{18,19,20}$**), 28.1 (3C, **$C_{13,15,17}$**) ppm.

HRMS (ESI$^+$): exact mass calculated for $[M+H]^+$ ($C_{18}H_{24}NO_2^+$) required *m/z* 286.1802; found *m/z* 286.1795.

FT-IR (neat) ν_{max}: 3188, 2922, 1605, 1254, 1028, 839 cm^{-1}.

1.5.5.4. *N*-(4-hydroxyphenly)cyclobutanecarboxamide (1.167)

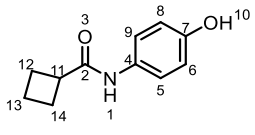

1.167

Chemical Formula: $C_{11}H_{13}NO_2$

Synthesised according to the general procedure described in chapter 1.5.2.2 starting from *N*-hydroxy-*N*-phenylcyclobutanecarboxamide **1.167sm** (1.01 mg, 5.28 mmol, 1.00 eq.) at 20°C for 1 h before being

heated to 100°C for 2 h to afford *N*-(4-hydroxyphenyl)cyclobutanecarboxamide **1.167** (711 mg, 3.70 mmol, 70%) as a white solid.

^{1}H-NMR (600 MHz, DMSO-d_6): δ 9.42 (s, 1H, **H_{10}**), 9.11 (s, 1H, **H_1**), 7.37-7.35 (m, 2H, **$H_{6,8}$**), 6.68-6.65 (m, 2H, **$H_{5,9}$**), 3.15 (pd, *J* = 8.6, 0.7 Hz, 1H, **H_{11}**), 2.23-2.16 (m, 2H, **$H_{12,14}$**), 2.09-2.03 (m, 2H, **$H_{12,14}$**), 1.95-1.87 (m, 1H, **H_{13}**), 1.81-1.75 (m, 1H, **H_{13}**) ppm.

^{13}C-NMR (150 MHz, DMSO-d_6): δ 172.1 (**C_2**), 153.1 (**C_7**), 131.0 (**C_4**), 120.9 (2C, **$C_{5,9}$**), 115.0 (2C, **$C_{6,8}$**), 39.5 (**C_{11}**), 24.6 (2C, **$C_{12,14}$**), 17.8 (**C_{13}**) ppm.

HRMS (ESI$^+$): exact mass calculated for $[M+H]^+$ ($C_{11}H_{14}NO_2^+$) required *m/z* 192.1019; found *m/z* 192.1016.

FT-IR (neat) ν_{max}: 3300, 2946, 1738, 1643, 1605, 1546, 1511, 1440, 1367, 1219, 833 cm^{-1}.

1.5.5.5. *N*-(4-hydroxyphenyl)-4-nitrobenzamide (1.168)

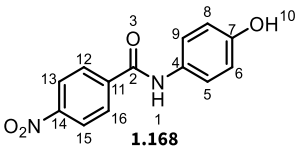

1.168

Chemical Formula: $C_{13}H_{10}N_2O_4$

Synthesised according to the general procedure described in chapter 1.5.2.2 starting from *N*-hydroxy-4-nitro-*N*-phenylbenzamide **1.168sm** (60.0 mg, 0.230 mmol, 1.00 eq.) at 20°C for 4 h to afford *N*-(4-hydroxyphenyl)-4-nitrobenzamide **1.168** (50.0 mg, 0.191 mmol, 83%) as a white solid.

^{1}H-NMR (600 MHz, DMSO-d_6): δ 10.34 (br. s, 1H, **H_{10}**), 9.38 (br. s, 1H, **H_1**), 8.33 (d, *J* = 8.7 Hz, 2H, **$H_{13,15}$**), 8.15 (d, *J* = 8.6 Hz, 2H, **$H_{12,16}$**), 7.54 (d, *J* = 8.8 Hz, 2H, **$H_{6,8}$**), 6.76 (d, *J* = 8.9 Hz, 2H, **$H_{5,9}$**) ppm.

^{13}C-NMR (150 MHz, DMSO-d_6): δ 163.4 (**C_2**), 154.2 (**C_{10}**), 149.0 (**C_{14}**), 140.9 (**C_{11}**), 130.3 (**C_4**), 129.1 (2C, **$C_{12,16}$**), 123.6 (2C, **$C_{13,15}$**), 122.5 (2C, **$C_{5,9}$**), 115.2 (2C, **$C_{6,8}$**) ppm.

HRMS (ESI$^+$): exact mass calculated for $[M+H]^+$ ($C_{13}H_{11}N_2O_4^+$) required *m/z* 259.0713; found *m/z* 259.0709.

FT-IR (neat) ν_{max}: 3247, 1625, 1584, 1521, 1348, 834, 718, 693 cm^{-1}.

1.5.5.6. *N*-(4-hydroxyphenyl)-4-methoxybenzamide (1.169)

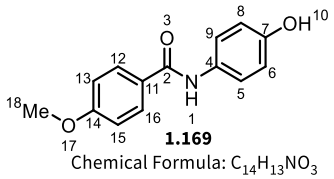

1.169

Chemical Formula: $C_{14}H_{13}NO_3$

Synthesised according to the general procedure described in chapter 1.5.2.2 starting from *N*-hydroxy-4-methoxy-*N*-phenylbenzamide **1.169sm** (60.0 mg, 0.250 mmol, 1.00 eq.) at 20°C for 2 h to afford *N*-(4-hydroxyphenyl)-4-methoxybenzamide **1.169** (37.0mg, 0.155 mmol, 62%) as a white solid.

^{1}H-NMR (600 MHz, DMSO-d_6): δ 9.85 (br. s, 1H, **H_{10}**), 9.22 (br. s, 1H, **H_1**), 7.93-7.91 (m, 2H, **$H_{12,16}$**), 7.51-7.48 (m, 2H, **$H_{6,8}$**), 7.05-7.02 (m, 2H, **$H_{12,16}$**), 6.73-6.71 (m, 2H, **$H_{5,9}$**), 3.83 (s, 3H, **H_{18}**) ppm.

^{13}C-NMR (150 MHz, DMSO-d_6): δ 164.0 (**C_2**), 161.7 (**C_{14}**), 153.6 (**C_{10}**), 130.8 (**C_4**), 129.4 (2C, **$C_{12,16}$**), 127.2 (**C_{11}**), 122.3 (2C, **$C_{5,9}$**), 115.0 (2C, **$C_{13,15}$**), 113.6 (2C, **$C_{6,8}$**), 55.4 (**C_{18}**) ppm.

HRMS (ESI$^+$): exact mass calculated for $[M+H]^+$ ($C_{14}H_{14}NO_3^+$) required *m/z* 244.0968; found *m/z* 244.0966.

FT-IR (neat) ν_{max}: 3188, 2922, 1605, 1254, 1028, 839 cm^{-1}.

1.5.5.7. *N*-(4-hydroxy-2,3-dimethylphenyl)cinnamamide (1.170)

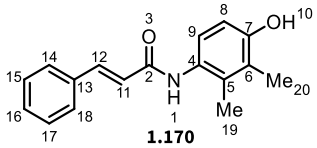

1.170

Chemical Formula: $C_{17}H_{17}NO_2$

Synthesised according to the general procedure described in chapter 1.5.2.2 starting from *N*-(2,3-dimethylphenyl)-*N*-hydroxycinnamamide **1.170sm** (60.0 mg, 0.220 mmol, 1.00 eq.) at 20°C for 8 h to afford *N*-(4-hydroxy-2,3-dimethylphenyl)cinnamamide **1.170** (44.0 mg, 0.161 mmol, 73%) as a white solid.

^{1}H-NMR (600 MHz, DMSO-d_6): δ 9.43 (s, 1H, **H_{10}**), 9.22 (s, 1H, **H_1**), 7.61, (d, *J* = 7.2 Hz, 2H, **$H_{14,18}$**), 7.53 (d, *J* = 15.8 Hz, 1H, **H_{12}**), 7.40-7.37 (m, 3H, **$H_{15\text{-}17}$**), 6.98 (d, *J* = 8.5 Hz, 1H, **H_9**), 6.89 (d, *J* = 15.8 Hz, 1H, **H_{11}**), 6.66 (d, *J* = 8.5 Hz, 1H, **H_8**), 2.08 (s, 3H, **H_{19}**), 2.06 (s, 3H, **H_{20}**) ppm.

^{13}C-NMR (150 MHz, DMSO-d_6): δ 164.0 (**C_2**), 153.1 (**C_7**), 139.5 (**C_{12}**), 135.1 (**C_{13}**), 133.0 (**C_4**), 129.6 (**C_5**), 129.1 (2C, **$C_{14,18}$**), 127.7 (2C, **$C_{15,17}$**), 127.6 (**C_{16}**), 124.0 (**C_6**), 122.8 (**C_{11}**), 122.5 (**C_9**), 112.0 (**C_8**), 14.7 (**C_{19}**), 12.3 (**C_{20}**) ppm.

HRMS (ESI$^+$): exact mass calculated for $[M+H]^+$ ($C_{17}H_{18}NO_2^+$) required *m/z* 268.1332; found *m/z* 268.1322.

FT-IR (neat) ν_{max}: 3360, 1660, 1620, 1578, 1528, 1269, 1203, 1048, 1022, 795, 539 cm^{-1}.

1.5.5.8. *N*-(4-hydroxyphenyl)-4-vinylbenzamide (1.171)

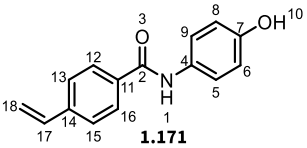

1.171

Chemical Formula: $C_{15}H_{13}NO_2$

Synthesised according to the general procedure described in chapter 1.5.2.2 starting from *N*-hydroxy-*N*-phenyl-4-vinylbenzamide **1.171sm** (55.0 mg, 0.230 mmol, 1.00 eq.) at 20°C for 8 h to afford *N*-(4-hydroxyphenyl)-4-vinylbenzamide **1.171** (31.0 mg, 0.129 mmol, 56%) as an off-white solid.

^{1}H-NMR (600 MHz, DMSO-d_6): δ 9.99 (s, 1H, **H_{10}**), 9.24 (s, 1H, **H_1**), 7.92 (d, *J* = 8.3 Hz, 2H, **$H_{12,16}$**), 7.60 (d, *J* = 8.3 Hz, 2H, **$H_{13,15}$**), 7.52 (d, *J* = 8.8 Hz, 2H, **$H_{6,8}$**), 6.81 (dd, *J* = 17.7, 11.0 Hz, 1H, **H_{17}**), 6.73 (d, *J* = 8.9 Hz, 2H, **$H_{5,9}$**), 6.98 (d, *J* = 17.8 Hz, 1H, **H_{18}**), 5.39 (d, *J* = 11.1 Hz, 1H, **H_{18}**) ppm.

^{13}C-NMR (150 MHz, DMSO-d_6): δ 164.4 (**C_2**), 153.7 (**C_7**), 139.8 (**C_{14}**), 135.9 (**C_{17}**), 134.2 (**C_{11}**), 130.7 (**C_4**), 127.9 (2C, **$C_{13,15}$**), 126.0 (2C, **$C_{12,16}$**), 122.3 (2C, **$C_{5,9}$**), 116.3 (**C_{18}**), 115.0 (2C, **$C_{6,8}$**) ppm.

HRMS (ESI$^+$): exact mass calculated for $[M+Na]^+$ ($C_{15}H_{13}NO_2Na^+$) required *m/z* 262.0839; found *m/z* 262.0844.

FT-IR (neat) ν_{max}: 3316, 2925, 2362, 1692, 1641, 1608, 1539, 1515, 1258, 1125, 918 cm^{-1}.

1.5.5.9. *N*-(4-hydroxyphenyl)acetamide, paracetamol (1.136)

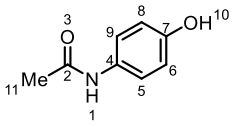

1.136

Chemical Formula: $C_8H_9NO_2$

Synthesised according to the general procedure described in chapter 1.5.2.2 starting from *N*-hydroxy-*N*-phenylacetamide **1.133x** (62.0 mg, 0.410 mmol, 1.00 eq.) at 20°C for 3 h to afford *N*-(4-hydroxyphenyl)acetamide **1.136** (47.0 mg, 0.312 mmol, 76%) as a white solid.

^{1}H-NMR (600 MHz, DMSO-d_6): δ 9.66 (s, 1H, **H_{10}**), 9.20 (s, 1H, **H_1**), 7.33 (d, *J* = 8.6 Hz, 2H, **$H_{6,8}$**), 6.67 (d, *J* = 8.6 Hz, 2H, **$H_{5,9}$**), 1.97 (s, 3H, **H_{11}**) ppm.

^{13}C-NMR (150 MHz, DMSO-d_6): δ 167.9 (**C_2**), 153.3 (**C_{10}**), 131.1 (**C_4**), 121.1 (2C, **$C_{5,9}$**), 115.2 (2C, **$C_{6,8}$**), 23.8 (**C_{11}**) ppm.

HRMS (ESI$^+$): exact mass calculated for $[M+H]^+$ ($C_8H_{10}NO_2^+$) required *m/z* 152.0706; found *m/z* 152.0697.

FT-IR (neat) ν_{max}: 3320, 3157, 2353, 2233, 1652, 1540, 1437, 1230, 969, 834, 682 cm^{-1}.

1.5.5.10. *N*-(4-hydroxynaphthalene-1-yl)acetamide (1.115)

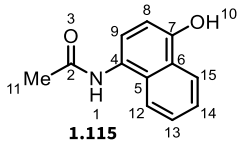

1.115

Chemical Formula: $C_{12}H_{11}NO_2$

Synthesised according to the general procedure described in chapter 1.5.2.2 starting from *N*-hydroxy-*N*-(naphthalene-1-yl)acetamide **1.115sm** (90.0 mg, 0.440 mmol, 1.00 eq.) at 20°C for 12 h to afford *N*-(4-hydroxynapthalene-1-yl)acetamide **1.115** (57.0 mg, 0.273 mmol, 62%) as an off-white solid.

^{1}H-NMR (600 MHz, DMSO-d_6): δ 10.08 (s, 1H, **H_{10}**), 9.62 (s, 1H, **H_1**), 8.14 (d, *J* = 8.0 Hz, 1H, **H_{15}**), 7.88 (d, *J* = 8.3 Hz, 1H, **H_{12}**), 7.51 (ddd, *J* = 8.3, 6.8, 1.3 Hz, 1H, **H_{13}**), 7.46 (ddd, *J* = 7.9, 6.8, 1.0 Hz, 1H, **H_{14}**), 7.30 (d, *J* = 8.0 Hz, 1H, **H_9**), 6.83 (d, *J* = 8.0 Hz, 1H, **H_8**), 2.33-2.10 (m, 3H, **H_{11}**) ppm.

^{13}C-NMR (150 MHz, DMSO-d_6): δ 168.9 (**C_2**), 151.2 (**C_7**), 129.8 (**C_4**), 126.0 (**C_6**), 125.0 (**C_5**), 124.7 (**C_{14}**), 124.6 (**C_{13}**), 123.6 (**C_{15}**), 122.8 (**C_{12}**), 122.3 (**C_8**), 107.3 (**C_9**), 23.1 (**C_{11}**) ppm.

HRMS (ESI$^+$): exact mass calculated for $[M+H]^+$ ($C_{12}H_{12}NO_2^+$) required *m/z* 202.0863; found *m/z* 202.0868.

FT-IR (neat) ν_{max}: 3256, 1657, 1553, 1511, 1257, 1236, 1047, 1023, 833 cm^{-1}.

1.5.5.11. *N*-(4-hydroxy-3-methylphenyl)acetamide (1.172)

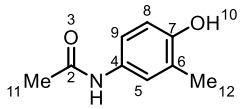

1.172

Chemical Formula: $C_9H_{11}NO_2$

Synthesised according to the general procedure described in chapter 1.5.2.2 starting from *N*-hydroxy-*N*-(*m*-tolyl)acetamide **1.172sm** (60.0 mg, 0.360 mmol, 1.00 eq.) at 20°C for 8 h to afford *N*-(4-hydroxy-3-methylphenyl)acetamide **1.172** (42.0 mg, 0.252 mmol, 70%) as an off-white solid.

^{1}H-NMR (600 MHz, MeOH-d_4): δ 7.17 (d, *J* = 2.2 Hz, 1H, **H_5**), 7.14 (dd, *J* = 8.5, 2.2 Hz, 1H, **H_9**), 6.67 (d, *J* = 8.5 Hz, 1H, **H_8**), 2.16 (s, 3H, **H_{12}**), 2.07 (s, 3H, **H_{11}**) ppm. (*The NH and OH protons are not observed in MeOH-d_4*).

^{13}C-NMR (150 MHz, MeOH-d_4): δ 171.3 (**C_2**), 153.5 (**C_7**), 131.4 (**C_4**), 125.8 (**C_6**), 124.7 (**C_5**), 120.6 (**C_9**), 115.4 (**C_8**), 23.5 (**C_{11}**), 16.3 (**C_{12}**) ppm.

HRMS (ESI$^+$): exact mass calculated for $[M+H]^+$ ($C_9H_{12}NO_2^+$) required *m/z* 166.0863; found *m/z* 166.0866.

FT-IR (neat) ν_{max}: 3284, 1636, 1617, 1503, 1415, 1263, 1209, 1114, 818 cm^{-1}.

1.5.5.12. *N*-(4-hydroxy-2,6-dimethylphenyl)acetamide (1.175)

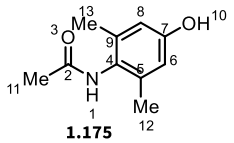

1.175

Chemical Formula: $C_{10}H_{13}NO_2$

Synthesised according to the general procedure described in chapter 1.5.2.2 starting from *N*-hydroxy-*N*-(2,6-dimethylphenyl)acetamide **1.175sm** (60.0 mg, 0.360 mmol, 1.00 eq.) at 100°C for 8 h to afford *N*-(4-hydroxy-2,6-dimethylphenyl)acetamide **1.175** (28.0 mg, 0.169 mmol, 47%) as an off-white solid.

^{1}H-NMR (600 MHz, MeOH-d_4): δ 6.51 (s, 2H, **$H_{6,8}$**), 2.13 (s, 3H, **H_{11}**), 2.12 (s, 6H, **$H_{12,13}$**) ppm. (*The NH and OH protons are not observed in MeOH-d_4*).

^{13}C-NMR (150 MHz, MeOH-d_4): δ 172.6 (**C_2**), 157.3 (**C_7**), 138.0 (2C, **$C_{5,9}$**), 127.4 (**C_4**), 115.2 (2C, **$C_{6,8}$**), 22.3 (**C_{11}**), 18.4 (2C, **$C_{12,13}$**) ppm.

HRMS (ESI$^+$): exact mass calculated for $[M+H]^+$ ($C_{10}H_{14}NO_2^+$) required *m/z* 180.1019; found *m/z* 180.1023.

FT-IR (neat) ν_{max}: 3254, 2954, 1704, 1637, 1597, 1523, 1291, 1150, 1028, 830 cm^{-1}.

1.5.5.13. *N*-(4-hydroxy-3,5-dimethylphenyl)acetamide (1.176)

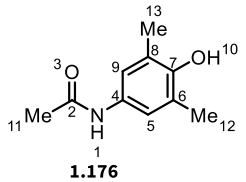

1.176

Chemical Formula: $C_{10}H_{13}NO_2$

Synthesised according to the general procedure described in chapter 1.5.2.2 starting from *N*-hydroxy-*N*-(3,5-dimethylphenyl)acetamide **1.176sm** (60.0 mg, 0.360 mmol, 1.00 eq.) at 100°C for 8 h to afford *N*-(4-hydroxy-3,5-dimethylphenyl)acetamide **1.176** (36.0 mg, 0.216 mmol, 60%) as an off-white solid.

^{1}H-NMR (600 MHz, MeOH-d_4): δ 7.06 (s, 2H, **$H_{5,9}$**), 2.18 (s, 6H, **$H_{12,13}$**), 2.06 (s, 3H, **H_{11}**) ppm. (*The NH and OH protons are not observed in MeOH-d_4*).

^{13}C-NMR (150 MHz, MeOH-d_4): δ 171.3 (**C_2**), 151.1 (**C_7**), 131.5 (**C_4**), 126.0 (2C, **$C_{6,8}$**), 122.1 (2C, **$C_{5,9}$**), 23.5 (**C_{11}**), 16.8 (2C, **$C_{12,13}$**) ppm.

HRMS (ESI$^+$): exact mass calculated for [M+H]$^+$ ($C_{10}H_{14}NO_2^+$) required *m/z* 180.1019; found *m/z* 180.1019.

FT-IR (neat) ν_{max}: 3297, 2954, 2923, 2853, 1639, 1619, 1552, 1508, 1325, 1114, 964, 794, 757 cm^{-1}.

1.5.5.14. *N*-(4-hydroxy-3-methoxyphenyl)acetamide (1.173)

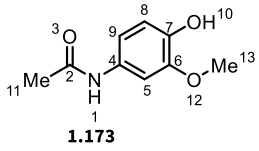

1.173

Chemical Formula: $C_9H_{11}NO_3$

Synthesised according to the general procedure described in chapter 1.5.2.2 starting from *N*-hydroxy-*N*-(3-methoxyphenyl)acetamide **1.173sm** (56.0 mg, 0.310 mmol, 1.00 eq.) at 20°C for 18 h to afford *N*-(4-hydroxy-3-methoxyphenyl)acetamide **1.173** (38.0 mg, 0.211 mmol, 68%) as a purple solid.

^{1}H-NMR (700 MHz, DMSO-d_6): δ 9.66 (s, 1H, **H_{10}**), 8.66 (s, 1H, **H_1**); 7.23 (dd, *J* = 1.8 Hz, 1H, **H_5**), 6.91 (dd, *J* = 8.5, 1.9 Hz, 1H, **H_9**), 6.66 (d, *J* = 8.5 Hz, 1H, **H_8**), 3.71 (s, 3H, **H_{13}**), 1.97 (s, 3H, **H_{11}**) ppm.

^{13}C-NMR (175 MHz, DMSO-d_6): δ 167.5 (**C_2**), 147.1 (**C_7**), 142.3 (**C_6**), 131.5 (**C_4**), 115.1 (**C_8**), 111.6 (**C_9**), 104.7 (**C_5**), 55.5 (**C_{13}**), 23.8 (**C_{11}**) ppm.

HRMS (ESI$^+$): exact mass calculated for [M+H]$^+$ ($C_9H_{12}NO_2^+$) required *m/z* 182.0812; found *m/z* 182.0812.

FT-IR (neat) ν_{max}: 3304, 3169, 2965, 2841, 1658, 1620, 1549, 1513, 1452, 1418, 967 cm^{-1}.

1.5.5.15. *N*-(3-acetyl-4-hydroxyphenyl)acetamide (1.174)

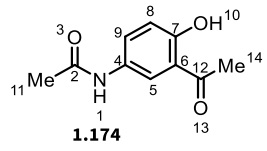

1.174

Chemical Formula: $C_{10}H_{11}NO_3$

Synthesised according to the general procedure described in chapter 1.5.2.2 starting from *N*-(3-acetylphenyl)-*N*-hydroxyacetamide **1.174sm** (48.0 mg, 0.250 mmol, 1.00 eq.) at 100°C for 10 h to afford *N*-(3-acetyl-4-hydroxyphenyl)acetamide **1.174** (22.0 mg, 0.113 mmol, 45%) as a white solid.

^{1}H-NMR (600 MHz, DMSO-d_6): δ 10.1 (s, 1H, **H_{10}**), 8.14 (t, *J* = 1.8 Hz, 1H, **H_1**), 7.84 (ddd, *J* = 8.1, 2.0, 0.8 Hz, 1H, **H_5**), 7.64 (ddd, *J* = 7.7, 1.5, 1.1 Hz, 1H, **H_8**), 7.44 (t, *J* = 7.9 Hz, 1H, **H_9**), 2.55 (s, 3H, **H_{14}**), 2.06 (s, 3H, **H_{11}**) ppm.

^{13}C-NMR (150 MHz, DMSO-d_6): δ 197.7 (**C_{12}**), 168.6 (**C_2**), 139.7 (**C_7**), 137.3 (**C_4**), 129.1 (**C_6**), 123.5 (**C_9**), 123.1 (**C_5**), 118.1 (**C_8**), 26.7 (**C_{14}**), 24.0 (**C_{11}**) ppm.

HRMS (ESI$^+$): exact mass calculated for $[M+H]^+$ ($C_{10}H_{12}NO_3^+$) required *m/z* 194.0812; found *m/z* 194.0815.

FT-IR (neat) ν_{max}: 3245, 2922, 1681, 1372, 1275, 797, 687 cm^{-1}.

1.5.5.16. *N*-(3-fluoro-4-hydroxy-5-iodophenyl)acetamide (1.177)

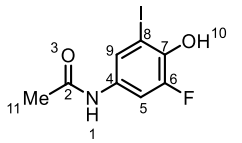

1.177
Chemical Formula: $C_8H_7FINO_2$

Synthesised according to the general procedure described in chapter 1.5.2.2 starting from *N*-(2-fluoro-6-iodophenyl)-*N*-hydroxyacetamide **1.177sm** (60.0 mg, 0.200 mmol, 1.00 eq.) at 100°C for 18 h to afford *N*-(3-fluoro-4-hydroxy-5-iodophenyl)acetamide **1.177** (31.0 mg, 0.104 mmol, 52%) as an off-white solid.

^{1}H-NMR (600 MHz, MeOH-d_4): δ 7.63-7.61 (m, 1H, **H_9**), 7.46 (dd, *J* = 12.5, 4.4 Hz, 1H, **H_5**), 2.08 (s, 3H, **H_{11}**) ppm. (*The NH and OH protons are not observed in MeOH-d_4*).

^{13}C-NMR (150 MHz, MeOH-d_4): δ 171.4 (**C_2**), 151.0 (d, J_{CF} = 241.2 Hz, **C_6**), 142.9 (d, J_{CF} = 16.0 Hz, **C_7**), 133.4 (d, J_{CF} = 10.0 Hz, **C_4**), 126.6 (d, J_{CF} = 3.3 Hz, **C_9**), 109.7 (d, J_{CF} = 24.2 Hz, **C_5**), 85.7 (**C_8**), 23.6 (**C_{11}**) ppm.

^{19}F-NMR (565 MHz, MeOH-d_4): δ –133.41 - –133.43 (m) ppm.

HRMS (ESI$^+$): exact mass calculated for $[M+H]^+$ ($C_8H_8NO_2FI^+$) required *m/z* 295.9578; found *m/z* 295.9575.

FT-IR (neat) ν_{max}: not measured.

1.5.5.17. *N*-(3-fluoro-4-hydroxyphenyl)acetamide (1.178)

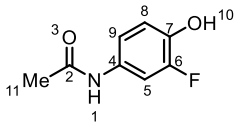

1.178
Chemical Formula: $C_8H_8FNO_2$

Synthesised according to the general procedure described in chapter 1.5.2.2 starting from *N*-(3-fluorophenyl)-*N*-hydroxyacetamide **1.178sm** (60.0 mg, 0.360 mmol, 1.00 eq.) at 100°C for 12 h to afford *N*-(3-fluoro-4-hydroxyphenyl)acetamide **1.178** (34.0 mg, 0.205 mmol, 57%) as an off-white solid.

^{1}H-NMR (700 MHz, DMSO-d_6): δ 9.82 (br. s, 1H, **H_{10}**), 9.50 (br. s, 1H, **H_1**), 7.50 (dd, *J* = 13.6, 2.4 Hz, 1H, **H_5**), 7.04 (dd, *J* = 8.7, 1.3 Hz, 1H, **H_8**), 6.85 (t, *J* = 9.3 Hz, 1H, **H_9**), 1.99 (s, 3H, **H_{11}**) ppm.

^{13}C-NMR (175 MHz, DMSO-d_6): δ 167.9 (**C_2**), 150.2 (d, J_{CF} = 238.6 Hz, **C_6**), 140.3 (d, J_{CF} = 12.3 Hz, **C_7**), 131.5 (d, J_{CF} = 9.2 Hz, **C_5**), 117.5 (d, J_{CF} = 3.8 Hz, **C_4**), 115.2 (d, J_{CF} = 3.1 Hz, **C_9**), 107.6 (d, J_{CF} = 22.8 Hz, **C_8**), 23.8 (**C_{11}**) ppm.

^{19}F-NMR (659 MHz, DMSO-d_6): δ –135.00 ppm.

HRMS (ESI$^+$): exact mass calculated for $[M+H]^+$ ($C_8H_9NO_2F^+$) required *m/z* 170.0612; found *m/z* 170.0611.

FT-IR (neat) ν_{max}: 3314, 1642, 1517, 1287, 755, 694 cm^{-1}.

1.5.5.18. *N*-(2-fluoro-4-hydroxyphenyl)acetamide (1.179)

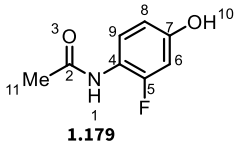

1.179
Chemical Formula: $C_8H_8FNO_2$

Synthesised according to the general procedure described in chapter 1.5.2.2 starting from *N*-(2-fluorophenyl)-*N*-hydroxyacetamide **1.179sm** (60.0 mg, 0.360 mmol, 1.00 eq.) at 100°C for 12 h to afford *N*-(2-fluoro-4-hydroxyphenyl)acetamide **1.179** (33.0 mg, 0.198 mmol, 55%) as a white solid.

^{1}H-NMR (600 MHz, MeOH-d_4): δ 7.39 (td, *J* = 8.9, 0.6 Hz, 1H, **H_9**), 6.58-6.55 (m, 2H, **$H_{6,8}$**), 2.11 (s, 3H, **H_{11}**) ppm. (*The NH and OH protons are not observed in MeOH-d_4*).

^{13}C-NMR (150 MHz, MeOH-d_4): δ 172.2 (**C_2**), 157.7 (d, J_{CF} = 11.0 Hz, **C_7**), 157.4 (d, J_{CF} = 245.5 Hz, **C_5**), 127.9 (d, J_{CF} = 3.0 Hz, **C_9**), 118.1 (d, J_{CF} = 12.7 Hz, **C_4**), 111.9 (d, J_{CF} = 2.9 Hz, **C_8**), 103.8 (d, J_{CF} = 22.6 Hz, **C_6**), 22.9 (**C_{11}**) ppm.

^{19}F-NMR (470 MHz, MeOH-d_4): δ –112.67 ppm.

HRMS (ESI$^+$): exact mass calculated for $[M+H]^+$ ($C_8H_9NO_2F^+$) required *m/z* 170.0612; found *m/z* 170.0612.

FT-IR (neat) ν_{max}: 3163, 1634, 1591, 1437, 1378, 1262, 1108, 862, 846, 775, 680 cm^{-1}.

1.5.5.19. *N*-(4-hydroxy-3-(trifluoromethyl)phenyl)acetamide (1.180)

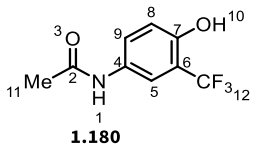

1.180

Chemical Formula: $C_9H_8F_3NO_2$

Synthesised according to the general procedure described in chapter 1.5.2.2 starting from *N*-(3-(trifluoromethyl)phenyl)-*N*-hydroxyacetamide **1.180sm** (74.0 mg, 0.340 mmol, 1.00 eq.) at 100°C for 12 h to afford *N*-(4-hydroxy-3-(trifluoromethyl)phenyl)acetamide **1.180** (37.0 mg, 0.170 mmol, 50%) as a white solid.

^{1}H-NMR (600 MHz, MeOH-d_4): δ 7.39 (td, *J* = 8.9, 0.6 Hz, 1H, **H_5**), 6.58-6.55 (m, 2H, **$H_{8,9}$**), 2.11 (s, 3H, **H_{11}**) ppm. (*The NH and OH protons are not observed in MeOH-d_4*).

^{13}C-NMR (150 MHz, MeOH-d_4): δ 171.5 (**C_2**), 153.6 (d, J_{CF} = 1.6 Hz, **C_7**), 131.5 (**C_4**), 126.6 (**C_9**), 125.2 (d, J_{CF} = 271.4 Hz, **C_{12}**), 120.0 (q, J_{CF} = 5.4 Hz, **C_5**), 117.9 (**C_8**), 117.7 (q, J_{CF} = 30.8 Hz, **C_6**), 23.5 (**C_{11}**) ppm.

^{19}F-NMR (565 MHz, MeOH-d_4): δ –63.95 ppm.

HRMS (ESI$^+$): exact mass calculated for $[M+H]^+$ ($C_9H_9NO_2F_3^+$) required *m/z* 220.0580; found *m/z* 220.0585.

FT-IR (neat) ν_{max}: 3125, 1630, 1580, 1410, 1251, 1100, 810, 732, 580 cm^{-1}.

1.5.5.20. *N*-(3-bromo-4-hydroxy-2-methylphenyl)acetamide (1.181)

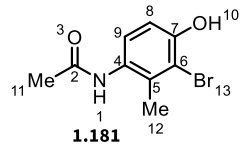

1.181
Chemical Formula: $C_9H_{10}BrNO_2$

Synthesised according to the general procedure described in chapter 1.5.2.2 starting from *N*-(3-bromo-2-methylphenyl)-*N*-hydroxyacetamide **1.181sm** (225 mg, 0.920 mmol, 1.00 eq.) at 20°C for 3 h and at 100°C for 1 h to afford *N*-(3-bromo-4-hydroxy-2-methylphenyl)acetamide **1.181** (96.8 mg, 0.396 mmol, 43%) as a white solid.

^{1}H-NMR (600 MHz, MeOH-d_4): δ 7.02 (d, *J* = 8.6 Hz, 1H, **H_9**), 6.76 (d, *J* = 8.6 Hz, 1H, **H_8**), 2.28 (s, 3H, **H_{12}**), 2.12 (s, 3H, **H_{11}**) ppm. (*The NH and OH protons are not observed in MeOH-d_4*).

^{13}C-NMR (150 MHz, MeOH-d_4): δ 172.7 (**C_2**), 154.3 (**C_7**), 136.8 (**C_4**), 127.8 (2C, **$C_{5,6}$**), 114.1 (2C, **$C_{8,9}$**), 22.7 (**C_{11}**), 18.9 (**C_{12}**) ppm.

HRMS (ESI^+): exact mass calculated for $[M+H]^+$ ($C_9H_{11}NO_2{}^{79}Br^+$) required *m/z* 243.9968; found *m/z* 243.9969.

FT-IR (neat) ν_{max}: 3297, 3251, 1738, 1642, 1524, 1433, 1371, 1290, 1217, 1026, 811 cm^{-1}.

1.5.5.21. *N*-(4-hydroxy-2-iodophenyl)acetamide (1.182)

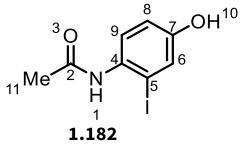

1.182
Chemical Formula: $C_8H_8INO_2$

Synthesised according to the general procedure described in chapter 1.5.2.2 starting from *N*-(2-iodophenyl)-*N*-hydroxyacetamide **1.182sm** (199 mg, 0.720 mmol, 1.00 eq.) at 20°C for 12 h to afford *N*-(4-hydroxy-2-iodophenyl)acetamide **1.182** (140 mg, 0.504 mmol, 70%) as a white solid.

^{1}H-NMR (600 MHz, MeOH-d_4): 7.30 (d, *J* = 2.7 Hz, 1H, **H_6**), 7.13 (d, *J* = 8.6 Hz, 1H, **H_9**), 6.79 (dd, *J* = 8.6, 2.7 Hz, 1H, **H_8**), 2.12 (s, 3H, **H_{11}**) ppm. (*The NH and OH protons are not observed in MeOH-d_4*).

^{13}C-NMR (150 MHz, MeOH-d_4): δ 172.6 (**C_2**), 157.9 (**C_7**), 132.1 (**C_4**), 129.5 (**C_9**), 126.4 (**C_6**), 116.8 (**C_8**), 97.9 (**C_5**), 22.9 (**C_{11}**) ppm.

HRMS (ESI^+): exact mass calculated for $[M+H]^+$ ($C_8H_9NO_2I^+$) required *m/z* 277.9672; found *m/z* 277.9674.

FT-IR (neat) ν_{max}: 3244, 1702, 1655, 1519, 1425, 1346, 1250, 1029, 806, 503 cm^{-1}.

1.5.6. Synthesis of pharmaceutically relevant *para*-Aminophenols

1.5.6.1. Synthesis of paracetamol (1.136) and practolol (1.188)

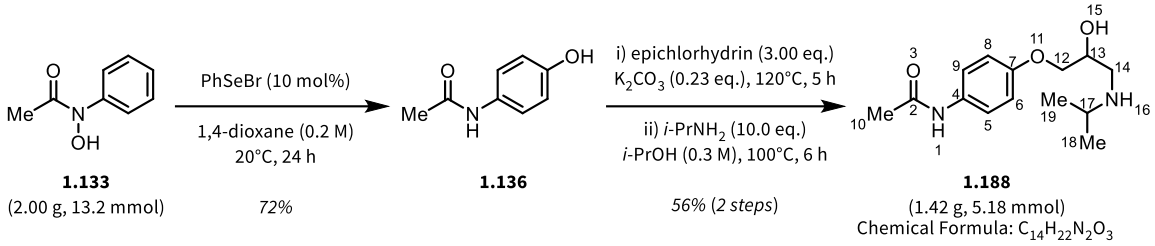

1.133 (2.00 g, 13.2 mmol)

72%

1.136

56% (2 steps)

1.188 (1.42 g, 5.18 mmol)
Chemical Formula: $C_{14}H_{22}N_2O_3$

To a solution of hydroxamic acid **1.133** (2.00 g, 13.2 mmol, 1.00 eq.) in 1,4-dioxane (0.2 M) at room temperature was added PhSeBr (312 mg, 1.32 mmol, 0.100 eq.). The resulting mixture was stirred at room temperature for 24 h, after which the solvent was removed *in vacuo*. The crude product was subsequently purified by flash column chromatography (SiO_2, heptane/EtOAc) to afford paracetamol (**1.136**) (1.44 g, 9.50 mmol, 72%) as a white solid.

All spectroscopic data are in accordance with the reported literature.[112]

Paracetamol (**1.136**) (1.44 g, 9.50 mmol, 1.00 eq.) was dissolved in epichlorhydrin (2.18 mL, 27.8 mmol, 3.00 eq.). To the solution was then added K_2CO_3 (306 mg, 2.20 mmol, 0.23 eq.) and the resulting mixture was heated to 120°C for 5 h. Afterwards, the solution was allowed to cool to room temperature and was subsequently concentrated under reduced pressure. The crude epoxide was used in the next step without further purification.

The crude epoxide (1.97 g, 9.50 mmol, 1.00 eq.) was dissolved in isopropanol (0.3 M) at room temperature and isopropylamine (7.60 mL, 92.8 mmol, 9.77 eq.) was added. The reaction mixture was heated to 100°C for 6 h. After the reaction time had elapsed, the solution was concentrated *in vacuo* to yield crude practolol. The crude product was purified by flash column chromatography (SiO_2, heptane/EtOAc) to afford practolol (**1.188**) (1.42 g, 5.18 mmol, 56% over two steps) as a white solid.

^{1}H-NMR (600 MHz, MeOH-d_4): δ 7.40 (d, *J* = 8.9 Hz, 2H, **$H_{6,8}$**), 6.90 (d, *J* = 9.0 Hz, 2H, **$H_{5,9}$**), 4.05-4.01 (m, 1H, **H_{13}**), 3.96-3.91 (m, 2H, **H_{12}**), 2.86-2.81 (m, 2H, **H_{14}**), 2.67-2.64 (dd, *J* = 11.9, 8.6 Hz, 1H, **H_{17}**), 2.09 (s, 3H, **H_{10}**), 1.11-1.09 (m, 6H, **$H_{18,19}$**) ppm. (*The NH and OH protons are not observed in MeOH-d_4*).

^{13}C-NMR (125 MHz, MeOH-d_4): δ 171.3 (**C_2**), 157.0 (**C_4**), 133.2 (**C_7**), 123.0 (2C, **$C_{5,9}$**), 115.7 (2C, **$C_{6,8}$**), 72.2 (**C_{13}**), 69.8 (**C_{17}**), 50.9 (**C_{12}**), 49.9 (**C_{14}**), 23.6 (**C_{10}**), 22.7 (**C_{18}**), 22.5 (**C_{19}**) ppm.

HRMS (ESI^+): exact mass calculated for $[M+H]^+$ ($C_{14}H_{23}N_2O_3^+$) required *m/z* 267.1703; found *m/z* 267.1707.

FT-IR (neat) ν_{max}: 3250, 2952, 1700, 1632, 1540, 1280, 1120, 1021, 829 cm^{-1}.

1.5.6.2. Synthesis of diloxanide furoate 1.191

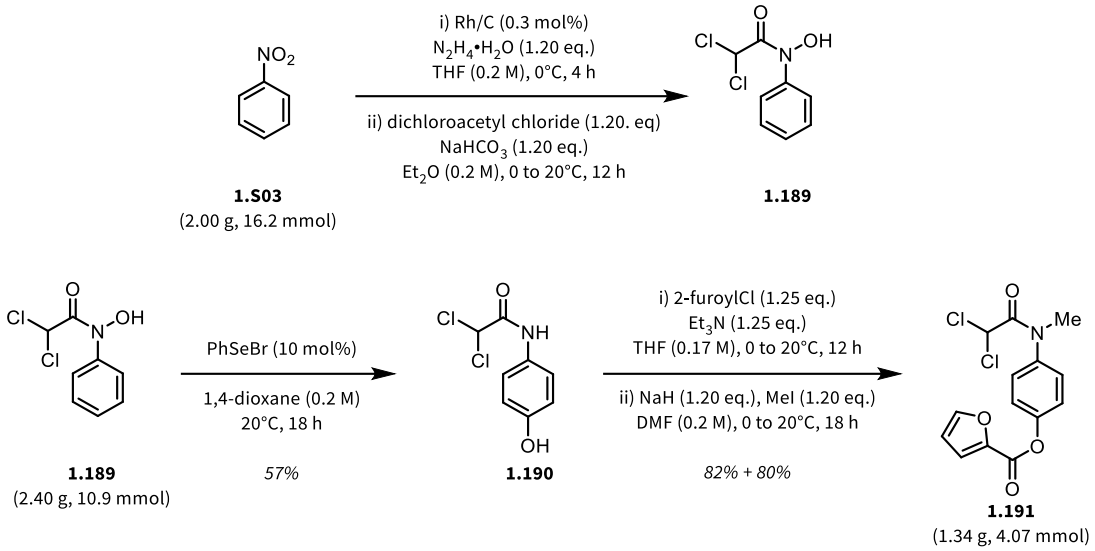

To a solution of nitrobenzene (2.00 g, 16.2 mmol, 1.00 eq.) in THF (0.2 M) at 0°C was added Rh/C (5-wt%) (100 mg, 0.3 mol%) followed by hydrazine hydrate (0.900 mL, 19.5 mmol, 1.20 eq.) and the resulting reaction mixture was stirred at 0°C for 4 h. Afterwards, the reaction mixture was filtered through a pad of Celite® and the filtrate was concentrated under reduced pressure.

The crude hydroxylamine was redissolved in Et_2O (0.2 M) and cooled to 0°C. To the solution was then added $NaHCO_3$ (1.64 g, 19.5 mmol, 1.20 eq.) and dichloroacetyl chloride (1.90 mL, 19.5 mmol, 1.20 eq.). The resulting reaction mixture was allowed to warm to room temperature while being continuously stirred for 12 h. After the starting material had been consumed (as indicated by TLC analysis), the reaction mixture was filtered through a paper filter. The filtrate was concentrated to yield the crude hydroxamic acid **1.189** (2.40 g, 10.9 mmol, 66% over two steps). As **1.189** is unstable, it was used in the next step without further purification.

To a solution of crude hydroxamic acid **1.189** (2.40 g, 10.9 mmol, 1.00 eq.) in 1,4-dioxane (0.2 M) at room temperature was added PhSeBr (264 mg, 1.09 mmol, 0.100 eq.). The resulting reaction mixture was stirred at room temperature for 18 h. After the reaction time had elapsed, the solvent was removed *in vacuo* and the crude *p*-aminophenol was purified by flash column chromatography (SiO_2, heptane/EtOAc) to afford *p*-aminophenol **1.190** (1.40 g, 6.21 mmol, 57%) as a white solid.

To a solution of *p*-aminophenol **1.190** (1.40 g, 6.21 mmol, 1.00 eq.) in THF (0.17 M) at 0°C was added Et_3N (1.08 mL, 7.82 mmol, 1.26 eq.) and 2-furoyl chloride (0.77 mL, 7.82 mmol, 1.26 eq.). The resulting reaction

mixture was stirred for 12 h, during which time it was allowed to warm to room temperature. After the reaction time had elapsed, the reaction mixture was diluted with water (20.0 mL) and EtOAc (20.0 mL) and the layers were separated. The aqueous layer was extracted with EtOAc (3 x 20.0 mL) and the combined organic layers were dried over $MgSO_4$, the solids were filtered off and the solvents were removed *in vacuo* to yield the crude furoate **1.190b**. The crude product was purified by flash column chromatography (SiO_2, heptane/EtOAc) to afford the pure product (1.60 g, 5.09 mmol, 82%) as a white solid.

The furoate **1.190b** (1.60 g, 5.09 mmol, 1.00 eq.) was dissolved in DMF (0.21 M) and cooled to 0°C. To the cold solution was then added NaH (60-wt% in paraffin oil, 244 mg, 6.11 mmol, 1.20 eq.) and the resulting reaction mixture was stirred for 30 min at 0°C before MeI (0.380 mL, 6.11 mmol, 1.20 eq.) was added dropwise. The reaction mixture was allowed to warm to room temperature and was continuously stirred for 18 h. The reaction was quenched by careful addition of water (20.0 mL; *Nota bene: on larger scale it is recommended to cool the reaction mixture to 0°C before quenching carefully with water*) and EtOAc (20.0 mL) was added. The layers were separated and the aqueous layer was extracted with EtOAc (3 x 20.0 mL). The combined organic layers were dried over $MgSO_4$, the solids were filtered off and the solvents were removed *in vacuo* to yield the crude diloxanide furoate. The crude product was purified by flash column chromatography (SiO_2, heptane/EtOAc) to afford diloxanide furoate (**1.191**) (1.34 g, 4.07 mmol, 80%) as a white solid.

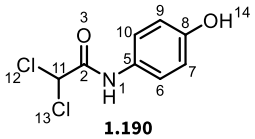

1.190

Chemical Formula: $C_8H_7Cl_2NO_2$

^{1}H-NMR (600 MHz, MeOH-d_4): δ 7.39-7.37 (m, 2H, **$H_{6,10}$**), 6.79-6.76 (m, 2H, **$H_{7,9}$**), 6.34 (s, 1H, **H_{11}**) ppm. (*The NH and OH protons are not observed in MeOH-d_4*).

^{13}C-NMR (150 MHz, MeOH-d_4): δ 164.1 (**C_2**), 156.2 (**C_8**), 130.3 (**C_5**), 123.4 (2C, **$C_{7,9}$**), 116.4 (2C, **$C_{6,10}$**), 68.2 (**C_{11}**) ppm.

HRMS (ESI$^+$): exact mass calculated for $[M+H]^+$ ($C_8H_8NO_2{}^{35}Cl_2{}^+$) required *m/z* 219.9927; found *m/z* 219.9925.

FT-IR (neat) ν_{max}: 3290, 1669, 1608, 1513, 1439, 1363, 1222, 1167, 832, 812, 664 cm^{-1}.

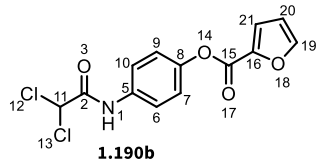

1.190b

Chemical Formula: $C_{13}H_9Cl_2NO_4$

^{1}H-NMR (600 MHz, MeOH-d_4): δ 7.86 (dd, *J* = 1.7, 0.8 Hz, 1H, **H_{19}**), 7.69-7.67 (m, 2H, **$H_{6,10}$**), 7.46 (dd, *J* = 3.5, 0.8 Hz, 1H, **H_{21}**), 7.25-7.22 (m, 2H, **$H_{7,9}$**), 6.70 (dd, *J* = 3.5, 1.8 Hz, 1H, **H_{20}**), 6.39 (s, 1H, **H_{11}**) ppm. (*The NH and OH protons are not observed in MeOH-d_4*).

^{13}C-NMR (150 MHz, MeOH-d_4): δ 164.4 (**C_2**), 158.4 (**C_{15}**), 149.3 (**C_8**), 148.5 (**C_{16}**), 145.1 (**C_{19}**), 136.7 (**C_5**), 123.3 (2C, **$C_{7,9}$**), 122.5 (2C, **$C_{6,10}$**), 120.9 (**C_{21}**), 113.4 (**C_{20}**), 68.2 (**C_{11}**) ppm.

HRMS (ESI^+): exact mass calculated for $[M+H]^+$ ($C_{13}H_{10}NO_4{}^{35}Cl_2{}^+$) required *m/z* 313.9981; found *m/z* 313.9979.

FT-IR (neat) ν_{max}: 1697, 1611, 1567, 1537, 1509, 1470, 1393, 1295, 1198, 1173, 1089, 1015, 929, 885, 806, 764 cm^{-1}.

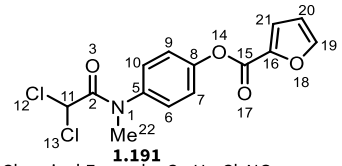

1.191

Chemical Formula: $C_{14}H_{11}Cl_2NO_4$

^{1}H-NMR (600 MHz, MeOH-d_4): δ 8.00 (d, *J* = 3.2 Hz, 1H, **H_{19}**), 7.71 (d, *J* = 4.7 Hz, 1H, **$H_{6\ or\ 10}$**), 7.37-7.33 (m, 4H, **$H_{6\ or\ 10,\ 7,9,21}$**), 7.21-7.20 (m, 1H, **H_{20}**), 5.91 (s, 1H, **H_{11}**), 3.35 (s, 3H, **H_{22}**) ppm.

^{13}C-NMR (150 MHz, MeOH-d_4): δ 164.1 (**C_2**), 160.2 (**C_{15}**), 150.8 (**C_{19}**), 139.2 (**C_8**), 135.3 (**C_5**), 134.3 (**C_{16}**), 132.2 (**C_{21}**), 128.43 (2C, **$C_{7,9}$**), 128.35 (**C_{20}**), 123.8 (2C, **$C_{6,8}$**), 63.6 (**C_{11}**), 38.8 (**C_{22}**) ppm.

HRMS (ESI^+): exact mass calculated for $[M+H]^+$ ($C_{14}H_{12}NO_4{}^{35}Cl_2{}^+$) required *m/z* 328.0138; found *m/z* 328.0137.

FT-IR (neat) ν_{max}: 1739, 1682, 1503, 1470, 1391, 1234, 1232, 1199, 1170, 1086, 929, 884, 805, 769, 753, 664 cm^{-1}.

1.5.7. Crossover Experiment

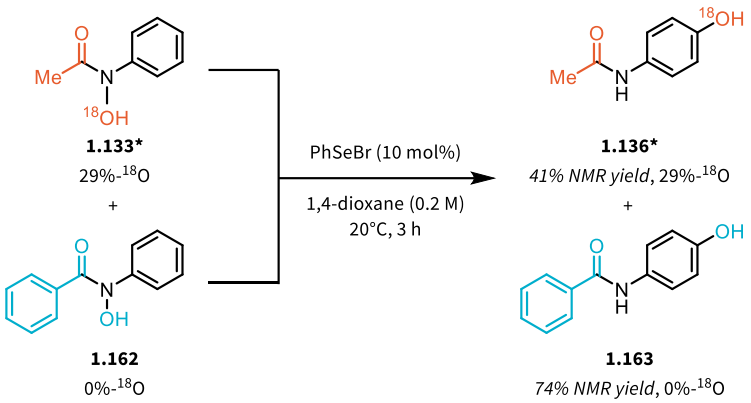

The labelled starting material **1.133*** (27.0 mg, 0.180 mmol, 1.00 eq.) and **1.162** (38.4 mg, 0.180 mmol, 1.00 eq.) were dissolved in 1,4-dioxane (0.1 M). To the solution was then added PhSeBr (8.49 mmol, 0.0360 mmol, 20 mol% overall, 10 mol% per substrate) and the resulting mixture was stirred at 20°C for 3 h. After the reaction time had elapsed, an internal standard was added (1,3,5-trimethoxybenzene) and the NMR yields were determined (41% **1.136***, 74% **1.163**). The crude product mixture was analysed by HRMS to analyse the ^{18}O-content for each of the products.

HRMS (ESI^+): exact mass calculated for $[M+H]^+$

- **1.136*** ($C_8H_{10}NO^{18}O^+$) required *m/z* 154.0749; found *m/z* 154.0758.
- **1.163** ($C_{13}H_{12}NO_2^+$) required *m/z* 214.0863; found *m/z* 214.0867.
- **1.163*** ($C_{13}H_{12}NO^{18}O^+$, hypothetical) required *m/z* 216.0905; found: no fitting mass found within error range.

No signal in HRMS consistent with the formation of the labelled crossover product **1.163*** could be detected, while no loss of ^{18}O incorporation from hydroxamic acid **1.133*** to the corresponding product **1.136*** was detected. It was therefore concluded that no crossover of intermediates took place.

1.5.8. Computational Details

Conformational space analysis of all molecules has been initially established using meta-dynamics simulations based on tight-binding quantum chemical calculations in CREST.[90,113,114] Structures within CREST were then subjected to PBE0-D3BJ/def2-SVP geometry optimisation.[115–119] The nature of stationary points (transition states and minima) was verified through the computation of vibrational frequencies. Thermal correction to Gibbs free energy were combined with single point energies calculated at the PBE0-D3BJ/def2-TZVP level of theory to give Gibbs free energies ("G_{298}") at 298.15 K. All energies are given in kcal·mol^{-1}. The polarisable continuum model (PCM) with SMD parameters was applied to consider solvent effects (THF) for both geometries and energies.[120,121] Free energies in solution were corrected to a reference state of 1 mol·L^{-1} at 298.15 K through the addition of RTln/24.46) = +7.925 kJ·mol^{-1} to the gas phase (1 atm) free energies. DFT calculations were performed with Gaussian 16-program package.

2. Synthesis and Biological Evaluation of FR252921 and Derivatives thereof

2.1. Introduction

2.1.1. Human Health and the Immune System

Over the past centuries, human health care has undergone several revolutions, which have raised the life expectancy dramatically. Such revolutions can be found in the advancement of vaccination,[122] the implementation of stricter hygiene,[123] development of medical imaging technologies,[124] or the discovery of antibiotics,[125–127] which have overall reduced mortality from diseases at different points in life, but have also had a tremendous impact on the fight for reducing child mortality. However, in everyday life, these medical interventions are only required or should only be applied after a first line of defence has been overcome, namely the immune system.

The immune system consists of all cells and molecules involved in immunity, and their coordinated response against foreign pathogens or substances is referred to as the immune response.[128] It can be divided into the *innate* immune system, responsible for a first unspecific response, and the *adaptive* immune system, which is highly specific and capable of generating immunologic memory. The innate arm of the immune system is typically active within hours of infection, with the adaptive arm taking over on a timescale of days (Figure 2.1). The adaptive immune system is the specific part of the immune system which can be trained by vaccination and by previous infection, and is therefore capable of suppressing reinfection with a similar pathogen even years after the first encounter.

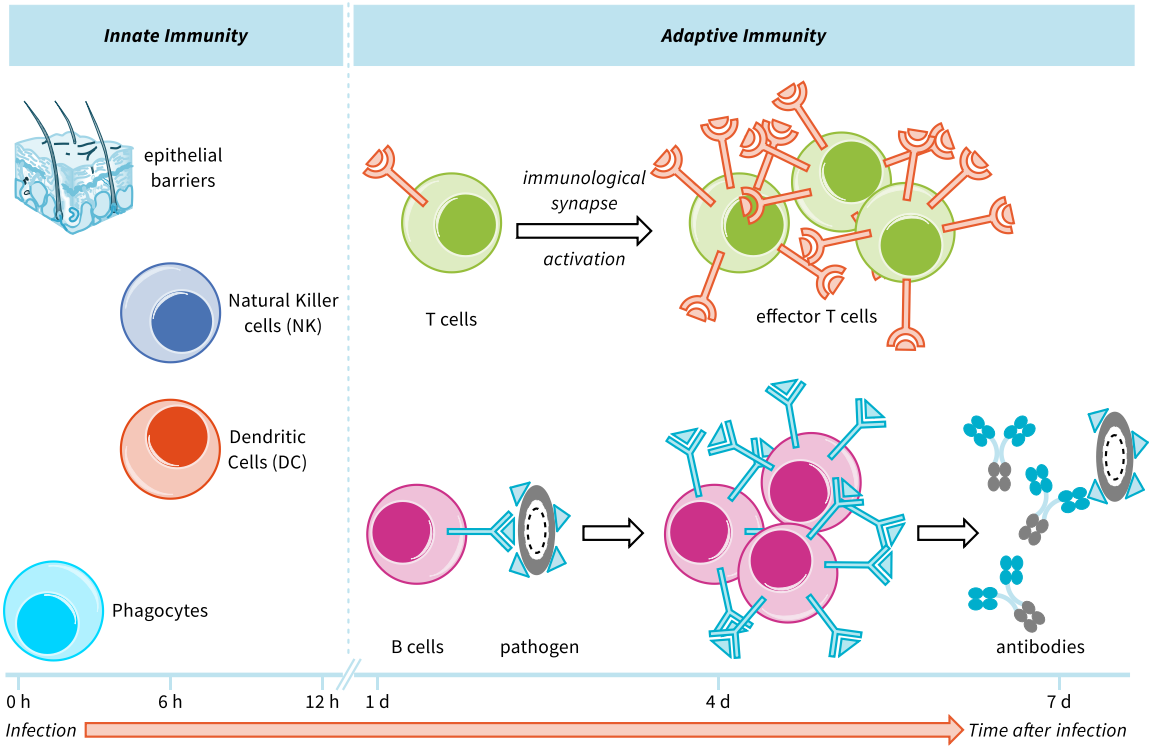

Figure 2.1: Overview of the components and time scale involved in innate and adaptive immunity. Figure adapted from Ref.[128]

Cells belonging to the immune system are found in virtually all tissues of the body, as they are part of the blood and lymphatic system and thus circulate throughout the organism. This dispersion of immune cells to all parts of the body is of critical importance in detecting and fighting off pathogens in a timely manner, regardless of their localisation within the body. Within the immune system, there is a large range of different cell types, which can be identified by their surface antigens (*i.e.* $CD4^+$ T cells or $CD8^+$ T cells, B cells, NK cells, dendritic cells, macrophages, neutrophils, basophils and others) and are readily separated or sorted by modern purification techniques; among these, a commonly experimentally employed group of immune cells are known as peripheral blood mononuclear cells (PBMCs). PBMCs consist, as the name suggests, of all peripheral blood cells with a round nucleus, which are mostly lymphocytes such as B cells, T cells, NK cells, dendritic cells and macrophages.[128]

Immune cells communicate through signalling molecules, typically called cytokines or interleukins (IL), or through the immunological synapse. Cytokine production within immune cells and release of those cytokines can be induced through activation of the immune cells, for example by binding to an infected cell displaying foreign antigens on its surface. Upon activation, immune cells produce and release more cytokines and start proliferating rapidly to expand the immune cell population capable of recognising the

foreign antigen and which are therefore able to adequately respond to the threat. The activation of immune cells is tightly regulated within the human body, as a full-blown immune response can inflict severe damage onto the responding organisms as well.[128]

However, in some cases, the immune system can be triggered against its own organism, leading to what is typically referred to as autoimmune disease. Additionally, while a fully functional immune system is irreplaceable as a means to fight off pathogens, it can be detrimental for patients that require organ transplantation for survival. In both cases, autoimmune disease and organ transplantation, the immune system must be suppressed to ensure the survival of those affected by the condition.[128]

A detailed explanation of the mechanism at play in immune response would go beyond the scope of this thesis and the interested reader is referred to textbooks on immunology for further study.[128]

2.1.2. Immunosuppression, Immunosuppressive Natural Products and their Applications

While an intact immune system is a perfect line of defence for healthy individuals, it can be detrimental in cases where a disease burden can only be lifted through organ transplantation, for example in cases of acute heart or kidney failure. In transplantation settings, the donor tissue or organ is referred to as the graft, while the patient receiving the graft is termed host.

A first approach to immunosuppression was found in the application of the endogenous (*i.e.* produced and found within the human body) glucocorticoid cortisol (**2.001**) (Scheme 2.1). Glucocorticoids like cortisol enact their immunomodulatory properties through binding to the glucocorticoid receptors, which in turn influence the expression of several genes involved in immune response, leading to inhibition of the immune system.[128–130] Glucocorticoids remain an effective treatment option today to modulate the immune system, and derivatives of cortisol, in particular dexamethasone, found widespread application in the COVID-19 pandemic, saving countless lives.[131,132]

Cortisol (**2.001**) remained the only immunosuppressive natural product applied in a clinical setting until the late 1970's, with synthetic drugs being introduced in the meantime (Scheme 2.1). These exhibit their immunosuppressive properties mostly through interference with general DNA synthesis and stability and are therefore most efficacious in rapidly dividing cells, which is one part of the immune response in the proliferation of effector cells.

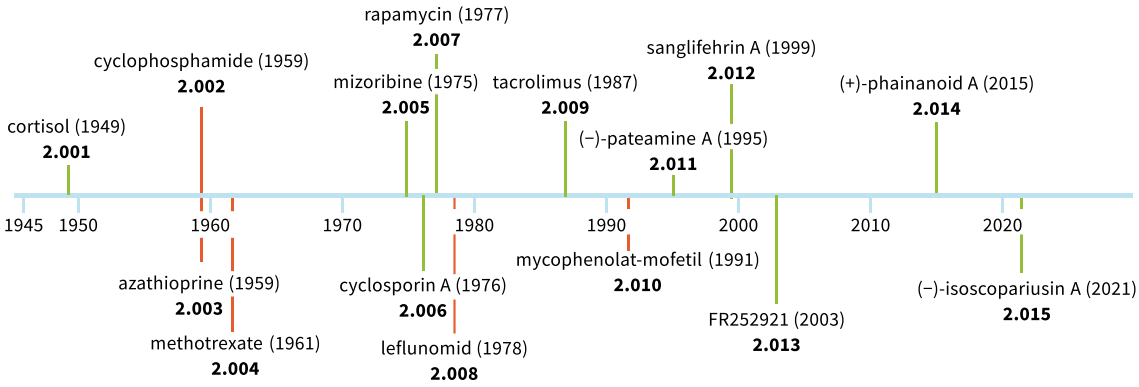
rapamycin (1977)
2.007
cyclophosphamide (1959)
2.002
mizoribine (1975)
2.005
tacrolimus (1987)
2.009
sanglifehrin A (1999)
2.012
(+)-phainanoid A (2015)
2.014
cortisol (1949)
2.001
(−)-pateamine A (1995)
2.011
1945
1950
1960
1970
1980
1990
2000
2010
2020
mycophenolat-mofetil (1991)
2.010
azathioprine (1959)
2.003
cyclosporin A (1976)
2.006
FR252921 (2003)
2.013
(−)-isoscopariusin A (2021)
2.015
methotrexate (1961)
2.004
leflunomid (1978)
2.008

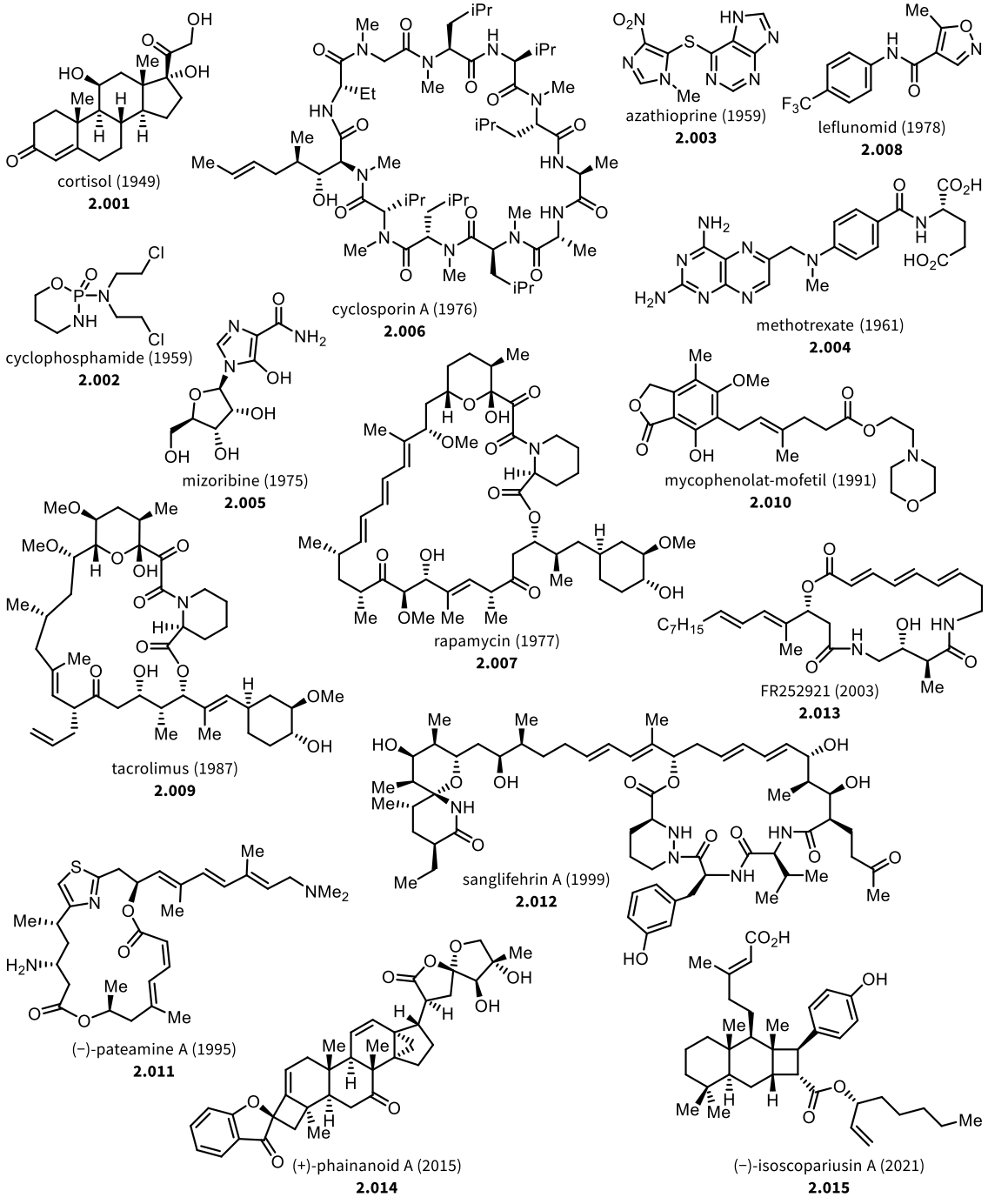
cortisol (1949)
2.001
azathioprine (1959)
2.003
leflunomid (1978)
2.008
cyclosporin A (1976)
2.006
methotrexate (1961)
2.004
cyclophosphamide (1959)
2.002
mizoribine (1975)
2.005
mycophenolat-mofetil (1991)
2.010
rapamycin (1977)
2.007
FR252921 (2003)
2.013
tacrolimus (1987)
2.009
sanglifehrin A (1999)
2.012
(−)-pateamine A (1995)
2.011
(+)-phainanoid A (2015)
2.014
(−)-isoscopariusin A (2021)
2.015

Scheme 2.1: Overview of different molecules capable of suppressing or modulating the immune response. Natural products are connected to the time scale with a green bar, while synthetic molecules are connected with a red bar. The year in parentheses give the year in which the immunomodulating capabilities of the structures were discovered, not the year in which the molecule was discovered or first synthesised.

The discovery of cyclosporin A (CsA, **2.006**) and its immunosuppressive properties sparked research into its clinical application, which ultimately succeeded in the 1980's. It was shown to be more efficacious in preventing graft rejection compared to the previously employed azathioprine (**2.003**), ensuring patient survival after receiving the transplantation.[133–136] Later, the mode of action of CsA was elucidated, showing that CsA exhibits its immunosuppressive properties by binding to a protein called cyclophilin A, which then leads to binding of the CsA-cyclophilin complex to a phosphatase named calcineurin. Calcineurin is responsible for dephosphorylation of a signalling protein (transcription factor) NFAT (nuclear factor of activated T cells). The activation of NFAT through dephosphorylation leads to the transcription of genes responsible for the production of interleukin-2 (IL-2). IL-2 is one of the main signalling molecules required for the activation of T cells, therefore the suppression of the activation of NFAT by inhibition of calcineurin leads to immunosuppression (Figure 2.2).[129,130,136,137] However, it was also found that CsA can be toxic to the kidneys and therefore it is commonly employed in combination with corticosteroids, enabling application of a lower dose, thus leading to reduced toxicity. These toxicity issues also led to the desire to find other immunosuppressive agents, which could be applied in the clinic.[129,136]

Following the success of the calcineurin inhibitor CsA (**2.006**) in suppressing the immune response after organ transplantation, interest in the field of immunosuppressive natural products grew and led to the discovery and application of two other natural products which are still applied as immunosuppressants today: tacrolimus (**2.009**, also referred to as FK506) and rapamycin (**2.007**, also referred to as sirolimus) (Scheme 2.1). Tacrolimus (**2.009**) was first isolated in 1987 and its immunosuppressive properties were discovered alongside its isolation.[138–140] Following initial publication, tacrolimus was quickly enrolled in clinical trials to evaluate its immunosuppressive properties in patients, ultimately being applied successfully and enabling rescue of graft rejection under CsA treatment.[141] Soon after its discovery and the publication of its structure, tacrolimus (**2.009**) became a target for the synthetic community to achieve a total synthesis of this compound, with several total syntheses having been published since.[142–145] Crucially, the synthesis of tacrolimus enabled synthetic material and derivatives to be employed in

mechanistic assays, which led to elucidation of the mode of action of the parent compound.[142,146] It was found that, while structurally distinct from CsA, tacrolimus also suppresses the immune response through inhibition of calcineurin; however, tacrolimus is not capable of binding to calcineurin directly. First, tacrolimus binds to a protein named FKBP-12 (FK506 binding protein), leading to a FK506-FKBP-12 complex capable of binding to calcineurin, which results in immunosuppression.[130,146–148] In this sense, CsA and tacrolimus are similar, in that they first bind to immunophilin proteins (cyclophilin A or FKBP-12) and the thusly formed complexes are capable of binding calcineurin, thereby suppressing the activation of NFAT and ultimately suppressing the T cell response of the immune system (Figure 2.2).

The last immunosuppressive natural product currently used clinically is rapamycin (**2.007**) (Scheme 2.1). Interestingly, rapamycin was discovered more than a decade prior to the discovery of tacrolimus (**2.009**), albeit research interest was initially low, a fact that remained unchanged despite the discovery of its immunosuppressive properties in 1977.[149–151] Rapamycin and tacrolimus (FK506) share some structural similarities which mediate their binding to FKBP-12. However, while the FK506-FKBP12-complex binds to calcineurin, the rapamycin-FKBP12 complex does not. Rapamycin mediates its immunosuppressive properties through the binding of the rapamycin-FKBP12-complex to a protein deemed the mechanistic target of rapamycin (mTOR).[152,153] Again, the elucidation of the mode of action of rapamycin was enabled by the synthetic effort of several working groups, providing synthetic rapamycin as well as derivatives.[154–161] mTOR is a serine-threonine kinase with several functions and is crucial in cell proliferation. Under physiological conditions without inhibition, mTOR is, among other functions, involved in the activation of the S6 kinase through phosphorylation and the activated S6 kinase then phosphorylates S6, a ribosomal protein which is involved in cell proliferation.[162] As a result of this crucial activity of mTOR, its inhibition by the rapamycin-FKBP12 complex leads to inactivated S6 kinase and ultimately to the arrest of cell proliferation in the transition of the G_1 to S phase of the cell cycle. While cell proliferation is affected throughout the whole organism, the effects are most detrimental in rapidly dividing cell populations, including stimulated T cells, thereby leading to immunosuppression (Figure 2.2).

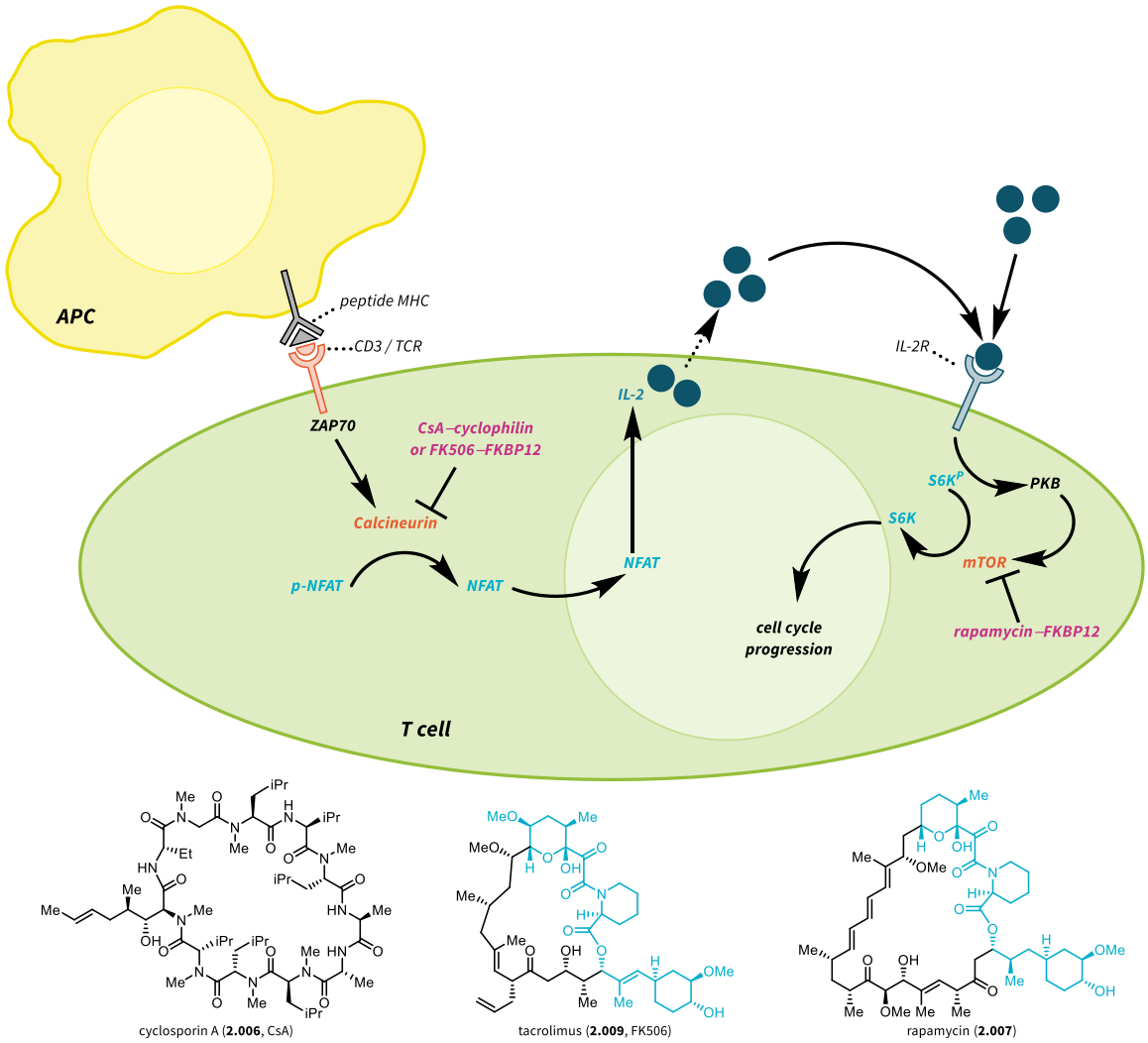

Figure 2.2: Schematic depiction of the cellular signalling pathways inhibited by cyclosporin A (**2.006**), tacrolimus (**2.009**, FK506) and rapamycin (**2.007**). Structurally similar features in tacrolimus and rapamycin are highlighted in blue, as this part of the molecule binds to FKBP12. Activation of a T lymphocyte (green) by an APC (yellow) through MHC-TCR binding is depicted, leading to the activation of calcineurin and subsequent pathways. The activity of calcineurin can be blocked through the action of CsA-cyclophilin or FK506-FKBP12 complexes. The T lymphocyte can alternatively be activated through the binding of IL-2 to the IL-2-Receptor (IL-2R), leading to activation *via* an mTOR-mediated pathway. This activation can be blocked through the action of the rapamycin-FKBP12 complex, leading to cell cycle arrest. Information presented in this scheme was taken and heavily adapted from Kahan.[130]

The seminal discoveries of these immunosuppressive natural products and their unique modes of action have inspired research ever since. Based on these molecules, the field of molecular glue degraders has been established and research into other, novel immunosuppressive natural products with new modes of action has been stimulated, revealing the promising properties of compounds such as (−)-pateamine A (**2.011**), sanglifehrin A (**2.012**), (−)-isoscopariusin A (**2.015**), among many others.[161,163–174] The discovery of novel modes of action additionally bears the potential to reveal further mechanisms at play in immunology and may help alleviate patient suffering, if translated into the clinic.

2.1.3. Electrocyclisations and Torquoselectivity

Electrocyclic reactions are part of the larger class of pericyclic reactions, as introduced in chapter 1.1.,[20,163] and electrocyclic reactions typically involve electrocyclisations, leading to the formation of a cyclic compound, and electrocyclic ring opening reactions, going from a cyclic starting material to an open-chain product. Both processes are theoretically interlinked through an equilibrium, favouring the most thermodynamically stable product. In an electrocyclisation, a new σ-bond is formed, connecting two ends of a conjugated π-system, with the electrocyclic ring opening causing the reverse process, the cleavage of a σ-bond to form a linear (unbranched), conjugated π-system. One of the simplest systems in which such a process can occur is the interconversion of 1,3-butadiene and cyclobutene, however the consideration of substituted p-systems, such as in the case of (*E*.*E*)-2,4-hexadiene (**2.016**) is more insightful (Scheme 2.2).

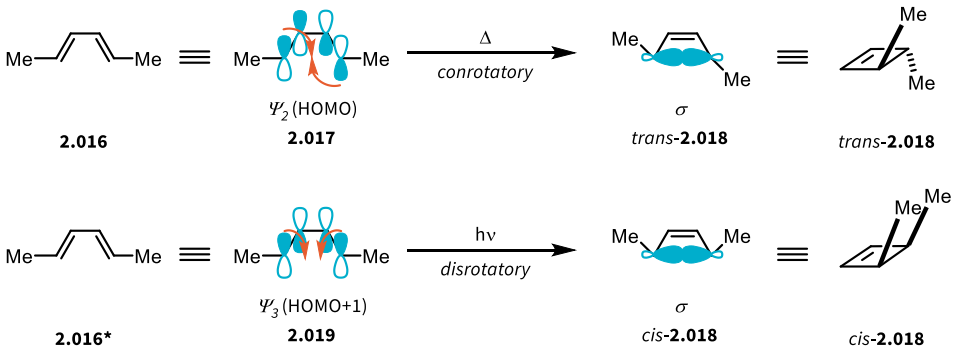

Table 2.1

Amount of electrons	Thermal	Photochemical
4n	conrotatory	disrotatory
4n + 2	disrotatory	conrotatory

Scheme 2.2: Representation of conrotatory and disrotatory electrocyclisations from (*E*,*E*)-2,4-hexadiene (**2.016**) to the *trans*- and *cis*-cyclobutene products (**2.018**). Depending on the orbitals involved, the reaction occurs in a stereoselective fashion to yield a single product through the mechanism depicted above, where n is a natural number or 0.

Much like other pericyclic reactions, the fate of electrocyclic reactions can also be anticipated by consideration of the Woodward–Hoffmann rules for the conservation of orbital symmetry.[20,175] Due to this required conservation of orbital symmetry, electrocyclic reactions can occur in either a conrotatory or disrotatory fashion, depending on the number of electrons involved and the mode of activation

dictating the orbitals involved in the process (Scheme 2.2, Table 2.1). Systems involving larger π-systems are amenable to the same processes and the same rules apply.

In the example above, the use of a (*Z*,*E*)-2,4-hexadiene would lead to similar products, which are accessible through the other mode of rotation, meaning that *trans*-**2.018** would be the product of disrotatory electrocyclisation and *cis*-**2.018** being the product of conrotatory electrocyclisation. The terms disrotatory and conrotatory refer to the direction of rotation the orbitals involved in bond formation undergo. If these orbitals rotate in the same direction, the process is termed conrotatory, while rotation in different directions is termed disrotatory.

When considering the reverse process, the electrocyclic ring opening of substituted cyclobutenes, one has to consider the direction of dis- or conrotation, as well as the orientation of substituents in the cyclobutene (*cis*- or *trans*-configured), as a range of products is theoretically possible from the electrocyclic ring opening. For the context of the topics discussed within this thesis, the thermal, conrotatory electrocyclic ring opening of substituted cyclobutenes involving four π-electrons will be considered going forward.

As described by the Woodward-Hoffmann rules and outlined above, the thermal electrocyclic ring opening of cyclobutenes has to follow a conrotatory mechanism to afford the open-chain products. Within this limitation, the conrotation may still proceed through two pathways, as R^1 can potentially rotate either inward or outward and, depending on the configuration of the starting material (*cis* or *trans*-**2.020**), all four possible isomers of the resulting diene are theoretically accessible (**2.021**, Scheme 2.3). As the whole process is conrotatory, the rotation of R^1 determinates the rotation of R^2 and vice versa.

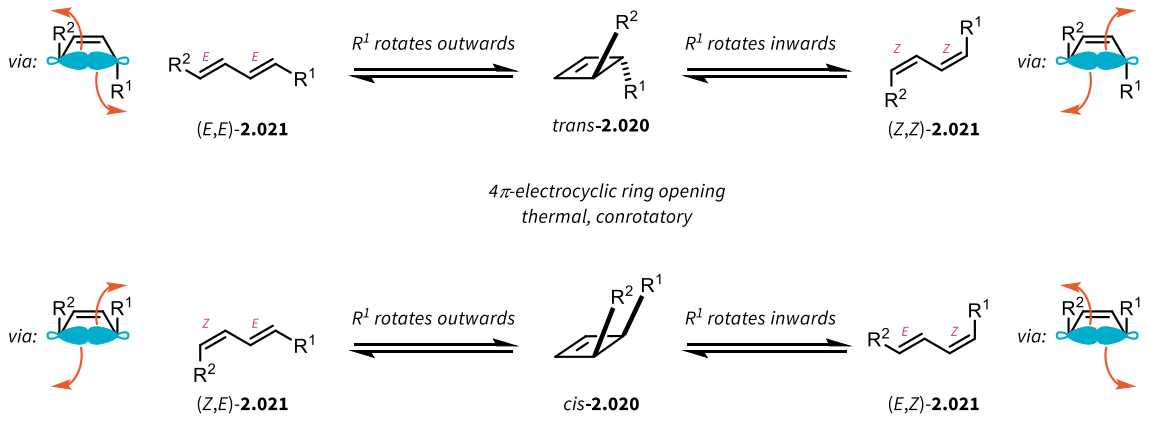

Scheme 2.3: All possible modes of 4π-electrocyclic ring opening of *trans*- and *cis*-configured disubstituted cyclobutenes in a conrotatory fashion.

After the theoretical groundwork had been established by Woodward and Hoffmann, establishing that thermal 4π-electrocyclic ring openings progress in a conrotatory fashion, its predictions were confirmed through experimental work by many groups.[176] However, while only the predicted products of conrotatory 4π-electrocyclic ring openings for thermal processes were detected,[176–178] it remained unexplained why only one of the two possible products of conrotatory ring opening was found for unsymmetrically 3,4-disubstituted cyclobutenes (not shown).

Later, Frey found that 3,3-disubstituted cyclobutenes underwent thermal conrotatory 4π-electrocyclic ring opening to preferentially form the product resulting from inward rotation of the larger substituent,[179] and these studies were later expanded Curry and Stevens, who conducted systematic studies of 3,3-disubstituted cyclobutenes (**2.022**) to find that the observed products could not be explained by sterics alone (**2.023** and **2.024**, Scheme 2.4).

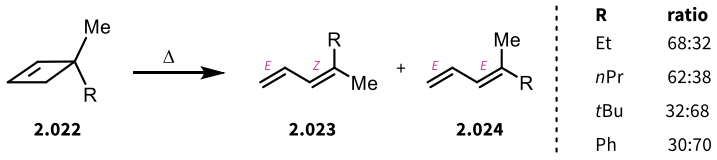

R	ratio
Et	68:32
*n*Pr	62:38
*t*Bu	32:68
Ph	30:70

Scheme 2.4: Systematic study of Curry and Stevens on the conrotatory opening of 3,3-disubstituted cyclobutenes (**2.022**) to find a change in selectivity for product formation across different substituents.

These results were taken as inspiration by Houk *et al.* to develop what is today known as the principle of *torquoselectivity*, which describes the preference of a given substituent to rotate inward or outward in electrocyclic ring opening reactions.[176,180–184] Within torquoselective electrocyclic ring-opening reactions it was established that the direction of rotation of substituents depends on steric as well as electronic effects. Outside of the fairly obvious steric explanation, *i.e.* that very large substituents are required to rotate outward due to their respective size, the electronic side of the substituent effect is more complex. For a given substituent R, the outward rotation of the substituent is favoured if it: a) stabilises the overlap between the bonding $\sigma(C_3–R)$ orbital and the antibonding $\sigma^*(C_3–C_4)$ orbital and b) leads to a reduction in repulsion between the $\sigma(C_3–R)$ and $\sigma(C_3–C_4)$ orbitals (Scheme 2.5A). These conditions are fulfilled well if R is of electron-donating character and in the case that R is a strong electron acceptor, the inward rotation is favoured. In extreme cases, these electronic requirements trump steric effects, as was demonstrated by Houk *et al*. using 3-(*t*Bu)-3-methoxycyclobutene (**2.026**, X = OMe). This molecule underwent thermal

conrotatory 4π-electrocyclic ring opening to yield **2.027**, resulting from inward rotation of the sterically encumbered *tert*-butyl moiety, demonstrating the strong electronic effects displayed by the electron-donating methoxy moiety, forcing its own outwards rotation over that of the significantly more demanding *t*Bu group (Scheme 2.5B).[185]

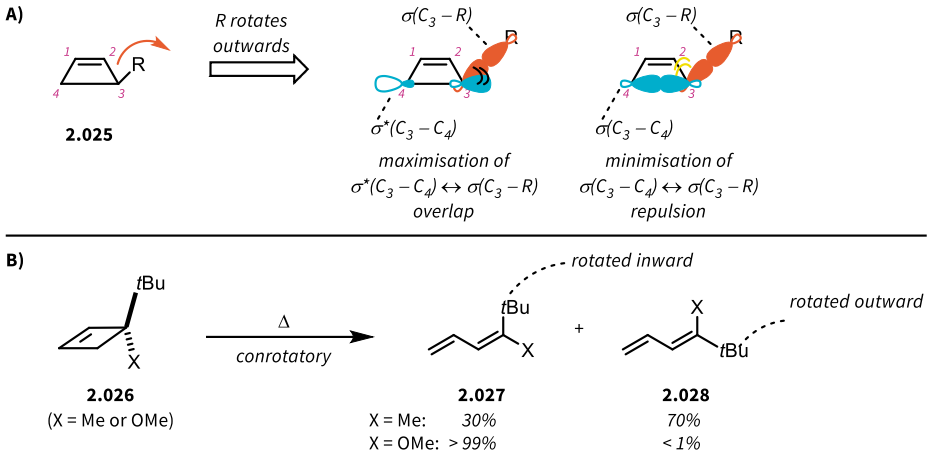

Scheme 2.5: A) Orbital considerations for the propensity of substituents to force outward rotation upon electrocyclic ring opening. B) Strong electronic influence overcoming steric demand to force a *t*Bu group to rotate inward.

2.1.4. The Chemistry of Cyclobutenes

Among the several syntheses for cyclobutenes, the 4π-electrocyclisation of 2-pyrone (**2.029**) under photochemical conditions, leading to 2-oxabicyclo[2.2.0]hex-5-en-3-one (**2.030**, referred to as bicyclo[2.2.0]lactone), which contains the desired cyclobutene moiety has proven particularly useful (Scheme 2.6). This method was first developed by Corey *et al*. and has recently been modernised to be amenable to flow chemistry.[186–188] Photochemical electrocyclisation is possible *via* the predicted disrotatory pathway, as described by the Woodward-Hoffmann rules from the Ψ_4 orbital of **2.029**, with a corresponding thermal disrotatory process being impossible due to the required *trans*-configuration of the product, which is not possible in a four membered ring. The bicyclo[2.2.0]lactone could also be viewed as the smallest possible allylic lactone, as the double bond is in the allylic position relative to both the oxygen as well as the carbonyl-C of the molecule. When viewing this substituted cyclobutene as an allylic system, the reactions used to modify allylic systems in general could be considered to be applied here.

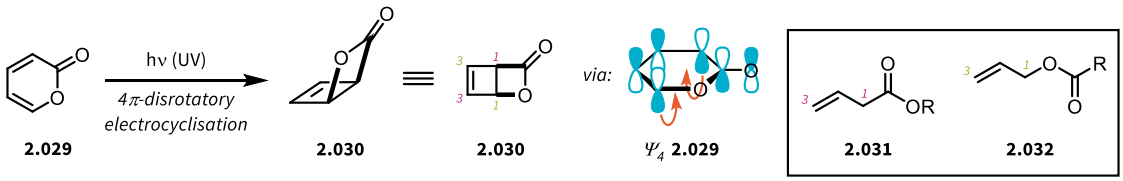

Scheme 2.6: Synthesis of bicyclo[2.2.0]lactone **2.030** from 2-pyrone (**2.029**) *via* a photochemical disrotatory process enabled by the Ψ_4 orbital of **2.029**. The allylic character of **2.030** is highlighted by numbering with respect to the carbonyl-C (pink numbers) or the hydroxy-O (green numbers) and comparative allylic systems (**2.031** and **2.032**) are given.

A prime example of reactions on allylic systems is the venerable Tsuji-Trost reaction, which describes the modification of allylic substrates bearing a leaving group *via* a palladium catalyst and a nucleophile to deliver the product of nucleophilic substitution (Scheme 2.7).[189,190] The reaction can be rendered enantioselective by the use of chiral ligands to coordinate the catalytically active Pd species, which has led to the broad application of this reaction within the context of total synthesis and beyond.[191,192] Two representative examples are displayed in Scheme 2.7, showcasing the application of the Tsuji-Trost reaction. In a first example, the asymmetric Tsuji-Trost reaction is applied in the total synthesis of wine

lactone, (−)-**2.036**, starting from allylic acetate **2.033**. The OAc moiety can act as a leaving group upon the addition of the chiral palladium species to form the required allyl palladium intermediate. Addition of the nucleophile then leads to the highly enantioselective formation of the desired product (**2.035**) in excellent yield (Scheme 2.7A; general mechanism depicted in Scheme 2.10).

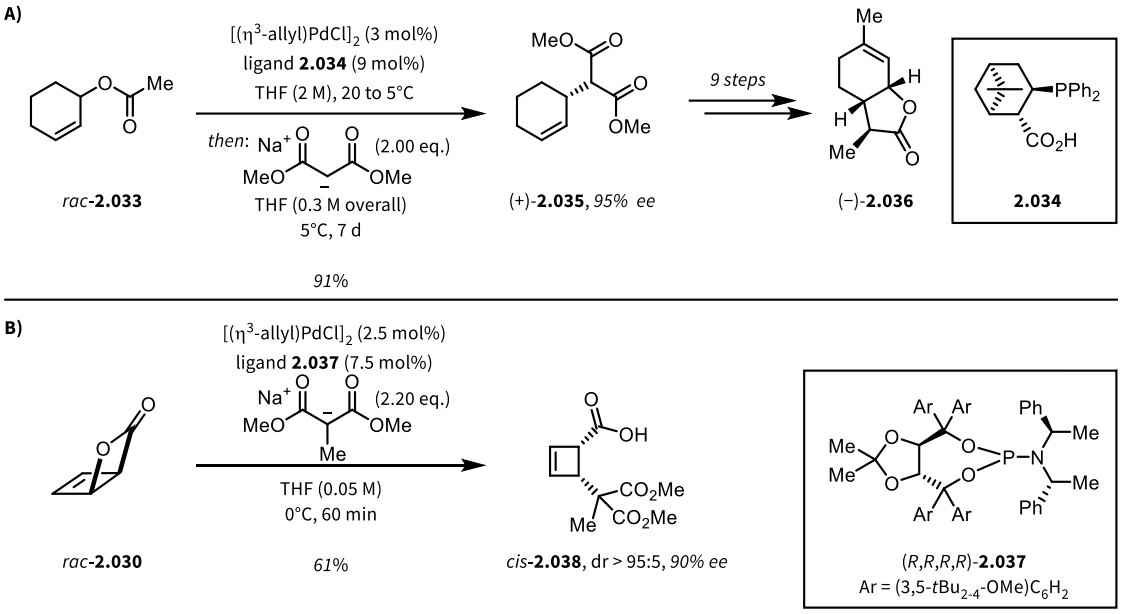

Scheme 2.7: A) Representative asymmetric allylic alkylation of *rac*-**2.033** to form (+)-**2.035** using a malonate nucleophile. B) Asymmetric allylic alkylation of *rac*-bicyclo[2.2.0]lactone (**2.030**) using a chiral phosphoramidite ligand (**2.037**).

Showing how closely related the bicyclo[2.2.0]lactone (**2.030**) is to open-chain allylic systems, a similar transformation was realised by Maulide *et al*. in their diastereo- and enantioselective asymmetric allylic alkylation of a racemic starting material to yield the alkylated cyclobutenecarboxylic acid product **2.038**.[193] The reaction progresses in a similar fashion to the typical Tsuji-Trost reaction, with the added benefit that the leaving group, the carboxylate, remains in the molecule to form the carboxylic acid of the product (Scheme 2.7B). It could be shown that the asymmetric allylic alkylation of racemic bicyclo[2.2.0]lactone **2.030** could be conducted in a diastereo- and enantiodivergent manner, meaning that from one racemic starting material, **2.030**, each and every of the four diastereo- and enantiomers could be synthesised, with the outcome being determined solely by the choice of ligand for the palladium species (Scheme 2.8).

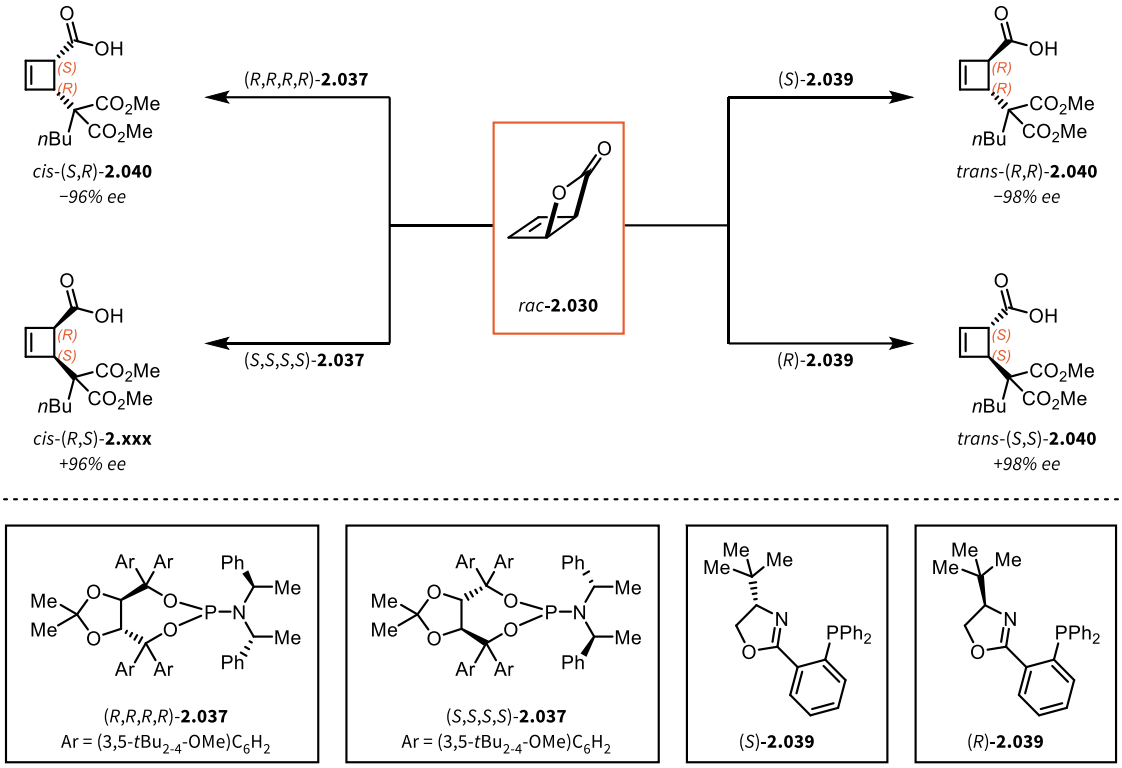

Scheme 2.8: Diastereo- and enantiodivergent synthesis of alkylated cyclobutenecarboxylic acids through an asymmetric Tsuji-Trost reaction as presented by Maulide *et al*.

When trying to expand the developed methodology to a broader range of nucleophiles, as is possible for the Tsuji-Trost reaction on regular allylic systems, it was found that for some nucleophiles the desired cyclobutenecarboxylic acids are not the products of the reaction, but rather a range of diene products was afforded (Scheme 2.9).[194,195] In the event, the attack of the nucleophile on the allylic system leads to the expected formation of the *cis*- or *trans*-configured product, depending on the character of the nucleophile (*vide infra*, Scheme 2.10). Subsequently, some products undergo spontaneous thermal conrotatory 4π-electrocyclic ring opening to yield dienecarboxylic acids (Scheme 2.9). Together, these methods to synthesise functionalised cyclobutenes have been expanded upon to yield valuable building blocks, such as aryl vinyl ether **2.043**, dieneyne **2.046** and vinyl azide **2.048**.[188,193–200]

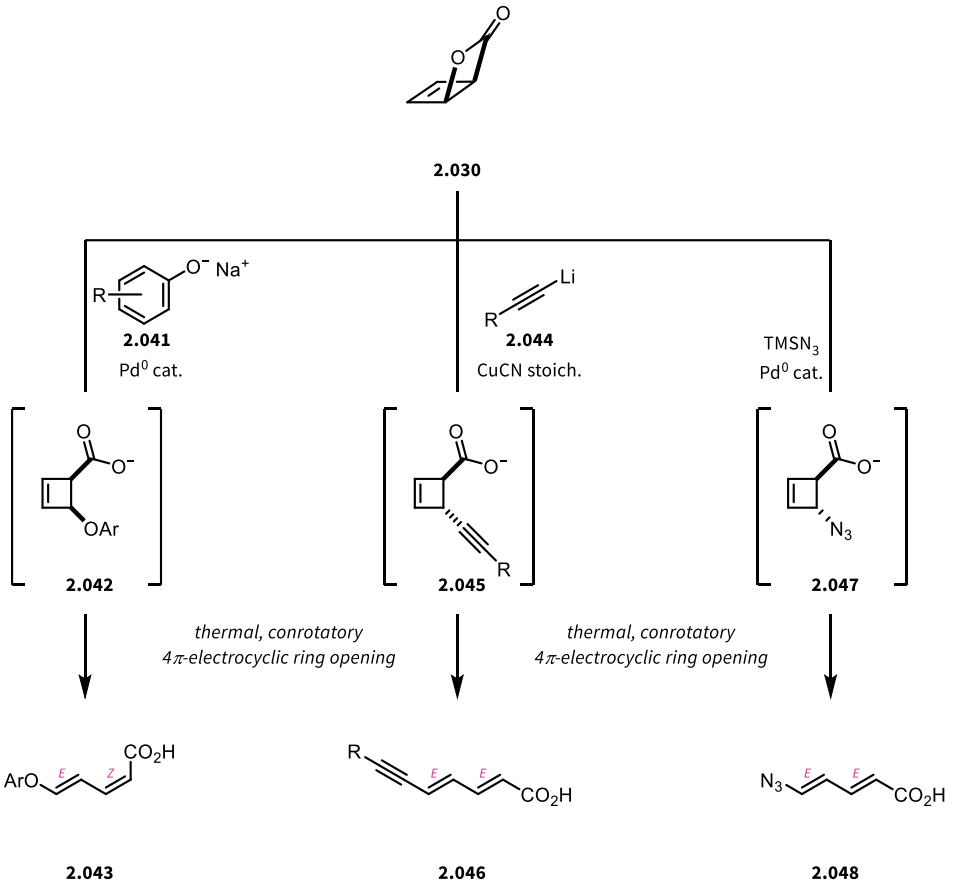

Scheme 2.9: Functionalisation of bicyclo[2.2.0] lactone **2.030** with phenolic (**2.042**), acetylenic (**2.044**) and azide nucleophiles, leading to the formation of either *cis*- or *trans*-cyclobutenecarboxylate intermediates, which undergo spontaneous thermal conrotatory 4π-electrocyclic ring opening to yield functionalised dienecarboxylic acids.

To fully understand how different stereoisomers of dienes, (*E*,*E*) and (*Z*,*E*), can be obtained from the same starting material under seemingly similar conditions, the mechanism of the Tsuji-Trost reaction needs to be more deeply examined (Scheme 2.10). The oxidative addition of a Pd^0-species to an allylic system bearing a leaving group X occurs with inversion of configuration to yield the η^3-allyl palladium(II) complex (**2.050**). This η^3-complex is capable of isomerisation, allowing (in the case of substrates possessing the required symmetry) the kinetic resolution of material and enantioselective transformations. In the special case of cyclobutene substrates, the putative η^3-allyl complex is symmetrical and therefore enantioselective reactions are enabled by the ability of chiral ligands to direct the trajectory of incoming nucleophiles to form the enantiomerically pure products from a symmetric intermediate (**2.054**). As mentioned, the η^3-complex is consumed by the nucleophile employed in the reaction. Here, nucleophiles can be grouped according to the stabilisation of their negative charge, with “hard” nucleophiles referring to species in which the charge is not stabilised, while “soft” refers to nucleophiles with a stabilised

negative charge.[201,202] Soft nucleophiles tend to engage the η^3-allyl palladium complex from outside of the coordination sphere (so-called outer-sphere addition), leading to inversion of configuration upon reductive elimination of the Pd^0-species. Since the addition of Pd^0 also occurred with inversion of configuration, this second inversion leads to global retention of configuration. In contrast to this, hard nucleophiles are more prone to attack the metal center of the complex, an inner-sphere addition, and subsequently engage the allylic system from the same face as the palladium upon reductive elimination, a process with retention of configuration relative to the palladium complex. Since, as previously mentioned, oxidative addition to the allylic system occurs with inversion of configuration, hard nucleophiles lead to products with inverted configuration, as reductive elimination does not lead to a second inversion.

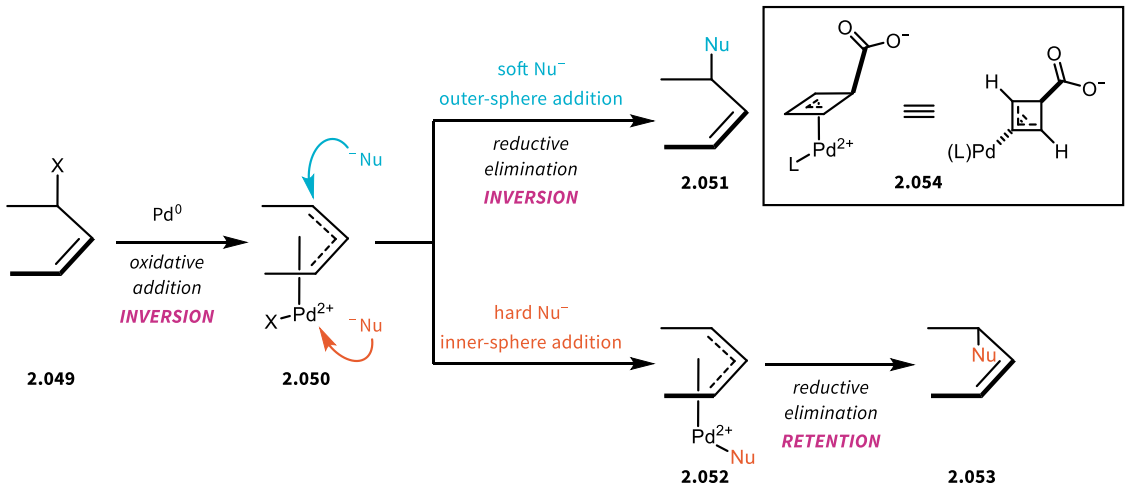

Scheme 2.10: Simplified overview of the stereochemical considerations for the Tsuji-Trost allylic alkylation reaction. Oxidative addition to form the η^3-allyl palladium species (**2.050**) occurs with inversion of configuration. **2.050** can then be attacked by the nucleophile present. Depending on the character of the nucleophile, hard or soft, the attack occurs either with a second inversion of configuration, as is the case for soft nucleophiles, to directly form **2.051** under global retention or, for hard nucleophiles, the attack occurs on the metal center to form **2.052**. This intermediate can then undergo reductive elimination under retention of configuration to yield the product **2.053** with global inversion of configuration.

Lastly, in order to synthesise cyclobutenecarboxylic acid building blocks to enable further functionalisation and application as building blocks in complex synthetic sequences, Maulide *et al.* surmised that simple nucleophiles, such as halides, are capable of opening the bicyclo[2.2.0]lactone to furnish either *cis*- or *trans*-halocyclobutenecarboxylic acids (**2.055** or **2.057**).[196] These can directly be applied as building blocks in their own right or the cyclobutenes can be thermally opened under microwave irradiation to yield the corresponding dienes (Scheme 2.11).

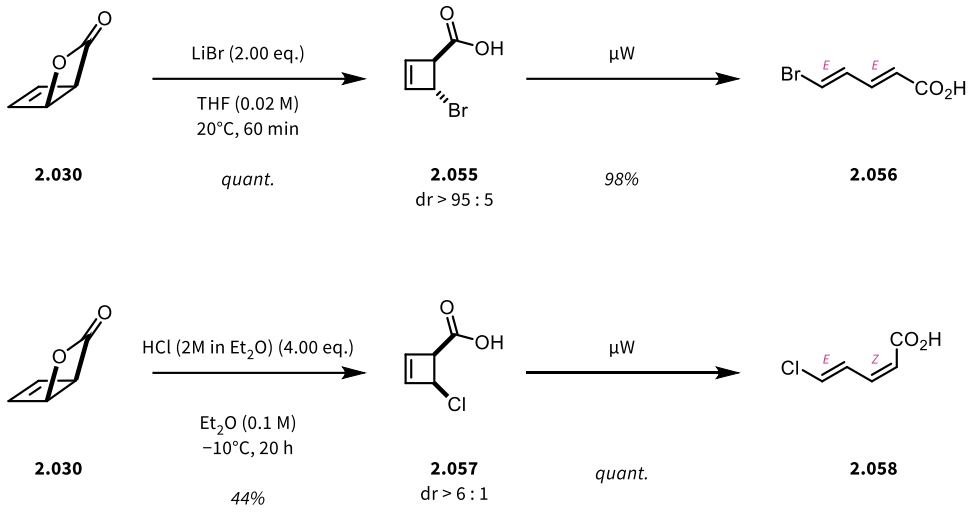

2.030 *quant.* **2.055** dr > 95 : 5 *98%* **2.056**

2.030 *44%* **2.057** dr > 6 : 1 *quant.* **2.058**

Scheme 2.11: Synthesis of halogenated cyclobutenecarboxylic acids and open diene products as a result of thermal electrocyclic ring opening.

2.1.5. Different Approaches towards Macrocyclisations

When exploring the realm of biologically active natural products, regardless whether in an immunosuppressive, antiproliferative, antibacterial or other context, one is quick to notice the ubiquity of compounds containing cyclic structures or substructures. For example, if Figure 2.1 from within this thesis is recalled, all of the natural products depicted therein contain cyclic structural features with most of the immunosuppressive natural products, such as rapamycin (**2.007**), CsA (**2.006**), tacrolimus (**2.009**) or sanglifehrin A (**2.012**), containing a macrocyclic core. This observation is most commonly explained by the structural preorganisation of the molecular structure lowering the entropic penalty arising from binding of the natural product to its target protein. Such entropic influences on the biological activity of macrocyclic compounds can be quite dramatic and, if reduced through introducing more degrees of freedom, the biological activity may be completely lost.[203] The term "macrocycles" typically refers to a cyclic structure of twelve atoms or more, but in the context of this thesis, cyclic moieties of ten or more atoms shall be considered.

A comparison of the open-chain and macrocyclic forms of a given molecule showcases the higher degree of freedom of the former and the ring strain of the latter, macrocyclisation events are typically key strategic events in a given synthetic sequence towards the construction of biologically active natural products bearing macrocyclic structures. Among the established macrocyclisation techniques to forge the cores of complex natural products, macrolactonisations,[166,204–208] macrolactamisations,[209–211] and alkene or alkyne ring-closing metathesis reactions are dominant.[212–220] These reactions typically need to be conducted at high dilution of the linear precursors, as the macrocyclisation inevitably competes with dimer formation.

With respect to the large class of macrolactonisation reactions, three commonly employed named macrolactonisation reactions are the Yamaguchi,[221] Mukaiyama,[222] and Shiina macrolactonisations.[223,224] Each of these methods relies on the generation of a mixed acid anhydride to activate the carboxylic acid, facilitating intramolecular attack of the hydroxy moiety to enable ring closure. For example, a Shiina macrocyclisation process was used in the recent synthesis of the antibiotic

macrolide luminamicin (**2.062**) by Sunazuka *et al.* to cyclise the precursor **2.059**, yielding product **2.061**, which contains a 10-membered ring (Scheme 2.12).

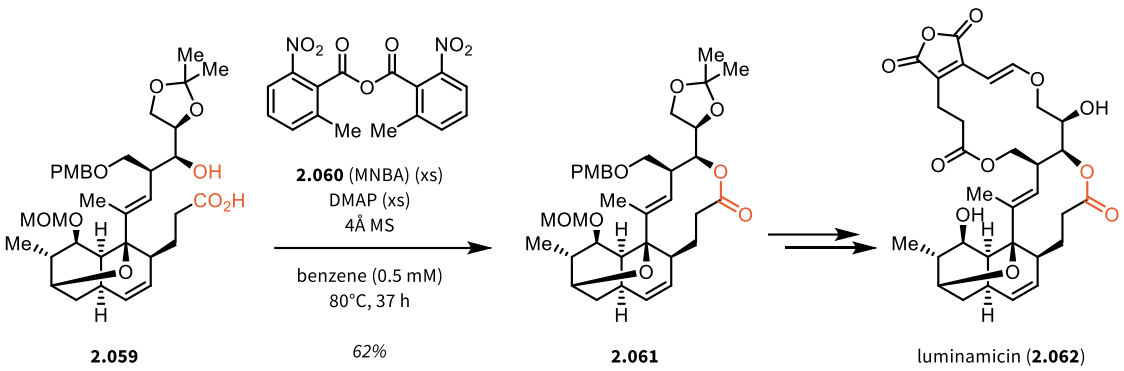

Scheme 2.12: Crucial Shiina cyclisation event in the total synthesis of luminamicin (**2.062**).

The Larock indole synthesis,[225] typically conducted catalytically and intermolecularly and not often used to form macrocyclic structures, has been recently applied by Sarlah *et al.* and Baran *et al.* in their independent approaches towards darobactin A (**2.064**),[226,227] a natural product with promising activity against Gram-negative bacteria.[228] In the final steps of the Sarlah synthesis of darobactin A, an advanced precursor carrying an alkyne and a bromoaniline moiety (**2.063**) was engaged in an intramolecular Larock reaction to yield the western macrocycle of the natural product darobactin A (Scheme 2.13). Interestingly, the Larock reaction seemed to be the only viable option to forge the two macrocycles present in darobactin A, as both the Sarlah and the Baran syntheses applied Larock reactions for the formation of all macrocycles.

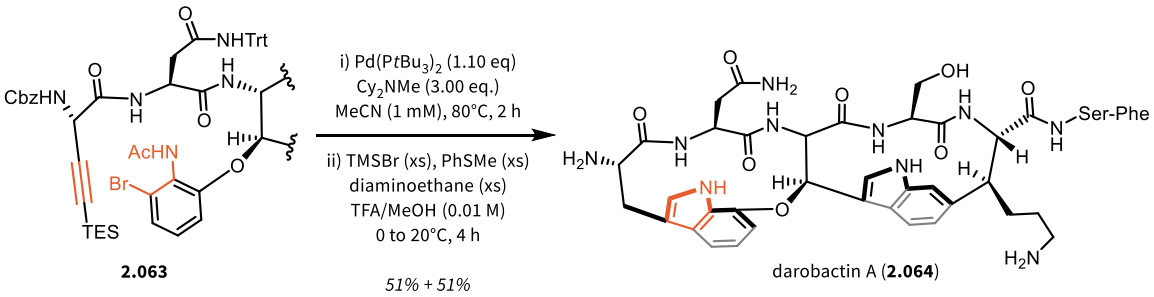

Scheme 2.13: Late-stage Larock cyclisation as applied by Sarlah *et al.* in their approach to darobactin A (**2.064**), a novel antibiotic active against Gram-negative pathogens.

Staying on the topic of Pd-catalysed reactions, two more natural product total syntheses with remarkable macrocyclisation steps shall be considered, namely the syntheses of sanglifehrin A (**2.012**),[171,229] and rapamycin (**2.007**), two immunosuppressive polyene natural products.[154–160,220–226] While there are several completed total synthesis campaigns for both natural products,[154–160,173,230–235] the total syntheses by

Nicolaou *et al*. for both sanglifehrin A as well as rapamycin include inspiring macrocyclisation approaches.

The discovery of sanglifehrin A (**2.012**) was disclosed in 1999 and soon after, the first synthetic approaches were published. As depicted in Scheme 2.1, sanglifehrin A bears immunosuppressive biological activity and was therefore also investigated in a biological context to reveal its capability to bind to calcineurin.[172,236–238] In terms of the synthetic approach towards sanglifehrin A by Nicolaou *et al*., one key aspect in the synthetic sequence was found in the selective macrocyclisation of bis-vinyl iodide **2.065** (Scheme 2.14).[173,231] This compound, when subjected to Pd-catalysis at high dilutions, was found to form the desired 22-membered macrocycle in a regioselective fashion, differentiating between the two vinyl iodide moieties present within the precursor.

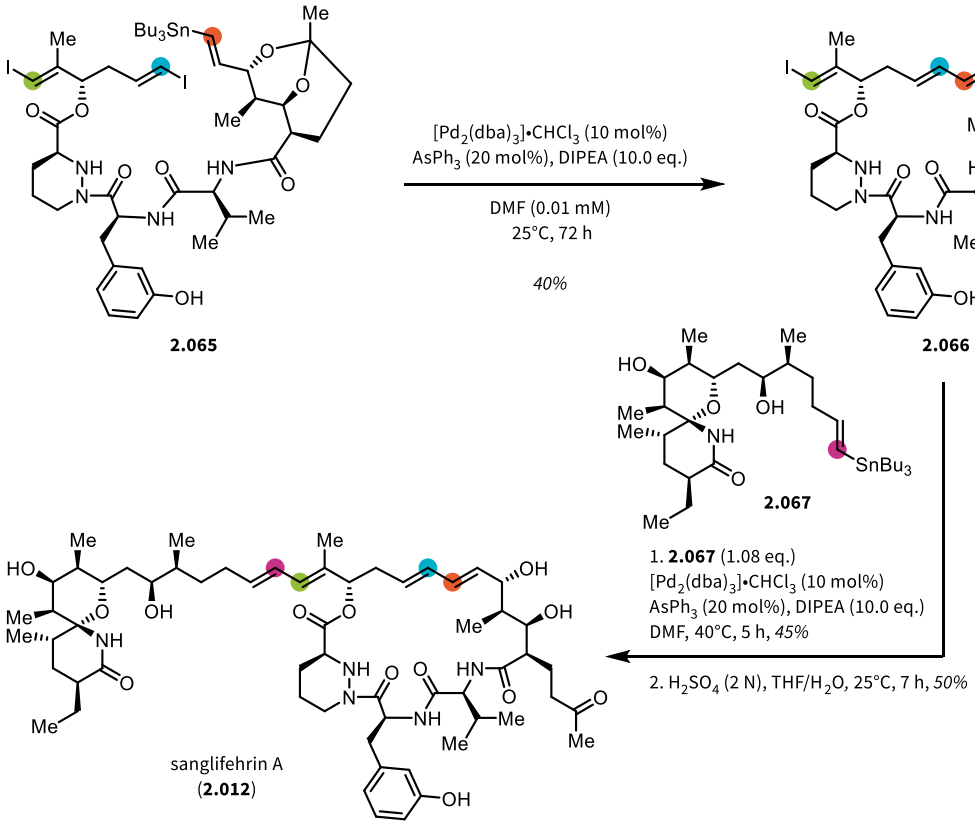

Scheme 2.14: Total synthesis of sanglifehrin A (**2.012**) as carried out by Nicolaou *et al*. to forge the 22-membered macrocyclic core *via* a regioselective Stille coupling of bis-vinyl iodide **2.065**.

Another stunning feat in total synthesis can be found in the "stitching" approach to rapamycin by Nicolaou *et al*.[154,156–160] In this synthesis of rapamycin (**2.007**), the 29-memebered macrocyclic core of the natural product was closed at the very end of the synthetic sequence. To achieve this, the unprotected bis-vinyl iodide **2.068** was reacted with vinyl-1,2-bisstannane **2.069** to form the desired macrocycle to

yield rapamycin (**2.007**) without the need for further deprotection operations after a double Stille-coupling. Additionally, unreacted starting material could be reisolated alongside the intermediate vinylstannane **2.070**. This by-product grants insight into the order of regioselective Stille couplings occurring in the reaction mixture. First, the intermolecular Stille coupling between **2.069** and the more accessible iodide of **2.068** takes place to deliver the lynchpin-precursor for the anticipated macrocyclisation. Since the reaction is carried out at high dilution, the second Stille coupling occurs, this time in an intramolecular fashion to form the desired macrocycle and deliver rapamycin (**2.007**).

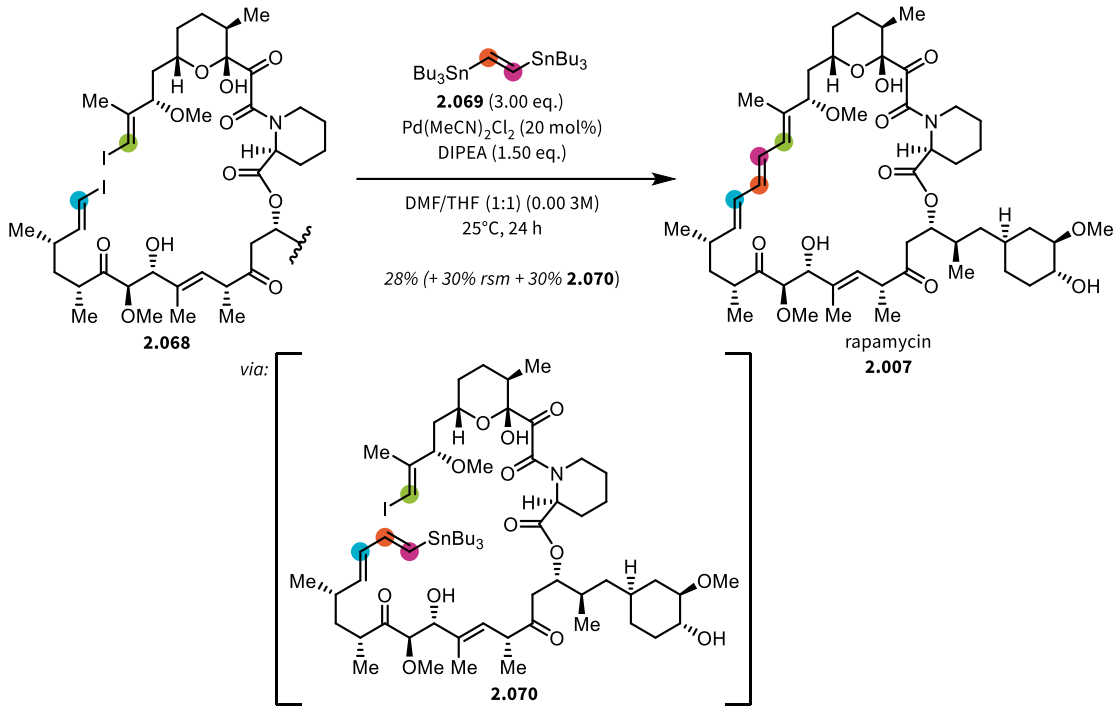

Scheme 2.15: Late-stage "stitching" double Stille-coupling / macrocyclisation of **2.068** towards rapamycin (**2.007**) *via* the intermediate vinylstannane **2.070**, which can be isolated as part of the product mixture.

Rapamycin (**2.007**) itself has sparked highly creative synthetic approaches, summarised in Scheme 2.16.[154] For example, while Nicolaou's first total synthesis of rapamycin relied on the "stitching" double Stille coupling process to facilitate formation of the 29-membered macrocyclic core of the natural product, Schreiber *et al*. forged the macrocycle through an adaptation of Mukaiyama macrolactonisation conditions to their precursor, resulting in smooth macrolactamisation of the amino acid precursor **2.071**.[156] Danishefsky *et al.*, also publishing their work in 1993, chose an entirely different route to achieve macrocyclisation. In this approach, the use of a Lewis acid ($TiCl_3(OiPr)$) enabled an intramolecular aldol reaction of aldehyde **2.072**, which simultaneously closed the macrocycle and set one of the

stereocentres of rapamycin.[157] Later, Ley *et al*. chose a catechol-templated macrocyclisation approach starting from **2.073**. In this case, the catechol is later eliminated from the intermediate to ultimately yield rapamycin.[231–233] Finally, Smith *et al*. published their synthesis of rapamycin, which featured a more traditional Stille coupling to close the macrocycle from the open-chain precursor **2.074**.[159,160]

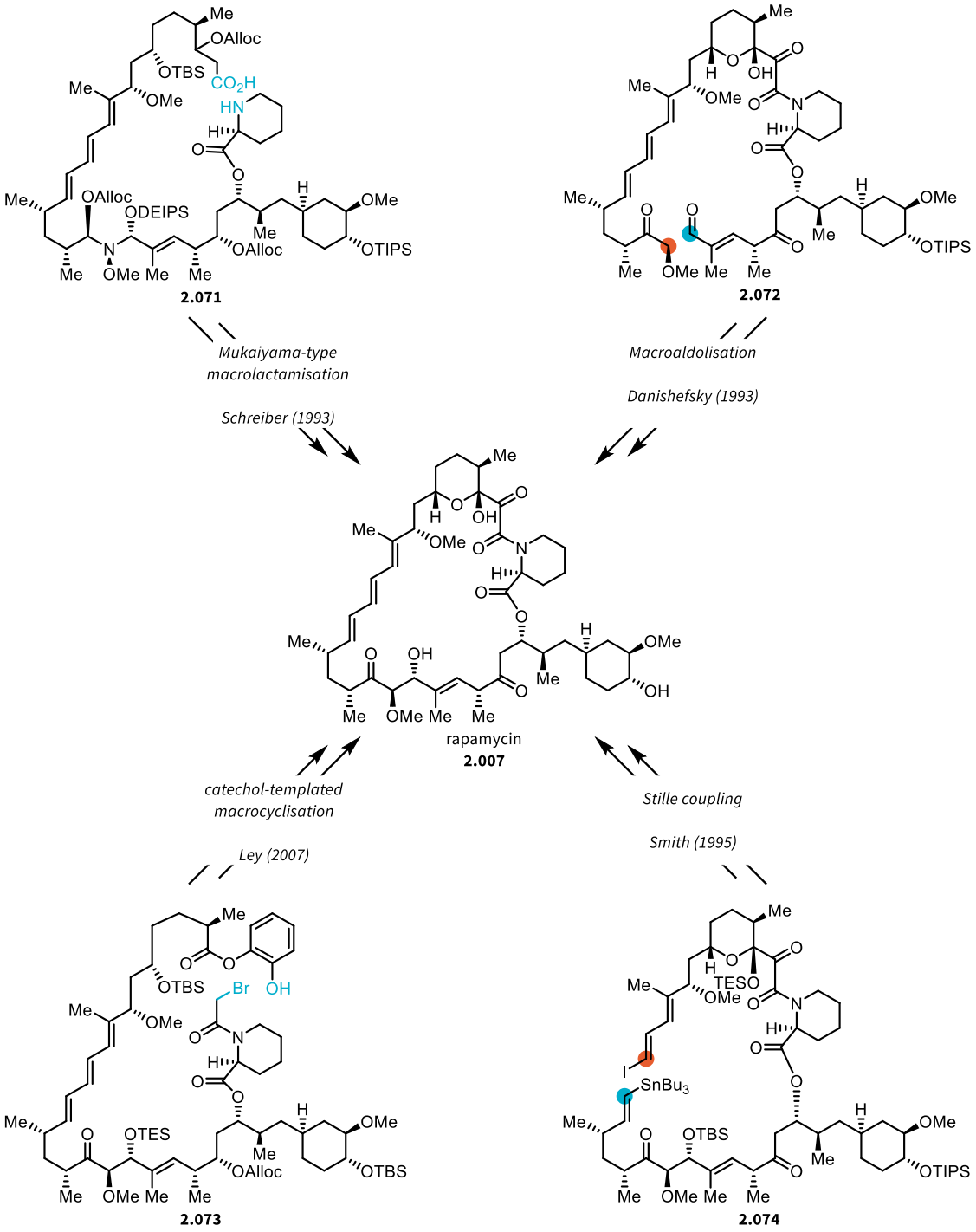

Scheme 2.16: Alternative approaches to rapamycin (**2.007**) by Schreiber *et al*., Danishefsky *et al*., Smith *et al.* and Ley *et al.* The various approaches feature Mukaiyama-type macrolactamisation (Schreiber), intramolecular aldol reaction (Danishefsky), Stille macrocyclisation (Smith) and a templated macrocyclisation (Ley).

2.1.6. The FR252921 Family of Immunosuppressive Natural Products

2.1.6.1. Discovery of the FR Molecules and their Immunosuppressive Properties

After the breakthroughs enabled by the application of immunosuppressive natural products in medicine, several research programs were initiated aiming at discovering the next generation of immunosuppressive agents. One of these research programs, conducted at Fujisawa Pharmaceutical Co., Ltd. in Japan, ultimately led to the discovery of the FR252921 family of natural products, which includes three compounds, FR252921 (**2.013**), FR252922 (**2.075**) and FR256523 (**2.076**), which will be referred to as the "FR molecules" for the remainder of this thesis (Scheme 2.17). The FR molecules were isolated from a cultural broth of the Gram-negative bacterial species *Pseudomonas fluorescens* No. 408813 (abbreviated *P. fluorescens*) and were subsequently shown to possess immunosuppressive biological activity in a range of biological assays.[239–241]

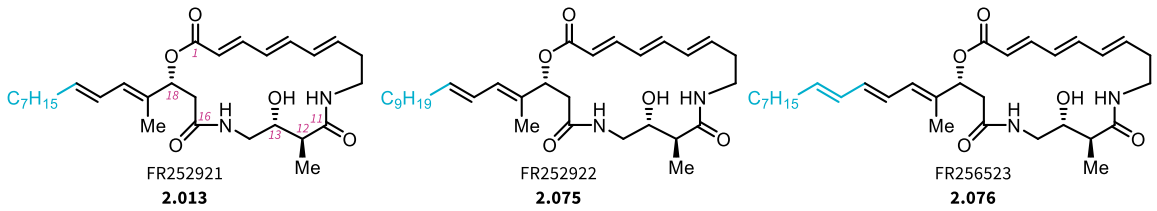

Scheme 2.17: The FR252921 family of natural products with its three members, FR252921 (**2.013**), FR252922 (**2.075**) and FR256523 (**2.076**).

Structurally, the FR molecules are composed of a 19-memberd macrocyclic core, to which a side-chain, differentiating the three natural products, is attached. While the side-chain does bear functional groups through the presence of (*E*)-configured double bonds, the main structural features of the FR molecules are located within the 19-membered macrocyclic core. The macrocycle contains all three stereocentres (12*S*, 13*R*, 18*R*), as well as two lactams (C-11 and C-16) and one lactone (C-1). Crucially, the macrocycle also contains three conjugated double bonds adjacent to the lactone carbonyl, forming a trienoate. All double bonds are of (*E*)-orientation, thereby potentially exerting strain onto the macrocycle.

The FR molecules were deemed of high interest following their isolation, as their immunosuppressive biological activity was found to be synergistic with tacrolimus (**2.009**) in a murine skin graft experiment. Therein, the combination of tacrolimus with FR252921 was shown to prolong, when compared to either drug alone, survival of the hosts receiving the allograft. Since the use of tacrolimus can be assumed to fully block the calcineurin pathway, this would indicate a mode of action for FR252921 that is distinct. However, whether the immunosuppressive action of FR252921 is mediated through the mTOR pathway was not investigated originally.[240,241]

2.1.6.2. Synthetic Approaches towards FR252921

As is the case for most biologically interesting natural products, soon after the publication of the structure and biological activity of the FR molecules, the first synthetic efforts were disclosed. In 2007, both Falck *et al.*[242] and Cossy *et al.*[243,244] reported their approaches towards FR252921. Several other approaches featuring semisynthesis,[245] alternative total synthesis,[246,247] and formal syntheses have since been reported.[248,249]

In their synthetic efforts towards FR252921, both Falck *et al.* and Cossy *et al.* aimed to construct the core 19-membered *all*-(*E*)-triene macrocycle through a macrolactonisation reaction. Both approaches employed Shiina conditions on a linear hydroxy acid (**2.077**), as depicted in Scheme 2.18.[242,243] However, while these reaction conditions were capable of eliciting ring-closure, the desired product of the reaction, FR252921 (**2.013**), could only be observed in low yields, while the main product of the macrolactonisation was found to be the (*Z*,*E*,*E*)-stereoisomer of FR252921 (**2.078**). The authors argued that this product was likely formed through isomerisation of the double bond adjacent to the carboxylic acid following a Michael/Retro-Michael reaction of the C-18 hydroxy moiety. While the C-13 hydroxyl moiety might also be capable of inducing a Michael/Retro-Michael process, the undesired (*Z*,*E*,*E*)-product was also formed in the presence of a OTIPS-protected C-13 hydroxyl moiety.[243] The formation of this byproduct is further rationalised to arise from the reduced ring-strain evoked by a (*Z*)-olefin, compared to FR252921, thereby favouring isomerisation before macrocyclisation.

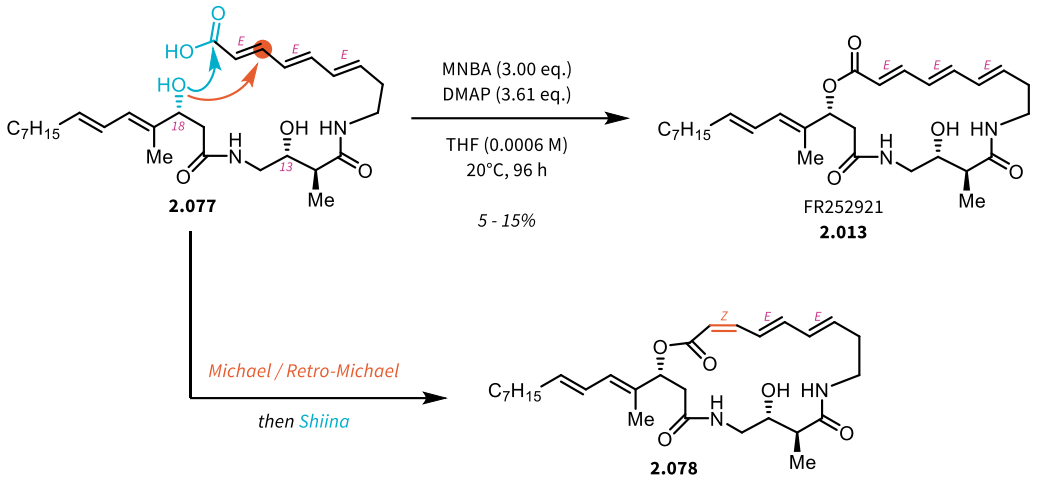

Scheme 2.18: Shiina macrolactonisation of linear acid **2.077** leading to FR252921 in low yield. The main competitive pathway for isomerisation appears to be a Michael/Retro-Michael reaction by the C-18 hydroxyl moiety leading to **2.078**.

As the natural product FR252921 could only be obtained in low amounts, no further biological explorations or investigations of potential derivatives of FR252921 were undertaken.

2.1.6.3. The Cyclobutene Approach to FR252921

The investigation of the chemistry of *cis*- and *trans*-cyclobutene acids by Maulide *et al.*, as outlined in chapter 2.1.4, led to the serendipitous discovery that some cyclobutene products underwent spontaneous, thermal 4π-electorcyclic ring opening upon formation of the lactone. Further investigations revealed that the reaction of *cis*-chlorocyclobutene acid methyl ester (**2.079**) with vinyl-Bpin species (**2.080**) in a Suzuki-Miyaura cross-coupling reaction also did not enable isolation of the anticipated *trans*-vinylcyclobutene species **2.081**, but rather the product of concomitant 4π-electrocyclic opening of said *trans*-cyclobutene, the *all*-(*E*)-triene carboxylic acid methyl ester **2.082** (Scheme 2.19).[250–253]

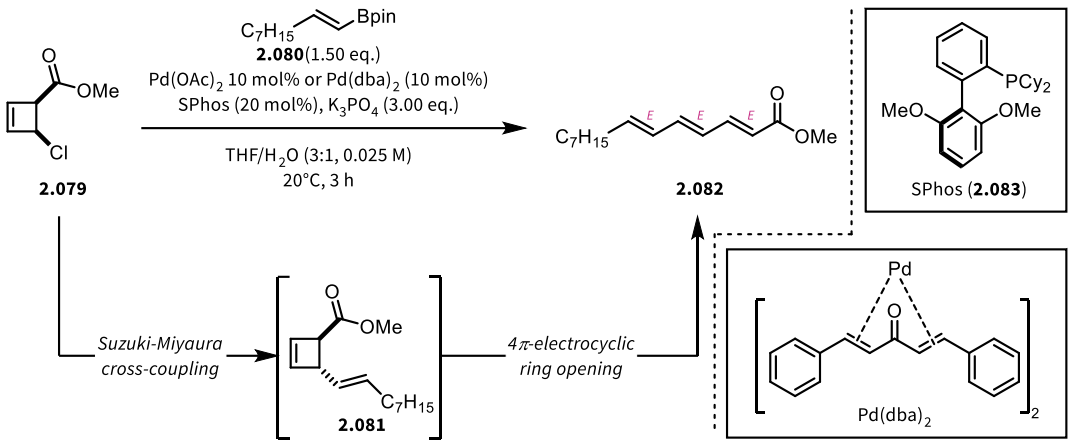

Scheme 2.19: Domino reaction cascade of Suzuki-Miyaura cross-coupling between *cis*-chlorocyclobutene acid methyl ester (**2.079**) and vinyl-Bpin species **2.080** to form *all*-(*E*)-triene product **2.082** *via trans*-vinylcyclobutene intermediate **2.081**.

The discovery of a synthetic tool allowing for the synthesis of *all*-(*E*)-triene carbonyl species spurred research into the total synthesis of FR252921, which ultimately culminated in the first generation total synthesis reported by Maulide *et al*. in 2019.[253] Dissecting the target molecule retrosynthetically, the forward synthesis was envisioned to construct the natural product from four distinct building blocks, with **2.057**, **2.084** and **2.087** being used to construct the macrocycle, while **2.086** was used to introduce the side-chain of the FR molecules (Scheme 2.20).

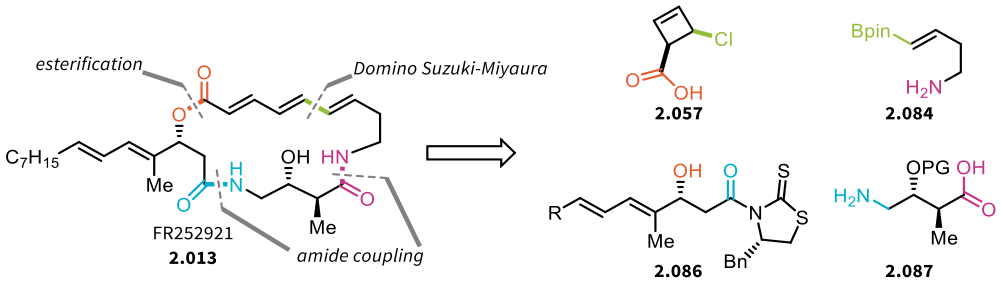

Scheme 2.20: Retrosynthetic analysis of the FR molecules by Maulide *et al*. featuring key domino Suzuki-Miyaura cross-coupling / 4π-electrocyclic ring opening.

Scheme 2.21 shows the synthetic approach to FR252921 as carried out by Maulide *et al*. The first building block, homoallyl-Bpin amine (**2.084**/**2.091**), was constructed starting from commercially available pentynoic acid (**2.088**) in three steps. First, pentynoic acid **2.088** was converted to the *N*-Boc-protected amine **2.089** *via* a Curtius rearrangement enabled by diphenylphosphoryl azide (DPPA) and *tert*-butanol. Subsequently, the alkyne was converted to the required vinyl-Bpin moiety by an *E*-selective hydroboration using Schwartz's reagent to form **2.090**. Afterwards, the *N*-Boc protecting group was removed by the action of trifluoroacetic acid (TFA) to yield the required building block **2.091**.

The synthesis of the second building block, azidoacid **2.094**, started from commercially available, enantiopure chlorohydroxy ester **2.092**. First, the chloride moiety was displaced by an azide through S_N2 reaction in DMF, yielding an azidoalcohol, which was subsequently methylated α to the carbonyl through diastereoselective Fráter-Seebach alkylation, to yield the methylated product **2.093**.[254,255] Protection of the hydroxyl moiety in **2.093** with TBSOTf and 2,6-lutidine was followed by hydrolysis of the ester, leading to azidoacid **2.094**.

With acid **2.094** and amine **2.091** in hand, a HATU-mediated amide coupling was conducted to form **2.095**, after reduction of the azide moiety with Zn dust and ammonium chloride. Next, the side-chain was introduced using another amide coupling reaction with **2.096** promoted by a substoichiometric amount of 4-dimethylaminopyridine (DMAP) to yield linear secondary alcohol **2.097**, setting the stage for the last three steps of the total synthesis.

The first of these was the crucial esterification between secondary alcohol **2.097** and *cis*-chlorocyclobutenecarboxylic acid **2.057**. It was found that this reaction is highly sensitive to epimerisation of the cyclobutenecarboxylic acid, often leading to the formation of undesired *trans*-cyclobutene ester (not shown). Following extensive optimisation, the authors identified the combination of Ghosez's reagent and pyridine as optimal, enabling the reproducible synthesis of *cis*-cyclobutene ester **2.098** as a mixture of two *cis*-diastereomers (a result of the use of racemic *cis*-cyclobutene acid). Having introduced the last building block, the macrocyclisation precursor **2.098** was consumed in the anticipated key step, the domino Suzuki-Miyaura / 4π-electrocyclic ring opening macrocyclisation reaction. This reaction proceeded smoothly under Pd-catalysis, employing the commonly utilised combination of $Pd(PPh_3)_4$ and Cs_2CO_3, to yield the macrocyclic *all*-(*E*)-triene product in high yield and with excellent selectivity. Comparing this macrocyclisation approach to the previous total syntheses, it is clear that avoiding ring-strain before cyclisation is key to ensuring high (*E*,*E*,*E*)-selectivity. In the final step, the C-13 hydroxyl moiety was deprotected to yield FR252921 (**2.013**) after ten steps in the longest linear sequence.

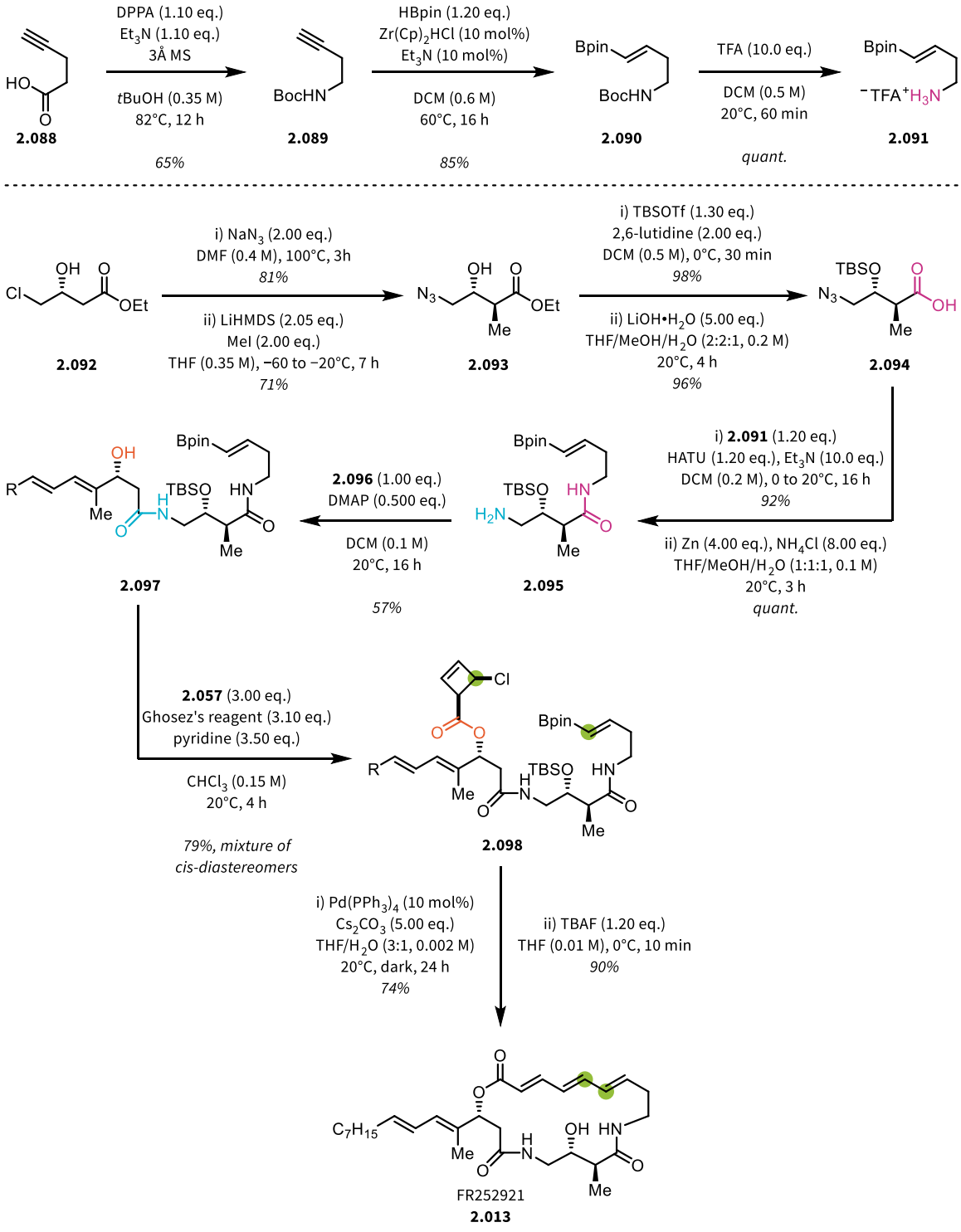

Scheme 2.21: Total synthesis of FR252921 by Maulide *et al*. *via* a key macrocyclisation event consisting of a domino Suzuki-Miyaura cross-coupling / 4π-electrocyclic ring opening.

Since the natural FR molecules only differentiate in the side-chain, all three natural products alongside a range of synthetic analogues were produced by simple exchange of the side-chain precursor and their biological activity was tested in an antiproliferation assay against EL4 T cells, a murine T cell-derived cancer cell line. This enabled a first evaluation of the structure-activity relationship (SAR) of the FR molecules and their derivatives (Scheme 2.22).[253]

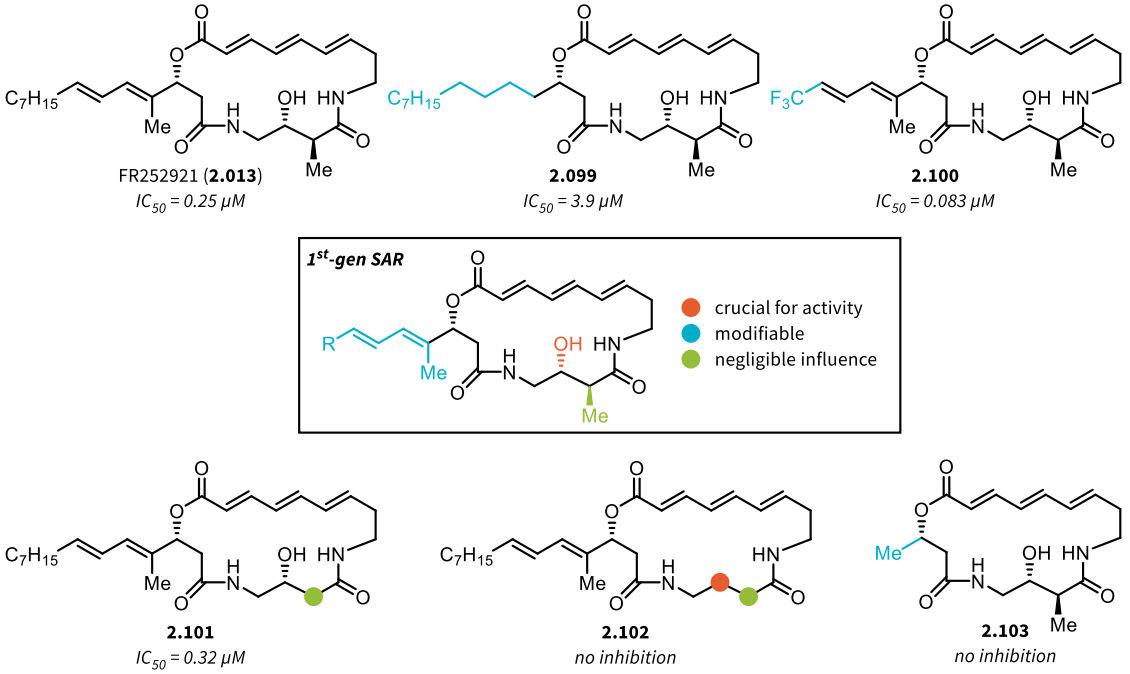

Scheme 2.22: First generation SAR as evaluated in an antiproliferation assay against EL4 T cells.

From these SAR considerations, it was concluded that the C-13 hydroxyl moiety was crucial for biological activity (**2.102**), while the influence of the C-12 methyl group was found to be negligible (**2.101**). The side-chain, while generally required for activity, could be modified and activity was retained (**2.099**, **2.103**). In one stunning example, it was found that the CF_3-side-chain-modified analogue **2.100** even showed higher activity than the natural products themselves.

2.2. Aims of the Project

Within this project, several synthetically and biologically relevant properties of the FR252921 family of natural products and their derivatives are to be explored. Our aims were:

a) Reoptimising the total synthesis of FR252921 and synthesising novel analogues to establish a second-generation structure-activity-relationship (Scheme 2.23A).

b) Probing the immunosuppressive biological activity of all FR analogues in human primary cell material and their interactions with approved medication (Scheme 2.23B).

c) Understanding the mechanistic details of the domino macrocyclisation reaction (Scheme 2.23C).

These aims separate this chapter into three subchapters, which will be explored below.

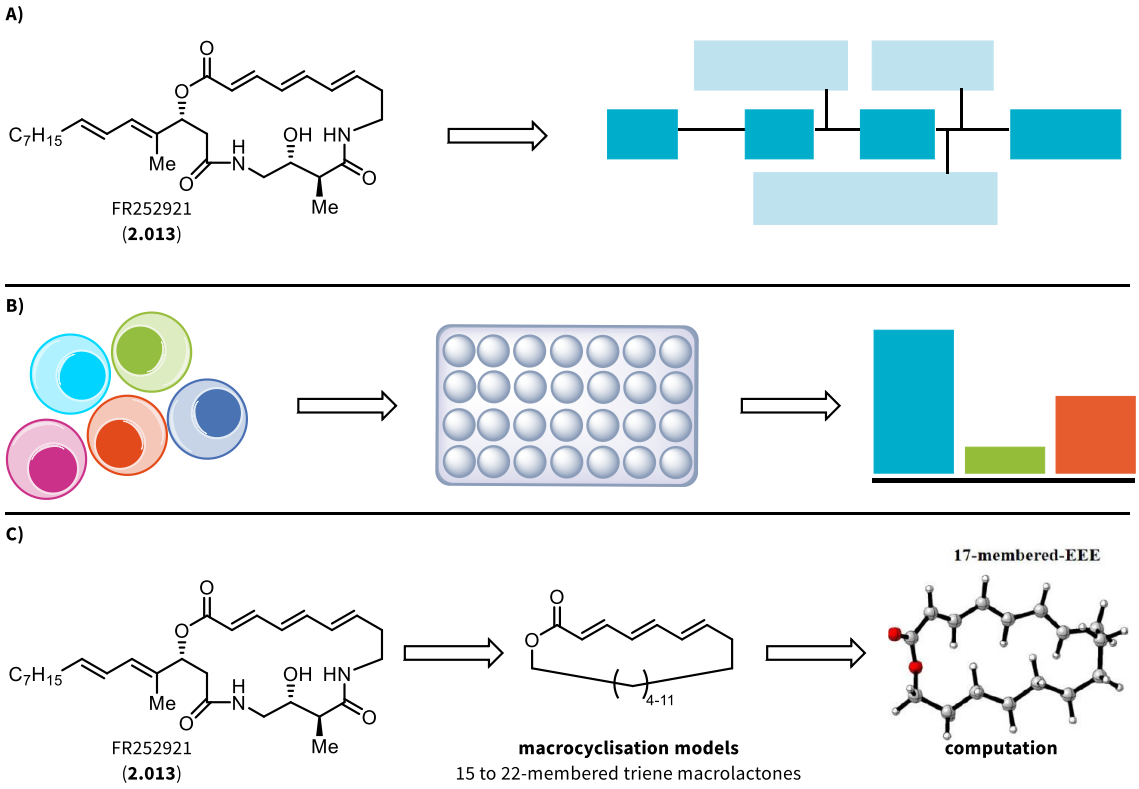

Scheme 2.23: Overview on the different aims of the FR project as presented within this thesis. A) Synthesis of FR252921 (**2.013**) and novel immunosuppressive natural products analogues. B) Biological evaluation of the synthesised compounds within different cellular settings. C) Towards a general application of the domino Suzuki-Miyaura/4π-electrocyclic ring opening macrocyclisation towards macrocyclic *all*-(*E*)-triene lactones.

2.3. Results & Discussion

The results described in this chapter were acquired in collaboration with:

a) *Synthetic results: Dr. Iakovos Saridakis, Haoqi Zhang, Dr. Thomas Leischner, Martina Drescher, Dr. Yong Chen, Dr. Guilhem Coussanes, Dr. Margaux Riomet, Filip Gallob (CeMM), Herwig Weißinger, Florian Doubek, Anne Fischer and Quentin Riedl.*

b) *Biological experiments: Laura Marie Gail (CeMM / Medical University of Vienna), Dr. Tuan-Anh Nguyen (CeMM), Anna Koren (CeMM), Assoc. Prof. Dr. Georg Stary (CeMM / Medical University of Vienna), Dr. Stefan Kubicek (CeMM).*

c) *Computational studies: Jingran Shan (UCLA), Dr. Xiangyang Chen (UCLA), Prof. Dr. Kendall N. Houk (UCLA)*

2.3.1. Revisiting and Reoptimisation of the Synthesis of FR252921

When embarking on the repetition of the total synthesis of FR252921 and the translation towards the development of a discovery platform for novel immunosuppressive natural product analogues, some key reaction steps in the synthetic sequence were revisited in order to improve their robustness. Two out of the three last synthetic operations are particularly sensitive to perform and a successful macrocyclisation requires a clean *cis*-cyclobutene ester starting material. This is the result of the fact that, during the esterification reaction, some amount of *cis*-chlorocyclobutenecarboxylic acid (**2.057**) may be epimerised to the *trans*-isomer, leading to the undesired *trans*-ester of **2.098**. While the two *trans*-diastereomers can be separated from the two desired *cis*-diastereomers, this process is tedious, time consuming and suboptimal. The *trans*-isomers are undesired byproducts, as a hypothetical macrocyclisation reaction *via* the aforementioned domino process would inevitably lead to the (*Z*,*E*,*E*)-macrocyclic product, whereas only the two *cis*-diastereomers lead to the *all*-(*E*)-product, as outlined in chapter 2.1.4.

In the initial publication,[253] Ghosez's reagent was used to activate acid **2.057** under mild conditions, avoiding epimerisation in the process. However, significant amounts of the *trans*-acid were still formed through impurities or sub-par quality of the Ghosez's reagent. While the amount of *trans*-product formed can be reduced by distillation of both pyridine and Ghosez's reagent, the need for the latter distillation to be performed immediately before the reaction led to a desire to find a suitable alternative. The desire was met by the use of T3P® (propanephosphonic acid cyclic anhydride), a reagent commonly applied in amide coupling reactions.[256,257] An added benefit to the use of T3P® over Ghosez's reagent (aside the *cis*-/*trans*-diastereomer issue) is the ease of purification, as the byproducts of T3P® hydrolysis are water soluble and therefore readily washed out during workup (whereas Ghosez's reagent hydrolyses to the corresponding *N*,*N*-dimethylisopropylamide, which co-elutes with the desired products of the reaction during purification by flash column chromatography). A brief overview of the reoptimisation process and its results is presented in table 2.2, within Scheme 2.24. The lower rate of epimerisation leading to the undesired *trans*-products can be rationalised by consideration of the potential acidity of the α-proton of the intermediate activated acids **2.108** and **2.109.** Indeed, with the acid chloride **2.108** derived from **2.057** and Ghosez's reagent is likely more acidic—and therefore more prone to epimerisation—than its T3P®-derived counterpart **2.109**, as the more electronegative chlorine substituent is more capable of further stabilisation of a negative charge than the phosphate substituent. Additionally, when comparing the pKa values of the corresponding acids, hydrochloric acid and phosphoric acid, a similar picture emerges, as hydrochloric acid posses pKa = −7.0, while phosphoric acid is much less acidic with pKa = 2.16.[258]

Overall, the replacement of Ghosez's reagent with T3P® was implemented without further adjustments to the optimal reaction conditions. Additional experiments conducted on a model scaffold (chapter 2.3.4.), concerned with changing the order of addition of different reagents as well as the equivalents of reagents used, did not lead to a further increase in yield or suppression of epimerisation. The general optimised reaction procedure for the esterification can be found in chapter 2.5.2.17., and due to limited availability of the linear precursors and similar behaviour of these compounds across different analogues, various different linear alcohols (*ent*-**2.097**, **2.104**, **2.106**) were used for the reoptimisation endeavours.

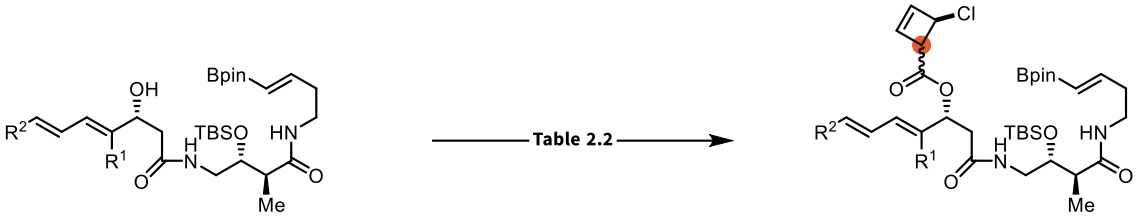

ent-**2.097**, R^1 = Me, R^2 = C_7H_{15}
2.104, R^1 = H, R^2 = C_7H_{15}
2.106, R^1 = Me, R^2 = C_9H_{19}

ent-**2.098**, R^1 = Me, R^2 = C_7H_{15}
2.105, R^1 = H, R^2 = C_7H_{15}
2.107, R^1 = Me, R^2 = C_9H_{19}

Table 2.2

Substrate	Reagent	distilled	Base	distilled	Yield (isolated)	*cis*/*trans*
2.104	Ghosez's	yes	pyridine	yes, fresh	–	2.5:1
2.104	Ghosez's	yes	pyridine	yes, old	–	2:1
2.104	Ghosez's	yes	pyridine	no	–	decomp.
ent-**2.097**	Ghosez's	yes	pyridine	yes, old	*13 % cis*	n.d.
ent-**2.097**	Ghosez's	yes, fresh	pyridine	yes, old	*21 % cis*	n.d.
2.106	Ghosez's	yes, fresh	pyridine	yes, fresh	*73 % cis (NMR)*	3.6:1
2.106	T3P	–	pyridine	yes, fresh	*57 % cis (NMR)*	4.8:1

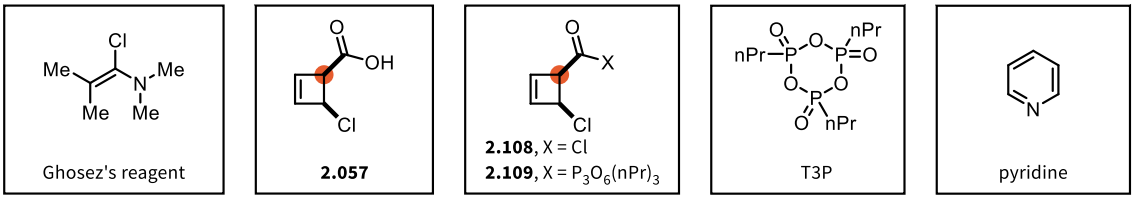

Ghosez's reagent

2.057

2.108, X = Cl
2.109, X = $P_3O_6(nPr)_3$

T3P

pyridine

Scheme 2.24: Optimisation of esterification conditions through the application of freshly distilled reagents or replacing Ghosez's reagent with T3P®.

2.3.2. Second-Generation Structure-Activity Relationship

The first generation of fully synthetic FR252921 analogues, as published by Maulide *et al*. in 2019, did establish two rules for the design of further compounds, namely the necessity to include both the C-13 hydroxyl moiety and the requirement for all structures to bear a side-chain. However, this leaves large parts of the molecule unexplored, and several new analogues were envisioned to address the open questions posed in Scheme 2.25. The synthetic access to these novel, second generation analogues is outlined in the following chapter, followed by their biological evaluation.

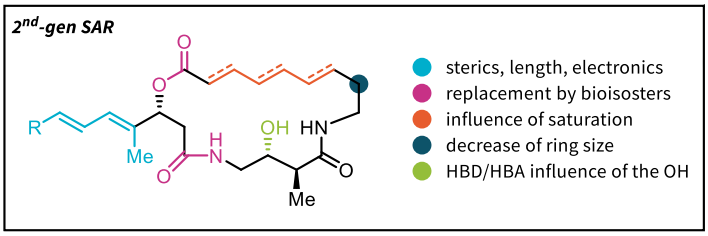

Scheme 2.25: Representative depiction of the points of modification explore for the second generation of structure-activity relationship investigations. HBD = hydrogen-bond donor; HBA = hydrogen-bond acceptor.

These investigations are made possible by the high convergence of the synthetic route towards FR252921. As outlined in chapter 2.1.6.3., our approach builds upon the synthesis of four building blocks, which are then joined together during the final stages of the synthesis. Using this building block-based synthesis logic allows for the rapid generation of novel product structures by systematically replacing one of the aforementioned building blocks, thereby reducing the requirement to repeat every step of the synthetic sequence. A visualisation of this idea is shown in Scheme 2.26, depicting how changing the building blocks influences the outcome at the end of the synthetic sequence without deviating from the main pathway.

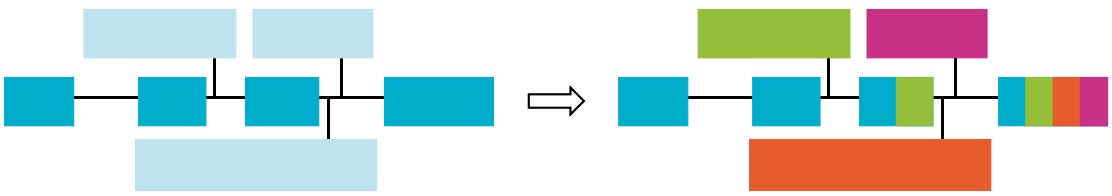

Scheme 2.26: Depiction of the idea of transforming the total synthesis of one molecule into a discovery platform capable of producing a range of different analogues without tedious repetition of every synthetic transformation.

2.3.2.1. Novel Side-chain Analogues of FR252921

As previously discussed, the FR molecules are three natural products which are similar in their macrocyclic core but differentiate in their side-chain. Taking inspiration from this, most of the first-generation structure-activity relationship investigation was spent systematically permutating the properties of said side-chain, ultimately finding an analogue of improved activity in the EL4 T cell assay. This analogue, henceforth referred to as FR5 (**2.100**), contains a shortened side-chain, replacing the *n*-heptyl chain with a simple CF_3-moiety, which was found to increase the activity three-fold (Scheme 2.22). Other modifications of the side-chain, such as the inclusion of aromatic moieties, were also tested, but these analogues presented higher IC_{50} values or no inhibition, while also giving an indication that an electron-withdrawing group appended to the side-chain may be beneficial.[253]

Taking these results into consideration, several analogues were designed to bridge the gaps between the synthetic analogues and the natural products, as well as to explore new ideas in analogue design (Scheme 2.27). As the removal of the double bonds had been previously found to be detrimental, it was decided to tune the electronic properties of an analogous side-chain through the variation of the α-substituent present in FR252921 (Scheme 2.27). To this end, several possible changes were explored, particularly in the form of removal of the α-substituent altogether (αH-FR, **2.110**) or in the form of replacement of the methyl group with electron-withdrawing substituents such as an α-F moiety (αF-FR, **2.111**) or an α-CF_3 group (αCF_3-FR, **2.112**).

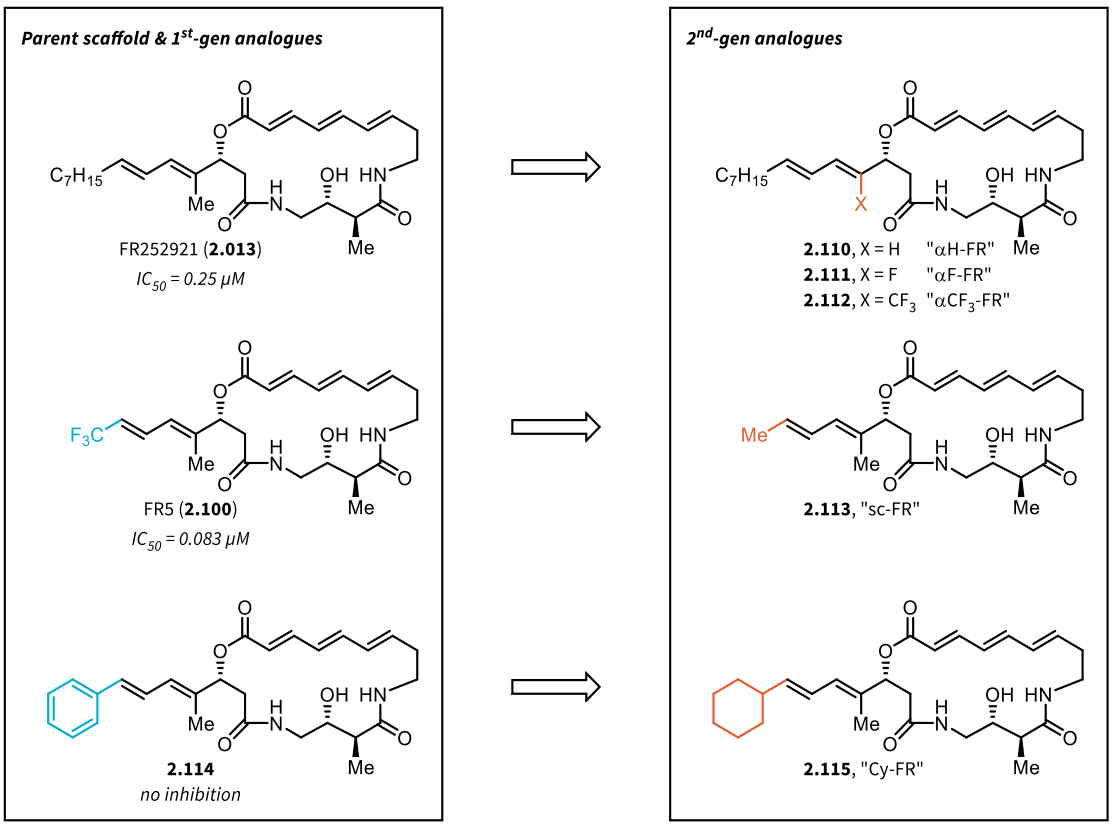

Scheme 2.27: Comparison between the previously synthesised natural product FR252921 (**2.013**), FR5 (**2.100**) and **2.114**, bearing an aromatic side-chain and the newly designed analogues. αH-FR (**2.110**), αF-FR (**2.111**) and αCF$_3$-FR (**2.112**) explore the modification of the α–Me group of the natural product, whereas sc (short-chain)-FR (**2.113**) and Cy-FR (**2.115**) are aimed at bridging the gaps between previously synthesised compounds and the natural product.

Taking into consideration the success of the first generation analogue FR5 (**2.100**), bearing a shortened ω-CF$_3$ side-chain, the short-chain FR analogue sc-FR (**2.113**) was proposed to bridge the gap between the long, aliphatic sidechain of the natural product FR252921 and the shortened, electron-withdrawing side-chain present in FR5.

Lastly, several fully synthetic analogues bearing aromatic side-chains, such as **2.114** were previously synthesised, but all led to lower antiproliferative activity compared to the natural product FR252921. Again, the gap between the aliphatic sidechain of the natural product and the analogues bearing an aromatic side-chain was bridged by the design of an analogue bearing a side-chain capped by a cyclohexyl group (**2.115**). This serves as a saturated benzene analogue, thus posing the question whether it is a cyclic substituent or an aromatic character, that led to lowered activity in **2.114**.

The side-chain building blocks required for these investigations are synthesised through a short sequence starting from commercial aldehydes and the α-substituents are typically introduced *via* a Horner-Wadsworth-Emmons[259,260] or Wittig[261] olefination. Further manipulations include redox operations to

yield the required aldehyde for a diastereoselective Evans–Crimmins-type aldol reaction.[262] The aldehydes required for the synthesis of Cy-FR and sc-FR (**2.129** and **2.131**, Scheme 2.29) were prepared from commercially available starting materials by the standard route and without any noteworthy complication, and aldehyde **2.125** was sourced from a commercial supplier.[253] The two side-chain aldehydes bearing electron-withdrawing substituents, **2.119** and **2.123**, were synthesised as outlined in Scheme 2.28.

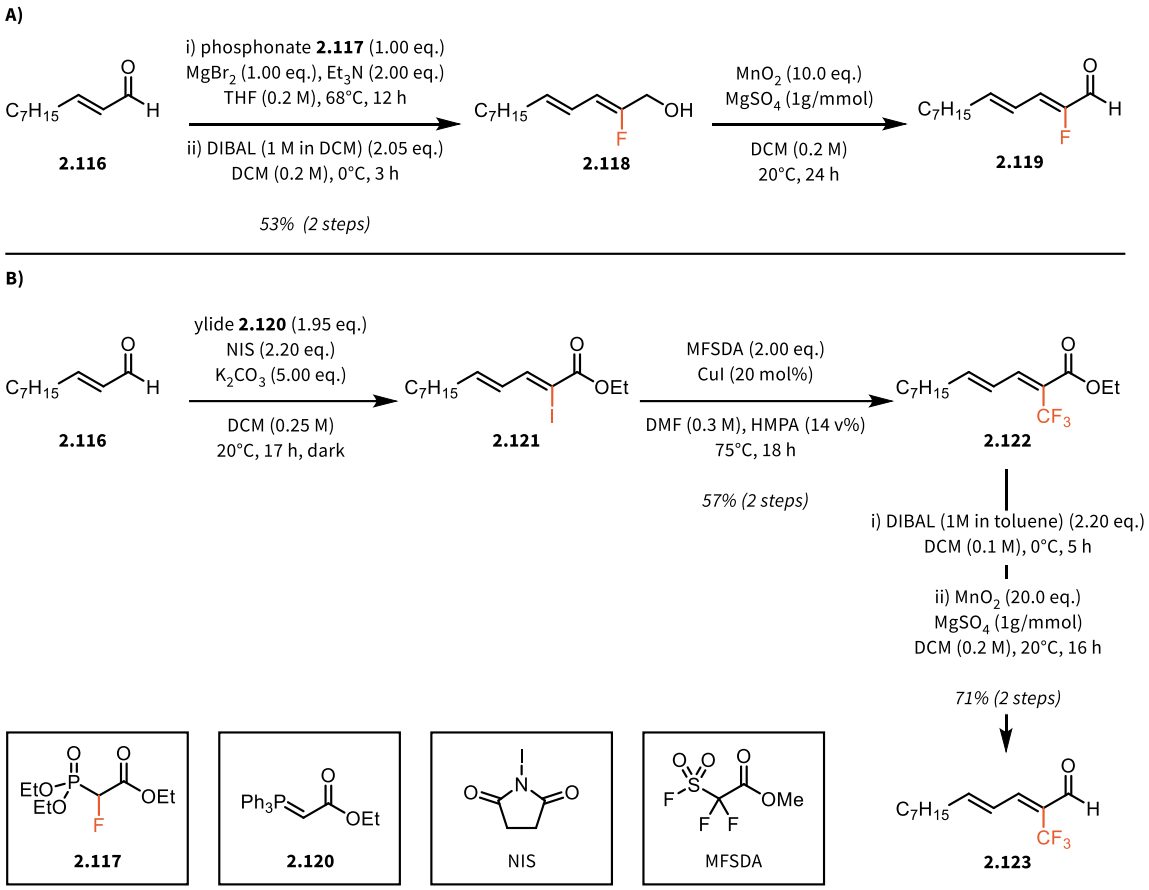

Scheme 2.28: Synthesis of the αF- and the αCF$_3$-side-chain aldehyde (**2.119** and **2.123**) from commercially available *trans*-decene-2-al (**2.116**).

With the required aldehydes in hand, the Evans–Crimmins aldol reaction was conducted, converting the aldehydes (**2.119**, **2.123**, **2.125**, **2.129**, **2.131**) to the β-hydroxy carbonyl building blocks amenable to amide formation with the core FR precursor (**2.095**) (Scheme 2.29). In some cases, the crude diastereomeric ratio could not be determined due to overlap in ^{1}H-NMR, however the observed diastereomeric ratio upon isolation of the two isomers was typically in the range of >10:1 to 3:1.

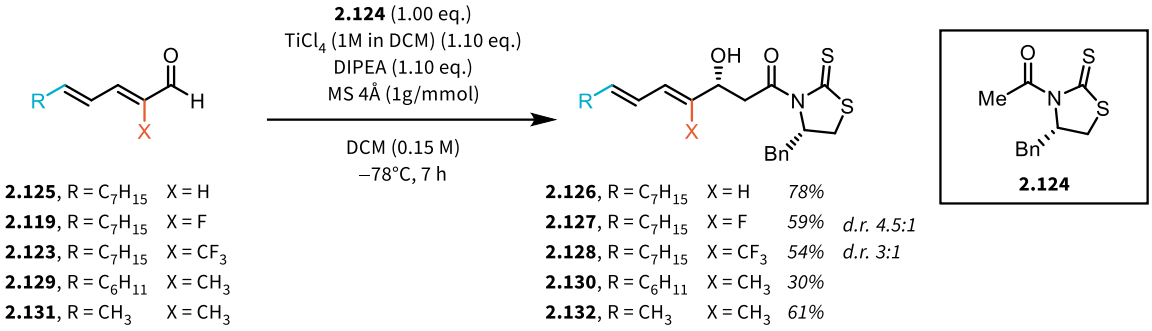

Scheme 2.29: Aldol reaction to synthesise the side-chain building blocks to be applied in the syntheses of novel FR252921 analouges.

After successful isolation of the diastereomerically pure precursors (**2.126**, **2.127**, **2.128**, **2.130**, **2.132**), these building blocks, in combination with the core building block **2.095**, were used in the synthesis of novel FR analogues without any alteration of the previously discussed reaction conditions to afford five new final compounds (αH-FR (**2.110**), αF-FR (**2.111**), αCF$_3$-FR (**2.112**), Cy-FR (**2.115**) and sc-FR (**2.113**)), as outlined in Scheme 2.30.

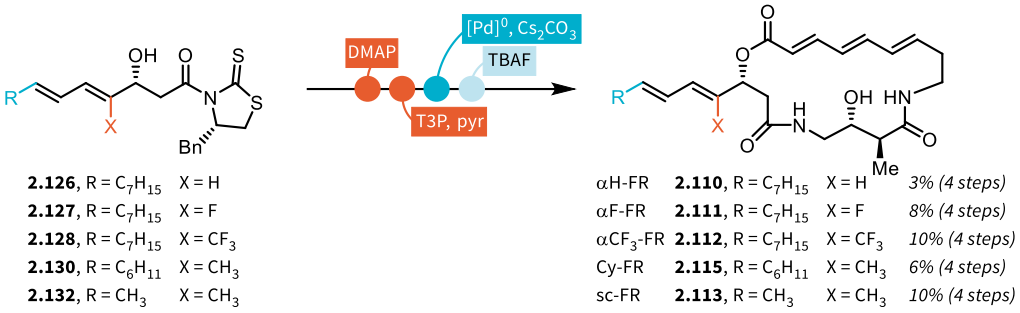

Scheme 2.30: Synthesis of five novel FR analogues from the side-chain precursors following the standard synthetic route.

2.3.2.2. Novel Core Analogues of FR252921

Apart from modifications of the side-chain to generate analogues for the second-generation evaluation of the structure-activity relationship of FR252921, new core modifications were envisioned to probe the influence of different functional groups within the macrocyclic core. These analogues can be grouped according to the hemisphere of the macrocycle they aim to modify, into northern and southern modifications, as depicted in Scheme 2.31.

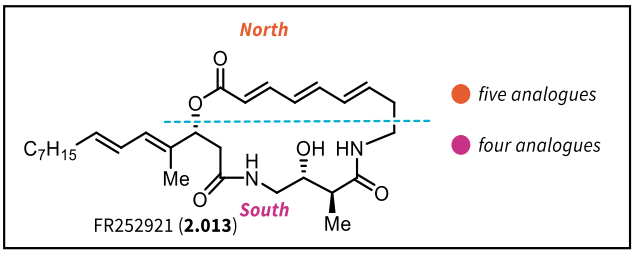

Scheme 2.31: Grouping of core modifications applied to FR252921 to generate novel analogues for biological testing.

2.3.2.2.1. Northern Macrocycle Modification of FR252921

Overall, five analogues were designed and synthesised, addressing the functionality located within the northern hemisphere of the macrocyclic core of FR252921. Among these is the synthesis of a hydrolysed analogue, possessing the terminal carboxylic acid as well as the C-18 hydroxyl moiety, as well as different analogues surveying changes in the configuration and presence of the iconic *all*-(*E*)-triene. Lastly, a bioisosteric replacement of the lactone by a lactam was attempted and synthetic progress towards this goal is described.

2.3.2.2.1.1. Open-FR252921

To mediate a biological effect, effector molecules typically need to bind to a cellular target. For some natural products, this target is the DNA, the key genetic information at the heart of the cell. Such compounds, for example enediyne antibiotics, typically show very high activity against a range of cell lines, as the presence of DNA, and therefore of the target, is the same across cell lines.[263,264] However, most biologically active molecules convey their action by binding to a protein through different binding modes (reversible, covalent, allosteric *etc.*). When binding to a protein, several thermodynamic barriers have to be overcome, such as the binding enthalpy and the entropy associated with the process. One major contributor to the entropic barrier is associated with the orientation of the binding moieties within the ligand, as these need to reside in an optimal orientation. However, if the functional groups necessary for binding are fixed in place by virtue of a macrocycle, the entropic penalty dwindles in importance.[265,266] This theoretical consideration is typically confirmed experimentally by comparing the binding affinities of macrocyclic ligands and their open-chain counterparts.

As FR252921 (**2.013**) contains a 19-membered macrocyclic core, itself containing the C-13 hydroxy group, which has been shown to be key for biological activity, several questions about the significance of said macrocycle were raised. The entropic consideration as outlined above was taken into account, as well as the potential for metabolic inactivation of FR252921 by virtue of ester-hydrolysing enzymes. The sum of these considerations led to the design of a route to open-FR252921 (**2.133**). In the event, its synthesis was swiftly accomplished from the commonly employed advanced FR252921 precursor **2.097** (Scheme 2.32).

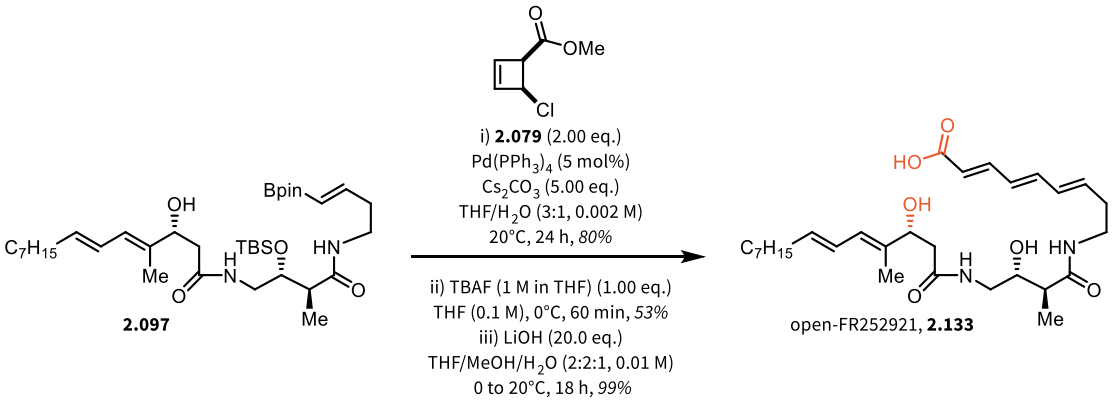

Scheme 2.32: Synthesis of the open-chain FR252921 analogue (open-FR252921, **2.133**) from the standard precursor **2.097** and *cis*-chlorocyclobutenecarboxylic acid methyl ester **2.079**.

The linear vinyl-Bpin precursor **2.097** was first engaged in an intermolecular domino Suzuki-Miyaura/4π-electrocyclic ring opening process with **2.079** to yield an *all*-(*E*)-triene carboxylic acid methyl ester (not shown). Subsequent cleavage of the silyl ether, mediated by TBAF, followed by hydrolysis of the ester yielded **2.133** ("open-FR252921"), with no change in the length of the longest linear sequence (10 steps).

2.3.2.2.1.2. EZE-FR252921

During investigations to establish generality for the domino macrocyclisation process (*cf.* chapter 2.3.4.), it was found that the macrocyclisation reaction is capable of producing an unexpected isomer in the form of the (*E*,*Z*,*E*)-triene macrolactone—a particularly stark contrast to the reports by Falck and Cossy, which highlighted the observation of the (*Z*,*E*,*E*)-triene.[242,243] While this isomer had not been detected in the total synthesis of FR252921 on the typically applied scale (20 µmol), scaling the reaction to 58 µmol led to the discovery of the undesired (*E*,*Z*,*E*)-isomer (**2.135**) as a byproduct of the macrocyclisation event (Scheme 2.33).

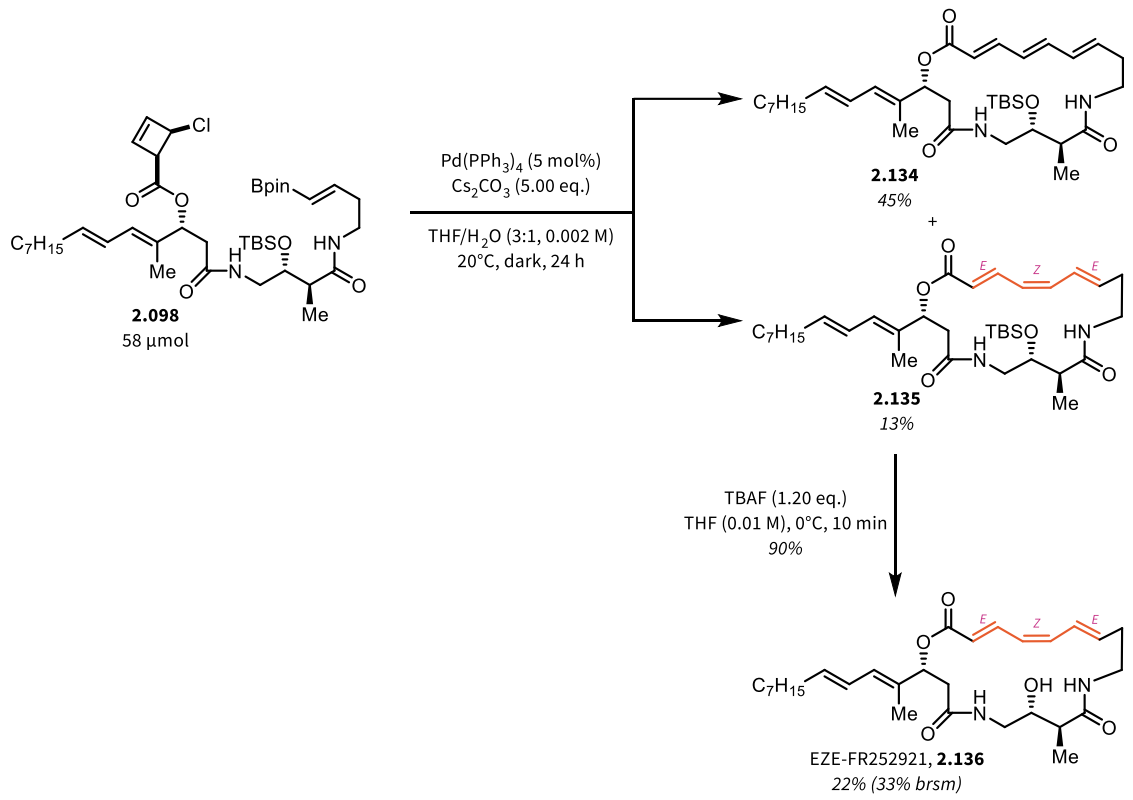

Scheme 2.33: Synthesis of EZE-FR252921 (**2.136**) from the undesired macrocyclisation product **2.135**.

This discovery is interesting for two major theoretical considerations. First, the formation of an (*E*,*Z*,*E*)-isomer should be ruled out by the Woodward-Hoffmann rules as well as the torquoselectivity considerations outlined in chapter 2.1., as this undesired product would be the result of a counter-torquoselective thermal disrotatory 4π-electrocyclic ring opening of a *trans*-vinylcyclobutene derivative. Second, the (*E*,*Z*,*E*)-product, while thermodynamically favoured over the *all*-(*E*)-triene, is not the most thermodynamically stable product for FR252921. It has been established *via* quantum chemical calculations that the unnatural (*E*,*E*,*Z*)-isomer would be thermodynamically favoured, if accessible; however, these calculations were conducted on the natural product scaffold, meaning that the C-13 hydroxyl moiety was able to contribute to the overall stabilisation by intramolecular hydrogen bonding.[253] As, within the synthetic sequence, at the time of macrocyclisation, this functionality is protected as the corresponding silyl ether (TBS), the results of the computational considerations should be seen as an orientation rather than a definitive answer.

However, outside of theoretical considerations on how the product may be formed, which were conducted in collaboration with Houk *et al*., deprotection of **2.135** by means of TBAF yielded EZE-FR252921 (**2.136**) in quantities allowing for biological evaluation of this unexpected isomer.

2.3.2.2.1.3. Saturated-FR252921 and Anti-Michael-FR252921

As previously alluded to, the shape of the macrocycle present in FR252921 may be crucial for high-affinity binding to its target, with the overall appearance of the core scaffold being mostly shaped by rigid structural features located therein. When considering modifications to the rigidifying parts of the macrocycle, the removal of double bonds would result in a more flexible macrocycle, enabling the investigation of the influence of ring shape.

A first foray into probing the role of the double bonds was found in a fully saturated analogue, a molecule aptly named saturated-FR252921 (**2.142**), the synthesis of which is outlined in Scheme 2.34. Starting from commercially available acid **2.137**, first the carboxylic acid moiety was converted to a *N*-Boc protected amine followed by deprotection to yield ammonium salt **2.138**. Subsequent amide bond formation with common precursor **2.094** and reduction of the azide moiety produced amine **2.139**, which was reacted with the common side-chain building block **2.096** to furnish the macrocyclisation precursor **2.140** after ester hydrolysis mediated by LiOH. Unlike the regular synthetic route, the macrocycle was forged by a Shiina macrolactonisation, mediated by 2-methyl-6-nitrobenzoic anhydride (MNBA) and DMAP, swiftly followed by TBS removal to yield the saturated FR252921 analogue **2.142**.

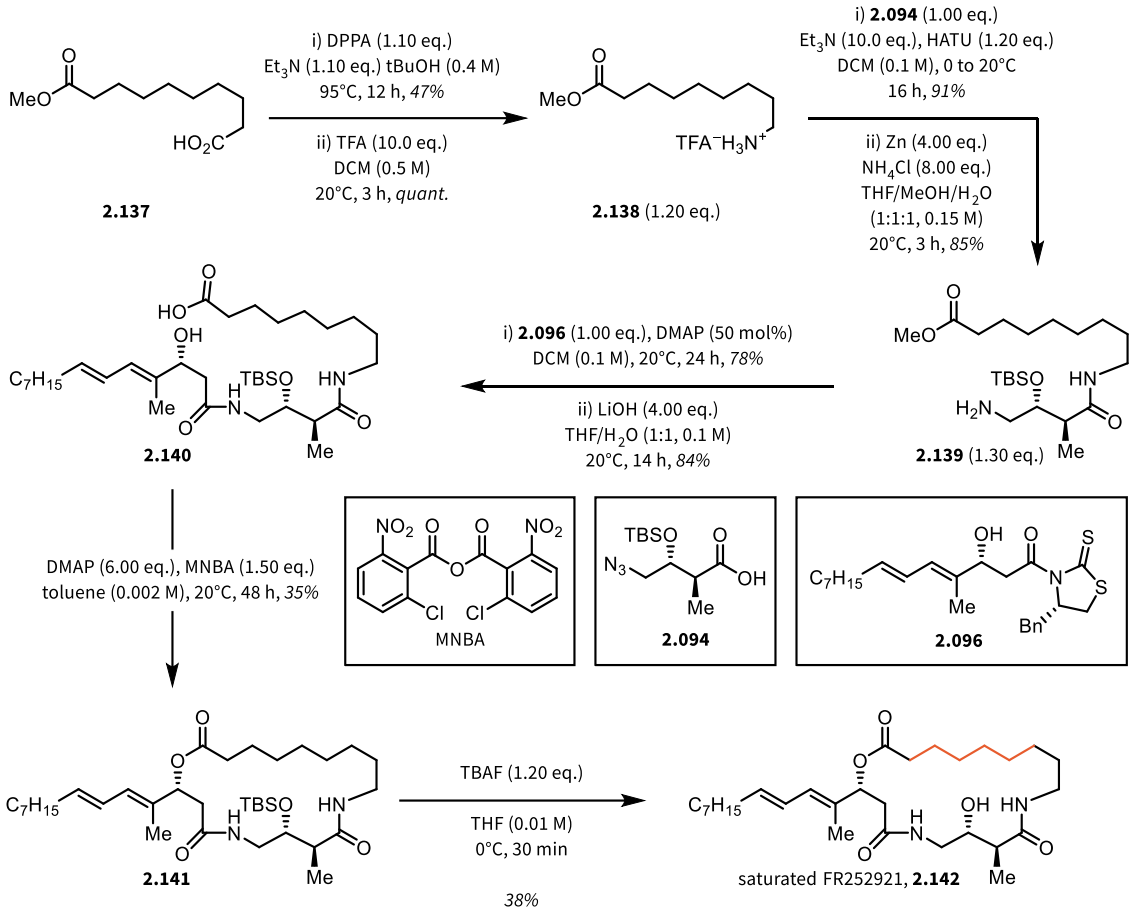

Scheme 2.34: Synthesis to access the saturated FR252921 analogue (**2.142**). The key step is a Shiina macrolactonisation of precursor **2.140**.

One major concern with regard to the stability of the FR compounds is the possibility of transannular Michael addition by attack of the C-13 hydroxyl moiety onto any of the conjugated double bonds on the opposing side of the macrocycle, as depicted in Scheme 2.35A. To render this process impossible, as well as to probe the potential immunosuppressive properties of the resulting analogue, so-called "anti-Michael-FR252921" (**2.147**) was envisioned. The removal of the α,β-double bond adjacent to the carbonyl would result in a compound unable to undergo Michael addition to any of the atoms highlighted in Scheme 2.35A, while still retaining some of the rigidity instilled by the presence of an sp^2-carbon-rich chain.

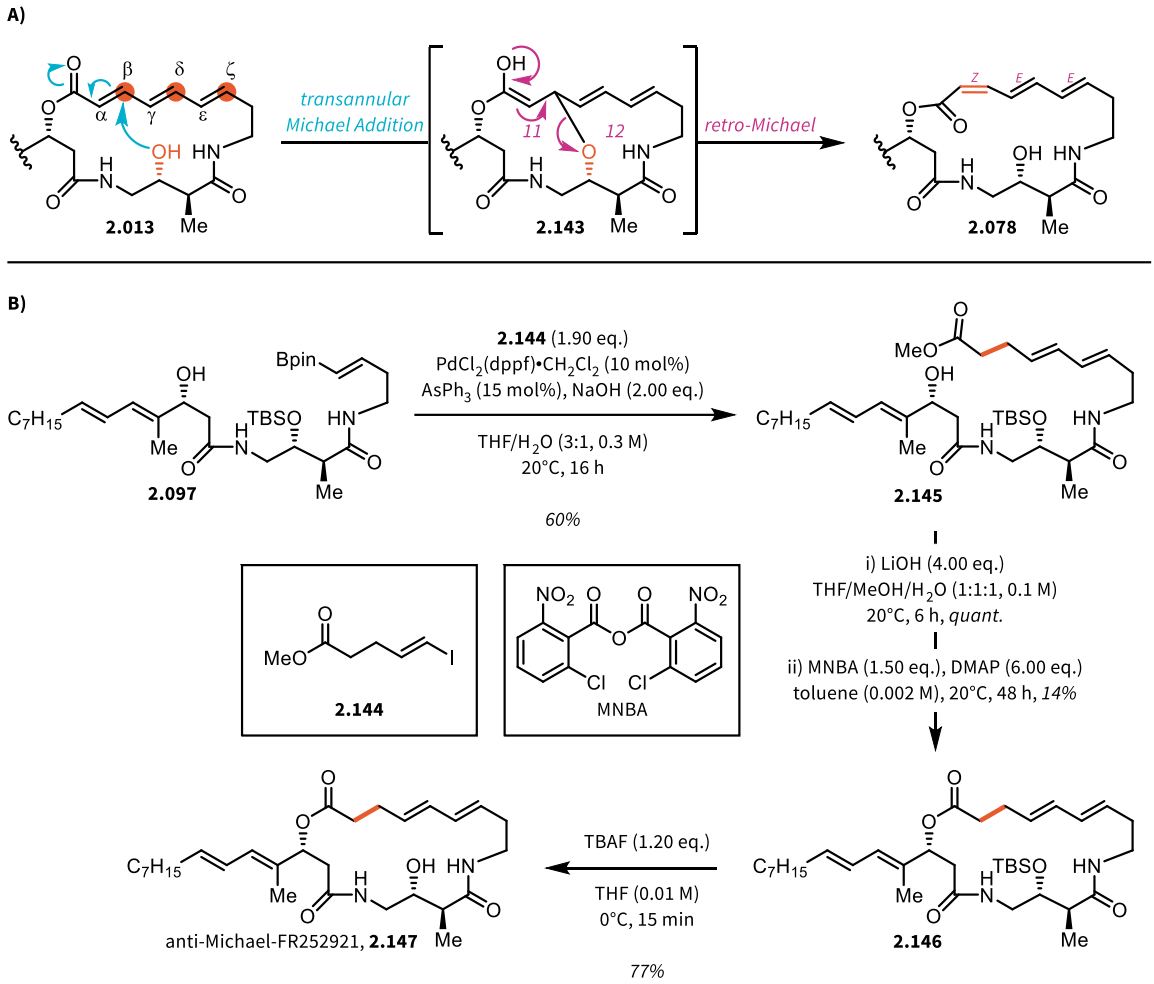

Scheme 2.35: A) Simplified depiction for the hypothetical transannular Michael/retro-Michael process from **2.013** to lead to an isomer such as **2.078**. B) Synthesis of anti-Michael-FR252921 starting from the standard FR252921 building block **2.097** *via* intermolecular Suzuki-Miyaura coupling followed by ester hydrolysis, Shiina macrolactonisation and TBS removal to yield **2.147**.

The synthesis of anti-Michael-FR252921 (**2.147**) started with the standard building block developed for the synthesis of FR252921 (**2.097**), once more highlighting the flexibility and modularity of our approach to analogue synthesis (Scheme 2.35B). The vinyl-Bpin moiety is reacted with vinyl iodide **2.144** in a Suzuki-Miyaura cross-coupling to yield **2.145**, which is converted to the macrolactonisation precursor by means of LiOH-mediated hydrolysis of the ester. Following successful synthesis of the linear carboxylic acid (not shown), this substrate was consumed in a Shiina macrolactonisation to yield the TBS-protected precursor **2.146**, which was readily converted to anti-Michael-FR252921 (**2.147**) following removal of the silyl protecting group.

It should be noted that in the approaches to FR252921 by Falck *et al*. and Cossy *et al*. isomerisation of the α,β-double bond occurred in the presence of a protected C-13 hydroxyl group, indicating that the

observed isomerisation arose from the attack of the C-18 hydroxy group. As the macrocyclisation strategy by Falck *et al*. and Cossy *et al*. relies on this moiety being unprotected, isomerisation is inevitable in their case and arises during macrolactonisation of the linear precursor rather than being caused by transannular Michael addition.

2.3.2.2.1.4. Trilactam-FR252921

Nature typically produces biologically active compounds in order for the producing organism to gain an advantage over competitors in the relevant biological niche. However, since it was discovered that natural products may be isolated and applied to humans in order to elicit their effects for the cure or treatment of diseases, it was also found that not every natural product can be applied in medicine without modification. One of the cases where modification was required to convert a biologically active natural product into a drug suitable for clinical application can be found in the development of epothilone B (**2.148**) towards its application in cancer therapy.

Epothilone B is part of the epothilone family of natural products, which were found to possess powerful cytotoxic activity through a mode of action similar to taxol (**2.150**) and (+)-discodermolide (**2.151**), namely the induction of tubulin polymerisation and stabilisation of microtubules, leading to cell cycle arrest.[267–269] During investigation into the application of epothilone B, it was found that, while the natural product was highly active *in vitro*, this activity was not reflected *in vivo*; an observance which was reasoned to arise from cleavage of the macrolactone core of epothilone B. In order to overcome this metabolic barrier, scientists at Bristol-Myers-Squibb (BMS) developed a macrolactam analogue (**2.149**, BMS-247550, azaepothilone B or ixabepilone), replacing the labile lactone with a more stable, bioisosterically matching lactam, resulting in a molecule which is sold today as Ixempra for the treatment of advanced breast cancer (Scheme 2.36).[269–272]

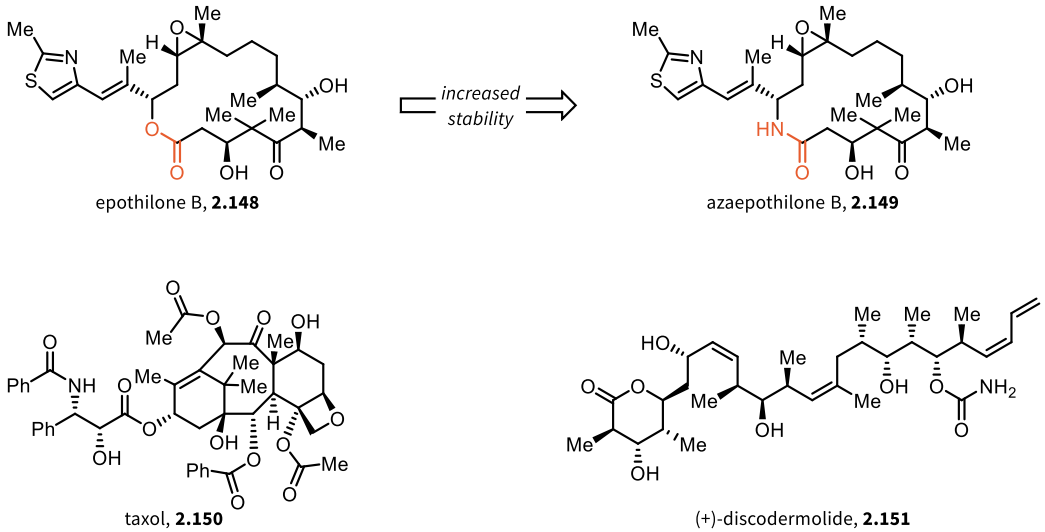

Scheme 2.36: Overview on the range of antiproliferative natural products, which elicit their biological effects through interference with microtubule assembly and stability, namely epothilone B (**2.148**), taxol (**2.150**) and (+)-discodermolide (**2.151**). Additionally, the macrolactam analogue of epothilone B, azaepothilone B (**2.149**) is shown.

As the FR molecules are macrolactones similar to epothilone B (**2.148**), a process similar to the development of azaepothilone B (**2.149**) was envisioned to lead to a novel analogue of FR252921 in the form of Trilactam-FR252921 (**2.152**) as depicted in Scheme 2.37.

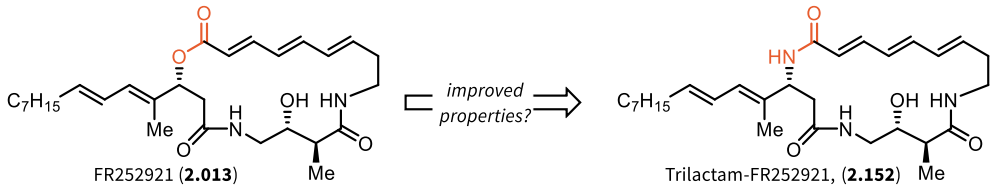

Scheme 2.37: Proposed conversion of the macrolactone FR252921 to its trilactam analogue (**2.152**).

In order to achieve the synthesis of this analogue, several strategies were investigated to synthesise an advanced precursor and the different approaches to Trilactam-FR252921 (**2.152**) are explored in the following chapters.

2.3.2.2.1.4.1. The BMS-like Approach to Trilactam-FR252921

The synthesis of azaepothilone B (**2.149**) by Bristol-Myers-Squibb relies on the semisynthetic modification of the natural product epothilone B (**2.148**), which can be acquired from its natural source organism *Sorangium cellulosum*. The conversion of epothilone B to its lactam analogue can be carried out in three synthetic steps, all conducted without isolation of intermediates, to yield the desired

product.[269] Starting with epothilone B (**2.148**), the allylic lactone is opened through the action of a palladium catalyst (Scheme 2.38A) and the resulting Pd-complex is substituted by an azide anion in a Tsuji-Trost reaction to form **2.153** with retention of stereochemistry. The newly introduced azide moiety is subsequently reduced in a Staudinger reduction to yield amino acid **2.154**, which undergoes macrolactamisation mediated by HOBt and EDCI to yield azaepothilone B (**2.149**). This reaction sequence can be applied on larger scales (5.06 g of epothilone B) and can be conducted in a one-pot fashion without isolation of the intermediates, to deliver the desired product **2.149** in 23% yield.

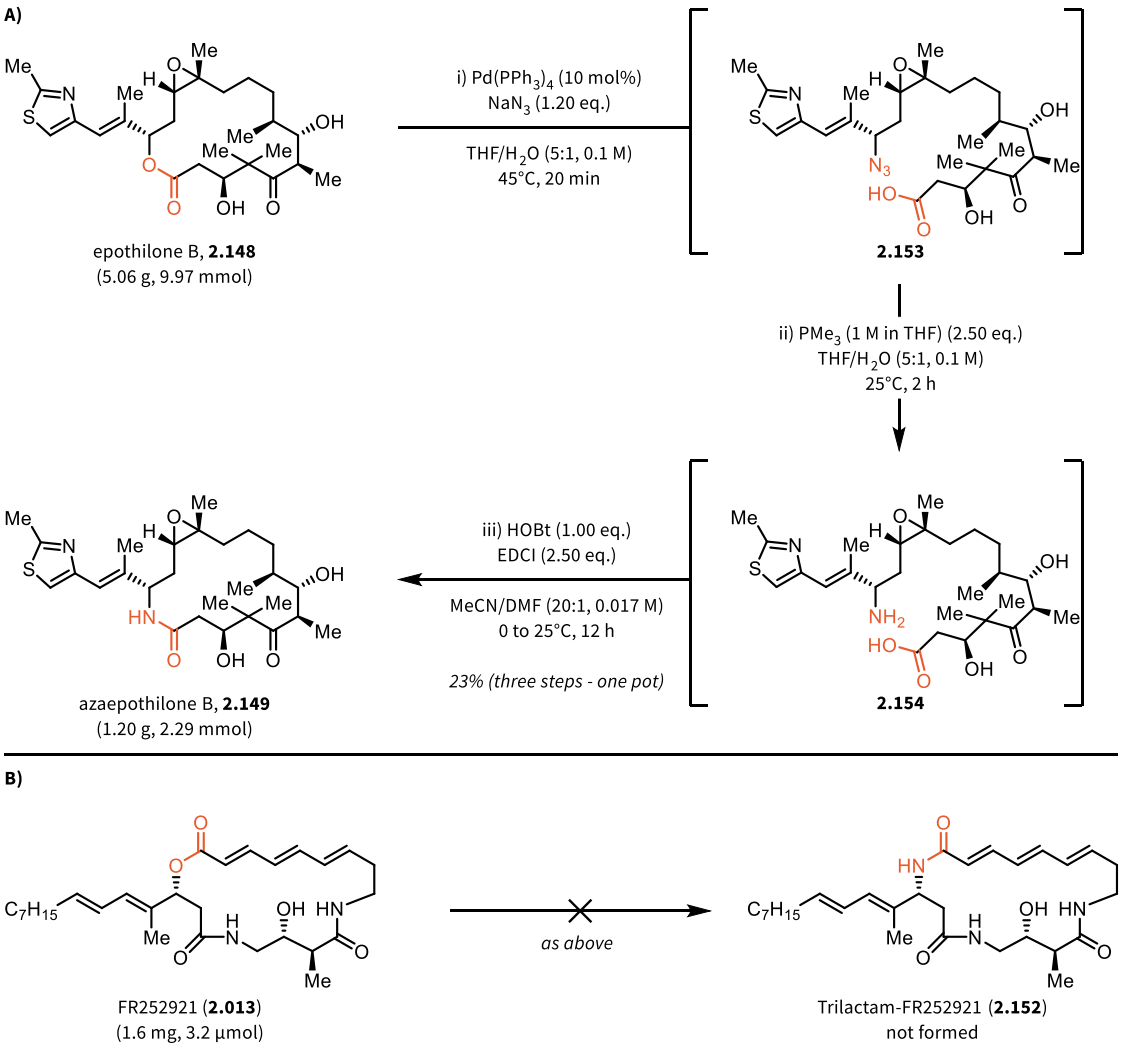

Scheme 2.38: A) BMS-Synthesis of azaepothilone B (**2.149**) from epothilone B (**2.148**) *via* a three-step-one-pot approach featuring Tsuji-Trost ring opening/allylic substitution, Staudinger reduction and macrolactamisation. B) Analogous application of reaction conditions to FR252921 (**2.013**) failed to deliver Trilactam-FR252921 (**2.152**).

When applying the exact same reaction conditions to FR252921, in order to convert it to Trilactam-FR252921 (**2.152**), it was found that the allylic ester in FR252921 does not undergo ring-opening mediated by the palladium catalyst. Rather than forming a novel complex and being consumed in the desired

fashion, the starting material FR252921 was found to be entirely unreactive under the employed reaction conditions and could be reisolated from the reaction mixture (Scheme 2.38B), leading to the exploration of other possibilities to access Trilactam-FR252921.

2.3.2.2.1.4.2. Modifications of the Side-chain Building Block to access Trilactam-FR252921

The failure of the direct route to Trilactam-FR252921 (**2.152**) as inspired by the synthesis of azaepothilone B (**2.149**) led to the reconsideration of the synthetic approach towards this FR analogue. Since the concept of a diversifiable synthetic platform is at the heart of the synthetic efforts, modification of the side-chain building block to access Trilactam-FR252921 was explored next (Scheme 2.39).

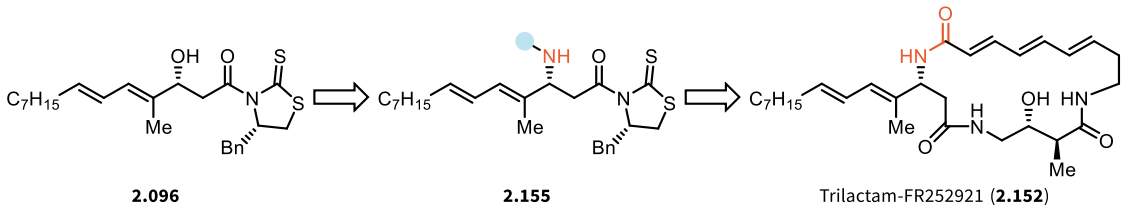

2.096 **2.155** Trilactam-FR252921 (**2.152**)

Scheme 2.39: Outlined synthetic plan to convert the side-chain hydroxyl moiety to a nitrogen-containing functional group to then serve as a building block in the approach towards Trilactam-FR252921 (**2.152**).

The experiments towards probing the feasibility to convert the regular FR252921 side-chain building block (**2.096**) into a modified building block carrying either a leaving group amenable for displacement or a nitrogen-containing moiety are summarised in Table 2.3. First, attempts to convert the hydroxyl moiety into a leaving group amenable to Tsuji-Trost reaction or S_N2 displacement were explored. Converting the hydroxyl moiety into a tosylate, hoping to invoke its properties as a leaving group, either led to decomposition (reagent grade pyridine, entry 1) or to no conversion of the starting material when distilled pyridine was employed (entry 2). However, conversion of **2.096** to acetate **2.156** (X = OAc) was achieved in mediocre yield through reaction with acetic anhydride in distilled pyridine (entry 3) and the thusly generated acetate was used in a Tsuji-Trost reaction with sodium azide, aiming to introduce an azide moiety (entry 4). To our dismay, this reaction failed to produce the desired product and resulted in decomposition of the starting material. In cases where the products of decomposition could be analysed,

it was found that decomposition could occur *via* the hydrolysis of the auxiliary, resulting in a carboxylic acid, or *via* elimination of the hydroxyl moiety to yield a triene decomposition product.

Diphenylphosphoryl azide (DPPA) is a commonly employed reagent to convert hydroxyl moieties to the corresponding azides, hinging on the high oxophilicity of phosphorus enabling sufficient activation of the hydroxyl group to enable displacement by the azide. However, when applied to the side-chain building block **2.096**, DPPA was found to lead to immediate decomposition of the starting material without producing any trace of the desired product (entry 5 and 6). Switching to $TMSN_3$, an alternative activating agent bearing an azide moiety, led to disappointing outcomes. Its use in conjunction with a Cu(II) catalyst returned only byproducts of unspecific decomposition (entry 7), whereas using $TMSN_3$ together with catalytic amounts of $BF_3 \cdot OEt_2$ led to no reaction at all (entry 8). Aiming to activate the secondary alcohol in **2.096** prior to the addition of DPPA, which previously led to immediate decomposition, conditions reminiscent of a Mitsunobu reaction were employed (entry 9). Here, the alcohol was activated with PPh_3 and diisopropyl azodicarboxylate (DIAD), followed by addition of DPPA. It was found that this combination of reagents led to no reaction.

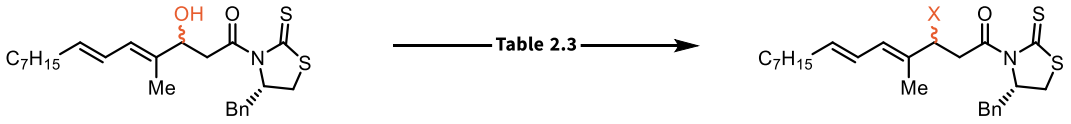

2.096 **2.156**, X = N_3, OAc, OTs

Table 2.3

Entry	Reagent	Catalyst	Base	Conditions	Result
1	TsCl (1.10 eq.)	–	pyridine (xs)	pyridine (0.2 M), 20°C, 18 h	*decomposition*
2	TsCl (1.10 eq.)	–	distilled pyridine (xs)	pyridine (0.2 M), 20°C, 18 h	*no conversion*
3	Ac_2O (1.10 eq.)	–	distilled pyridine (xs)	pyridine (0.2 M), 20°C, 18 h	*38%, 4:1 d.r.*
4	**2.156**, X = OAc + NaN_3 (1.10 eq.)	$Pd(PPh_3)_4$ (5 mol%)	–	THF/H_2O (3:1, 0.3 M), 20°C, 18 h	*decomposition*
5	DPPA (1.20 eq.)	–	DBU (1.20 eq.)	toluene (0.2 M), 20 °C, 18 h	*decomposition*
6	DPPA (1.20 eq.)	–	DBU (1.20 eq.)	toluene (0.2 M), 20°C, 18 h	*decomposition*
7	$TMSN_3$ (1.50 eq.)	$Cu(OTf)_2$ (5 mol%)	–	DCM (0.5 M), 0 to 20°C, 18 h	*decomposition*
8	$TMSN_3$ (1.50 eq.)	BF_3•OEt_2 (10 mol%)	–	DCM (0.5 M), 0 to 20°C, 18 h	*no conversion*
9	DIAD (1.50 eq.), PPh_3 (1.50 eq.) DPPA (1.50 eq.)	–	–	THF (0.05 M), 0 to 20°C, 18 h	*no conversion*

Table 2.3: Summary of the experiments to convert secondary alcohol **2.096** to any of the proposed products (**2.156**).

Since the modification of the side-chain building block **2.096** proved to be cumbersome, primarily due to the instability of the precursor under various reaction conditions, we considered two new approaches, described in the following subchapters.

2.3.2.2.1.4.3. The Isoxazolin-Approach to Trilactam-FR252921

The synthesis of Trilactam-FR252921 is in essence a problem of selective synthesis of a chiral β-amino acid building block, in which the amino group is both secondary as well as adjacent to a (*E*,*E*)-diene system. One promising approach towards the synthesis of such a building block can be found in the total synthesis of epothilone A and B by Carreira *et al.*, in which a directed 1,3-dipolar cycloaddition (Huisgen reaction) of a nitrile oxide onto an olefin is used to construct the northern half of epothilone B **2.148** (Scheme 2.40A).[208] Precedent for this reaction was found in research conducted by Kanemasa *et al*. and was further developed towards general applicability and ultimately β-amino acid synthesis by Carreira *et al.* and Mapp *et al*.[273–278] One key advantage of the directed nitrile-oxide Huisgen reaction is that phosphonates are accepted as bystander moieties in the substrate, resulting in the retrosynthetic approach towards Trilactam-FR252921 (**2.152**) outlined in Scheme 2.40B. Therein, Trilactam-FR252921 is deconstructed using the disconnections established for the synthesis of the FR molecules, namely Domino Suzuki-Miyaura macrocyclisation (green), introduction of a *cis*-chlorocyclobutene acid (orange) and amide bond formation (blue).

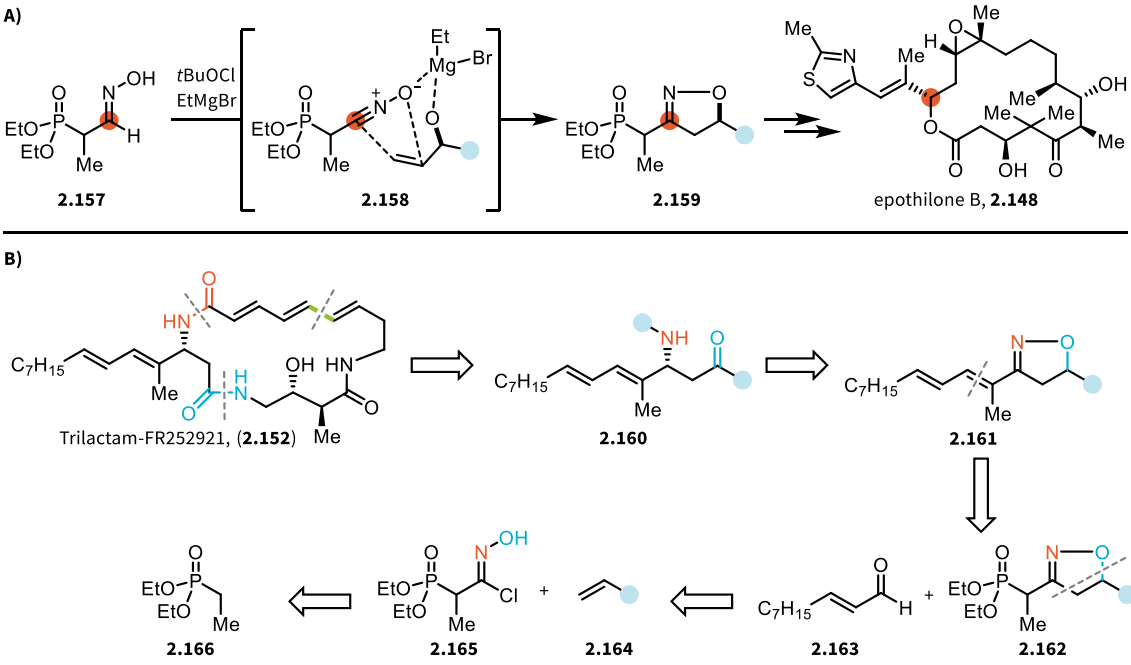

Scheme 2.40: A) Simplified approach to epothilone B (**2.148**) as reported by Carreira *et al*. B)Retrosynthetic approach towards Trilactam-FR252921 (**2.152**) *via* a directed 1,3-dipolar cycloadditon followed by HWE-olefination and opening of the isoxazoline **2.162**.

The forward synthesis followed literature precedent,[208] and started from commercially available diethyl ethylphosphonate (**2.166**), which was deprotonated using *n*BuLi, reacted with DMF to form a hemiaminal and hydrolysed upon workup to yield an aldehyde (not shown). This aldehyde was subsequently condensed with hydroxylamine to yield aldoxime **2.157** (Scheme 2.41). Aldoxime **2.157** was then converted through reaction with freshly generated *t*BuOCl to its corresponding hydroxyimidoyl chloride (**2.165**, Scheme 2.40B), which, due to its instability, was used in the next step without isolation. The newly synthesised hydroxyimidoyl chloride was reacted in a directed 1,3-dipolar cycloaddition with 1-buten-3-ol after being converted to the corresponding nitrile oxide *in situ*, a process requiring deprotonation (mediated by the excess amount of Grignard reagent — EtMgBr) and elimination of a chloride anion. Due to the presence of the Grignard reagent additionally leading to the deprotonation of 1-buten-3-ol, the charged species coordinate the magnesium ions present in the reaction mixture (*cf.* Scheme 2.40A). This induced proximity of the dipole nitrile oxide and the dipolarophile 1-buten-3-ol led to the regioselective 1,3-dipolar cycloaddtion yielding phosphonate **2.167** with a 1,2-*syn* relation of the hydroxyl substituents.[274,275] The phosphonate **2.167** was engaged in a Horner-Wadsworth-Emmons (HWE) olefination reaction with *trans*-2-decenal (**2.116**), the precursor for the regular FR252921 side-chain, to form the advanced Trilactam-FR252921 side-chain precursor **2.168**. In order to progress **2.168** further towards the desired β-amino acid building block (**2.160**), the isoxazoline ring needed to be reductively opened to yield **2.169**. The required reduction was extensively explored, as outlined in Table 2.4, however, the desired product **2.169** could not be formed in sufficient amounts for isolation and full characterisation. $LiAlH_4$ at temperatures between 0 and 20°C was the only reductant capable of producing detectable amounts of the desired product, in either protected or unprotected form (entries 1, 2 and 9), while other reductants, including mixed nickel(II) borohydride species, led to overreduction by reducing the diene in the side-chain (entries 3 – 5). Lastly, $LiAlH_4$ at cryogenic temperatures, as well as DIBAL (entries 6-8), were not effective at reducing the starting material. These efforts were further complicated by the high polarity of the anticipated product **2.169**, which, paired with its generation in only trace amounts, thwarted efforts of isolation and characterisation and brought this synthetic route to a halt.

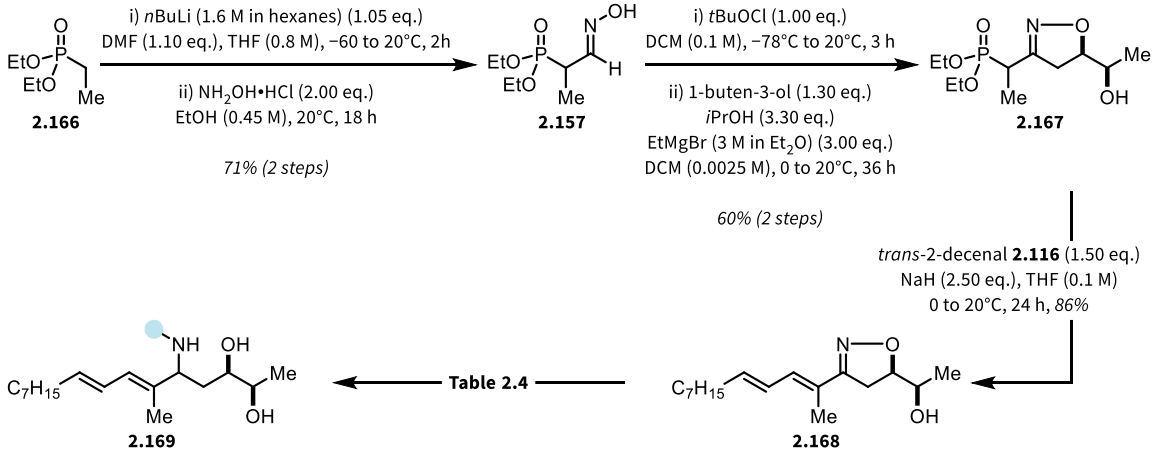

Table 2.4

Entry	Reagent	Conditions	Result
1	i) $LiAlH_4$ (1 M in THF) (4.00 eq.) ii) Boc_2O (3.00 eq.)	i) THF (0.7 M), 0 to 20°C, 2 h ii) EtOAc (0.2 M), 20°C, 12 h	*N-Boc amine **2.169** mass detected*
2	$LiAlH_4$ (4.00 eq.)	THF (0.1 M), 0 to 20°C, 18 h	*mass detected*
3	$NiCl_2$ (3.00 eq.), $NaBH_4$ (10.0 eq.)	DCM/MeOH (1:1, 0.05 M), −30°C, 18 h	*overreduction*
4	$NiCl_2$ (4.00 eq.), $NaBH_4$ (10.0 eq.), Boc_2O (1.50 eq.)	MeOH (0.1 M), 0 to 20°C, 18 h	*overreduction*
5	$NiCl_2•6H_2O$ (3.00 eq.), $NaBH_4$ (10.0 eq.)	MeOH/THF (3:1, 0.05 M), −30°C, 18 h	*overreduction*
6	$LiAlH_4$ (4.00 eq.)	THF (0.1M), −78°C, 2 h	*no conversion*
7	$LiAlH_4$ (4.00 eq.)	THF (0.1M), −60°C, 2 h	*no conversion*
8	DIBAL (1 M in THF) (4.00 eq.)	THF (0.1M), −78°C, 2 h	*no conversion*
9	$LiAlH_4$ (4.00 eq.)	THF (0.1M), −20 to 0°C, 18 h	*mostly no conversion trace of product detected*

Scheme 2.41: Synthesis of isoxazoline side-chain precursor (**2.168**) over five steps from commercially available phosphonate **2.166**. Following successful synthesis of **2.168**, the reductive opening of the isoxazoline to form **2.169** was investigated and the approaches towards this are summarised in Table 2.4.

While the synthetic challenges encountered in this route towards Trilactam-FR252921 may eventually be overcome, another strategy based on D-homoserine, which will be discussed in the following subchapter, was also formulated.

2.3.2.2.1.4.4. The Homoserine-Approach to Trilactam-FR252921

Another promising approach towards Trilactam-FR252921 was identified to arise from the use of D-homoserine (**2.170**), which by itself solves the problem of setting the desired stereochemistry at C-18 of the anticipated analogue, as the stereocentre is set by the starting material. The retrosynthetic approach, with regard to the requirement of a β-amino acid side-chain building block (**2.160**), is similar to the one presented in Scheme 2.40, therefore only the forward synthesis will be presented below in Scheme 2.42 and Table 2.5.

The commercially available starting material D-homoserine was first cyclised to the corresponding lactone in the presence of HCl, and the primary amine was protected with a Boc group to yield **2.171** in 83% yield over two steps. Subsequently, the lactone was converted to the Weinreb amide **2.172** through the action of $AlMe_3$ in near-quantitative yield. The primary alcohol of Weinreb amide **2.172** was then protected with a TBS-group and the Weinreb amide was converted to the methyl ketone to ultimately form **2.173**.

Overall, olefination of the methyl ketone **2.173** proved to be more complex than anticipated. First, the venerable HWE reaction was explored (Table 2.5, entries 1 – 13), as a review of the literature seemed promising for the olefination of methyl ketones with this reaction.[279,280] Aiming for the synthesis of the required building block **2.174**, methyl ketone **2.173** and phosphonate **2.177** were reacted with a range of strong bases, however the anticipated product was not formed (entries 1 – 4). In order to explore whether the methyl ketone **2.174** was at all capable of undergoing HWE olefination, commercially available phosphonate **2.179** was used and it could be shown that the test product **2.180** was formed through HWE olefination (entries 5 – 8). The phosphonate **2.179** is distinct from the required phosphonate **2.177** by the presence of an ester moiety in the β-position to the phosphorous atom. This makes the α-proton of phosphonate **2.179** much more acidic compared to aliphatic or allylic phosphonates, resulting in a more reactive phosphonium ylide capable of converting the methyl ketone **2.173** to the olefin **2.180**.

Having established that methyl ketone **2.173** is in principle able to undergo HWE olefination, more forcing conditions and the application of different bases were explored (entries 9 – 13), but were unsuccessful, except for the detection of the mass of the expected product **2.174** in trace amounts (entry 11). Following the limited success of the exploration of the HWE olefination, the approach was changed to involve a Wittig olefination. To this end, phosphonium ylide **2.178** was synthesised and tested in the reaction (entry 14), with the first attempt leading to the formation of the desired product **2.174** in 50% yield on 0.1 mmol scale.[281] Upon scale-up to 3.4 mmol (1.13 g), the yield increased to 67% to afford the desired olefination product **2.174**. With the fully protected diene **2.174** in hand, the attention was turned to the oxidation towards the carboxylic acid.

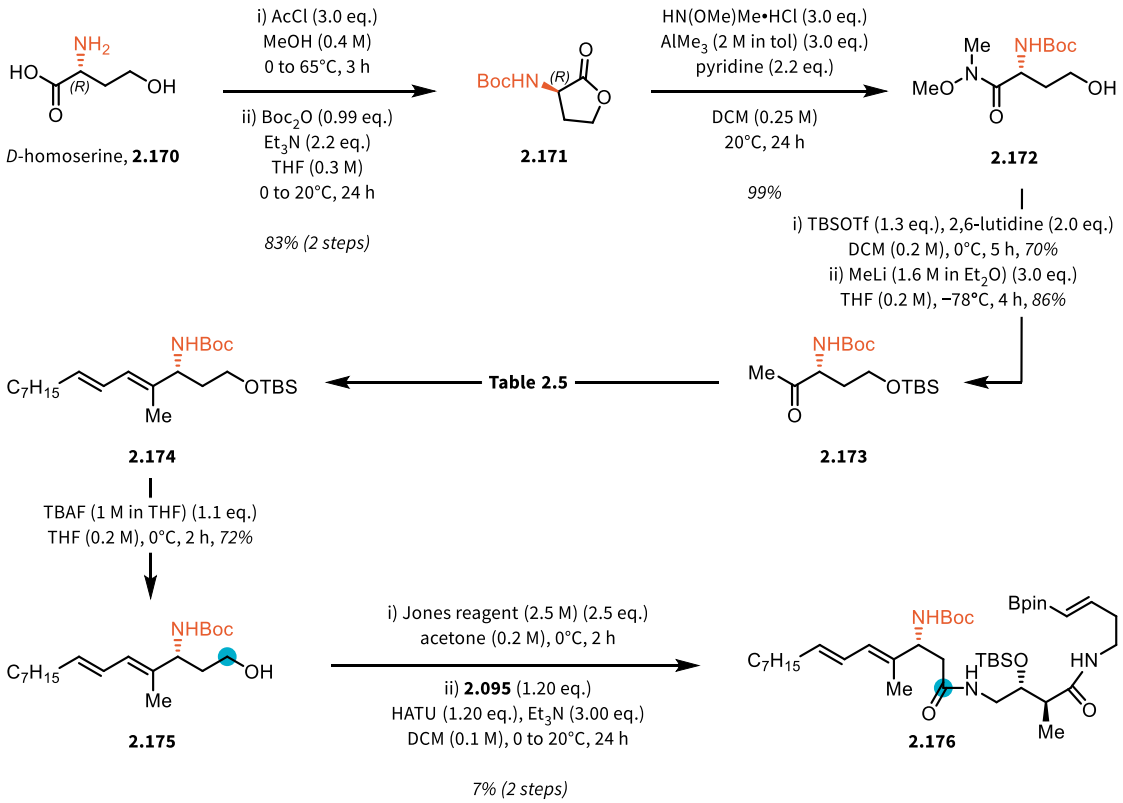

Table 2.5

Entry	Ylide	Base / Reagent	Conditions	Result
1	**2.177** (2.20 eq.)	LiHMDS (2.20 eq.)	THF (0.04 M), 0 to 20°C, 14 h	*no conversion*
2	**2.177** (2.20 eq.)	NaH (2.20 eq.)	THF (0.1 M), 0 to 20°C, 4 h	*no conversion*
3	**2.177** (2.20 eq.)	*n*BuLi (2.20 eq.)	THF (0.1 M), 0 to 20°C, 4 h	*no conversion*
4	**2.177** (2.20 eq.)	NaH (5.00 eq.)	THF (0.1 M), 0 to 20°C, 4 h	*no conversion*
5	**2.179** (2.20 eq.)	NaH (2.50 eq.)	THF (0.1 M), 0 to 20°C, 4 h	***2.180** formed*
6	**2.179** (2.20 eq.)	NaH (2.50 eq.) (inverted addition)	THF (0.1 M), 0 to 20°C, 4 h	***2.180** formed*
7	**2.179** (2.20 eq.)	LiHMDS (7.50 eq.)	THF (0.1 M), 0 to 20°C, 24 h	***2.180** formed*
8	**2.179** (2.20 eq.)	*n*BuLi (2.50 eq.)	THF (0.1 M), 0 to 60°C, 24 h	***2.180** formed*
9	**2.177** (2.20 eq.)	NaHMDS (2.25 eq.)	THF (0.1 M), −78 to 0°C, 5 h	*decomposition*
10	**2.177** (2.20 eq.)	LiHMDS (2.10 eq.) + HMPA (3.00 eq.)	THF (0.03 M), 0 to −78 to 20°C, 2 h	*no conversion*
11	**2.177** (2.20 eq.)	NaHMDS (2.10 eq.)	THF (0.1 M), −78 to 20°C, 24 h	*trace of **2.174** formed*
12	**2.177** (2.20 eq.)	*n*BuLi (2.10 eq.)	THF (0.1 M), −78 to 20°C, 24 h	*no conversion*
13	**2.177** (2.20 eq.)	NaHMDS (5.00 eq.)	THF (0.1 M), −78 to 60°C, 16 h	*decomposition*
14	**2.178** (2.00 eq.)	*n*BuLi (2.00 eq.)	THF (0.07 M), 0 to 20°C, 48 h	*50% **2.174** (0.1 mmol scale)*
15	**2.178** (2.00 eq.)	*n*BuLi (2.00 eq.)	THF (0.07 M), 0 to 20°C, 24 h	*67% **2.174** (3.4 mmol scale)*

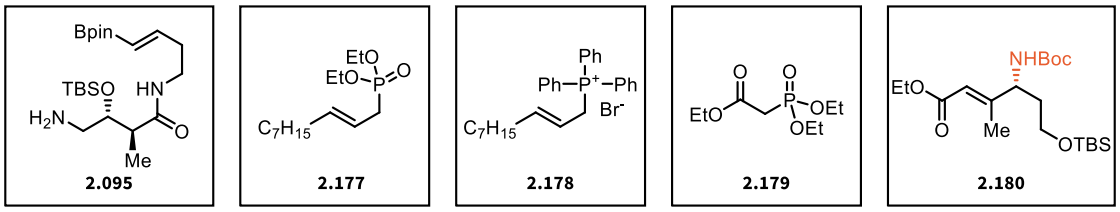

Scheme 2.42: Synthetic route to the advanced Trilactam-FR252921 precursor **2.176** over nine steps, starting from D-homoserine (**2.170**). The optimisation required for successful installation of the aliphatic side-chain is summarised in Table 2.5, with entries 1 to 13 exploring the HWE olefination and entries 14 and 15 exploring Wittig olefination. LiHMDS, NaHMDS and *n*BuLi were used as solutions either in THF (1 M; LiHMDS, NaHMDS) or hexanes (1.6 M; *n*BuLi).

This was achieved by removing the TBS protecting group to reveal the primary alcohol (**2.175**), which was then oxidised by virtue of the Jones reagent (CrO_3 in H_2SO_4) to afford the crude carboxylic acid, which was

used without further purification in a HATU-mediated amide coupling with FR core precursor **2.095** to afford the linear Trilactam-FR252921 precursor **2.176** in 7% over two steps. The low yield can be attributed to the unoptimised oxidation protocol to generate the carboxylic acid, which could be further explored in the future. Alternatively to Jones oxidation,[282] DMP oxidation followed by Pinnick oxidation,[283–286] or other oxidation methods could be explored in order to increase the yield of the key building block **2.176**.[287,288]

Due to the scarcity of the available material, as well as requirements to deliver other analogues for biological testing, the synthetic efforts towards Trilactam-FR252921 were concluded after demonstrating that **2.176** could be accessed. In order to complete the synthesis, it is required to cleave the *N*-Boc protecting group (TFA) and form an amide with *cis*-chlorocyclobutene acid (**2.057**), followed by the key macrocyclisation event, catalysed by Pd(0), and TBS deprotection to yield Trilactam-FR252921 (**2.152**).

2.3.2.2.2. Southern Macrocycle Modification of FR252921

Four modifications of the southern hemisphere of the macrocyclic core of FR252921 were completed and are described herein. First, the synthesis of the enantiomer of FR252921 is described, followed by the preparation of a bioisoster of FR252921. Lastly, two modifications of the C-13 hydroxyl moiety are explored.

2.3.2.2.2.1. *Ent*-FR252921

One key theory within biochemistry and drug design is the idea that an effector molecule binds tightly into the pocket of a protein, leading to an observable impact, *i.e.* inhibition of an enzyme or mediation of protein-protein interactions. This "lock and key" principle is at the heart of modern drug development efforts. Since proteins are themselves chiral and given a ligand which itself is also chiral, it is generally expected that one enantiomer binds while the other does with reduced affinity or not at all.

To probe whether FR252921 poses its biological effects through protein binding or through alternative pathways (*e.g.* metabolic disturbance, oxidative stress), the assumption that the enantiomers possess different levels of activity was tested through the synthesis of *ent*-FR252921 (*ent*-**2.013**). Since enantiomers behave identically in a non-chiral environment, the synthesis of *ent*-FR252921 was conducted in an identical manner, starting from the opposite enantiomers of the starting building blocks (Scheme 2.43). The synthesis of *ent*-FR252921 is listed herein as a modification of the southern hemisphere, although it may be considered a *global* modification of the macrocycle.

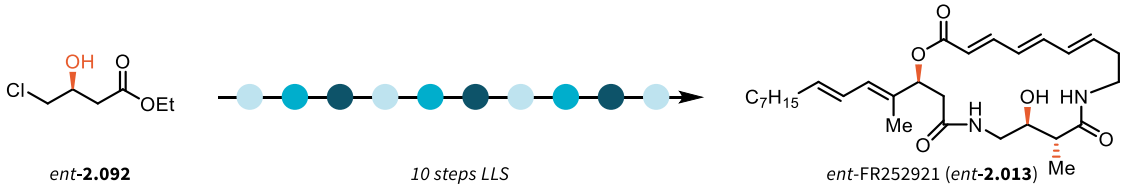

ent-**2.092** *ent*-FR252921 (*ent*-**2.013**)

Scheme 2.43: Simplified depiction of the synthesis of *ent*-FR252921 (*ent*-**2.013**) from the opposite enantiomer of commercially available *ent*-**2.092**.

2.3.2.2.2.2. OMe-FR252921 and OTBS-FR252921

Based on the prior publication of Maulide *et al*., the removal of the C-13 hydroxyl moiety led to inactive FR analouges. However, it remained unclear whether the lack of activity arose from the missing potential hydrogen bond donor (hydrogen attached to the oxygen) or if the hydrogen bond acceptor properties of the oxygen atom are crucial to the activity. Calculations indicated the presence of intramolecular hydrogen bonding between the oxygen of the hydroxyl moiety located at C-13 and NH-15 (Scheme 2.44).[253] Additionally, it was expected that these analogues should be more stable compared to the parent FR molecule, as the removal of the nucleophilic hydroxy moiety renders the transannular Michael addition impossible.

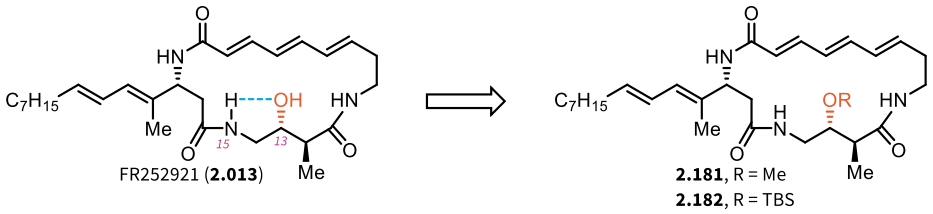

Scheme 2.44: Logic behind the proposed analogues **2.181** and **2.182** to probe the influence of the HBA/HBD properties of the C-13 hydroxyl moiety. The calculated hydrogen bond between NH-15 and the C-13 alcohol is depicted in blue.

To probe this, two analogues were envisioned, one of which was found in the TBS-protected precursor to FR252921 (**2.182**). This compound allows for the evaluation of activity for a sterically encumbered HBA-oxygen atom at C-13, while also being readily available through the synthesis of FR252921 (Scheme 2.21). Synthetic access to OMe-FFR252921 (**2.181**) was ultimately achieved by an early alteration of the synthetic sequence. Starting from the previously described azidoalcohol **2.093** (Scheme 2.21),[253] the route was altered to introduce a methylation event (Scheme 2.45). Successful methylation was conducted using MeI and Ag_2O to yield **2.183**. Notably, hydrolysis of the ester using LiOH led to epimerisation of the methyl group in the α-position, which could be circumvented by replacing LiOH with an excess Me_3SnOH, a mild reagent for the hydrolysis of epimerisable esters,[289] affording β-methoxy acid **2.184** in quantitative yield. The acid was then engaged in an amide coupling reaction mediated by HATU to be joined with ammonium salt **2.091** to furnish amidoazide **2.185**. Reduction of azide **2.185** was achieved using Staudinger reduction conditions (PEt_3 in THF/H_2O), as the reduction using Zn dust led to decomposition of the material. Consequently, a second amide coupling with the side-chain building

block **2.096** yielded the linear secondary alcohol **2.186**, amenable to esterification. *Cis*-chlorocyclobutene ester **2.187** was formed from alcohol **2.186** and *cis*-chlorocyclobutenecarboxylic acid **2.057** applying the improved esterification protocol using T3P as an activation reagent. Finally, the domino Suzuki-Miyaura cross-coupling / 4π-electrocyclic ring opening macrocyclisation reaction was conducted to yield OMe-FR252921 (**2.181**) over nine steps in the longest linear sequence and modification of three steps.

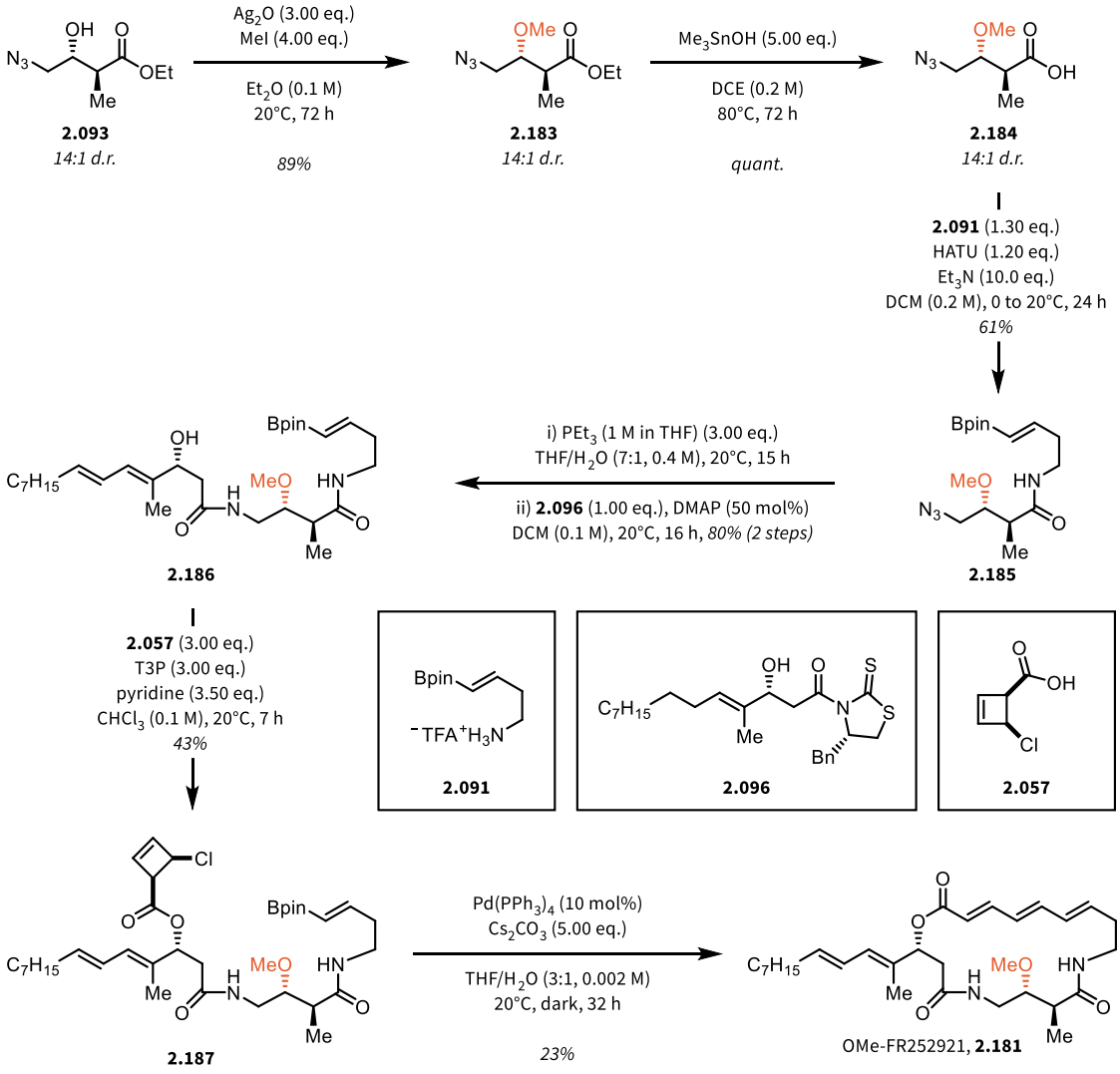

Scheme 2.45: Synthesis of OMe-FR252921 (**2.181**) through a modification of the established route to introduce the methoxy moiety early in the synthesis. The presence of a methoxy group rendered the molecule sensitive to epimerisation, requiring the choice of Me_3SnOH to mediate the hydrolysis of the ester. The reduction of the azide had to be conducted using Staudinger conditions, as the reduction using Zn dust (*cf* Scheme 2.21) led to decomposition.

2.3.2.2.2.3. Bioiso-FR252921

One concept of biological and medicinal chemistry previously briefly introduced is the introduction of structural modifications which aim to mimic the steric and electronic properties of the parts of the molecule being replaced, while allowing for alteration of the properties of the molecule. These replacements are especially relevant in contexts where the conversion of a metabolically labile group into a more stable moiety can convert an inactive compound into an important drug, as has been the case for azaepothilone B (**2.149**; Scheme 2.38). In general, this concept is referred to as bioisosteric replacement and is commonly applied in the development of drug molecules.[290] One of the most commonly encountered types of bonds in biomolecules are amide bonds, as they are ubiquitous in proteins as well as other biologically relevant molecules. The bioisosteric replacement of amide bonds is a widely used strategy to improve the properties of a given molecule in a pharmaceutical context. Having two amide bonds in the FR molecules, it was envisioned that a bioisosteric replacement could be of interest. Replacing the western lactam within the macrocycle by a triazole seemed to be synthetically feasible given the building block-based approach to FR analogues and the resulting Bioiso-FR252921 (**2.188**) is shown in Scheme 2.46 alongside a visualisation of the HBA/HBD-properties of an amide bond and a triazole.

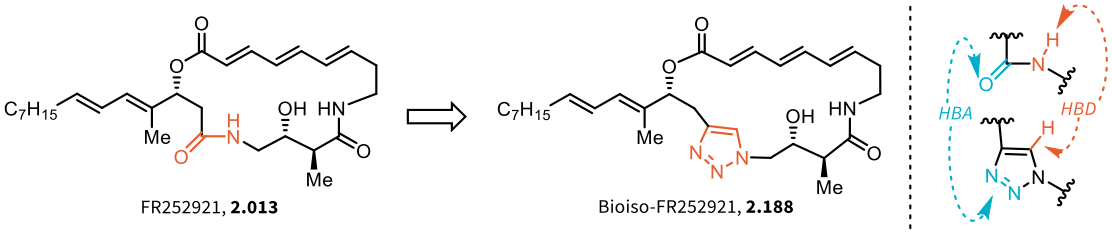

Scheme 2.46: Proposed modification of FR252921 (**2.013**) by replacing the highlighted western lactam with a triazole, a moiety which possesses similar HBA/HBD-properties, leading to Bioiso-FR252921 (**2.188**).

The synthesis of bioiso-FR252921 (**2.188**) began with the side-chain building block **2.096**, which is available in diastereomerically pure form in multi-gram amounts due to its ubiquity in FR analogues and is depicted in Scheme 2.47. First, the allylic hydroxy group was protected using TBSOTf and 2,6-lutdine to yield **2.189**, which was subsequently reduced to aldehyde **2.190** using DIBAL at −78°C in excellent yield. Aldehyde **2.190** was subjected to the Bestmann-Ohira modification of the Seyferth-Gilbert reaction to yield terminal alkyne **2.192** after removal of the TBS protecting group.[10,291,292] With terminal alkyne **2.192**

in hand, the Cu(I)-mediated cycloaddition between alkyne **2.192** and azide **2.193** was conducted to yield the linear bioiso-FR252921 precursor **2.194** in good yield. The use of copper ensures the synthesis of the desired 1,4-triazole, whereas the use of ruthenium would be expected to lead to mixture of 1,4- and 1,5-triazoles, favouring the latter.[293–295] Triazole **2.194** was then taken forward in the last three steps of the synthetic sequence without alteration of reaction conditions to first form the *cis*-chlorocyclobutene ester, followed by the key macrocyclisation event and TBS removal to yield bioiso-FR252921 (**2.188**) over twelve steps in the longest linear sequence.

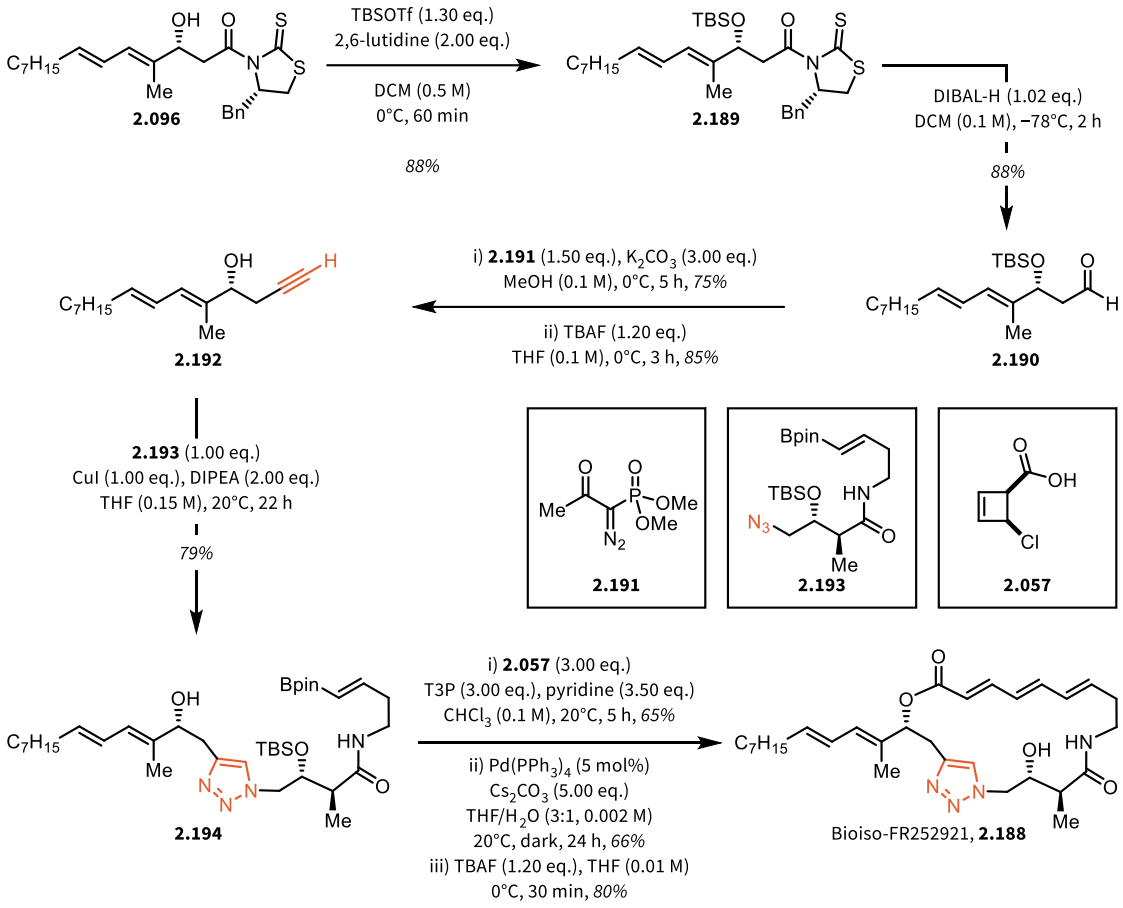

Scheme 2.47: Synthetic route to Bioiso-FR252921 (**2.188**) from the common side-chain building block **2.096** *via* Bestmann-Ohira reaction and Cu(I)-mediated azide-alkyne cycloaddition.

The synthesis of bioiso-FR252921 (**2.188**) concludes the synthetic work conducted on novel analogues of FR252921. In summary, the synthesis of fourteen novel analogues was attempted and thirteen analogues could be produced. The finished analogues, together with FR252921, FR4 and FR5, were evaluated in a range of biological assays to determine their immunosuppressive properties.

2.3.3. Biological Evaluation of FR252921 and its Analogues

When evaluating natural products or synthetic biologically active molecules, modern biology offers a range of possibilities to gather information on different aspects of the investigated compounds. Generally, biological experiments can be conducted on immortalised cell lines, which have been generated from an originator cell. The cell can originate from the tissue of interest or from primary samples taken directly from a healthy or diseased donor to evaluate the activity of a certain molecule. Cell lines derived from primary material are also common practise and they are typically not immortal, meaning that the cells start to die off after a certain number of cell divisions. Each model system has benefits as well as drawbacks (*i.e.* availability, reproducibility, closeness to relevant disease, cost, ethics considerations), which have to be taken into account when designing biological experiments.

For example, evaluation of presumed immunosuppressive compounds against so-called EL4 T cells, an immortalised T lymphocyte derived cancer (lymphoma) cell line originating from a C57BL mouse (a breed of laboratory mice), is used to gain a first understanding of the properties of the molecule.[239,253] Alternatively, immunosuppressive properties can be evaluated against so-called PBMCs, the fraction of white blood cells with one nucleus, which can be readily isolated from fresh whole blood of donors. In either case, the evaluation could be based on cell survival or proliferation, cytokine production, protein expression (so-called transcriptomics) or a number of different experimental parameters.

We originally planned to evaluate our novel analogues against EL4 T cells, as had been the case for the first generation of analogues.[253] As chapter 2.3.3.1. will describe, some reproducibility problems were encountered when running a number of analogues against the EL4 T cells, leading to a decreased activity of the FR molecules and their analogues. Following these results, a novel experimental setup was envisioned using human PBMCs, moving the evaluation of immunosuppressive properties closer to human application and allowing for a much deeper evaluation of bioactivity, as shall be detailed in chapter 2.3.3.2 and 2.3.3.3.

2.3.3.1. Evaluation of FR molecules against EL4 T cells

These experiments were conducted in close collaboration with Dr. Tuan-Anh Nguyen, Anna Koren and Dr. Stefan Kubicek at CeMM.

Following the previously established protocol, a panel of analogues was evaluated for their antiproliferative activity against EL4 T cells. First, the novel saturated-FR252921 (**2.142**) analogue was tested alongside FR252921 (**2.013**) at a range of concentrations from 5 nM to 20 µM. It was found that FR252921 showed activity with an IC_{50} = 1.2 µM, which is a five-fold decrease compared to the data published in 2019, whereas saturated-FR252921 showed no inhibition of proliferation across the range of concentrations tested (Figure 2.3).

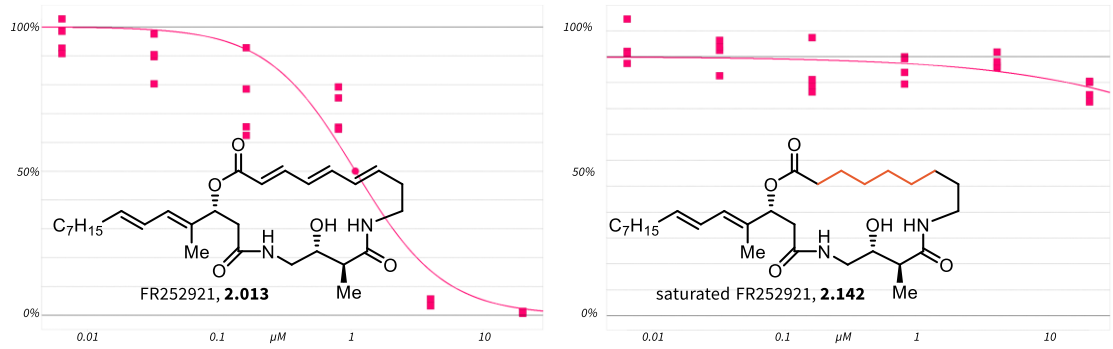

Figure 2.3: EL4 T cell proliferation assay of FR252921 (**2.013**, left) and saturated-FR252921 (**2.142**, right).

Following up on these results, a second panel of analogues was subjected to the same assay to evaluate their antiproliferative activity against EL4 T cells in order to derive information on the structure-activity relationship of these compounds and the results are shown in Figure 2.4. In summary, the results showed: i) no analogue possesses good activity against EL4 T cells at relevant concentrations (< 0.5 µM) and ii) the activity of FR252921 was 30-fold lower compared to the published data. As a result of this experiment, it was decided to cease the evaluation of novel analogues against EL4 T cells. In addition to the low reproducibility paired with the decrease in observed activity for the natural product, expanding the investigations towards human PBMCs enables a deeper investigation of the immunosuppressive properties of these compounds.

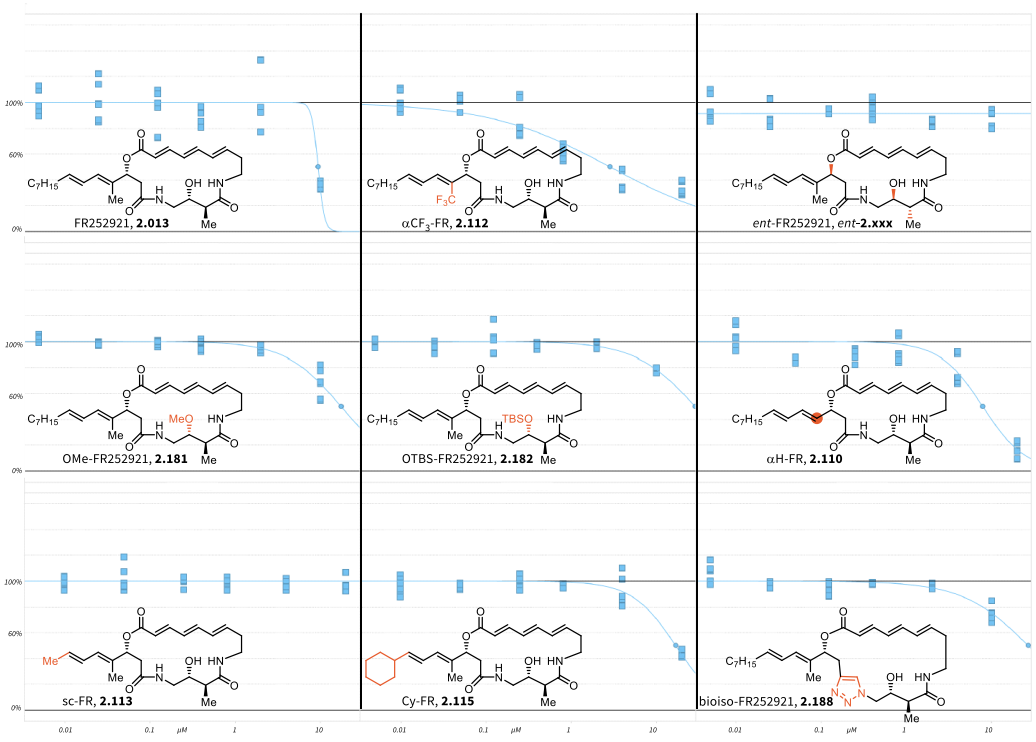

Figure 2.4: Structure-activity relationship exploration for a panel of eight new analogues as well as FR252921.

2.3.3.2. PBMC Assays, Validation Experiments and Synergy Experiment

These experiments were conducted in close collaboration with Laura Marie Gail, and Assoc. Prof. Dr. Georg Stary at CeMM and the Medical University of Vienna.

2.3.3.2.1. Establishment of Biological Activity against PBMCs

The translation from one biological model system, EL4 T cells, towards human PBMCs was first explored by the evaluation of three compounds, namely FR252921 (**2.013**), FR4 (**2.102**) and FR5 (**2.100**). These compounds were selected as they represent a range of activity according to the EL4 T cell assay. FR4 is expected to be inactive, whereas FR5 is expected to be more active than FR252921, with FR252921 being expected to show immunosuppressive activity in a range between the two fully synthetic analogues. Additionally, this first evaluation allowed for a thorough investigation of different cytokines and cell surface markers to inform the design of the antibody panel prior to evaluation of the full analogue array (*vide infra*).

In this first assay, PBMCs were isolated from one healthy donor's whole blood and were incubated with the FR compounds (FR252921, FR4 and FR5; Figure 2.5) at concentrations of 10 nM, 500 nM and 1µM. The cells were then activated with a cell activation cocktail (CAC) containing phorbol 12-myristate 13-acetate, a protein kinase C activator capable of activating T cells, and ionomycin, an ionophore which raises intracellular Ca^{2+} levels, which leads to activation of the remaining lymphocytes.[296] After several hours, the cells were stained for viability, cell surface markers and intracellular cytokines in order to enable further analysis by fluorescence-based cell sorting. Before the potentially immunosuppressive effects of the FR molecules could be evaluated, the viability of the stimulated $CD45^+$ cells was controlled, in order to exclude severely cytotoxic molecules, leading to the results displayed in Figure 2.5. It was shown that FR4 possesses no cytotoxic properties, while FR252921 and FR5 are slightly cytotoxic in a dose-dependent

manner. None of the compounds presented with severe cytotoxic effects and they could therefore be further evaluated with regards to their immunosuppressive properties within the viable fraction of cells.

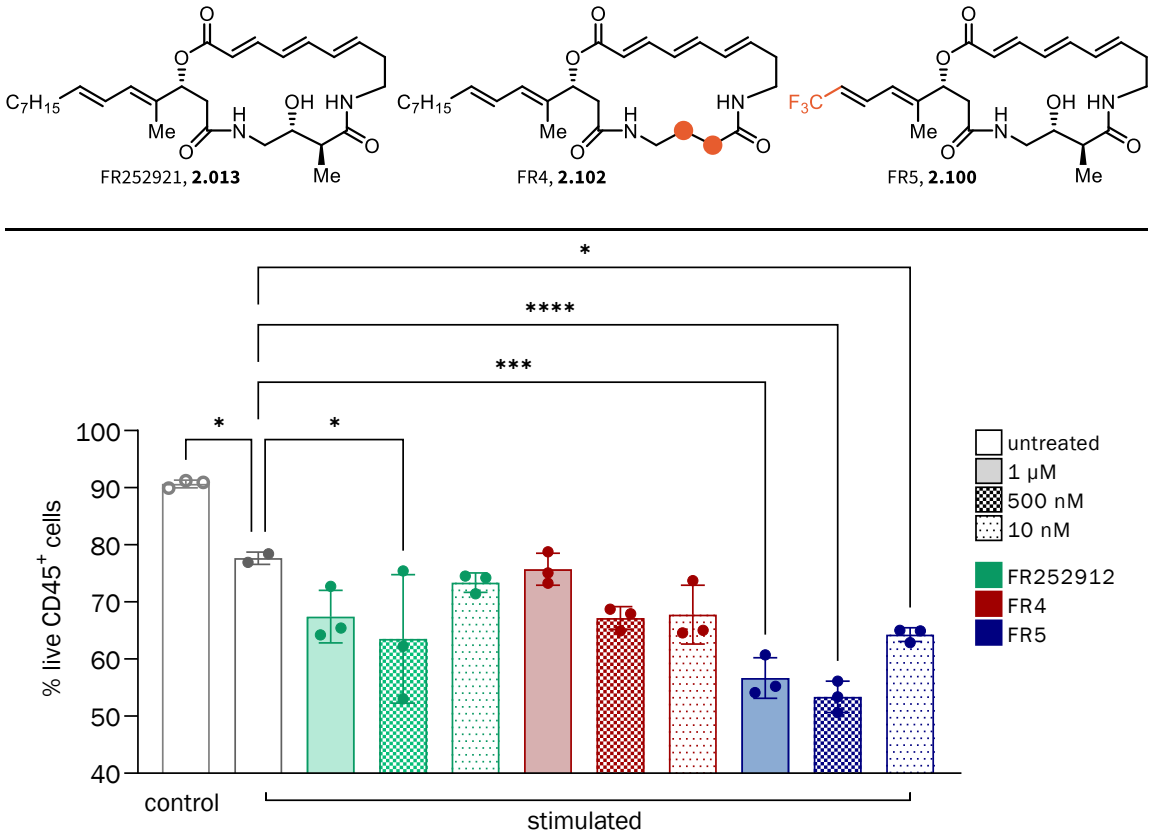

Figure 2.5: Viability readout for FR252921, FR4 and FR5 against stimulated CD45⁺ cells at concentrations of 1 µM (solid bars), 500 nM (checkered bars) and 10 nM (dotted bars). Negative control (left) and positive control (second from left) refer to untreated, unactivated cells (negative control) or untreated, activated cells (positive control). The *p* values for statistical significance are depicted as: * = $p < 0.05$; ** = $p < 0.01$; *** = $p < 0.001$; **** = $p < 0.0001$ and refer to the likeliness of an error in the correlation.

The small panel of three FR compounds was then evaluated in their capability to suppress the response of different types of immune cells following incubation and activation. As depicted in Figure 2.6, the presence of FR252921 and FR5 has a pronounced effect on IFN-γ expression, while FR4 shows a distinct lack of activity. The picture is less clear for the suppression of TNF-α, as FR252921 only exhibits non-significant activity, however FR5 is again highly active in suppressing TNF-α at 1 µM and 500 nM concentrations. IL-6, IFN-γ and TNF-α are cytokines which are produced by immune cells upon activation and can therefore be used as an indicator of the immune response or its suppression.

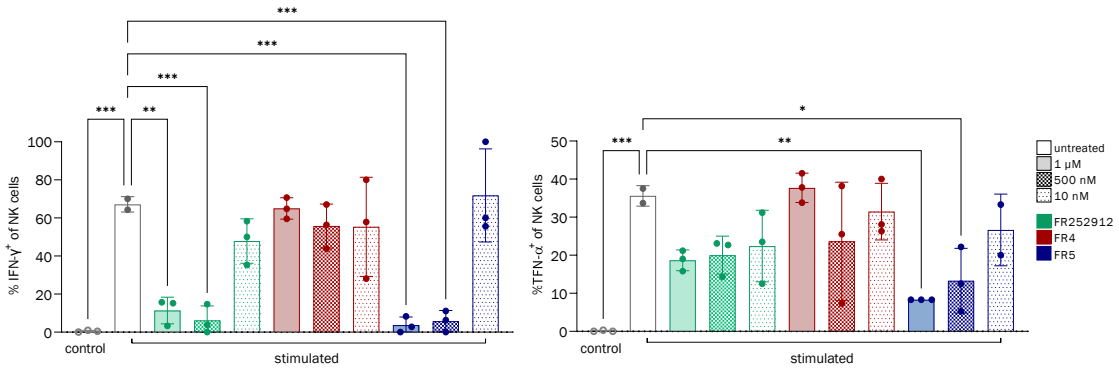

Figure 2.6: Influence of FR252921, FR4 and FR5 on the expression of IFN-γ and TNF-α in NK cells at the indicated concentrations. Negative control (left) and positive control (second from left) refer to untreated, unactivated cells (negative control) or untreated, activated cells (positive control). The *p* values for statistical significance are depicted as: * = $p < 0.05$; ** = $p < 0.01$; *** = $p < 0.001$; **** = $p < 0.0001$ and refer to the likeliness of an error in the correlation.

Next, a similar behaviour of the tested FR compounds in their immunosuppressive activity could be established across T cells and antigen-presenting cells (APCs). It was shown that both FR252921 and FR5 possess potent immunosuppressive activity at 1 µM and 500 nM concentrations (Figure 2.7), with FR5 showing some activity against IL-6 production in APCs at 10 nM. Additional cytokines in different cell types were evaluated as well, but are omitted for sake of brevity.

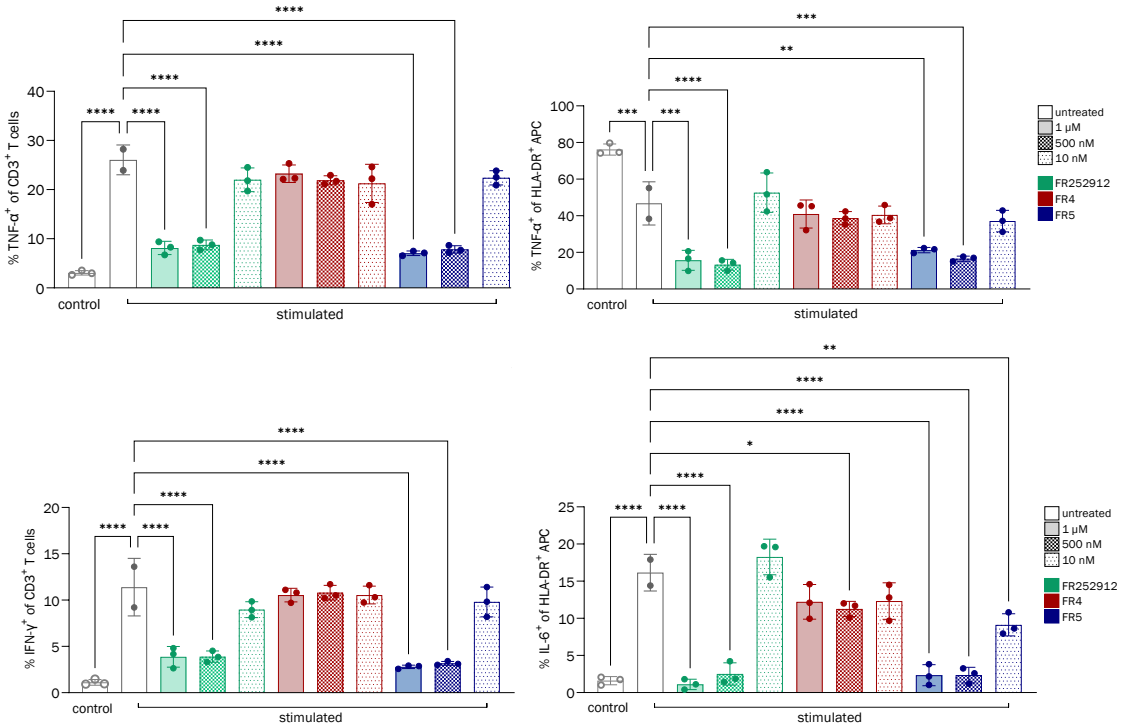

Figure 2.7: Effects of FR252921 (green), FR4 (red) and FR5 (blue) on the expression of TNF-α and IFN-γ in T cells and of TNF-α and IL-6 in APCs at 1µM (solid), 500 nM (checkered) and 10 nM (dotted). Negative control (left) and positive control (second from left) refer to untreated, unactivated cells (negative control) or untreated, activated cells (positive control). The *p* values for statistical significance are depicted as: * = $p < 0.05$; ** = $p < 0.01$; *** = $p < 0.001$; **** = $p < 0.0001$ and refer to the likeliness of an error in the correlation.

2.3.3.2.2. Evaluation of diverse FR252921 Analogues against PBMCs and Determination of IC_{50} values for the most active Compounds

After developing experimental conditions to evaluate the immunosuppressive properties of the FR compounds against human PBMCs, a large panel of analogues was prepared and the immunosuppressive properties as well as cytotoxicity of all analogues were evaluated in order to derive additional information with regards to their structure-activity relationship. The full panel of FR analogues is depicted in Figure 2.8 and consists of sixteen unique compounds.

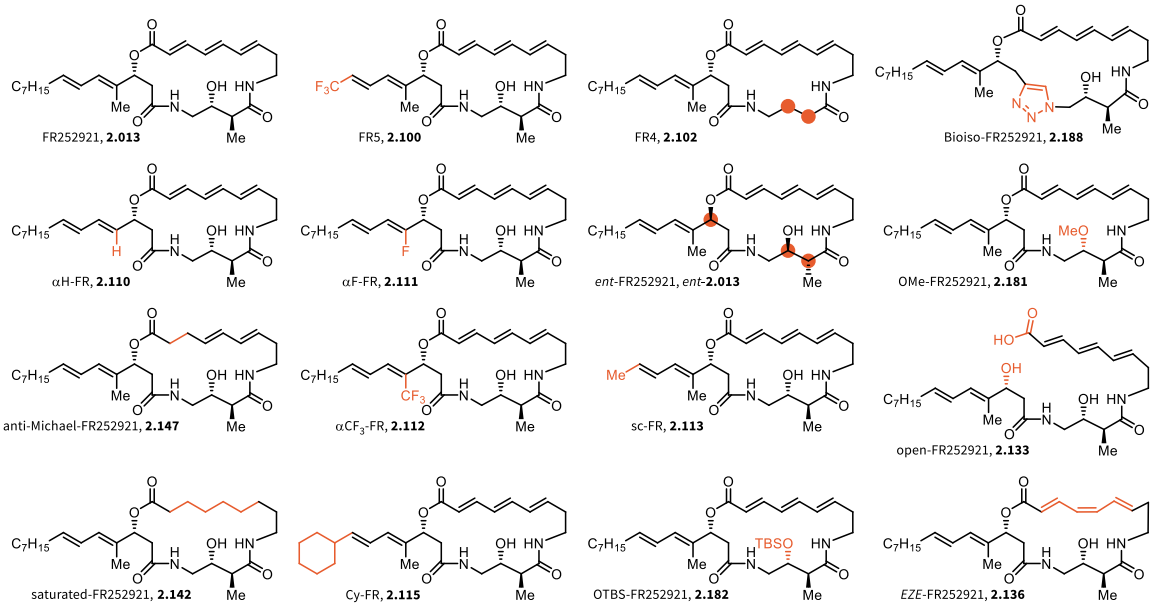

Figure 2.8: Panel of FR compounds to be tested against human PBMCs in a dose-response experiment.

All analogues were tested in a range of six concentrations (10 nM, 50 nM, 100 nM, 500 nM, 1 µM, 10 µM) in triplicate against positive and negative controls in order to generate dose-response curves amenable to determination of IC_{50} values. Thirteen different antibodies were used to label various cellular features and every compound was tested in triplicate at every concentration. Overall, deducting markers needed for cell type definition, this led to 36 data points per compound for each concentration or 216 data points per compound across six concentrations or 3456 data point excluding positive and negative controls overall. Due to the large amount of data generated, most activity data was preliminarily analysed at a concentration of 100 nM. Importantly, the natural product FR252921 produced strong

immunosuppressive effects against a range of cytokines and cell types at 100 nM while being non-cytotoxic. A first evaluation of cytotoxicity at 100 nM concentration is depicted in Figure 2.9.

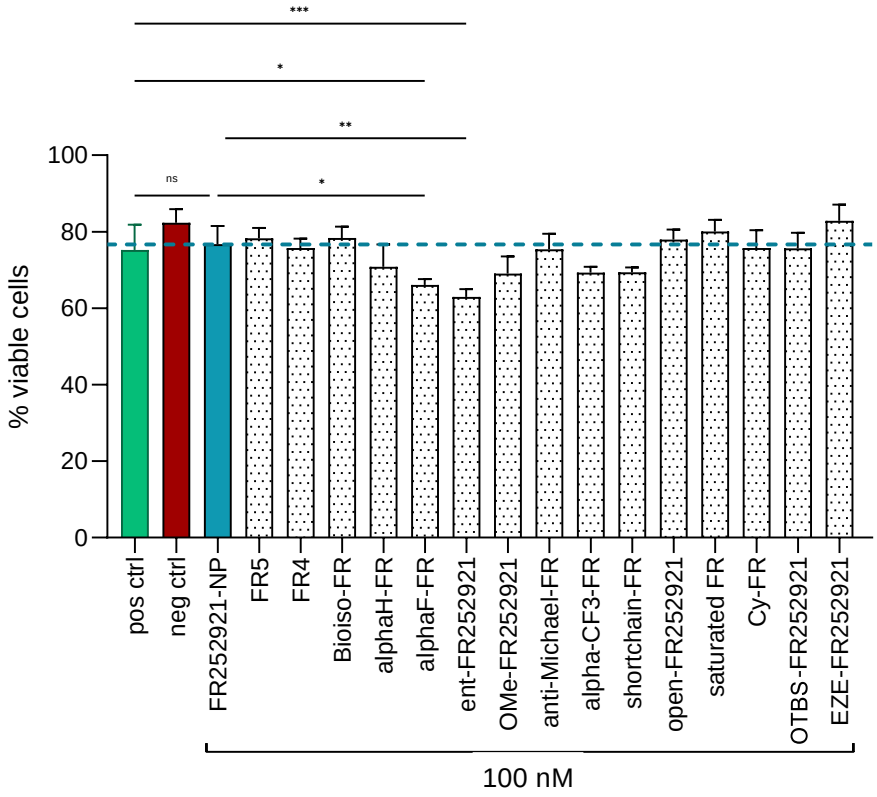

Figure 2.9: Cell viability evaluation of the panel of FR compounds at 100 nM concentration. Positive control (green) and negative control (red) refer to untreated, activated cells (positive control) or untreated, unactivated cells (negative control). The dashed blue line corresponds to the viability of cells in the presence of FR252921 at 100 nM. The *p* values for statistical significance are depicted as: * = $p < 0.05$; ** = $p < 0.01$; *** = $p < 0.001$; **** = $p < 0.0001$ and refer to the likeliness of an error in the correlation, with ns = not significant ($p \geq 0.05$).

The data presented in Figure 2.9 clearly showed that most of the novel FR analogues as well as FR252921, FR4 and FR5 are not cytotoxic at 100 nM concentration and these data suggest that the observed immunosuppressive effects across a range of assays are not due to antiproliferative activity of the FR compounds but that the observed effects arise from ligand-protein interactions within the cells. Two compounds appear to possess some cytotoxic properties at 100 nM concentration, namely αF-FR and *ent*-FR252921, albeit at a low level. The observation of cytotoxic effects of *ent*-FR252921 is counterintuitive at first, as one would expect both compounds to exhibit similar cytotoxic properties, if these properties were enabled through the generation of radical oxygen species or metabolic disturbances. However, the increased cytotoxicity of *ent*-FR252921 may be rationalised as it is, within the chiral environment of proteins within a cell, a compound entirely different from FR252921 and may therefore engage with other

proteins. This is supported by the finding that *ent*-FR252921 possesses little to no immunosuppressive activity, as would be expected if the interaction of two chiral partners, ligand and protein, is required for immunosuppression.

Next, the immunosuppressive activity of the FR compounds was evaluated against a range of cells and cytokines and strong dose-response dependency was found for TNF-α (T cells and NK cells), IFN-γ (T cells and NK cells) and IL-6 (B cells), which showed consistent results for each analogue, meaning that *e.g.* FR5 behaved as an immunosuppressant at 100 nM across all five cytokine/cell combinations rather than exhibiting strong effects in one but not the other. Figure 2.10 depicts the observed effects of the FR compound panel at 100 nM against the expression of TNF-α in T cells, IFN-γ in NK cells and IL-6 in B cells, which were selected to represent the more extensive results.

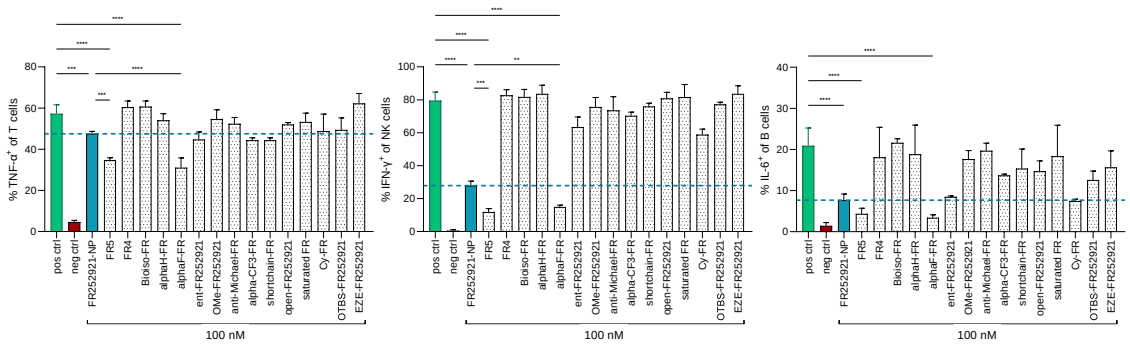

Figure 2.10: Immunosuppressive effects of the FR compounds against TNF-α in T cells, IFN-γ in NK cells and IL-6 in B cells at 100 nM concentration. Positive control (green) and negative control (red) refer to untreated, activated cells (positive control) or untreated, unactivated cells (negative control). The dashed blue line corresponds to the immunosuppressive potency of FR252921 at 100 nM. The *p* values for statistical significance are depicted as: * = $p < 0.05$; ** = $p < 0.01$; *** = $p < 0.001$; **** = $p < 0.0001$ and refer to the likeliness of an error in the correlation, with ns = not significant ($p \geq 0.05$).

At 100 nM, three compounds were identified to possess immunosuppressive biological activity across all cell types, which are FR252921, FR5 and αF-FR, with the latter two surpassing the activity of FR252921. Other analogues, such as *ent*-FR252921, αCF_3-FR, sc-FR and Cy-FR exhibit limited activity in certain settings, but their activities are not consistent across different cell types. This may serve as a benefit in future settings, as it would allow for the targeted suppression of certain cell types, however, the compounds consistently were less active compared to FR252921 and were therefore not considered in subsequent experiments.

Conclusions for SAR consideration could be drawn from these experiments, underlining previous findings in that modification of the side-chain of FR252921 is tolerated, leading to compounds of comparable

activity (αCF_3-FR, sc-FR and Cy-FR) or higher activity (FR5 and αF-FR). Modifications on the core of FR252921 are not tolerated, as only *ent*-FR252921 showed limited activity, with the remaining analogues (bioiso-FR252921, saturated-FR252921, anti-Michael-FR252921, OMe-FR252921, OTBS-FR252921, EZE-FR252921 and open-FR252921) displayed no immunosuppressive activity at 100 nM.

These results point towards a well-optimised macrocycle shape being required for binding to the target of FR252921, while the side-chain appears to benefit from electron-withdrawing substituents.

The four most active compounds (FR252921, FR5, αF-FR and *ent*-FR252921) were further evaluated with the data generated from the assay against PBMCs. Their immunosuppressive potency at different concentrations was graphed, aiming at estimation of an IC_{50} value could be attempted and the results are depicted in Figure 2.11.

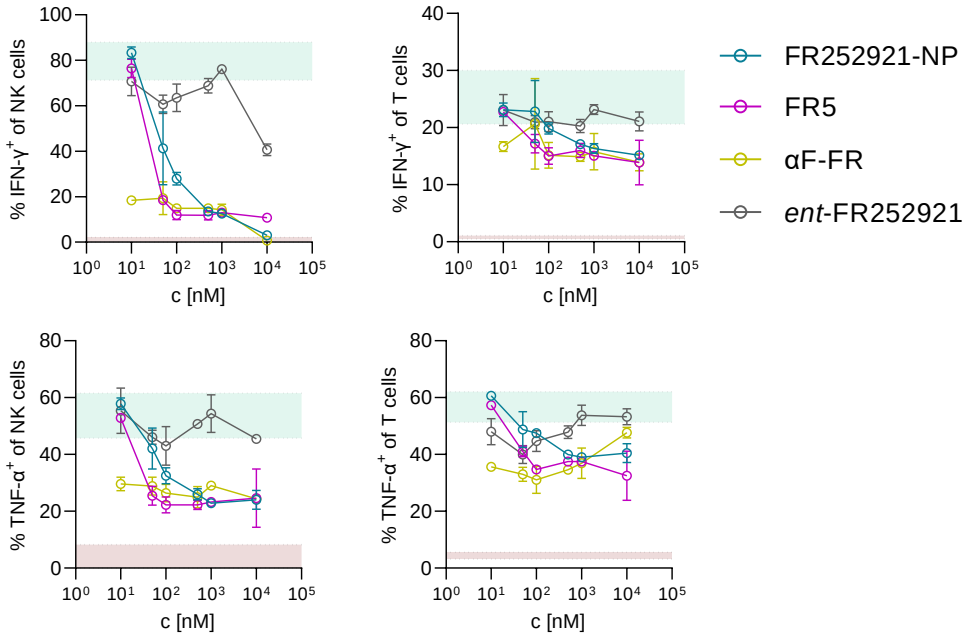

Figure 2.11: Dose-response curves for FR252921 (blue), FR5 (pink), αF-FR (yellow) and *ent*-FR252921 at six concentrations from 10 nM to 10 µM. The red area corresponds to the negative control (unactivated, untreated cells), while the green area corresponds to the positive control (activated, untreated cells). Each data point is depicted with the corresponding error bar.

Considering *ent*-FR252921, its dose-response dependant immunosuppressive activity appears to be unstable, fluctuating up and down with no correlation to concentration, and is mostly within the reach of the positive control. Therefore, it can be concluded that *ent*-FR252921 is not active as a non-cytotoxic, immunosuppressive analogue of FR252921. For all three remaining compounds, FR252921, FR5 and αF-FR, the dose-response curves adhere to the gradient of concentrations and the error appears to be

mostly small. FR252921 and FR5 exhibit a drop in activity at lower concentrations, with FR252921 decreasing in activity below 100 nM, whereas FR5 trails off below 50 nM concentration. Surprisingly, αF-FR appears to retain its activity at the lowest concentration tested (10 nM) across all four combinations of cell types and cytokines and, due to the retained activity at 10 nM, no IC_{50} could be determined for this analogue in the assay presented. FR252921 and FR5 however were taken forward and preliminary IC_{50} values could be determined, ultimately giving IC_{50} = 68 nM / 65 nM for FR252921 (IFN-γ in NK cells / IL-6 in B cells) and IC_{50} = 29 nM / 22 nM for FR5 (IFN-γ in NK cells / IL-6 in B cells). The IC_{50} values were deemed preliminary, as the inclusion of more concentrations would allow more accurate determination.

Next, FR252921, FR5 and αF-FR were evaluated at ten concentrations (0.5 nM, 1 nM, 5 nM, 10 nM, 25 nM, 50 nM, 100 nM, 250 nM, 500 nM, 1 µM) in triplicate against the established cell types and cytokines (*vide supra*). In between experimental runs, the cell activation cocktail had to be replaced, and the newly acquired CAC was found to perform as expected in a preliminary assay. However, when conducting the experiment to more accurately determine the IC_{50} values of the three most active FR molecules, it was found that the activation of T cells and NK cells was not sufficient to lead to observable effects, yet it was possible to determine the IC_{50} values for FR252921, FR5 and αF-FR in B cells against expression of IL-6 and are as follows (Figure 2.12): IC_{50} (FR252921) = 306 nM (95% range: 154 to 621 nM), IC_{50} (FR5) = 15.4 nM (95% range: 8.1 to 29.3 nM), IC_{50} (αF-FR) = 6.5 nM (95% range: 3.4 to 12.2 nM).

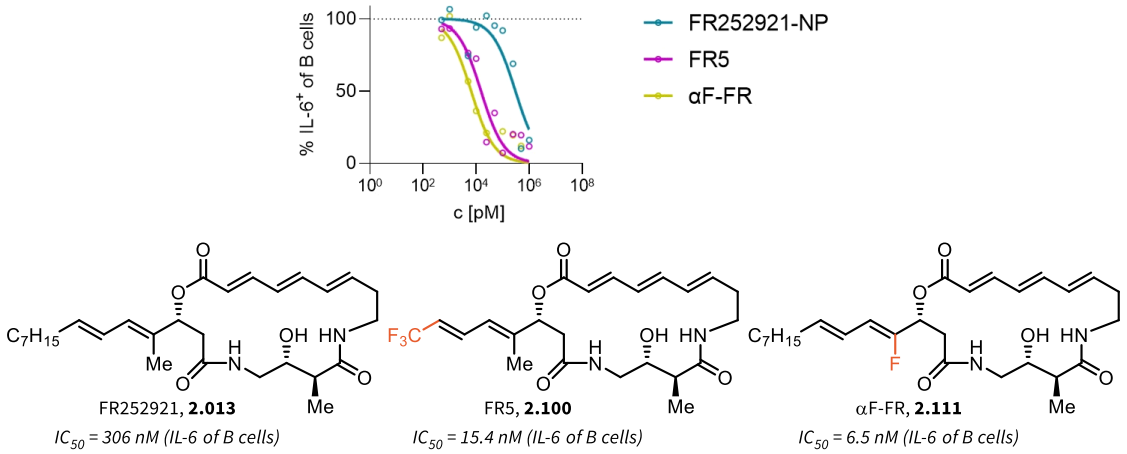

Figure 2.12: Dose-response curves for FR252921 (**2.013**), FR5 (**2.100**) and αF-FR (**2.111**). Experimentally determined measurements are depicted as hallow circles and the data is fitted with sigmoidal functions to determine the IC_{50} values, which are depicted below the corresponding molecules.

2.3.3.2.3. Validation Experiments and Synergistic Effects with Rapamycin and Cyclosporin A

The previously presented data was produced from the PBMCs of a sole healthy donor. While the observed effects were pronounced and consistent across different experiments, expanding these experiments to additional healthy donors is required in order to strengthen the relevance of the findings. To this end, three healthy donors were recruited, bringing the number of total donors to four (gender distribution: two male & two female, age distribution: male (29, 43), female (30, 27)) and the effects of FR252921, FR5 and αF-FR on PBMCs isolated from these individuals were evaluated at 100 nM and 10 nM across the previously established cell types and cytokines (T cells (TNF-α, IFN-γ), NK cells (TNF-α, IFN-γ), B cells (IL-6)). In order to further investigate the initially published finding on FR252921 exhibiting synergistic effects with the calcineurin inhibitor tacrolimus (**2.009**), the immunosuppressants cyclosporin A (**2.006**, calcineurin inhibitor) and rapamycin (**2.007**, mTOR inhibitor) were evaluated independently from the FR molecules. Selected results are depicted in Figure 2.13.

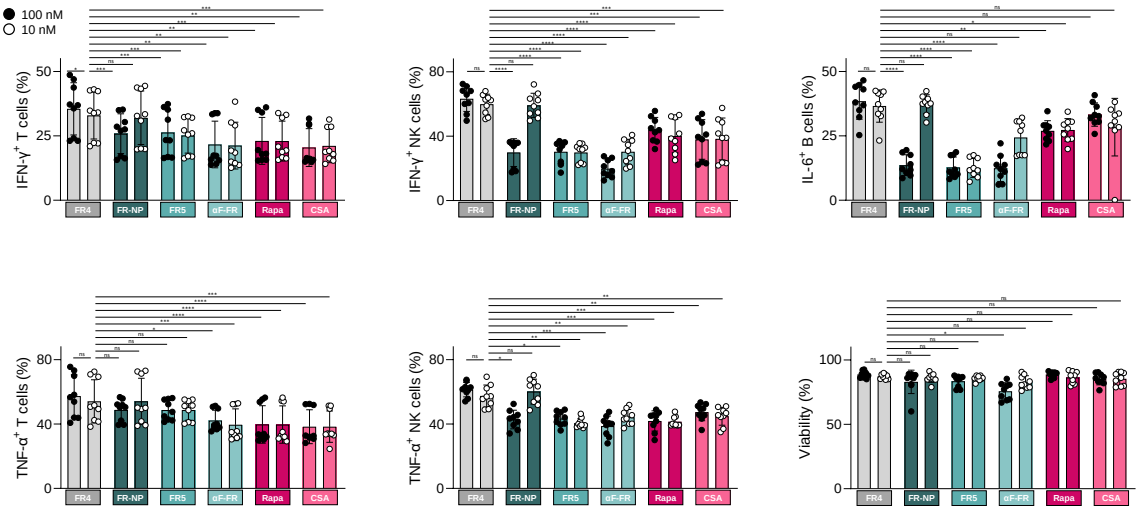

Figure 2.13: Three healthy donor evaluation of FR252921 (FR-NP), FR5, αF-FR, rapamycin (rapa) and cyclosporin A (CSA) at 100 nM (solid sphere) and 10 nM (hallow sphere). FR4 was used as positive control in this assay and activities of the other compounds are depicted relative to FR4. The *p* values for statistical significance are depicted as: * = $p < 0.05$; ** = $p < 0.01$; *** = $p < 0.001$; **** = $p < 0.0001$ and refer to the likeliness of an error in the correlation, with ns = not significant ($p \geq 0.05$).

In summary, it could be confirmed across three additional individuals that FR5 and αF-FR possess immunosuppressive biological activity surpassing FR252921 and that all FR compounds surpass the immunosuppressive potency of rapamycin and cyclosporin A in certain cell types (NK cells, B cells).

Lastly, the synergistic experiments were conducted at 100 nM concentration for FR252921, rapamycin and cyclosporin A across three healthy donors. These experiments were aimed to understand the interactions between different immunosuppressive natural products, as both rapamycin and cyclosporin A are known to be mostly active against T cells through two distinct mechanisms. Given the high activity of either of these two commercially used immunosuppressants, the presence of an additional molecule aiming to bind to the same targets should not impact the observed immunosuppressive effects, as rapamycin and cyclosporin A possess high affinities for their respective targets. The results of the combination experiments are depicted in Figure 2.14.

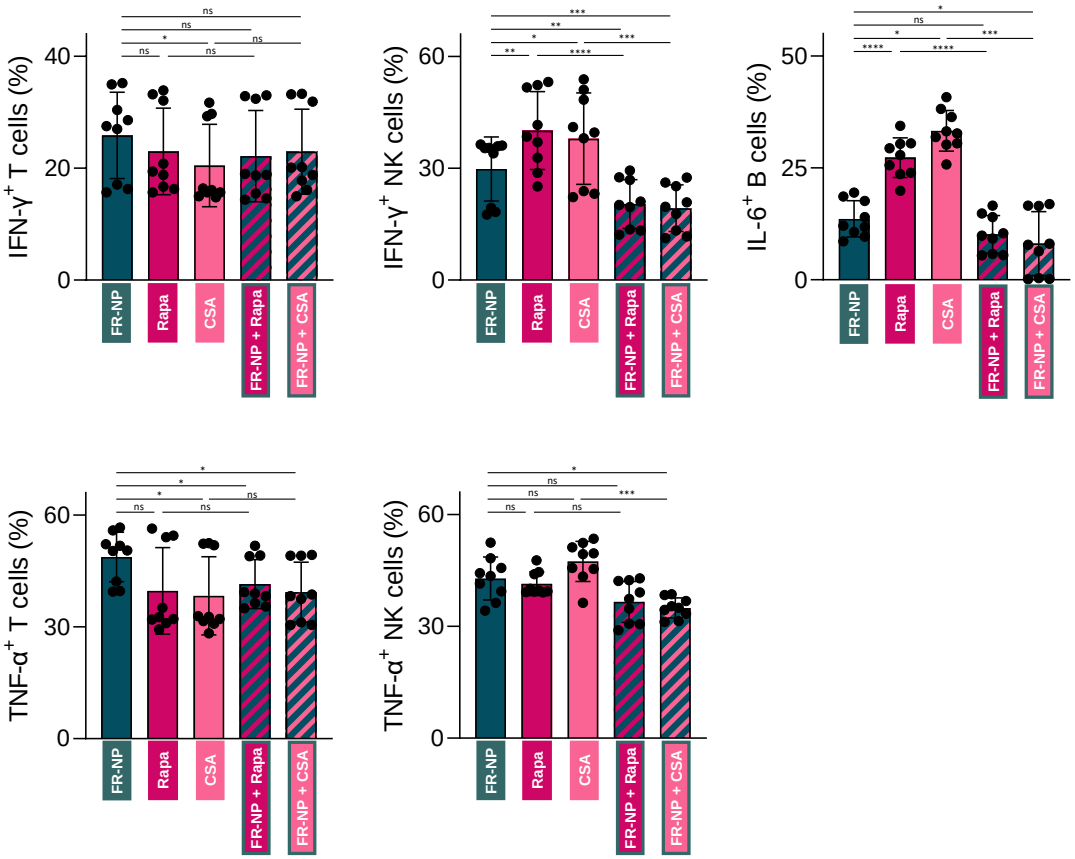

Figure 2.14: Synergy experiments between FR252921 (FR-NP), rapamycin (rapa) and cyclosporin A (CSA) at 100 nM concentration across three healthy donors. The *p* values for statistical significance are depicted as: * = $p < 0.05$; ** = $p < 0.01$; *** = $p < 0.001$; **** = $p < 0.0001$ and refer to the likeliness of an error in the correlation, with ns = not significant ($p \geq 0.05$).

Significant synergies could be observed in NK cells and B cells, while the combination of immunosuppressants in T cells did not lead to a significant increase in the immunosuppressive potency of the compounds. These results reinforce the observation that FR252921 appears to have broad activity across different cell types in suppressing the immune response, while eliciting its effects through a mode

of action that is distinct to the ones utilised by rapamycin (mTOR pathway) and cyclosporin A (calcineurin pathway).

In summary, the results presented in this chapter reveal the potential for the FR compounds to be further evaluated as potent immunosuppressants. It could be shown that analogues which could be readily generated from a building block-based discovery platform surpass the natural product in immunosuppressive potency while avoiding excess cytotoxicity. The evaluation of FR compounds was translated to human material for the first time and the FR compounds were highly active within healthy donor PBMCs. These results warrant further research into the biochemistry of FR compounds and should inspire the elucidation of the mode of action.

2.3.4. Cyclisation model systems to form *all*-(*E*)-triene macrolactones

Across the realm of natural products, many natural products feature one or more double bonds and these structural features can bear a significant synthetic challenge, especially if they are located with a strained macrocyclic scaffold (chapter 2.1.5.).[297,298] Finding a way to generalise the domino Suzuki-Miyaura/4π-electrocyclic ring opening macrocyclisation as developed by Maulide et al. towards different ring sizes, exploring its limitations and understanding the underlying mechanism promise were the objectives of the following subchapters.

2.3.4.1. Aliphatic cyclisation models

The synthesis of simplified macrocyclisation models started from commercially available terminal alkynes (**2.195**) which were deprotonated using *n*BuLi at −78°C to form the corresponding acetylide (Scheme 2.48). Following deprotonation, paraformaldehyde (PFA) was added to form the propargylic alcohols (**2.196**) in typically quantitative yields. The internal triple bond of the propargylic alcohols was isomerised to the ω-terminal position through the so-called alkyne zipper reaction. In this transformation, the sp^3-carbon atoms adjacent to the triple bond are deprotonated to form a propargyl anion, which is then reprotonated to either reform the triple bond at the starting position or on the other end of the allene, thereby moving the triple bond along one carbon on the chain. This process is terminated by the isomerisation of the triple bond to the terminal position, as deprotonation then leads to an acetylide which is not reprotonated under the reaction conditions, removing it from the equilibrium.[299,300] It is noteworthy that the reverse process, isomerisation of a terminal alkyne to an internal position, is also possible.[301] Following successful isomerisation to yield terminal alkynes (**2.197**), these compounds were subjected to (*E*)-selective hydroboration using Schwartz's reagent ($(Cp)_2ZrHCl$) to yield vinyl-Bpin-containing alcohols (**2.198**),[302] which were subsequently esterified with (±)-*cis*-chlorocyclobutene acid (**2.057**) to furnish the corresponding esters (**2.199**). This synthetic sequence was

applied to linear terminal alkynes of varying lengths, starting with nonye (**2.195** for n = 5) and ending with pentadecyne, ultimately delivering macrocyclisation precursors probing ring sizes ranging from 15- to 22-membered macrocyclic triene lactones.

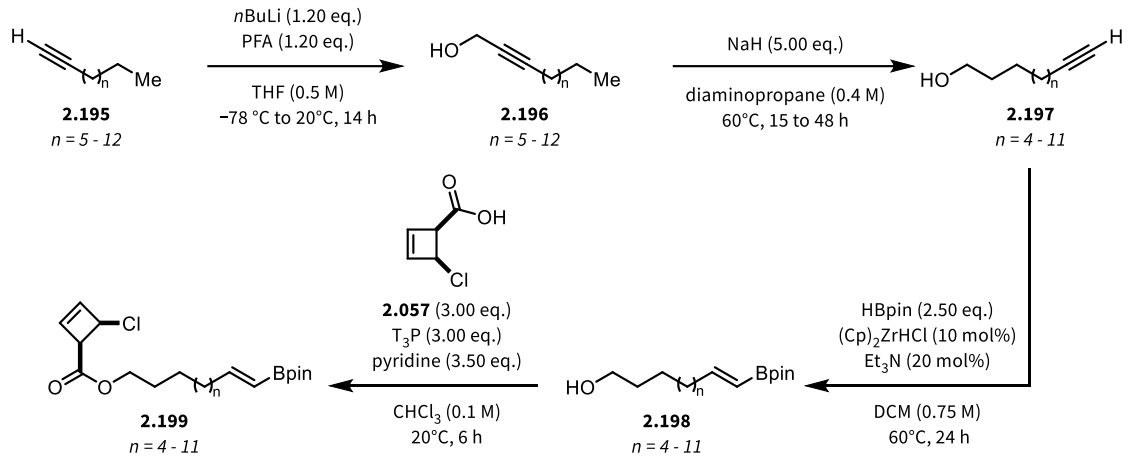

Scheme 2.48: Synthesis of *all*-(*E*)-macrolactone cyclisation model substrates through a four step sequence involving addiditon of PFA to an acetylide, alkyne zipper reaction, hydroboration and esterification with (±)-*cis*-chlorocyclobutene acid (**2.057**).

The linear macrocyclisation precursors (**2.199**) were then subjected to the optimised macrocyclisation conditions as established for the synthesis of FR252921 and its analogues (*vide infra*) using 5 mol% $Pd(PPh_3)_4$ and 5.00 eq. of Cs_2CO_3 in a THF/water mixture at 20°C in the dark (Scheme 2.49).[151,239,296,302,303] Upon treatment with a Pd-catalyst, the models were expected to undergo the desired Suzuki-Miyaura reaction through an oxidative addition – transmetallation – reductive elimination sequence to yield the *trans*-vinylcyclobutene ester intermediate (**2.200**). This would then trigger strain-induced torquoselective conrotatory electrocyclic 4π-ring opening to yield the desired *all*-(*E*)-triene macrolactones (**2.201**) of sizes ranging from 15- to 22-membered.

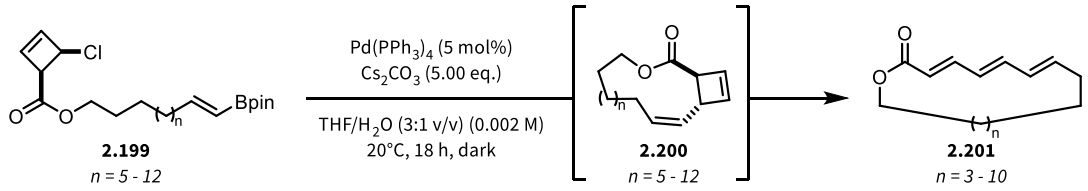

Scheme 2.49: Domino Suzuki-Miyaura/4π-electrocyclic ring opening model macrocyclisation of linear *cis*-cyclobutene esters (**2.199**) to deliver *all*-(*E*)-triene macrolactones (**2.201**) of different sizes.

As per the introduction to this chapter (chapter 2.1.), the ring-opening of cyclobutene esters should follow a torquoselective process to yield the aforementioned *all*-(*E*) trienes as the sole products. Surprisingly,

the results of the macrocyclisation study provided an unexpected outcome with several products being formed as a result of the macrocyclisation event (Scheme 2.50).

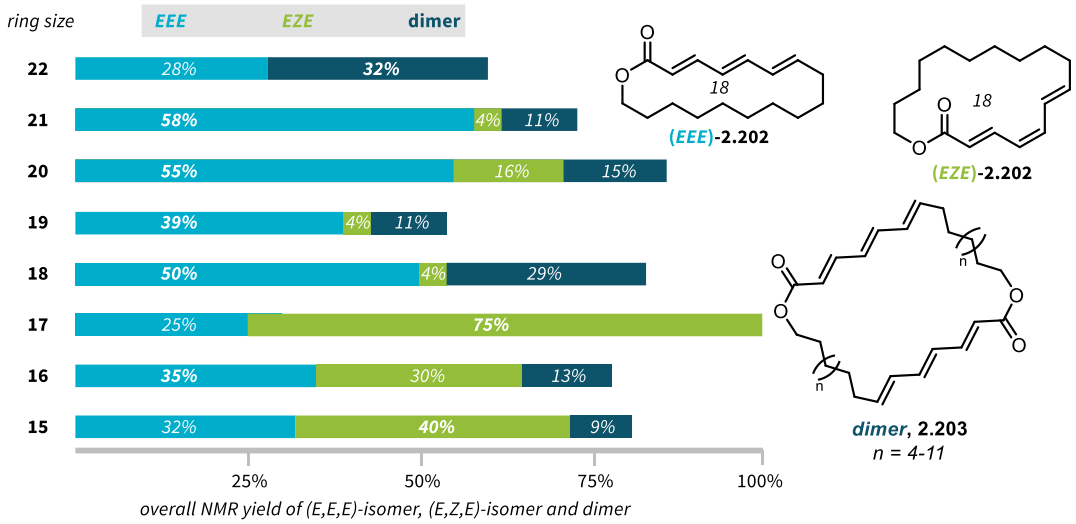

Scheme 2.50: Summary of the NMR yields of the macrocyclisation model study. NMR yields (white) are determined as an average of three experiments. The major product is depicted in **bold** and selected representative product structures are shown on the right. NMR yields were determined using $CHBr_3$ as an internal standard.

Contrary to the anticipated outcome of the yield increasing with ring size as the ring strain of the triene macrolactones diminishes and of consistently obtaining the *all*-(*E*)-triene product, it was found that the reaction produces significant amounts of unexpected (*E*,*Z*,*E*)-trienemacrolactones, such as (*EZE*)-**2.202**. Notably, the smallest macrocycle studied herein (15-membered triene) gave the 15-membered macrocycle in 72% overall yield with minimal dimerisation product observed (9%). However, the major product of the macrocyclisation could be shown to be the undesired (*E*,*Z*,*E*)-macrolactone in 40% NMR yield, while the desired *all*-(*E*)-macrolactone was produced in 32% NMR yield as the minor product. A similar result was observed for the 16-membered macrocycle model, in which both *all*-(*E*)-product and (*E*,*Z*,*E*)-product were produced in similar amounts (35% and 30% NMR yield) favouring the desired isomer in this case. Overall yield and production of dimer were comparable to the 15-membered model substrate. Moving to yet larger ring sizes, the 17-membered precursor showed high propensity to undergo the desired macrocyclisation (overall quantitative NMR yield) with no dimerisation; however, the reaction displayed a surprising 1:3 selectivity between the expected *all*-(*E*)-triene product and the (*E*,*Z*,*E*)-product at room temperature, delivering the products in 25% and 75% NMR yield respectively. This selectivity trend towards the undesired (*E*,*Z*,*E*)-triene macrolactone sharply inverts at the 18-membered model substrate. For this ring size and all following larger macrocycles, the (*E*,*Z*,*E*)-triene becomes the minor

product, with the *all*-(*E*)-triene being the major product. In the case of the 18-membered model substrate, the overall cyclisation efficiency was good with 54% combined NMR yield (50% NMR yield *all*-(*E*) + 4% NMR yield (*E*,*Z*,*E*)) albeit with 29% of dimer forming as a byproduct. The ease of formation of the 18-membered *all*-(*E*)-triene macrolactone stands in stark contrast with the unsuccessful outcome of progress towards a strained FR252921 analogue, possessing a 18-membered macrocycle, as will be discussed later in this thesis. Moving into the realm of the ring size found in FR252921, the 19-membered macrolactone was formed with high selectivity with only trace amounts of the undesired (*E*,*Z*,*E*)-product. While dimer formation could not be suppressed, it was only formed in 11% NMR yield. For the next two ring sizes, 20- and 21-membered macrolactones, the results are quite close. In both cases, the *all*-(*E*)-triene macrolactone was formed as the major product (55% and 58% NMR yield), while the (*E*,*Z*,*E*)-triene was observed in 16% and 4% yield, respectively. These results point towards the alleviation of ring strain from the system, as the large macrocycle allows the triene to be unstrained, whereas for smaller ring sizes the triene is likely distorted out-of-plane. For the largest ring size tested herein, the 22-membered macrocyclisation model, it was found that the *all*-(*E*) product is formed in an amount similar to the dimer, indicating macrocyclisation rates which are in a similar order of magnitude to the diffusion of the reactive intermediates in solution.

Taken together, these results provide a decent rationalisation in the avoidance of ring strain as to why polyene-macrocyclic natural products are typically found with ring sizes of 18 atoms or more, such as is the case for rapamycin (**2.007**), amphotericin B, stubomycin or FR252921 (**2.013**).[151,239,297,303,304]

It remained unclear how the observed (*E*,*Z*,*E*)-trienes were formed, as the presumed torquoselective ring opening would exclusively lead to the *all*-(*E*)-triene macrolactones, such as (*EEE*)-**2.202**. To investigate different aspects of the macrocycle formation, a range of mechanistic experiments were conducted (Scheme 2.51 A-D).

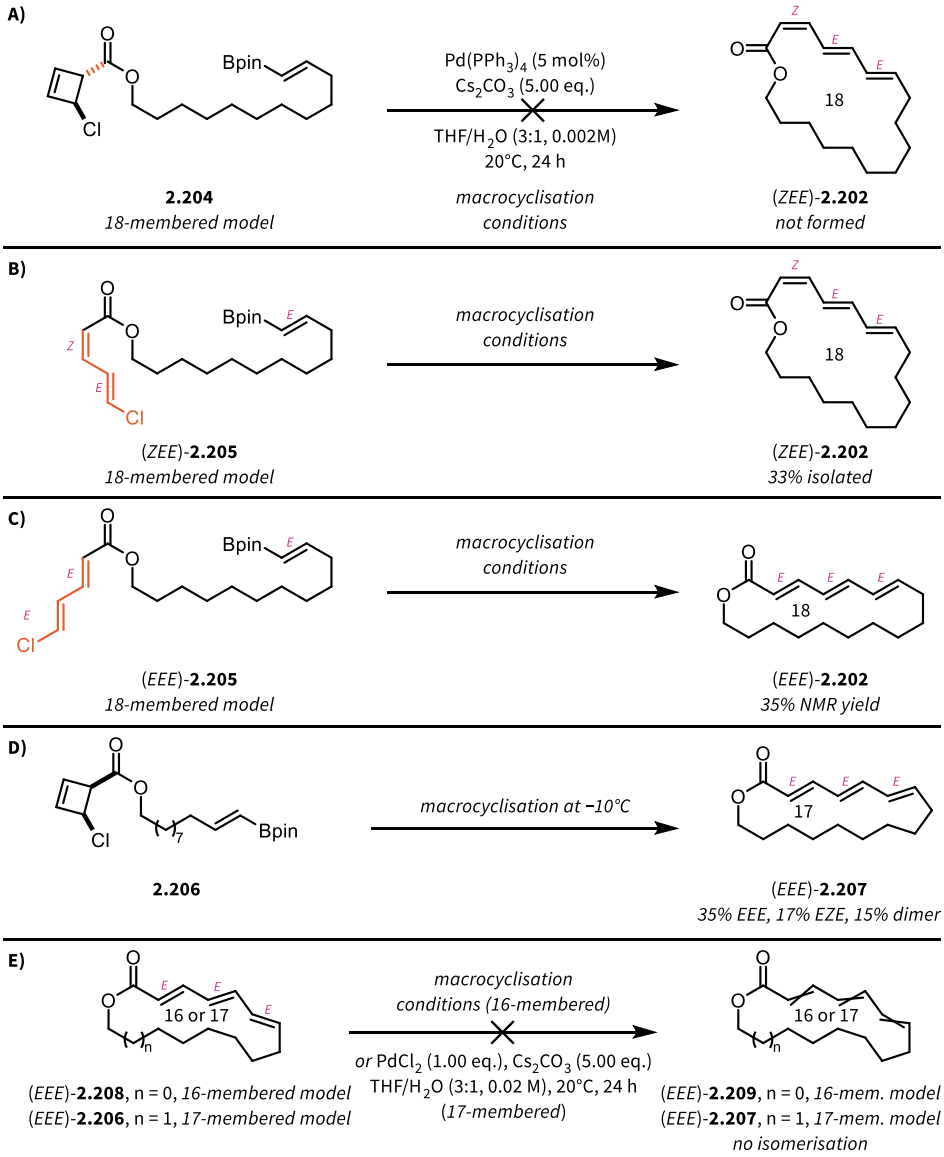

Scheme 2.51: Validation experiments to probe different possibilities for the formation of the (*E*,*Z*,*E*) byproduct.

First, it was investigated whether the (±)-*trans*-chlorocyclobutene ester **2.204** could also undergo the macrocyclisation to deliver the corresponding (*Z*,*E*,*E*)-triene macrolactone (*ZEE*)-**2.202** (Scheme 2.51A). However, (*ZEE*)-**2.202** was not obtained. Nevertheless, the starting material was slowly consumed but no clear product formation of any expected species could be observed. This could be rationalised as the oxidative addition step is happening from the backside of the allyl chloride moiety, leading to inversion of the configuration of the carbon atom. If the starting allyl chloride is *trans* to the carbonyl, an oxidative addition would lead to a *syn*-Pd species in relation to the carbonyl. Potential coordination of the Pd(II)-species by the carbonyl is assumed to stabilise this complex and hamper further reaction towards the macrolactone product.[305]

In two further experiments, the necessity of the cyclobutene moiety was investigated. To this end, *cis*- and *trans*-chlorocyclobutene ester were thermally opened to the corresponding (*Z*,*E*)-diene ((*ZEE*)-**2.205**) (Scheme 2.51B) and (*E*,*E*)-diene ((*EEE*)-**2.205**) (Scheme 2.51C). Both dienylchloride species were capable of undergoing macrocyclisation, albeit in lower yields and with remaining unreacted starting material. This reaction provided genuine samples of the corresponding (*Z*,*E*,*E*)- and (*E*,*E*,*E*)-triene macrolactones ((*ZEE*)-**2.202** and (*EEE*)-**2.202**) and could also show, that such a coupling is slower than the standard cyclobutene-involving reaction sequence. This is potentially due to the presence of a cyclobutene-tether, which allows the initial Suzuki-Miyaura process to take place without considerations towards ring strain, before releasing the fully strained *all*-(*E*) system in the following 4π-electrocyclic ring opening. For (*E*,*E*)-starting material ((*EEE*)-**2.205**), significant amounts of dimer were formed (27%) alongside 32% of recovered starting material, pointing again towards avoidance of macrocyclisation in favour of dimerisation, as a path to circumvent ring strain.

Additional control experiments were conducted in order to further elucidate the processes at play in the formation of the (*E*,*Z*,*E*)-products. To this end, the 17-membered macrocyclisation precursor **2.206** was subjected to the macrocyclisation conditions at −10°C to study the influence of the temperature on the formation of different isomers. While at 20°C the 17-membered macrocycle (**2.207**) was produced in a 3:1 ratio favouring the undesired (*E*,*Z*,*E*)-isomer over the *all*-(*E*)-isomer, this was inverted when performing the macrocyclisation at −10°C, leading to a 2:1 ratio between *all*-(*E*)-triene ((*EEE*)-**2.207**) and the (*E*,*Z*,*E*)-product (Scheme 2.51D). This result strongly suggests that the kinetic product is the *all*-(*E*)-triene, while the (*E*,*Z*,*E*)-product appears to be the thermodynamic product of the macrocyclisation reaction. It remains unclear how the (*E*,*Z*,*E*)-products are formed.

Finally, the potential for an isomerisation of the *all*-(*E*)-trienes after their formation through interaction with the catalyst was investigated. To achieve this, isolated, pure *all*-(*E*)-trienes of the 16- and 17-membered macrocycle were subjected to i) exact macrocyclisation conditions (16-membered *all*-(*E*)-triene macrolactone) or ii) conditions featuring a stoichiometric amount of a Pd(II) species (17-membered *all*-(*E*)-triene macrolactone) as depicted in Scheme 2.51E. In neither of the tested conditions could any trace of isomerisation be observed, pointing towards the potential formation of the (*E*,*Z*,*E*)-products prior to reductive elimination or disengagement of the catalytically active palladium species. These results

were taken into consideration for the calculation of a potential reaction mechanism as presented in chapter 2.3.4.3.

2.3.4.2. Lactam-containing cyclisation models

Since the aliphatic cyclisation models indicated a crucial role for the ring strain in the selectivity towards the desired *all*-(*E*)-triene, it was assumed that the presence of lactam moieties within the natural product FR252921 may play a role in stabilising the desired product through *e.g.,* intramolecular hydrogen bonding or the sp^2 character of the amide bond. To investigate this, several amide-containing macrocyclisation models were envisioned as derived from FR252921 (Scheme 2.52).

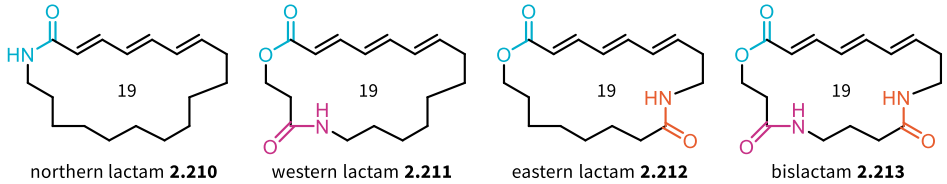

Scheme 2.52: Overview of the four envisioned lactam models to probe the selectivity of the macrocyclisation.

The lactam models consist of four 19-membered macrocyclic lactams, featuring a *northern* lactam model **2.210**, which replaces the lactone with a lactam, the *western* (**2.211**) and *eastern* (**2.212**) lactams, which each contain one of the two lactams found in FR252921 and finally a *bislactam-lactone* (**2.213**), reminiscent of FR252921 if most functionality was removed. The synthetic route design for each lactam borrowed from the experience acquired during the total synthesis of FR252921.

The synthesis of the northern lactam (**2.210**) started with the vinyl-Bpin-containing primary alcohol (**2.214**), which has previously been used to study the effect of ring size in the previous chapter as presented in Scheme 2.53A. The primary alcohol was converted to an azide (**2.215**) through the action of diphenylphosphoryl azide (DPPA) and DBU. Following successful incorporation of the azide, the primary amine was synthesised by its reduction, yielding **2.216** in quantitative yield. Amine **2.216** was subjected to the standard conditions for esterification (chapter 2.5.2.17) to form *cis*-chlorocyclobutene amide **2.217**, the required precursor for the macrocyclisation.

Western lactam precursor **2.223** was synthesised in a similar fashion to the northern lactam precursor. Vinyl-Bpin-containing primary alcohol **2.218** was converted to the corresponding azide (**2.219**) and subsequently reduced to the primary amine (**2.220**) as before (Scheme 2.53B). The amine was then reacted with β-propiolactone (**2.221**) to form the western amide bond delivering **2.222**, which also contained the crucial primary alcohol required for the following esterification step. Alcohol **2.222** was then coupled with *cis*-chlorocyclobutene acid (**2.057**) to form the macrocyclisation precursor **2.223**.

The synthesis of the eastern lactam model (**2.226**) started from commercially available acid **2.224**. The acid was subjected to amide bond formation with the FR252921 precursor **2.091**, conveniently produced in gram-scale for the synthesis of FR252921 (Scheme 2.53C). Amide **2.225** contained a primary alcohol at the distal end of the aliphatic chain, which was esterified using the established protocol to yield *cis*-chlorocyclobutene ester **2.226**.

Lastly, synthesis of the bislactam lactone progenitor **2.229** started from intermediate **2.227**, which is required for the synthesis of FR4. Amine **2.227** was reacted with β-propiolactone **2.221**, followed by esterification of the newly released primary alcohol **2.228** with *cis*-chlorocyclobutene acid to form the macrocyclisation precursor **2.229** (Scheme 2.53D).

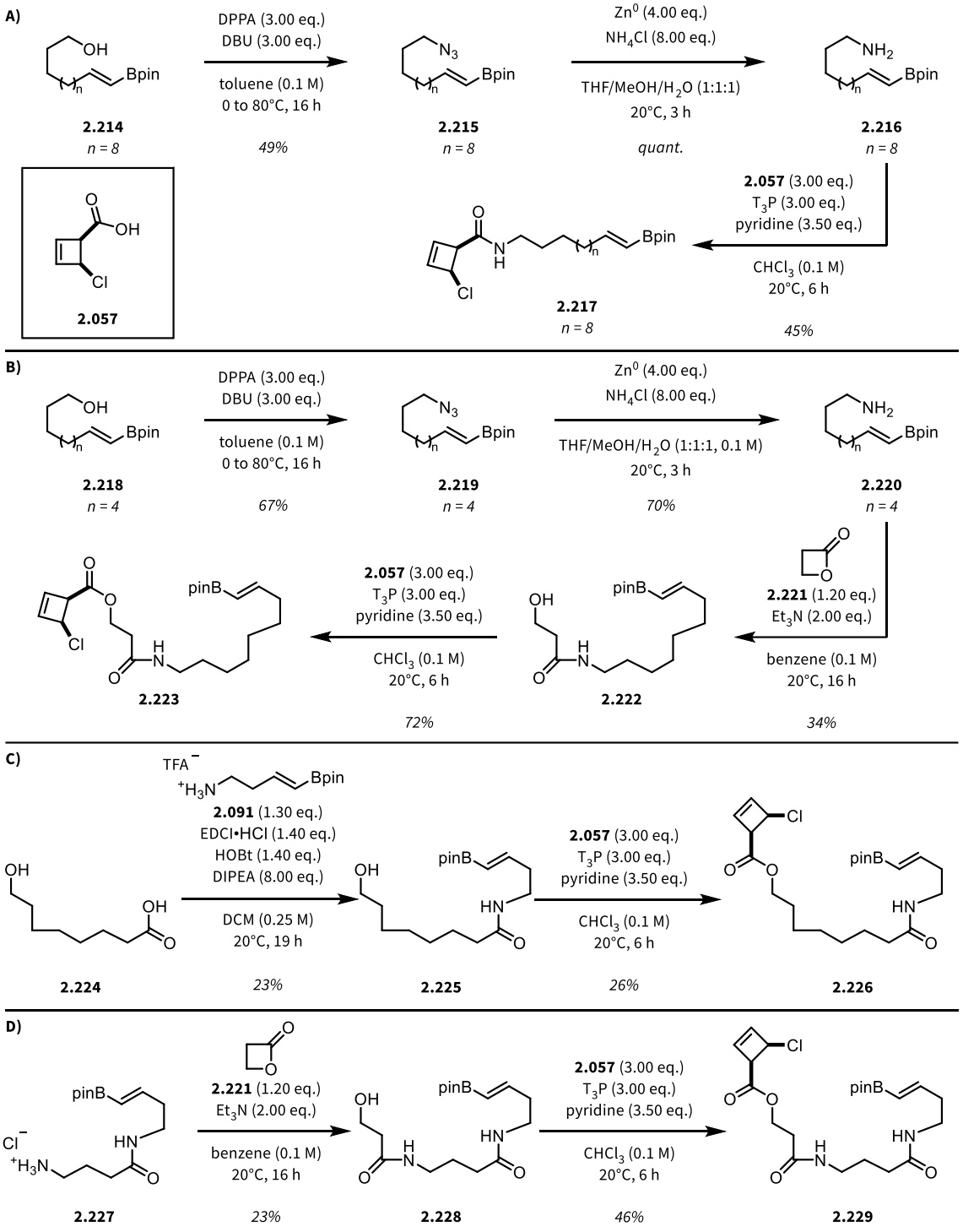

Scheme 2.53: Synthesis of four different lactam containing model substrates.

With all required *all*-(*E*)-triene macrolactam precursors in hand, the key cyclisation step was investigated. All four precursors were subjected to the standard macrocyclisation conditions to yield the corresponding 19-membered macrolactams and the results are summarised in Scheme 2.54.

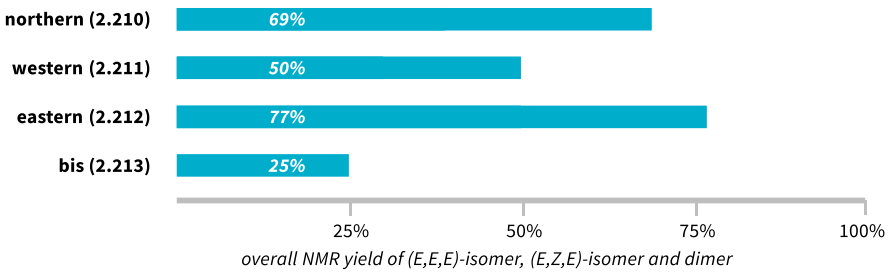

Scheme 2.54: Summary of the lactam macrocyclisation study. All tested precursors delivered the desired *all*-(*E*)-triene macrocycle as the sole product in mediocre to good NMR yield. NMR yield is averaged across three runs using $CHBr_3$ as an internal standard. NMR yields are given in **bold**.

Interestingly, these model substrates delivered the expected 19-membered (*E*,*E*,*E*)-triene macrocycles as single isomers in a range of yield from 25% for the bislactam lactone (**2.213**, incomplete conversion within 24 h) to 77% for the eastern lactam (**2.212**), with the northern lactam (**2.210**) and western lactam (**2.211**) being in between. This points towards the importance of the presence of lactams within the macrocycle to stabilise the product of the reaction, however the mechanism through which the byproducts are formed remains unclear. The observed low yield for the bislactam lactone model is difficult to rationalise alongside its slower reaction, as this model is closest to FR252921 or FR4 in structure, both of which in turn undergo macrocyclisation much more smoothly.

In order to further elucidate this mechanism, a cooperation with the group of Prof. Dr. Kendall N. Houk at UCLA was initiated and the investigation is still ongoing.

2.4. Conclusion & Outlook

This chapter has dealt with three aspects of the FR molecules in order to expand the synthesis, biology and synthetic methodology derived from the FR molecules.

First, several synthetic steps of the path towards natural product FR252921 were improved and the reoptimised protocol was taken forward to synthesise fourteen novel fully synthetic analogues and precursors, demonstrating the flexibility and efficiency of this building block-based approach.

Second, the fully synthetic analogues were evaluated alongside the natural product and two previously synthesised analogues, FR4 and FR5, in order to evaluate their biological activity both in terms of cytotoxicity and immunosuppressive activity. In PBMCs, it was found that FR252921 and some of its analogues possess impressive immunosuppressive properties at low concentrations without observable cytotoxicity. Additionally, it could be shown that the trend in activity could be translated from EL4 T cells to PBMCs and the application of the FR molecules in PBMCs represents the first experiments conducted on human material of this natural product and its analogues. Within the analogue panel evaluated, two analogues surpassed the activity of FR252921, leading to compounds with IC_{50} values below 50 nM in the form of FR5 and αF-FR. Interestingly, across the analogue panel, these two highly active compounds are some of the few which are not accessible to nature. However, most of the analogues which could theoretically be synthesised within a living organism showed decreased activity compared to FR252921.

Third, the observed formation of an isomer of the anticipated *all*-(*E*)-triene macrolactones in the form of (*E*,*Z*,*E*)-triene macrolactones was investigated. The cyclisation was applied across a range of model substrates to probe the influence of ring size as well as the influence of lactams present in the macrocycle, leading to stabilisation of certain confirmations. In addition, this process is being evaluated computationally in collaboration with the group of Prof. Dr. Kendall N. Houk at UCLA in order to elucidate the intriguing isomerisation process at play, delivering compounds which are not expected to be formed through classical torquoselective considerations of electrocyclic ring opening.

The future of the FR project should be concerned with the elucidation of the biological mode of action of these fascinating compounds. Since the FR molecules seem to act against a protein which is neither calcineurin nor mTOR, finding its biological target could unravel pathways within the immune system, which have thus far not been discovered or at least explored for immunosuppression. The potential discovery of a novel pathway to immunosuppression may stimulate research outside of the FR molecules and would be a milestone in the field.

One potential molecule capable of being ligated to a target molecule could be the diazirine-modified photo-FR25921 (**2.230**) (Scheme 2.55A). The diazirine moiety is readily cleaved by UV light irradiation to form a carbene *via* N_2-extrusion and the highly reactive carbene can bind to different amino acid residues within the target protein. The resulting conjugates can in turn be detected by proteomics approaches.[306,307]

Outside of the biological evaluation of FR analogues, the chemistry of cyclobutenes and cyclobutanes could be further explored in order to establish their properties as bioisosteres of *m*- or *p*-disubstituted benzene derivatives (**2.231**, Scheme 2.55B). The replacement of phenyl moieties by aliphatic isosteres has grown as an area of research over the past years, leading to the development of funtionalised cubanes,[308] and other complex aliphatic scaffolds.[309] To this end, modified cyclobutanes (**2.232**) could be synthesised from cyclobutenes (**2.233**) and the introduction of differentially protected carbonyl species would allow for a range of functionalised derivatives.[310]

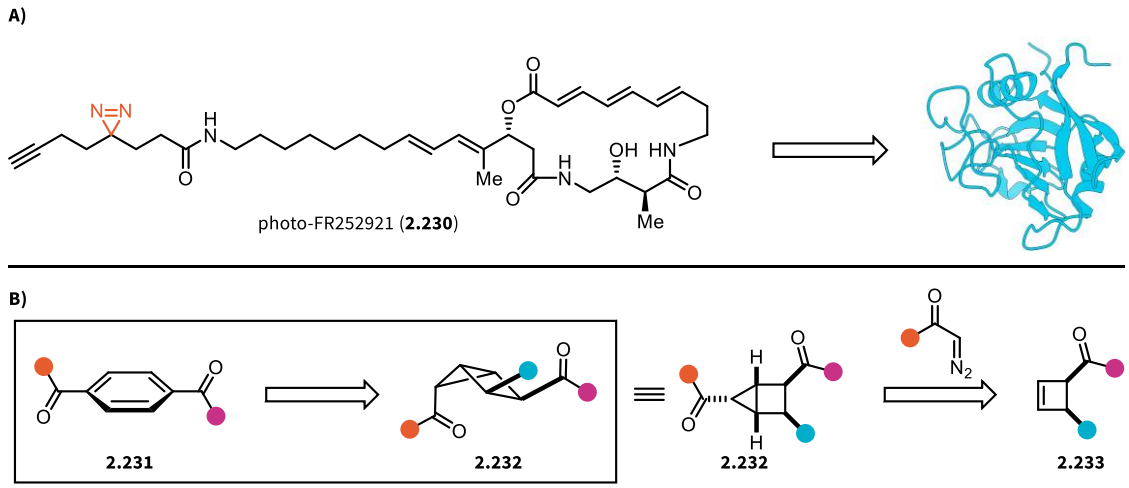

Scheme 2.55: A) proposed analogue photo-FR252921 (**2.230**) for photoaffinity labelling of potential target proteins. B) Proposed funtionalisation of cyclobutenes towards their application as isosteres for benzene derivatives.

2.5. Experimental Procedures and Data

2.5.1. General Information

Unless otherwise stated, all solvents were distilled from appropriate drying agents prior to use or used as received, if anhydrous. All reactions were carried out under an atmosphere of Argon in flame-dried glass vessels, unless otherwise stated. All reagents were used as received from commercial suppliers unless otherwise stated. For cyclobutene esterification reactions (Chapter 2.5.2.17.) pyridine was distilled prior to use from CaH_2 under an atmosphere of Argon and was subsequently stored in the dark under an atmosphere of Argon. For aldol reactions (Chapter 2.5.2.5) DIPEA was distilled prior to use twice (distillation from ninhydrin followed by distillation from KOH) under an atmosphere of Argon and was subsequently stored in the dark under an atmosphere of Argon. $TiCl_4$ (1 M in DCM) was used as received from the supplier after being transferred to a Schlenk flask for storage. Ghosez's reagent (1-Chloro-*N*,*N*,2-trimethyl-1-propenylamine) was distilled prior to use under an atmosphere of Argon and used without intermediate storage. Reaction progress was monitored by thin layer chromatography (TLC) performed on aluminium plates coated with silica gel F254 with 0.2 mm thickness. Chromatograms were visualised by fluorescence quenching with UV light at 254 nm or by staining using potassium permanganate, phosphomolybdic acid or ninhydrin. Flash column chromatography was performed using silica gel 60 (230-400 mesh, Merck and co.) or prepacked columns (Chromabond silica) using a Biotage Selekt Flash Purification System. Neat infrared spectra were recorded using a Perkin-Elmer Spectrum 100 FT-IR spectrometer. Wavenumbers (ν_{max}) are reported in cm^{-1}. Mass spectra were obtained using a Finnigan MAT 8200 or (70 eV) or an Agilent 5973 (70 eV) spectrometer, using electrospray ionisation (ESI). Optical rotation measurements were performed on a Perkin Elmer 341 polarimeter using a 100 mm path-length cell at λ = 589 nm (c given in g/100 mL). All ^{1}H-NMR, ^{13}C-NMR and ^{19}F-NMR spectra were recorded using Bruker AV-400, AV-600 or AV-700 spectrometers at 300K. Chemical shifts are given in parts per million (ppm, δ), referenced to the solvent peak of $CDCl_3$, defined at δ = 7.26 ppm (^{1}H-NMR) and δ = 77.16 ppm

(^{13}C-NMR), MeOH-d_4, defined at δ = 3.31 ppm (^{1}H-NMR) and δ = 49.00 ppm (^{13}C-NMR), and DMSO-d_6, defined at δ = 2.50 ppm (^{1}H-NMR) and δ = 39.52 ppm (^{13}C-NMR). Coupling constants are quoted in Hz (*J*). ^{1}H, ^{13}C and ^{19}F NMR splitting patterns are designated as singlet (s), doublet (d), triplet (t), quartet (q) as they appeared in the spectrum. If the appearance of a signal differs from the expected splitting pattern, the observed pattern is designated as apparent (app). Splitting patterns that could not be interpreted or easily visualised are designated as multiplet (m) or broad (br). Room temperature refers to 20°C.

2.5.2. General Procedures

2.5.2.1. Horner-Wadsworth-Emmons Olefination

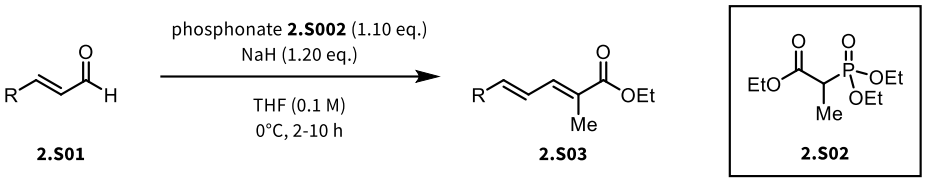

Phosphonate **2.S02** (1.10 eq.) was added to a suspension of NaH (60 wt% in paraffin) (1.20 eq.) in THF (0.2 M) at 0°C. The resulting mixture was stirred for one hour or until evolution of H_2 ceased before a solution of aldehyde **2.S01** (1.00 eq.) in THF (0.2 M) was added dropwise at 0°C. After 2–10 hours at 0°C, the starting material had been consumed (as indicated by TLC analysis) and the reaction mixture was carefully quenched by the dropwise addition of water at 0°C. The quenched reaction mixture was further diluted with water and was subsequently extracted with EtOAc (3 x equal volume to THF). The combined organic layers were dried over Na_2SO_4, the solids were filtered off and the solvents were removed *in vacuo* to yield the crude product. The crude product was purified by flash column chromatography (SiO_2, heptane/EtOAc) to yield the allylic esters **2.S03**.

2.5.2.2. Reduction of Allylic Esters to Allylic Alcohols

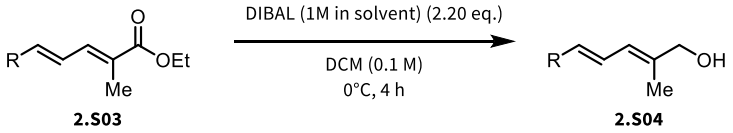

To a solution of allylic ester **2.S03** (1.00 eq.) in DCM (0.1 M) at 0°C was carefully added DIBAL (1 M in solvent; DCM, toluene or Et_2O) (2.20 eq.). Stirring was maintained at 0°C for 4 h or until the starting material had been consumed (as indicated by TLC analysis) before the reaction was quenched by either of two methods.

Method A: The reaction was quenched by careful addition of 0.2 mL of water and stirring was continued for 30 min. Then, $MgSO_4$ was added to dry the quenched reaction mixture and stirring was continued until an opaque gel formed (typically 15 to 30 min). The gel was filtered over a short pad of Celite® and the filter cake was washed with EtOAc. The filtrate was concentrated and the thusly afforded crude material was

purified by flash column chromatography (SiO_2, heptane/EtOAc) to afford the allylic alcohol **2.S04**. (*Nota bene: This method works well on smaller scales, up to typically 2 mmol. The method is limited by the capabilities to efficiently filter and wash large amounts of the formed opaque gel to extract the desired product.*)

Method B: The reaction was quenched by careful addition of (2 x solvent volume) mL of a saturated aqueous solution of Rochelle's salt (NaK tartrate) at 0°C and stirring was continued until two phases formed. The layers were separated and the aqueous layer was extracted with EtOAc (3 x equal volume to DCM). The combined organic layers were dried over Na_2SO_4, the solids were filtered off and the solvents were removed *in vacuo* to yield the crude product. The crude material was purified by flash column chromatography (SiO_2, heptane/EtOAc) to yield the pure allylic alcohols **2.S04**. (*Nota bene: This method works well for large scale reactions, typically > 2 mmol. The amount of Rochelle's salt solution necessary to quench the reaction and lead to separation should be considered when setting up the reaction and a suitable vessel should be selected*)

2.5.2.3. Oxidation of Allylic Alcohols to Allylic Aldehydes

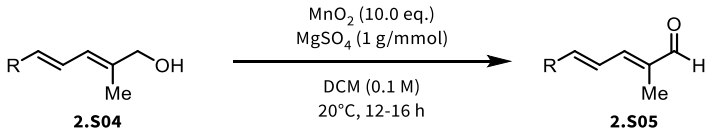

2.S04 **2.S05**

To a solution of allylic alcohol **2.S04** (1.00 eq.) in DCM (0.1 M) at 20°C was added $MgSO_4$ (1 g/mmol) followed by addition of MnO_2 (10.0 eq.). The reaction mixture was subsequently stirred at 20°C for 12-16 h or until the starting material had been consumed (as indicated by TLC analysis or ^{1}H-NMR). Subsequently, the reaction mixture was filtered through a short pad of Celite® to remove the solids and the filtrate was concentrated to yield the crude product. The crude material was subsequently purified by flash column chromatography (SiO_2, heptane/EtOAc) to yield the desired allylic aldehydes **2.S05**.

2.5.2.4. Synthesis of the Evans-Crimmins Auxiliary

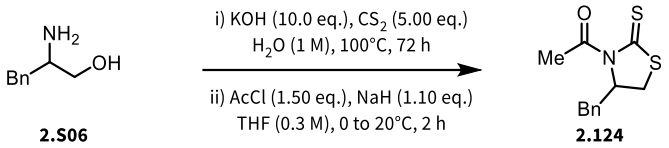

2.S06 **2.124**

To an aqueous solution of KOH (10.0 eq.) in water (5 M) at 20°C was added enantiopure alcohol **2.S06** (1.00 eq.) followed by CS_2 (5.00 eq.). The resulting reaction mixture was heated to 100°C and stirring at the indicated temperature was continued for 72 h. Afterwards, the reaction mixture was allowed to cool to room temperature and was extracted with DCM (4 x equal volume to H_2O). The combined organic layers were dried over Na_2SO_4, the solids were filtered off and the solvents were removed *in vacuo* to yield the crude material. The crude product was purified by recrystallisation from Et_2O to yield 4-benylthiazolidine-4-thione (not shown).

4-benylthiazolidine-4-thione (1.00 eq.) was dissolved in THF (0.3 M) and the resulting yellow solution was cooled to 0°C. NaH (60 wt% in paraffin) (1.10 eq.) was carefully added to the cold solution and the resulting mixture was stirred at 0°C for one hour or until H_2 evolution ceased. Subsequently, AcCl (1.50 eq.) was added to the cold reaction mixture and the resulting solution was allowed to warm to room temperature. Stirring was continued for two hours or until the starting material had been consumed (as indicated by TLC analysis) and the reaction mixture was subsequently quenched by careful addition of a saturated aqueous solution of NH_4Cl. The quenched reaction mixture was diluted with EtOAc and the layers were separated. The aqueous layer was extracted with EtOAc (3 x equal volume to THF) and the combined organic layers were washed with brine (1 x equal volume to THF). The organic layers were dried over Na_2SO_4, the solids were filtered off and the solvents were removed *in vacuo* to yield the crude auxiliary **2.124**. Purification was achieved by recrystallisation from Et_2O to yield **2.124** as yellow crystals.

2.5.2.5. Evans-Crimmins Aldol Reaction

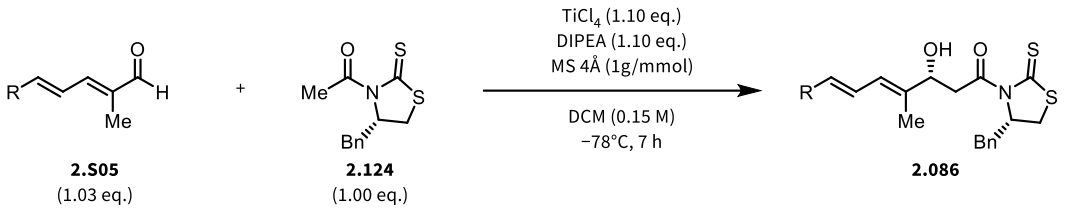

To a flame-dried Schlenk-tube under Argon containing activated molecular sieves 4Å (1 g/mmol) was added auxiliary **2.124** (1.00 eq.) and DCM (0.3 M). The resulting yellow solution was cooled to −78°C before $TiCl_4$ (1 M in DCM) (1.10 eq.) was carefully added dropwise to yield a dark orange slurry and stirring was continued for 10 min after complete addition. To the activated reaction mixture DIPEA (1.10 eq.) was subsequently carefully added dropwise at −78°C resulting in a change of colour to deep red/dark brown of the reaction mixture. The resulting reaction mixture was stirred for 30 min at −78°C before a solution of aldehyde **2.S05** (1.03 eq.) was carefully added dropwise (*Nota bene: the addition may occur more quickly if the solution of aldehyde is cooled to −78°C prior to addition and is added via transfer cannula. This is especially recommended on scales exceeding 2.00 mmol*). After the aldehyde had been added, the reaction was stirred at −78°C for 4 to 7 h or until all starting material had been consumed (as indicated by TLC analysis). The reaction was quenched by careful addition of a sat. aq. solution of NH_4Cl at −78°C (equal volume to reaction solvent) and stirring was continued for 5 min before the reaction was warmed to room temperature. The reaction mixture was filtered into a separatory funnel to remove the molecular sieves and the layers were separated. The aqueous layer was extracted with DCM (4 x reaction solvent volume) and the combined organic layers were washed with brine (1 x reaction solvent volume). The combined organic layers were dried over Na_2SO_4, the solids were filtered off and the solvents were removed *in vacuo*. The crude material was purified by flash column chromatography (SiO_2, heptane/EtOAc) to yield the aldol product **2.086**.

2.5.2.6. Curtius Rearrangement

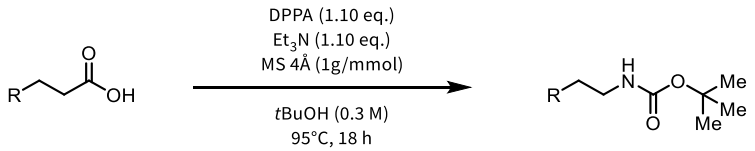

2.S07 **2.S08**

A flame-dried two-neck round bottom flask under Argon was fitted with a reflux condenser and a septum and to it were added carboxylic acid **2.S07** (1.00 eq.), MS 4Å (1 g/mmol) and *t*BuOH (0.3 M). The resulting mixture was stirred at room temperature for 30 min before DPPA (1.10 eq.) and Et_3N (1.10 eq.) were added. Subsequently, the reaction mixture was heated to reflux and stirring was continued for 18 h. Afterwards, the reaction was allowed to cool to room temperature, the solids were filtered off and the filtrate was concentrated *in vacuo* to afford the crude material. The crude material was purified by flash column chromatography (SiO_2, heptane/EtOAc) to afford primary *N*-Boc-protected amine **2.S08**.

2.5.2.7. Hydroboration of Alkynes

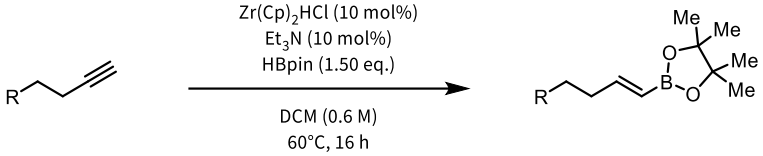

2.S09 **2.S10**

To a flame-dried three-neck round bottom flask under Argon fitted with a reflux condenser and two septa was added alkyne **2.S09** (1.00 eq.) and DCM (0.6 M). To the resulting mixture was added HBpin (1.50 eq.) followed by $Zr(Cp)_2HCl$ (10 mol%, Schwartz's reagent) and Et_3N (10 mol%). The reaction mixture was heated to reflux (typically 60°C) and stirring was continued for 16 h or until the starting material had been consumed (as indicated by ^{1}H-NMR analysis). Afterwards, the reaction mixture was cooled to room temperature and the solvents were removed *in vacuo*. The crude material was purified by flash column chromatography (SiO_2, heptane/EtOAc) to yield vinyl-Bpin species **2.S10**.

2.5.2.8. Removal of *N*-Boc Protecting Group

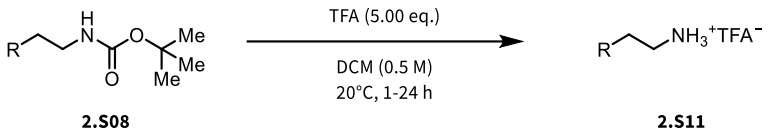

2.S08 **2.S11**

To a solution of *N*-Boc protected amine **2.S08** (1.00 eq.) in DCM (0.5 M) was added TFA (5.00 eq.) and the reaction mixture was stirred at room temperature until the starting material had been consumed (as indicated by TLC analysis). Afterwards, the volatiles were removed *in vacuo* and the resulting ammonium trifluoroacetate **2.S11** was directly used without further purification.

2.5.2.9. Synthesis of Azidoalcohols

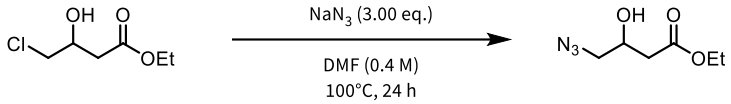

2.092 **2.S12**

To a solution of chlorohydrine **2.092** (1.00 eq.) in DMF (0.4 M) was added NaN_3 (3.00 eq.) and the resulting mixture was heated to 100°C. Stirring was continued at 100°C until the starting material had been consumed (as indicated by ^{1}H-NMR analysis). Afterwards, the reaction mixture was cooled to room temperature and the solids were removed by filtration. The residue was washed with EtOAc and the filtrate was concentrated under reduced pressure. The afforded crude material was purified by flash column chromatography (SiO_2, heptane/EtOAc) to yield azidoalcohol **2.S12**.

2.5.2.10. Fráter-Seebach Alkylation

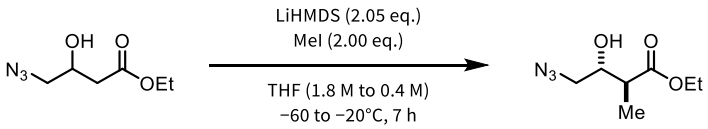

2.S12 **2.093**

To a solution of azidoalcohol **2.S12** (1.00 eq.) in THF (1.8 M) at −60°C was slowly added dropwise LiHMDS (1 M in THF) (2.05 eq.) and the resulting mixture was stirred at −60°C for an additional 30 min after

complete addition of LiHMDS. Afterwards, the reaction mixture was warmed to −35°C and stirred at the indicated temperature for 30 min before being cooled to −60°C. After reaching −60°C, MeI (2.00 eq.) was added dropwise and the resulting reaction mixture was stirred at −60°C for 2 h. Subsequently, the reaction solution was warmed to −40°C and stirred for 2 h and then to −20°C and was stirred at −20°C for 2 h. After the reaction time had elapsed, the reaction was quenched by addition of an aqueous solution of citric acid (15 wt%) at −20°C and the pH was adjusted to pH = 3-4. The quenched reaction mixture was warmed to room temperature and the layers were separated. The aqueous layer was extracted with EtOAc (3 x double reaction solvent volume) and the combined organic layers were dried over Na_sSO_4. The solids were filtered off, the solvents were removed *in vacuo* and the crude material was purified by flash column chromatography (SiO_2, heptane/EtOAc) to yield methylated azidoalcohol **2.093**.

2.5.2.11. TBS-Protection of Alcohols

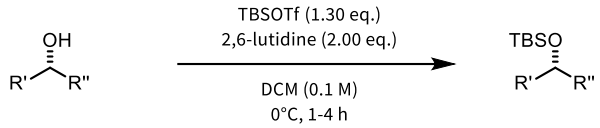

2.S13 **2.S14**

To a solution of unprotected alcohol **2.S13** in DCM (0.1 M) at 0°C was added TBSOTf (1.30 eq.) followed by addition of 2,6-lutidine (2.00 eq.). The resulting mixture was stirred at 0°C for 1 to 4 h or until the starting material had been consumed (as indicated by TLC analysis). The reaction was quenched by addition of a sat. aq. solution of NH_4Cl (1 x reaction solvent volume) and the layers were separated. The aqueous layer was extracted with DCM (3 x reaction solvent volume) and the combined organic layers were washed with brine (1 x reaction solvent volume). The combined organic layers were dried over $NaSO_4$, the solids were filtered off and the solvents were removed *in vacuo* to afford the crude material. The product was isolated through flash column chromatography (SiO_2, heptane/EtOAc) to yield protected alcohol **2.S14**.

2.5.2.12. Hydrolysis of Carboxylic Acid Ester with LiOH

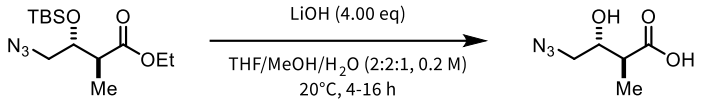

2.S15 **2.094**

To a solution of ester **2.S15** (1.00 eq.) in THF/MeOH/H_2O (2:2:1, 0.2 M) was added LiOH (4.00 eq., either LiOH or LiOH · H_2O) and the resulting reaction mixture was stirred at room temperature until the starting material had been consumed (typically 4 to 16 h, as indicated by TLC analysis). Afterwards, THF and MeOH were removed under reduced pressure and the remaining slurry was adjusted to pH = 2-3 by addition of 1 M HCl. The slurry was diluted with EtOAc and H_2O and the layers were separated. The aqueous layer (at pH = 2-3) was extracted with EtOAc (5 x reaction solvent volume) and the combined organic layers were washed with brine (1 x reaction solvent volume). The combined organic layers were dried over Na_2SO_4, the solids were filtered off and the solvents were removed *in vacuo* to afford the carboxylic acid **2.094** which was used without further purification.

2.5.2.13. Amide Coupling mediated by HATU

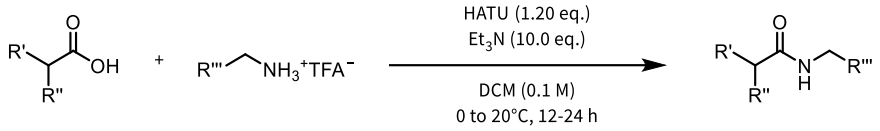

2.S16 (1.00 eq.) **2.S11** (1.20 eq.) **2.S17**

To a solution of carboxylic acid **2.S16** (1.00 eq.) and ammonium salt **2.S11** (1.20 eq.) in DCM (0.1 M) at 0°C was added Et_3N (10.0 eq.) followed by addition of HATU (1.20 eq.). The reaction mixture was allowed to warm to room temperature and was stirred for 12 to 24 h. Afterwards, the reaction was quenched by addition of 1 M HCl (11.0 eq) and the aqueous layer was extracted with DCM (3 x reaction solvent volume). The combined organic layers were washed with brine (1 x reaction solvent volume), dried over Na_2SO_4, the solids were filtered off and the solvents were removed *in vacuo* to afford the crude amide. The crude material was purified by flash column chromatography (SiO_2, heptane/EtOAc) to afford amide **2.S17**.

2.5.2.14. Reduction of Azide with Zn dust

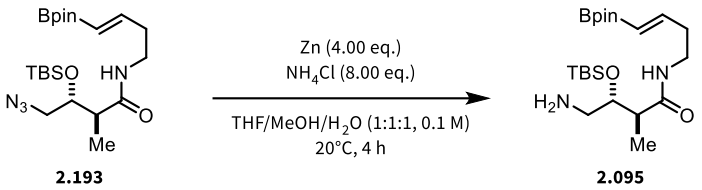

To a solution of azide **2.193** (1.00 eq.) in THF/MeOH/H_2O (1:1:1, 0.1 M) was added activated Zn dust (4.00 eq.) followed by addition of NH_4Cl (8.00 eq.). The resulting slurry was stirred at room temperature for 4 h or until the starting material had been consumed (as indicated by TLC analysis). Afterwards, the volatiles were removed under reduced pressure and the resulting slurry was basified by addition of a sat. aq. solution of $NaHCO_3$ to pH = 9 and the resulting aqueous phase was extracted with DCM (5 x reaction solvent volume). The combined organic layers were washed with brine, dried over Na_2SO_4, the solids were filtered off and the solvents were removed *in vacuo* to yield primary amine **2.095** which was used without further purification.

2.5.2.15. Amide Coupling mediated by DMAP

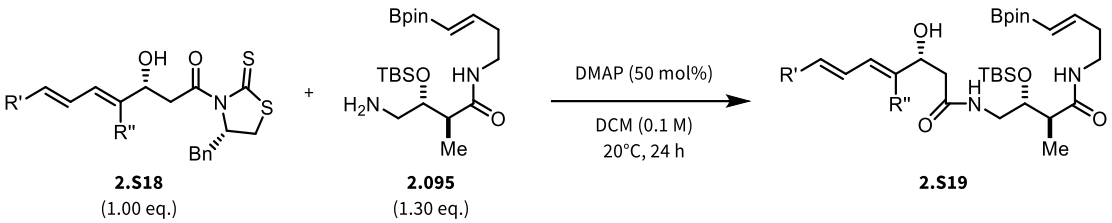

Side-chain precursor **2.S18** (1.00 eq.) and primary amine **2.095** (1.30 eq.) were dissolved in DCM (0.1 M) and DMAP (50 mol%) was added at room temperature. The resulting mixture was stirred for 24 h or until the starting material had been consumed (as indicated by TLC analysis). The reaction was quenched by addition of water (1 x reaction solvent volume) and the layers were separated. The aqueous layer was extracted with DCM (5 x reaction solvent volume) and the combined organic layers were washed with brine (1 x reaction solvent volume), dried over Na_2SO_4, the solids were filtered off and the solvents were

removed under reduced pressure to yield the crude material. The product was isolated by flash column chromatography (SiO_2, heptane/EtOAc to heptane/*i*PrOH) to yield amide **2.S19**.

2.5.2.16. Esterification with Cyclobutene Acid mediated by Ghosez's Reagent

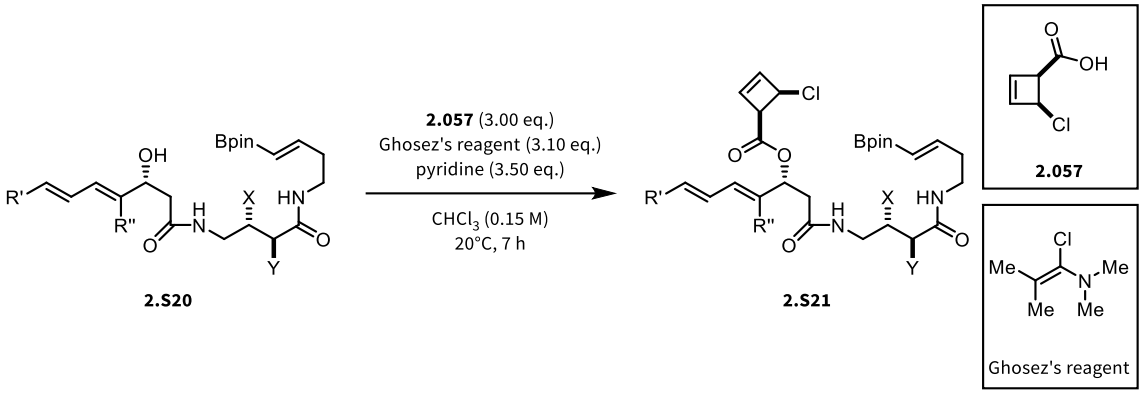

To a solution of carboxylic acid **2.057** (3.00 eq.) in $CHCl_3$ (0.3 M relative to the alcohol) at 20°C was added freshly distilled Ghosez's reagent (3.10 eq.). The resulting mixture was stirred at 20°C for 40 min before a solution of alcohol **2.S20** (1.00 eq.) in $CHCl_3$(0.3 M) was added followed by freshly distilled pyridine (3.50 eq.). The resulting reaction mixture was stirred for 7 h or until the starting material had been consumed (as indicated by TLC analysis). Afterwards, the reaction was quenched by addition of a sat. aq. solution of $NaHCO_3$ and the layers were separated. The aqueous layer was extracted with DCM (2 x reaction solvent volume) and the combined organic layers were dried over Na_2SO_4. The solids were removed by filtration and the solvents were evaporated under reduced pressure (*Nota bene: the bath temperature must not exceed 25°C to avoid opening of the cyclobutene*) to yield the crude ester. The crude material was purified by flash column chromatography (SiO_2, heptane/EtOAc, 10-15 mL c_v per 0.1 mmol of alcohol, gradient: 30% EtOAc (3 c_v) → 35% (2 c_v) → 40% (4 c_v) → 45% (2 c_v) → 50% (4 c_v)) to yield the pure *cis*-cyclobutene esters **2.S21**.

2.5.2.17. Esterification with Cyclobutene Acid mediated by T3P

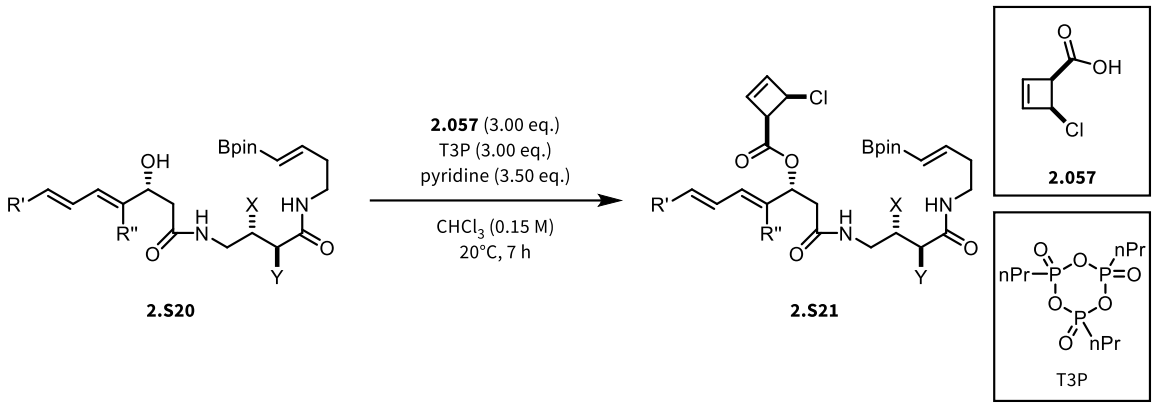

To a solution of carboxylic acid **2.057** (3.00 eq.) in $CHCl_3$ (0.3 M relative to the alcohol) at 20°C was added T3P (50 wt% in EtOAc) (3.00 eq.) and freshly distilled pyridine (3.50 eq.). The resulting mixture was stirred at 20°C for 40 min before a solution of alcohol **2.S20** (1.00 eq.) in $CHCl_3$(0.3 M) was. The resulting reaction mixture was stirred for 7 h or until the starting material had been consumed (as indicated by TLC analysis). Afterwards, the reaction was quenched by addition of 1.00 mL of MeOH and stirring was continued for 15 min before water was added. The aqueous layer was extracted with DCM (3 x reaction solvent volume) and the combined organic layers were washed with a sat. aq. solution of $NaHCO_3$ (2 x reaction solvent volume) and brine (2 x reaction solvent volume) before being dried over Na_2SO_4. The solids were removed by filtration and the solvents were evaporated under reduced pressure (*Nota bene: the bath temperature must not exceed 25°C to avoid opening of the cyclobutene*). The crude material was purified by flash column chromatography (SiO_2, heptane/EtOAc, 10-15 mL c_v per 0.1 mmol of alcohol, gradient: 30% EtOAc (3 c_v) → 35% (2 c_v) → 40% (4 c_v) → 45% (2 c_v) → 50% (4 c_v)) to yield pure *cis*-cyclobutene esters **2.S21**.

2.5.2.18. Domino Suzuki-Miyaura Macrocyclisation

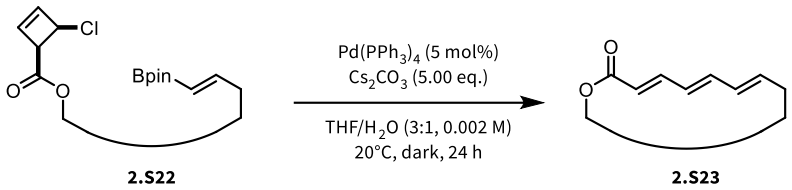

2.S22 **2.S23**

To a solution of linear macrocyclisation precursor **2.S22** (1.00 eq.) in THF/H_2O (3:1, 0.002 M) at 20°C was added Cs_2CO_3 (5.00 eq.) and the resulting reaction mixture was degassed for 20 min. Afterwards, $Pd(PPh_3)_4$ (5 mol%) was added and the reaction vessel was covered with aluminium foil and the reaction mixture was stirred in the dark at room temperature for 24 h. After the reaction time had elapsed, the reaction was quenched by addition of a sat. aq. solution of NH_4Cl and the layers were separated. The aqueous layer was extracted with DCM (5 x 25% of reaction solvent volume) and the combined organic layers were washed with brine (1 x 25% of reaction solvent volume). The combined organic layers were dried over Na_2SO_4, the solids were filtered off and the solvents were removed *in vacuo* to yield the crude macrocycle. The crude material was purified through flash column chromatography (SiO_2, heptanes/EtOAc) to yield **2.S23**.

2.5.2.19. Deprotection of TBS-protected Alcohols

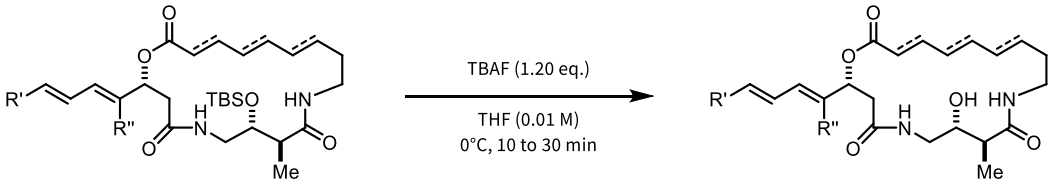

2.S24 **2.S25**

To a solution of protected alcohol **2.S24** (1.00 eq., typically 5 – 15 mg) in THF (1.00 mL) at 0°C was added TBAF (1 M in THF) (1.20 eq.) and the resulting mixture was stirred at 0°C for 10 to 30 min or until the starting material had been consumed (as indicated by TLC analysis, 10% MeOH in $CHCl_3$). The reaction was quenched by addition of one drop of a sat. aq. solution of NH_4Cl and the solvents were removed. The

crude material was purified by flash column chromatography (SiO_2, 5% MeOH in $CHCl_3$) to yield the desired natural product analogues **2.S25**.

2.5.2.20. Synthesis of Propargylic Alcohols

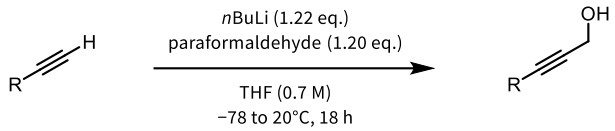

2.S26 **2.S27**

To a solution of terminal alkyne **2.S26** (1.00 eq.) in THF (0.7 M) at −78°C was added *n*BuLi (2.5 M in hexanes) (1.22 eq.) and the resulting reaction mixture was warmed to 0°C and stirred for 1 h. Afterwards, the reaction mixture was cooled to −78°C before paraformaldehyde (1.20 eq.) was added. Following addition, the reaction mixture was allowed to warm to room temperature and was stirred for 18 h. The reaction was quenched by addition of a sat. aq. solution of NH_4Cl (60 mL/100 mmol) and the aqueous layer was extracted with Et_2O (3 x reaction solvent volume). The combined organic layers were dried over Na_2SO_4, the solids were filtered off and the solvents were removed to yield the propargylic alcohol **2.S27** typically in pure form. If required, the product can be purified by flash column chromatography (SiO_2, heptane/EtOAc or pentane/Et_2O).

2.5.2.21. Alkyne Zipper Reaction

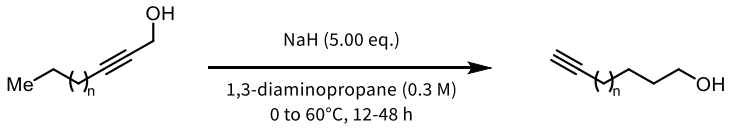

2.S28 **2.S29**

To a flame-dried two-neck round bottom flask capable of pressure release under Argon was added 1,3-diaminoproane (0.3 M, 41.0 eq.) and the flask was cooled to 0°C. To the cold diaminopropane was carefully portion wise added NaH (60 wt% in paraffin) (5.00 eq.). After addition of NaH and after gas evolution had ceased, the reaction mixture was heated to 60°C for 3 h. Subsequently, the reaction mixture was cooled

to 45°C and propargylic alcohol **2.S28** (1.00 eq.) was added (*Nota bene: for solid propargylic alcohols, **2.S28** was dissolved in a small amount of heptane prior to addition*). After full addition of the propargylic alcohol, the reaction mixture was heated to 60°C and stirring was continued for 12 to 48 h (*Nota bene: longer chains need longer reaction times to fully isomerise to the terminal position*). After the reaction time had elapsed, the reaction mixture was cooled to 0°C before being quenched by careful addition of conc. HCl and the pH was adjusted to pH = 1 – 2. The aqueous layer was then extracted with Et_2O (3 x reaction solvent volume) and the combined organic layers were dried over Na_2SO_4, the solids were filtered off and the solvents were removed *in vacuo* to afford the crude material, which was subsequently purified by flash column chromatography (SiO_2, heptane/EtOAc or pentane/Et_2O) to afford terminal alkyne **2.S29**.

2.5.2.22. Hydroboration of Alkynes in the Presence of unprotected Alcohols

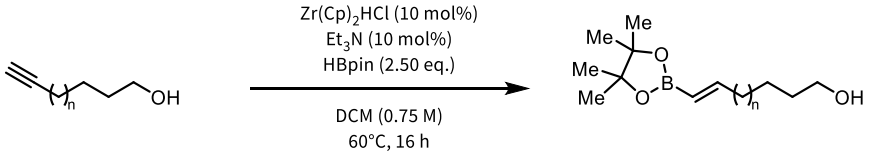

2.S29 **2.S30**

To a solution of alkyne **2.S29** (1.00 eq.) in DCM (0.75 M) at room temperature was added HBpin (2.50 eq.) (*gas evolution*) followed by $Zr(Cp)_2HCl$ (10 mol%) and Et_3N (10 mol%). The reaction was heated to 60°C, covered with aluminium foil and stirred for 16 h. After the starting material had been consumed (as indicated by ^{1}H-NMR analysis), the reaction was cooled to room temperature and the volatiles were removed *in vacuo*. The thusly afforded crude material was purified by flash column chromatography (SiO_2, heptane/EtOAc) to afford the hydroboration product **2.S30**.

2.5.3. Synthesis of general FR Building Blocks

2.5.3.1. (±)-*cis*-Chlorocyclobutene carboxylic acid (2.057)

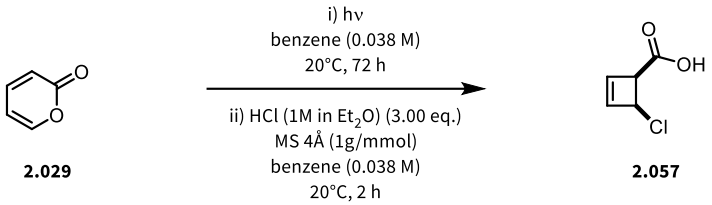

To a flame-dried 250 mL Schlenk-tube under Argon was added benzene (180 mL, 0.038 M) was added 2-pyrone **2.029** (650 mg, 6.76 mmol, 1.00 eq). The resulting solution was degassed while being sonicated for 15 min by bubbling with Argon before being placed in a 300 nm Rayonet apparatus for 72 h. After the starting material had been consumed (as indicated by ^{1}H-NMR analysis), the vessel was removed from the Rayonet and the solution of bicyclo[2.2.0]lactone was used in the next step without further purification.

To a flame-dried two-neck flask under Argon containing activated 4Å molecular sieves (1 g/mmol) was added a solution of bicyclo[2.2.0]lactone (0.038 M in benzene) and the mixture was stirred at room temperature for 10 min before HCl (2.0 M in Et_2O) (10.1 mL, 20.3 mmol, 3.00 eq.) was added. The resulting reaction mixture was stirred at 20°C for 2 h, after which HCl was removed under reduced pressure (aspirator pump). The solvents were removed under reduced pressure (*Nota bene: the bath temperature must not exceed 25°C to avoid ring opening*) to yield the crude carboxylic acid. The crude material was purified by flash column chromatography (SiO_2, 77% heptanes/20% EtOAc/3% AcOH) to yield (±)-*cis*-chlorocyclobutene carboxylic acid **2.057** (450 mg, 3.40 mmol, 50%) as a white powder.

All spectroscopic data are in accordance with the reported literature.[253]

TLC: R_f (50% EtOAc in heptane) = 0.40 (tailing); heating prior to $KMnO_4$ stain.

2.5.3.2. Ethyl (2*E*,4*E*)-2-methyldodeca-2,4-dienoate (2.S31)

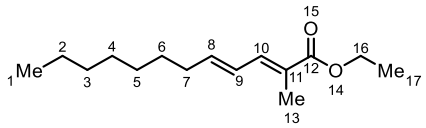

2.S31
Chemical Formula: $C_{15}H_{26}O_2$

The side-chain building block ethyl (2*E*,4*E*)-2-methyldodeca-2,4-dienoate (**2.S31**) was synthesised according to the general procedure outlined in chapter 2.5.2.1. on 30.0 mmol scale to yield **2.S31** (6.66 g, 27.9 mmol, 93%) as a colourless oil.

All spectroscopic data are in accordance with the reported literature.[253]

TLC: R_f (20% EtOAc in heptane) ~ 0.80; $KMnO_4$ stain.

2.5.3.3. (2*E*,4*E*)-2-Methyldodeca-2,4-dien-1-ol (2.S32)

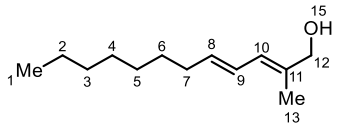

2.S32
Chemical Formula: $C_{13}H_{24}O$

The side-chain building block (2*E*,4*E*)-2-methyldodeca-2,4-dien-1-ol (**2.S32**) was synthesised according to the general procedure outlined in chapter 2.5.2.2. on 27.9 mmol scale to yield **2.S32** as a colourless oil, which was used without purification.

All spectroscopic data are in accordance with the reported literature.[253]

TLC: R_f (20% EtOAc in heptane) = 0.40; $KMnO_4$ stain.

2.5.3.4. (2*E*,4*E*)-2-Methyldodeca-2,4-dienal (2.S33)

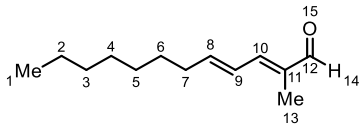

2.S33
Chemical Formula: $C_{13}H_{22}O$

The side-chain building block (2*E*,4*E*)-2-methyldodeca-2,4-dienal (**2.S33**) was synthesised according to the general procedure outlined in chapter 2.5.2.3. on 27.9 mmol scale to yield **2.S33** (3.99 g, 20.5 mmol, 74% over two steps) as a colourless oil.

All spectroscopic data are in accordance with the reported literature.[310]

TLC: R_f (20% EtOAc in heptane) ~ 0.80; $KMnO_4$ stain.

2.5.3.5. (*S*)-1-(4-Benzyl-2-thioxothiazolidin-3-yl)ethan-1-one (2.124)

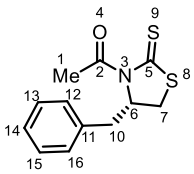

2.124
Chemical Formula: $C_{12}H_{13}NOS_2$

The chiral auxiliary (*S*)-1-(4-benzyl-2-thioxothiazolidin-3-yl)ethan-1-one (**2.124**) was synthesised according to the general procedure outlined in chapter 2.5.2.4. on 54.4 mmol scale to yield **2.124** (12.9 g, 51.3 mmol, 94%) as yellow crystals.

All spectroscopic data are in accordance with the reported literature.[311]

2.5.3.6. ((*R*,4*E*,6*E*)-1-((*S*)-4-Benzyl-2-thioxothiazolidin-3-yl)-3-hydroxy-4-methyltetradeca-4,6-dien-1-one (2.096)

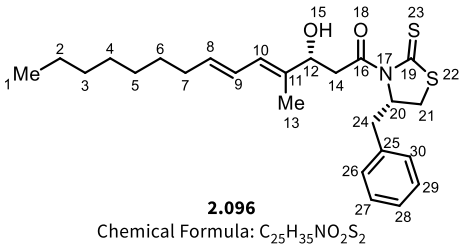

2.096
Chemical Formula: $C_{25}H_{35}NO_2S_2$

The side-chain building block (*R*,4*E*,6*E*)-1-((*S*)-4-benzyl-2-thioxothiazolidin-3-yl)-3-hydroxy-4-methyltetradeca-4,6-dien-1-one (**2.096**) was synthesised according to the general procedure outlined in chapter 2.5.2.5. on 20.2 mmol scale to yield **2.096** (7.29 g, 16.4 mmol, 81%, single diastereomer) as a yellow oil (overall: *13:1 d.r*, 7.83 g, 17.6 mmol, 87%.).

All spectroscopic data are in accordance with the reported literature.[253]

TLC: desired diastereomer: R_f (20% EtOAc in heptane) = 0.22; $KMnO_4$ stain;

undesired diastereomer: R_f (20% EtOAc in heptane) = 0.33; $KMnO_4$ stain.

2.5.3.7. *tert*-Butyl but-3-yn-1-ylcarbamate (2.089)

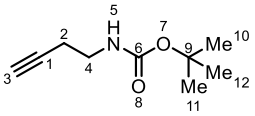

2.089
Chemical Formula: $C_9H_{15}NO_2$

tert-Butyl but-3-yn-1-ylcarbamate (**2.089**) was synthesised according to the general procedure outlined in chapter 2.5.2.6. on 81.5 mmol scale to yield **2.089** (6.36 g, 37.6 mmol, 46%) as a colourless oil.

All spectroscopic data are in accordance with the reported literature.[253]

TLC: R_f (20% EtOAc in heptane) = 0.44 (light tailing); $KMnO_4$ stain.

2.5.3.8. *tert*-Butyl (*E*)-(4-(4,4,5,5-tetramethyl-1,3,2-dioxaborolan-2-yl)but-3-en-1-yl)carbamate (2.090)

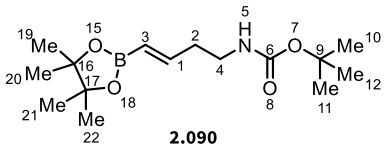

2.090

Chemical Formula: $C_{15}H_{28}BNO_4$

tert-Butyl (*E*)-(4-(4,4,5,5-tetramethyl-1,3,2-dioxaborolan-2-yl)but-3-en-1-yl)carbamate (**2.090**) was synthesised according to the general procedure outlined in chapter 2.5.2.7. on 37.6 mmol scale to yield **2.090** (9.30 g, 29.0 mmol, 77%) as a colourless oil.

All spectroscopic data are in accordance with the reported literature.[253]

TLC: R_f (20% EtOAc in heptane) = 0.40; $KMnO_4$ stain.

2.5.3.9. (*E*)-4-(4,4,5,5-tetramethyl-1,3,2-dioxaborolan-2-yl)but-3-en-1-ammonium trifluoroacetate (2.091)

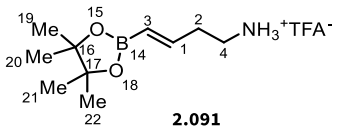

2.091

Chemical Formula: $C_{12}H_{21}BF_3NO_3$

(*E*)-4-(4,4,5,5-tetramethyl-1,3,2-dioxaborolan-2-yl)but-3-en-1-ammonium trifluoroacetate (**2.091**) was synthesised according to the general procedure outlined in chapter 2.5.2.8. on 29.0 mmol scale to yield **2.091** (9.06 g, 29.0 mmol, quantitative) as a colourless, viscous oil.

All spectroscopic data are in accordance with the reported literature.[253]

2.5.3.10. Ethyl (*R*)-4-azido-3-hydroxybutanoate (2.S12)

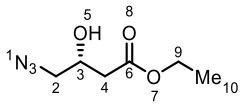

2.S12

Chemical Formula: $C_6H_{11}N_3O_3$

Ethyl (*R*)-4-azido-3-hydroxybutanoate (**2.S12**) was synthesised according to the general procedure outlined in chapter 2.5.2.9. on 180 mmol scale to yield azidoalcohol **2.S12** (19.4 g, 112 mmol, 62%) as a colourless, viscous oil.

All spectroscopic data are in accordance with the reported literature.[253]

TLC: R_f (30% EtOAc in heptane) = 0.33; $KMnO_4$ stain.

2.5.3.11. Ethyl (2*S*,3*R*)-4-azido-3-hydroxy-2-methylbutanoate (2.093)

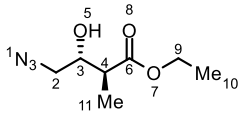

2.093

Chemical Formula: $C_6H_{11}N_3O_3$

Ethyl (2*S*,3*R*)-4-azido-3-hydroxy-2-methylbutanoate (**2.093**) was synthesised according to the general procedure outlined in chapter 2.5.2.10. on 53.4 mmol scale to yield **2.093** (5.65 g, 30.2 mmol, 57%) as a colourless oil.

All spectroscopic data are in accordance with the reported literature.[253]

TLC: R_f (30% EtOAc in heptane) = 0.44; $KMnO_4$ stain.

2.5.3.12. Ethyl (2*S*,3*R*)-4-azido-3-((*tert*-butyldimethylsilyl)oxy)-2-methylbutanoate (2.S34)

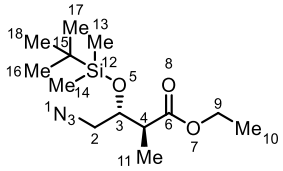

2.S34

Chemical Formula: $C_{13}H_{27}N_3O_3Si$

Ethyl (2*S*,3*R*)-4-azido-3-((*tert*-butyldimethylsilyl)oxy)-2-methylbutanoate (**2.S34**) was synthesised according to the general procedure outlined in chapter 2.5.2.11. on 47.8 mmol scale to yield **2.S34** (14.4 g, 47.8 mmol, quantitative) as a colourless oil.

All spectroscopic data are in accordance with the reported literature.[253]

TLC: R_f (20% EtOAc in heptane) = 0.80; $KMnO_4$ stain.

2.5.3.13. (2*S*,3*R*)-4-Azido-3-((*tert*-butyldimethylsilyl)oxy)-2-methylbutanoic acid (2.094)

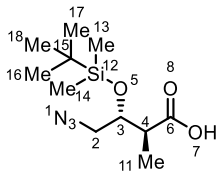

2.094

Chemical Formula: $C_{13}H_{29}N_3O_3Si$

(2*S*,3*R*)-4-Azido-3-((*tert*-butyldimethylsilyl)oxy)-2-methylbutanoic acid (**2.094**) was synthesised according to the general procedure outlined in chapter 2.5.2.12. on 26.1 mmol scale to yield **2.094** (6.90 g, 25.2 mmol, 97%) as a colourless oil.

All spectroscopic data are in accordance with the reported literature.[253]

TLC: R_f (20% EtOAc in heptane) = 0.20; $KMnO_4$ stain.

2.5.3.14. (2*S*,3*R*)-4-Azido-3-((*tert*-butyldimethylsilyl)oxy)-2-methyl-*N*-((*E*)-4-(4,4,5,5-tetramethyl-1,3,2-dioxaborolan-2-yl)but-3-en-1-yl)butanamide (2.193)

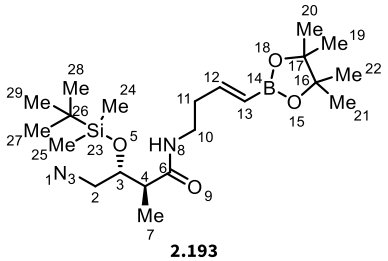

2.193
Chemical Formula: $C_{21}H_{41}BN_4O_4Si$

(2*S*,3*R*)-4-Azido-3-((*tert*-butyldimethylsilyl)oxy)-2-methyl-*N*-((*E*)-4-(4,4,5,5-tetramethyl-1,3,2-dioxaborolan-2-yl)but-3-en-1-yl)butanamide (**2.193**) was synthesised according to the general procedure outlined in chapter 2.5.2.13. on 16.4 mmol scale to yield **2.193** (5.79 g, 12.8 mmol, 78%) as a colourless oil.

All spectroscopic data are in accordance with the reported literature.[253]

TLC: R_f (40% EtOAc in heptane) = 0.40; $KMnO_4$ stain.

2.5.3.15. (2*S*,3*R*)-4-amino-3-((*tert*-butyldimethylsilyl)oxy)-2-methyl-*N*-((*E*)-4-(4,4,5,5-tetramethyl-1,3,2-dioxaborolan-2-yl)but-3-en-1-yl)butanamide (2.095)

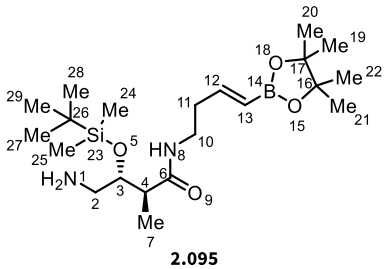

2.095
Chemical Formula: $C_{21}H_{43}BN_2O_4Si$

*(*2*S*,3*R*)-4-amino-3-((*tert*-butyldimethylsilyl)oxy)-2-methyl-*N*-((*E*)-4-(4,4,5,5-tetramethyl-1,3,2-dioxaborolan-2-yl)but-3-en-1-yl)butanamide (**2.095**) was synthesised according to the general procedure outlined in chapter 2.5.2.14. on 9.95 mmol scale to yield **2.095** (3.40 g, 7.97 mmol, 80%) as a colourless, viscous oil.

All spectroscopic data are in accordance with the reported literature.[253]

TLC: R_f (50% EtOAc in heptane) = 0.05; $KMnO_4$ stain.

2.5.3.16. (*R*,4*E*,6*E*)-*N*-((2*R*,3*S*)-2-((*tert*-butyldimethylsilyl)oxy)-3-methyl-4-oxo-4-(((*E*)-4-(4,4,5,5-tetramethyl-1,3,2-dioxaborolan-2-yl)but-3-en-1-yl)amino)butyl)-3-hydroxy-4-methyltetradeca-4,6-dienamide (2.097)

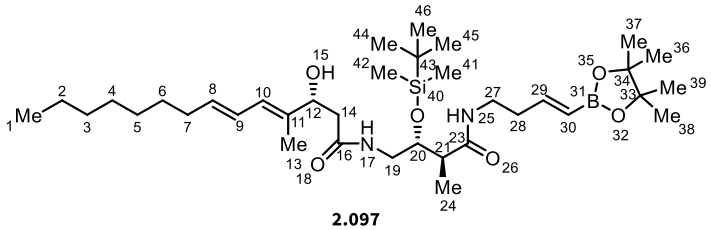

2.097

Chemical Formula: $C_{36}H_{67}BN_2O_6Si$

(*R*,4*E*,6*E*)-*N*-((2*R*,3*S*)-2-((*tert*-butyldimethylsilyl)oxy)-3-methyl-4-oxo-4-(((*E*)-4-(4,4,5,5-tetramethyl-1,3,2-dioxaborolan-2-yl)but-3-en-1-yl)amino)butyl)-3-hydroxy-4-methyltetradeca-4,6-dienamide (**2.097**) was synthesised according to the general procedure outlined in chapter 2.5.2.15. on 1.25 mmol scale to yield **2.097** (360 mg, 0.543 mmol, 43%) as a colourless, viscous oil.

All spectroscopic data are in accordance with the reported literature.[253]

TLC: R_f (20% *i*PrOH in heptane) = 0.70; PMA stain.

2.5.3.17. (*R*,4*E*,6*E*)-1-(((2*R*,3*S*)-2-((*tert*-butyldimethylsilyl)oxy)-3-methyl-4-oxo-4-(((*E*)-4-(4,4,5,5-tetramethyl-1,3,2-dioxaborolan-2-yl)but-3-en-1-yl)amino)butyl)amino)-4-methyl-1-oxotetradeca-4,6-dien-3-yl (1*R*,4*R*)-4-chlorocyclobut-2-ene-1-carboxylate (2.098)

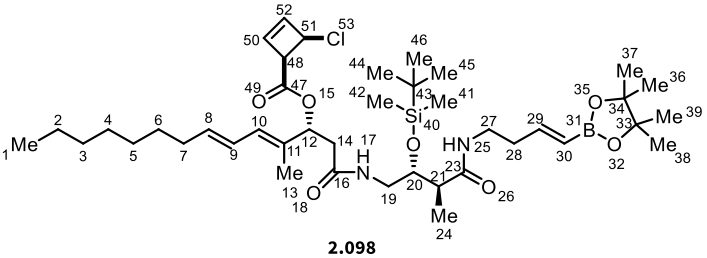

2.098

Chemical Formula: $C_{41}H_{70}BClN_2O_7Si$

(*R*,4*E*,6*E*)-1-(((2*R*,3*S*)-2-((*tert*-butyldimethylsilyl)oxy)-3-methyl-4-oxo-4-(((*E*)-4-(4,4,5,5-tetramethyl-1,3,2-dioxaborolan-2-yl)but-3-en-1-yl)amino)butyl)amino)-4-methyl-1-oxotetradeca-4,6-dien-3-yl (1*R*,4*R*)-4-chlorocyclobut-2-ene-1-carboxylate (**2.098**) was synthesised according to the general procedure outlined in chapter 2.5.2.17. on 280 µmol scale to yield **2.098** (53.1 mg, 68.3 µmol, 24%) as a colourless, viscous oil.

All spectroscopic data are in accordance with the reported literature.[253]

TLC: *trans*$_1$-**2.098**: R_f (50% EtOAc in heptane) = 0.43, heating prior to $KMnO_4$ or PMA stain;

trans$_2$-**2.098**: R_f (50% EtOAc in heptane) = 0.39, heating prior to $KMnO_4$ or PMA stain;

cis$_1$-**2.098**: R_f (50% EtOAc in heptane) = 0.29, heating prior to $KMnO_4$ or PMA stain;

cis$_2$-**2.098**: R_f (50% EtOAc in heptane) = 0.24, heating prior to $KMnO_4$ or PMA stain;

alcohol **2.097**: R_f (50% EtOAc in heptane) = 0.20, $KMnO_4$ or PMA stain.

2.5.3.18. (2*R*,7*R*,8*S*,13*E*,15*E*,17*E*)-7-((*tert*-butyldimethylsilyl)oxy)-2-((2*E*,4*E*)-dodeca-2,4-dien-2-yl)-8-methyl-1-oxa-5,10-diazacyclononadeca-13,15,17-triene-4,9,19-trione (2.182)

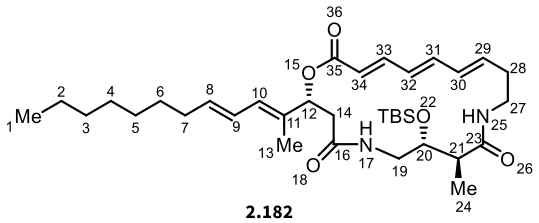

2.182

Chemical Formula: $C_{35}H_{58}N_2O_5Si$

(2*R*,7*R*,8*S*,13*E*,15*E*,17*E*)-7-((*tert*-butyldimethylsilyl)oxy)-2-((2*E*,4*E*)-dodeca-2,4-dien-2-yl)-8-methyl-1-oxa-5,10-diazacyclononadeca-13,15,17-triene-4,9,19-trione (**2.182**) was synthesised according to the general procedure outlined in chapter 2.5.2.18. on 24.8 µmol scale to yield **2.182** (7.80 mg, 12.7 µmol, 51%) as a colourless, viscous oil.

All spectroscopic data are in accordance with the reported literature.[253]

TLC: R_f (50% EtOAc in heptane) = 0.30, $KMnO_4$ stain.

2.5.3.19. (2*R*,7*R*,8*S*,13*E*,15*E*,17*E*)-2-((2*E*,4*E*)-dodeca-2,4-dien-2-yl)-7-hydroxy-8-methyl-1-oxa-5,10-diazacyclononadeca-13,15,17-triene-4,9,19-trione, FR252921 (2.013)

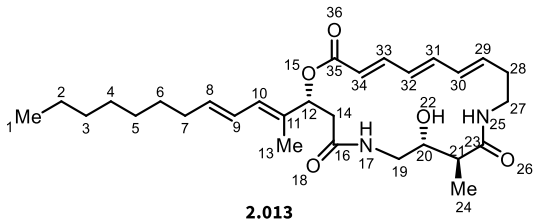

2.013

Chemical Formula: $C_{29}H_{44}N_2O_5$

FR252921 (**2.013**) was synthesised according to the general procedure outlined in chapter 2.5.2.19. on 12.7 µmol scale to yield **2.013** (4.90 mg, 9.79 µmol, 77%) as a white powder.

All spectroscopic data are in accordance with the reported literature.[311]

TLC: R_f (10% MeOH in $CHCl_3$) = 0.30, $KMnO_4$ stain.

2.6. Synthesis of FR Analogues

2.6.1. Synthesis of αH-FR

2.6.1.1. αH-FR ((2*R*,7*R*,8*S*,13*E*,15*E*,17*E*)-7-hydroxy-8-methyl-2-((1*E*,3*E*)-undeca-1,3-dien-1-yl)-1-oxa-5,10-diazacyclononadeca-13,15,17-triene-4,9,19-trione), αH-FR (2.110)

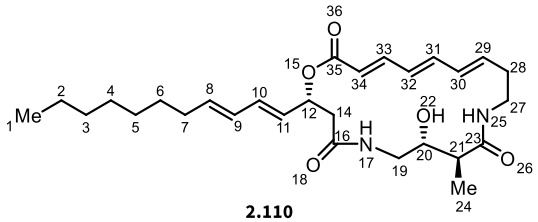

2.110

Chemical Formula: $C_{28}H_{42}N_2O_5$

αH-FR (**2.110**) was synthesised according to the general procedure outlined in chapter 2.5.2.19. on 8.00 µmol scale to yield **2.110** (1.60 mg, 3.29 µmol, 41%) as a white powder.

^{1}H-NMR (700 MHz, $CHCl_3$): δ 7.27-7.25 (m, 1H, **H_{33}**), 6.49 (dd, *J* = 14.9, 10.8 Hz, 1H, **H_{31}**), 6.31 (dd, *J* = 15.3, 10.5 Hz, 1H, **H_{19}**), 6.26 (d, *J* = 8.5 Hz, 1H, **H_{NH}**), 6.18 (dd, *J* = 14.9, 11.3 Hz, 1H, **H_{32}**), 6.07 (dd, *J* = 14.8, 11.6 Hz, 1H, **H_{30}**), 6.00 (dd, *J* = 15.1, 10.5 Hz, 1H, **H_9**), 5.81-5.72 (m, 4H, **$H_{8+12+29+34}$**), 5.68 (d, *J* = 7.2 Hz, 1H, **H_{NH}**), 5.60 (dd, *J* = 15.3, 6.5 Hz, 1H, **H_{11}**), 4.10 (ddd. *J* = 17.4, 14.9, 5.1 Hz, 1H, **H_{19}**), 3.80 (t, *J* = 10.0 Hz, 1H, **H_{27}**), 3.35-3.28 (m, 1H, **H_{20}**), 3.04 (d, *J* = 13.8 Hz, 1H, **H_{19}**), 2.65-2.60 (m, 1H, **H_{27}**), 2.58 (dd, *J* = 13.8, 2.8 Hz, 2H), 2.48 (dd, *J* = 13.9, 11.3 Hz, 2H), 2.29-2.18 (m, 2H, **H_{28}**), 2.07 (dd, *J* = 14.0, 6.8 Hz, 2H, **H_7**), 1.39-1.35 (m, 2H, **H_6**), 1.31-1.24 (m, 8H, **$H_{2\text{-}5}$**), 0.98 (d, *J* = 7.1 Hz, 3H, **H_{24}**), 0.88 (t, *J* = 7.1 Hz, 3H, **H_1**) ppm.

^{13}C-NMR (175 MHz, $CHCl_3$): δ 176.0 (**C_{23}**), 169.2 (**C_{16}**), 165.6 (**C_{35}**), 144.8, 140.9, 137.3, 136.1, 133.3 (**C_{10}**), 132.9 (**C_{30}**), 129.1 (**C_9**), 128.6 (**C_{32}**), 127.4 (**C_{11}**), 121.1, 72.3 (**C_{12}**), 71.6 (**C_{20}**), 44.1 (**C_{27}**), 43.1 (**C_{21}**), 43.0, 37.0 (**C_{19}**), 34.6, 32.8, 32.0 (**C_7**), 29.3 (**$C_{2\text{-}5}$**), 29.3 (**$C_{2\text{-}5}$**), 29.3 (**$C_{2\text{-}5}$**), 22.8 (**$C_{2\text{-}5}$**), 14.2 (**C_1**), 11.2 (**C_{24}**) ppm.

HRMS (ESI^+): exact mass calculated for $[M+Na]^+$ ($C_{28}H_{42}N_2O_5Na^+$) required *m/z* 509.2991; found *m/z* 509.2985.

FT-IR (neat) ν_{max}: 3314, 2957, 2921, 2851, 1739, 1702, 1645, 1630, 1614, 1540, 1234, 1216, 1009, 774 cm^{-1}.

$[a]_D^{20}$ = −67.1° (c = 0.07, $CHCl_3$).

TLC: R_f (10% MeOH in $CHCl_3$) = 0.30, $KMnO_4$ stain.

2.6.2. Synthesis of αF-FR

2.6.2.1. Ethyl (2*Z*,4*E*)-2-fluorododeca-2,4-dienoate (2.S35)

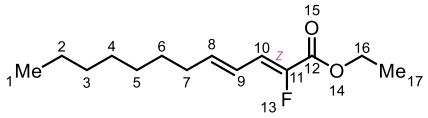

2.S35
Chemical Formula: $C_{14}H_{23}FO_2$

To a solution of triethyl 2-fluoro-2-phosphonoacetate (11.8 g, 44.0 mmol, 1.10 eq.) in THF (0.2 M) at 20°C was added Et_3N (11.2 mL, 80.0 mmol, 2.00 eq.), followed by $MgBr_2$ (7.36 g, 40.0 mmol, 1.00 eq.) and the resulting mixture was stirred for 10 min. Afterwards, *trans*-2-decenal (7.34 mL, 40.0 mmol, 1.00 eq.) was added and the reaction was heated to reflux for 12 h. Upon full consumption of the starting material (as indicated by ^{19}F-NMR analysis), the reaction was allowed to cool to room temperature before being diluted with Et_2O and the resulting suspension was filtered over a short pad of Celite®. The filtrate was washed with a sat. aq. solution of NH_4Cl (100 mL) and the aqueous layer was extracted with Et_2O (2 x 100 mL). The combined organic layers were washed with brine (1 x 100 mL), dried over Na_2SO_4, the solids were filtered off and the solvents were removed *in vacuo* to yield the crude material with a *Z*/*E* ratio of 3:1, which was used in the next step without further purification.

^{1}H-NMR (400 MHz, $CHCl_3$): δ 6.98-6.89 (m, 1H, *E* isomer), 6.58 (dd, *J* = 31.6, 11.3 Hz, 1H, *E* isomer), 6.45-6.31 (m, 1H, *E* + *Z* isomer), 6.14-5.96 (m, 1H, *E* + *Z* isomer), 4.30 (app dq, *J* = 14.3, 7.1 Hz, 2H, *E* + *Z* isomer), 2.18 (q, *J* = 7.1 Hz, 2H, *E* + *Z* isomer), 1.47-1.39 (m, 2H, *E* + *Z* isomer), 1.33-1.24 (m, 10H, *E* + *Z* isomer), 0.88 (t, *J* = 6.8 Hz, 3H, *E* + *Z* isomer) ppm.

^{19}F-NMR (376 MHz, $CHCl_3$): δ −126.9 (d, *J* = 20.1 Hz, *E* isomer), −131.2 (d, *J* = 31.7 Hz, *Z* isomer) ppm.

TLC: R_f (20% EtOAc in heptane) = 0.80 (*Z* isomer), $KMnO_4$ stain;

R_f (20% EtOAc in heptane) = 0.75 (*E* isomer), $KMnO_4$ stain.

2.6.2.2. (2*Z*,4*E*)-2-fluorododeca-2,4-dien-1-ol (2.118)

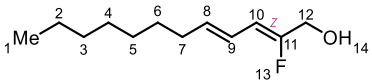

2.118

Chemical Formula: $C_{12}H_{21}FO$

(2*Z*,4*E*)-2-fluorododeca-2,4-dien-1-ol (**2.118**) was synthesised according to the general procedure outlined in chapter 2.5.2.2. on 40.0 mmol scale to yield **2.118** (4.44 g, 22.2 mmol, 56% over two steps) as a colourless oil.

^{1}H-NMR (600 MHz, $CHCl_3$): δ 6.26 (dd, *J* = 15.4, 10.8 Hz, 1H, **H_9**), 5.76-5.68 (m, 1H, **H_8**), 5.48 (dd, *J* = 35.3, 10.8 Hz, 1H, **H_{10}**), 4.15 (dd, *J* = 15.8, 6.4 Hz, 2H, **H_{12}**), 2.10 (q, *J* = 7.2 Hz, 2H, **H_7**), 1.63 (t, *J* = 6.4 Hz, 1H, **H_{OH14}**), 1.38 (m, 2H, **H_6**), 1.28 (dd, *J* = 7.5, 3.1 Hz, 8H, **$H_{2\text{-}5}$**), 0.88 (t, *J* = 6.9 Hz, 3H, **H_1**) ppm.

^{13}C-NMR (150 MHz, $CHCl_3$): δ 156.2 (d, J_{CF} = 261 Hz, **C_{11}**), 136.0 (d, J_{CF} = 3.2 Hz, **C_8**), 120.9 (d, J_{CF} = 4.6 Hz, **C_9**), 108.9 (d, J_{CF} = 10.7 Hz, **C_{10}**), 61.5 (d, J_{CF} = 31.1 Hz, **C_{12}**), 33.0 (**C_7**), 32.0 (**C_6**), 29.3 (3C, **$C_{3\text{-}5}$**), 22.8 (**C_2**), 14.2 (**C_1**) ppm.

^{19}F-NMR (565 MHz, $CHCl_3$): δ −118.95 (dt, *J* = 32.4, 15.9 Hz, **F_{13}**) ppm.

TLC: R_f (20% EtOAc in heptane) = 0.30 (*Z* isomer), $KMnO_4$ stain;

R_f (20% EtOAc in heptane) = 0.25 (*E* isomer), $KMnO_4$ stain.

2.6.2.3. (2*Z*,4*E*)-2-fluorododeca-2,4-dienal (2.119)

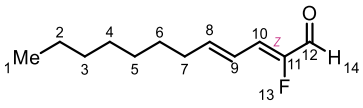

2.119

Chemical Formula: $C_{12}H_{19}FO$

(2*Z*,4*E*)-2-fluorododeca-2,4-dienal (**2.119**) was synthesised according to the general procedure outlined in chapter 2.5.2.3. on 3.98 mmol scale to yield **2.119** (642 mg, 3.24 mmol, 81%) as a colourless oil and was used in the next step without further purification.

^{1}H-NMR (400 MHz, $CHCl_3$): δ 9.21 (dd, *J* = 18.4 Hz, 1H, **H_{14}**), 6.51 (ddt, *J* = 13.6, 10.8, 1.2 Hz, 1H, **H_9**), 6.35 (dd, *J* = 30.1, 10.5 Hz, 1H, **H_{10}**), 6.32-6.24 (m, 1H, **H_8**), 2.24 (q, *J* = 7.2 Hz, 2H, **H_7**), 1.52-1.41 (m, 2H, **H_6**), 1.35-1.22 (m, 8H, **$H_{2\text{-}5}$**), 0.88 (t, *J* = 6.9 Hz, 3H, **H_1**) ppm.

^{19}F-NMR (376MHz, $CHCl_3$): δ −134.01 (dd, *J* = 30.6, 18.3 Hz, **F_{13}**) ppm.

TLC: R_f (20% EtOAc in heptane) = 0.63, $KMnO_4$ stain.

2.6.2.4. (*R*,4*Z*,6*E*)-1-((*S*)-4-benzyl-2-thioxothiazolidin-3-yl)-4-fluoro-3-hydroxytetradeca-4,6-dien-1-one (2.127)

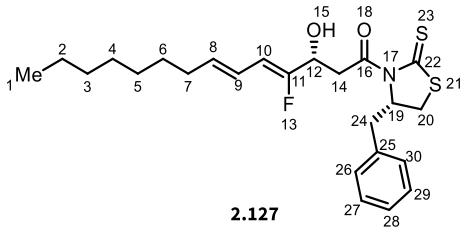

2.127

Chemical Formula: $C_{24}H_{32}FNO_2S_2$

(*R*,4*Z*,6*E*)-1-((*S*)-4-benzyl-2-thioxothiazolidin-3-yl)-4-fluoro-3-hydroxytetradeca-4,6-dien-1-one (**2.127**) was synthesised according to the general procedure outlined in chapter 2.5.2.5. on 3.15 mmol scale to yield **2.127** (942 mg, 2.09 mmol, 66%) as a yellow oil (overall: d.r. 5.3:1, 78%).

^{1}H-NMR (600MHz, $CDCl_3$): δ 7.36-7.34 (m, 2H, **H_{26+30}**), 7.29-7.26 (m, 3H, **$H_{27\text{-}29}$**), 6.26 (ddt, *J* = 15.2, 10.9, 1.3 Hz, 1H, **H_9**), 5.77–5.72 (m, 1H, **H_{10}**), 5.59 (dd, *J* = 36.2, 10.8 Hz, 1H, **H_8**), 5.39 (ddd, *J* = 10.7, 7.0, 4.1 Hz, 1H, **H_{19}**), 4.76-4.71 (m, 1H, **H_{15OH}**), 3.72 (dd, *J* = 17.7, 2.8 Hz, 1H, **H_{14}**), 3.51 (dd, *J* = 17.7, 9.0 Hz, 1H, **H_{14}**), 3.42 (ddd, *J* = 11.5, 7.2, 0.7 Hz, 1H, **H_{20}**), 3.23 (dd, *J* = 13.2, 3.9 Hz, 1H, **H_{24}**), 3.05 (dd, *J* = 13.2, 10.5 Hz, 1H, **H_{24}**), 2.93 (d, *J* = 1.6 Hz, 1H, **H_{12}**), 2.91 (d, *J* = 8.1 Hz, 1H, **H_{20}**), 2.10 (q, *J* = 7.1 Hz, 2H, **H_7**), 1.42-1.36 (m, 2H, **H_6**), 1.31-1.25 (m, 8H, **$H_{2\text{-}5}$**), 0.88 (t, *J* = 7.0 Hz, 3H, **H_1**) ppm.

^{13}C-NMR (151MHz, $CDCl_3$): δ 201.4 (**C_{22}**), 172.1 (**C_{16}**), 156.7 (d, *J* = 261.7 Hz, **C_{11}**), 136.5 (**C_{25}**), 136.2 (d, *J* = 3.0 Hz, **C_8**), 129.6 (2C, **$C_{27\&29}$**), 129.1 (2C, **$C_{26\&30}$**), 127.5 (**C_{28}**), 120.7 (d, *J* = 5.0 Hz, **C_9**), 107.7 (d, *J* = 9.7 Hz, **C_{10}**), 68.5 (**C_{19}**), 66.7 (d, *J* = 31.2 Hz, **C_{12}**), 43.1 (**C_{14}**), 37.0 (**C_{24}**), 33.0 (**C_7**), 32.3 (**C_{20}**), 32.0 (**C_2**), 29.3 (3C, **$C_{4\text{-}6}$**), 22.8 (**C_3**), 14.2 (**C_1**) ppm.

^{19}F-NMR (576MHz, $CDCl_3$): δ −121.89 (dd, *J* = 36.3, 11.7 Hz, **F_{13}**) ppm.

HRMS (ESI+): exact mass calculated for $[M+Na]^+$ ($C_{24}H_{32}NO_2FS_2Na^+$) required *m/z* 472.1756, found *m/z* 472.1725.

FT-IR (neat) ν_{max}: 2954, 2923, 2853, 1686, 1496, 1454, 1437, 1357, 1341, 1318, 1291, 1261, 1192, 1165, 1136, 1087, 1045, 969, 914, 890, 854, 744, 701, 683, 658, 641, 591, 554, 504, 480 cm^{-1}.

$[\alpha]_D^{20}$ = +115 (c = 1.00, $CDCl_3$).

TLC: R_f (20% EtOAc in heptane) = 0.26, $KMnO_4$ stain.

2.6.2.5. (*R*,4*Z*,6*E*)-*N*-((2*R*,3*S*)-2-((*tert*-butyldimethylsilyl)oxy)-3-methyl-4-oxo-4-(((*E*)-4-(4,4,5,5-tetramethyl-1,3,2-dioxaborolan-2-yl)but-3-en-1-yl)amino)butyl)-4-fluoro-3-hydroxytetradeca-4,6-dienamide (2.S36)

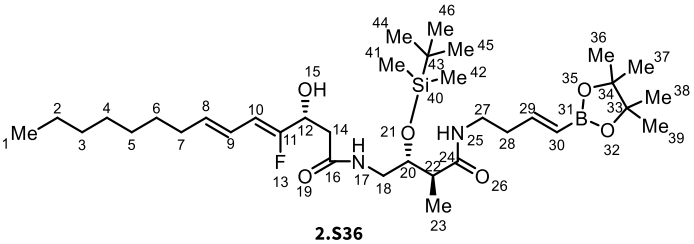

2.S36
Chemical Formula: $C_{35}H_{64}BFN_2O_6Si$

(*R*,4*Z*,6*E*)-*N*-((2*R*,3*S*)-2-((*tert*-butyldimethylsilyl)oxy)-3-methyl-4-oxo-4-(((*E*)-4-(4,4,5,5-tetramethyl-1,3,2-dioxaborolan-2-yl)but-3-en-1-yl)amino)butyl)-4-fluoro-3-hydroxytetradeca-4,6-dienamide (**2.S36**) was synthesised according to the general procedure outlined in chapter 2.5.2.15. on 0.700 mmol scale to yield **2.S36** (179 mg, 0.268 mmol, 38%) as a yellow foam.

^{1}H-NMR (600MHz, $CDCl_3$): δ 6.55 (dt, *J* = 18.0, 6.5 Hz, 1H, **H_{30}**), 6.46 (m, 1H, **H_{NH17}**), 6.22 (dd, *J* = 15.4, 10.9 Hz, 1H, **H_9**), 6.14 (t, *J* = 5.5 Hz, 1H, **H_{NH25}**), 5.73-5.68 (m, 1H, **H_8**), 5.58 (dd, *J* = 36.6, 10.9 Hz, 1H, **H_{10}**), 5.52 (d, *J* = 18.0 Hz, 1H, **H_{29}**), 4.55 (t, *J* = 9.4 Hz, 1H, **H_{12}**), 4.33 (d, *J* = 3.7 Hz, 1H, **H_{15}**), 3.89-3.85 (m, 1H, **H_{20}**), 3.68 (ddd, *J* = 13.6, 7.4, 4.3 Hz, 1H, **H_{18}**), 3.45 (td, *J* = 13.3, 6.6 Hz, 1H, **H_{28}**), 3.27 (td, *J* = 12.3, 6.4 Hz, 1H, **H_{28}**), 2.96 (ddd, *J* = 12.6, 7.6, 4.6 Hz, 1H, **H_{18}**), 2.59 (dd, *J* = 15.2, 3.3 Hz, 1H, **H_{14}**), 2.49 (dd, *J* = 15.2, 8.5 Hz, 1H, **H_{14}**), 2.41 (ddd, *J* = 14.4, 7.2, 4.9 Hz, 1H, **H_{22}**), 2.36 (dd, *J* = 13.2, 6.6 Hz, 2H, **H_{27}**), 2.08 (dd, *J* = 14.2, 7.0 Hz, 2H, **H_7**), 1.38-1.34 (m, 2H, **H_6**), 1.29-1.25 (m, 20H, **$H_{2\text{-}5\&36\text{-}39}$**), 1.14-1.12 (m, 3H, **H_{23}**), 0.92-0.86 (m, 12H, **$H_{1\&44\text{-}46}$**), 0.14-0.09 (m, 6H, **$H_{41\&42}$**) ppm.

^{13}C-NMR (151MHz, $CDCl_3$): δ 174.6 (**C_{24}**), 171.5 (**C_{16}**), 157.1 (d, *J* = 261.5 Hz, **C_{11}**), 150.4 (**C_{30}**), 135.8 (d, *J* = 2.8 Hz, **C_8**), 120.75 (d, *J* = 5.0 Hz, **C_9**), 120.72 (**C_{29}**, deducted from HSQC), 107.3 (d, *J* = 9.4 Hz, **C_{10}**), 83.4 (2C, **C_{33+34}**), 72.1 (**C_{20}**), 67.3 (d, *J* = 31.8 Hz, **C_{12}**), 44.8 (**C_{22}**), 42.9 (**C_{18}**), 39.7 (**C_{14}**), 37.9 (**C_{28}**), 35.8 (**C_{27}**), 33.0 (**C_7**), 32.0 (2C, **$C_{3\text{-}5}$**), 29.32 (**C_{pin}**), 29.29 (**C_{pin}**), 26.00 (3C, **$C_{44\text{-}46}$**), 25.01 (**C_{pin}**), 24.92 (2C, **$C_{3\text{-}5}$**), 24.91 (**C_{pin}**), 22.8 (**C_2**), 18.1 (**C_{43}**), 15.3 (**C_{23}**), 14.2 (**C_1**), -4.4 (**C_{41}**), -4.8 (**C_{42}**) ppm.

^{19}F-NMR (576MHz, $CDCl_3$): δ −122.73 (ddd, *J* = 73.8, 36.5, 11.0 Hz) ppm.

HRMS (ESI+): exact mass calculated for $[M+Na]^+$ ($C_{35}H_{64}N_2O_6BFSiNa^+$) required *m/z* 689.4503, found *m/z* 689.4494.

FT-IR (neat) ν_{max}: 3307, 2975, 2954, 2927, 2856, 1640, 1540, 1463, 1397, 1388, 1359, 1321, 1254, 1183, 1143, 1099, 1026, 1003, 970, 952, 847, 836, 812, 778, 750, 721, 680, 667, 648, 577 cm^{-1}.

$[\alpha]_D^{20}$ = +215 (c = 1.00, $CHCl_3$).

2.6.3. Synthesis of αCF$_3$-FR

2.6.3.1. ethyl (2*Z*,4*E*)-2-(trifluoromethyl)dodeca-2,4-dienoate (2.122)

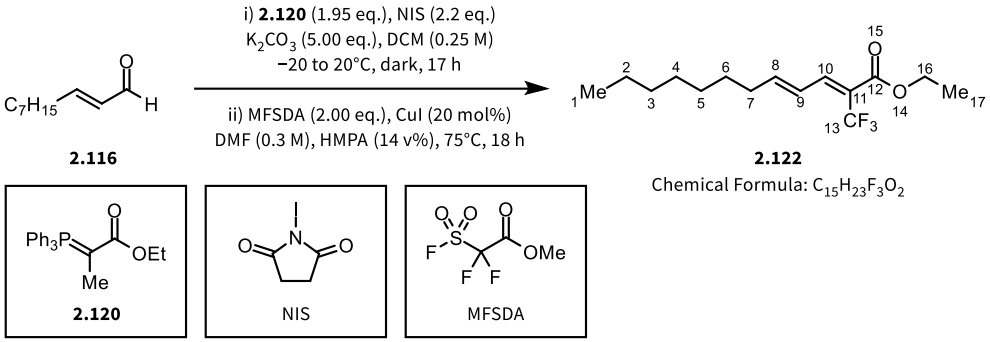

All reaction steps and work-up procedures were carried out in the dark. To a solution of ethyl (triphenylphosporanylidene)acetate (**2.120**) (16.3 g, 46.8 mmol, 1.95 eq.) in DCM (0.25 M) at −20°C was added NIS (11.9 g, 52.8 mmol, 2.20 eq.) and the resulting reaction mixture was stirred at −20°C for 20 min. Afterwards, K_2CO_3 (16.6 g, 120 mmol, 5.00 eq.) was added followed by *trans*-2-decenal (**2.116**) (4.40 mL, 24.0 mmol, 1.00 eq.). The resulting reaction mixture was allowed to warm to room temperature and stirring was continued for 17 h. After the reaction time had elapsed, the reaction mixture was filtered through a short pad of Celite® and the filter cake was washed with copious amounts of DCM. The filtrate was concentrated and the crude material was purified by flash column chromatography (SiO_2, heptane/EtOAc) to afford a mixture of *trans*-2-decenal and C11-I-**2.122** which was used in the next step without further purification.

C11-I-**2.122** (5.25 g, 15.0 mmol, 1.00 eq.) was dissolved in DMF (0.3 M) at room temperature and HMPA (11.3 mL, 65.2 mmol, 4.35 eq., 14 v% relative to DMF) and CuI (574 mg, 3.00 mmol, 0.200 eq.) were added. The resulting reaction mixture was heated to 75°C before MFSDA (3.94 mL, 30.0 mmol, 2.00 eq.) was added. Stirring was continued at 75°C for 14 h, after which the reaction mixture was allowed to cool to 20°C. The reaction mixture was diluted with Et_2O (50.0 mL) and the layers were separated. The organic layer was washed with water (5 x 50.0 mL), EDTA solution (1 x 50.0 mL) and brine (1 x 50.0 mL), dried over Na_2SO_4, the solids were filtered off and the solvents were removed *in vacuo* to yield the crude product as

a mixture with *trans*-2-decenal. The crude product was purified by flash column chromatography (SiO_2, heptanes/DCM) to yield **2.122** (2.49 g, 8.52 mmol, 36%; 57% brsm) as a colourless oil.

^{1}H-NMR (700MHz, $CDCl_3$): δ 7.50 (d, *J* = 11.9 Hz, 1H, **H_{10}**), 6.68 (dddd, *J* = 15.1, 13.4, 3.2, 1.4 Hz, 1H, **H_9**), 6.44-6.39 (m, 1H, **H_8**), 4.28 (q, *J* = 7.1 Hz, 2H, **H_{16}**), 2.26 (q, *J* = 7.3 Hz, 2H, **H_7**), 1.49-1.43 (m, 2H, **H_6**), 1.34-1.24 (m, 11H, **$H_{2\text{-}5,17}$**), 0.88 (t, *J* = 7.1 Hz, 3H, **H_1**) ppm.

^{13}C-NMR (176MHz, $CDCl_3$): δ 163.75 (d, *J* = 4.0, 2.0 Hz, **C_{12}**), 153.61 (app. d, *J* = 1.4 Hz, **C_8**), 147.78 (dd, *J* = 3.9, 1.9 Hz, **C_{10}**), 124.61 (q, *J* = 3.8 Hz, **C_9**), 123.05 (q, *J* = 273.6 Hz, **C_{13}**), 117.53 (q, *J* = 31.4 Hz,**C_{11}**), 61.62 (**C_{16}**), 33.64 (**C_7**), 31.88 (**$C_{2\text{-}5,}$**), 29.29 (**$C_{2\text{-}5}$**), 29.19 (**$C_{2\text{-}5}$**), 28.55 (**C_6**), 22.76 (**$C_{2\text{-}5}$**), 14.26 (**C_{17}**), 14.20 (**C_1**) ppm.

^{19}F-NMR (658MHz, $CDCl_3$): δ −58.09 (s, **F_{13}**) ppm.

HRMS (ESI+): exact mass calculated for $[M+Na]^+$ ($C_{15}H_{23}F_3O_2Na^+$) required *m/z* 315.1548, found *m/z* 315.1541.

TLC: **2.122** R_f (20% DCM in heptane) = 0.32, $KMnO_4$ stain;

trans-2-decenal R_f (20% DCM in heptane) = 0.23, $KMnO_4$ stain.

2.6.3.2. (2*Z*,4*E*)-2-(trifluoromethyl)dodeca-2,4-dien-1-ol (2.S37)

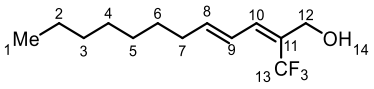

2.S37
Chemical Formula: $C_{13}H_{21}F_3O$

(2*Z*,4*E*)-2-(trifluoromethyl)dodeca-2,4-dien-1-ol (**2.S37**) was synthesised according to the general procedure outlined in chapter 2.5.2.2. on 5.00 mmol scale and was used in the next step without further purification.

2.6.3.3. (2*Z*,4*E*)-2-(trifluoromethyl)dodeca-2,4-dienal (2.123)

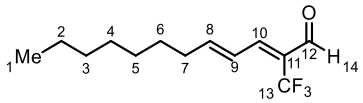

2.123
Chemical Formula: $C_{13}H_{19}F_3O$

(2*Z*,4*E*)-2-(trifluoromethyl)dodeca-2,4-dienal (**2.123**) was synthesised according to the general procedure outlined in chapter 2.5.2.3. on 5.00 mmol scale to yield **2.123** (233 mg, 0.938 mmol, 19%) as a colourless oil.

^{1}H-NMR (400MHz, $CDCl_3$): δ 9.52 (q, *J* = 1.7 Hz, 1H, **H_{14}**), 7.26 (d, *J* = 11.7 Hz, 1H, **H_{10}**), 6.74 (dddd, *J* = 13.1, 11.6, 2.7, 1.4 Hz, 1H, **H_9**), 6.63-6.54 (m, 1H, **H_8**), 2.32 (q, *J* = 7.2 Hz, 2H, **H_7**), 1.55-1.40 (m, 2H, **H_6**), 1.37-1.22 (m, 8H, **$H_{2\text{-}5}$**), 0.92-0.81 (m, 3H, **H_1**) ppm.

^{19}F-NMR (376MHz, $CDCl_3$): δ −59.55 (s, **F_{13}**) ppm.

2.6.3.4. (*R*,4*Z*,6*E*)-1-((*S*)-4-benzyl-2-thioxothiazolidin-3-yl)-3-hydroxy-4-(trifluoromethyl)tetradeca-4,6-dien-1-one (2.128)

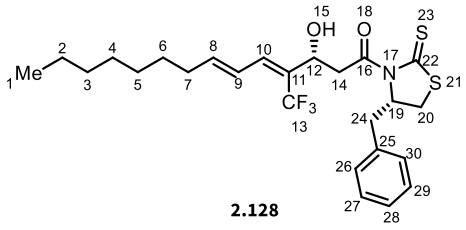

2.128
Chemical Formula: $C_{25}H_{32}F_3NO_2S_2$

(*R*,4*Z*,6*E*)-1-((*S*)-4-benzyl-2-thioxothiazolidin-3-yl)-3-hydroxy-4-(trifluoromethyl)tetradeca-4,6-dien-1-one (**2.128**) was synthesised according to the general procedure outlined in chapter 2.5.2.5. on 0.920 mmol scale to yield **2.128** (247 mg, 0.494 mmol, 54%) as a yellow oil (overall: d.r. 2:1, 81%).

^{1}H-NMR (400MHz, $CDCl_3$): δ 7.39-7.26 (m, 5H, **$H_{26\text{-}30}$**), 6.64 (d, *J* = 11.5 Hz, 1H, **H_{10}**), 6.53-6.42 (m, 1H, **H_9**), 6.04 (dt, *J* = 14.5, 7.1 Hz, 1H, **H_8**), 5.43-5.36 (m, 1H, **H_{19}**), 4.92 (d, *J* = 9.2 Hz, 1H, **H_{12}**), 2.73 (dd, *J* = 17.9, 2.2 Hz, 1H, **H_{14}**), 3.45-2.85 (m, 6H, **$H_{14,15,20,24}$**), 2.17 (q, *J* = 7.2 Hz, 2H, **H_7**), 1.46-1.36 (m, 2H, **H_6**), 1.33-1.22 (m, 8H, **$H_{2\text{-}5}$**), 0.90-0.84 (m, 3H, **H_1**) ppm.

^{19}F-NMR (376MHz, $CDCl_3$): δ −58.16 (s, **F_{13}**) ppm.

HRMS (ESI+): exact mass calculated for $[M+Na]^+$ ($C_{25}H_{32}F_3NO_2S_2Na^+$) required *m/z* 522.1724, found *m/z* 522.1716.

TLC: R_f (20% EtOAc in heptane) = 0.21, $KMnO_4$ stain (desired);

R_f (20% EtOAc in heptane) = 0.26, $KMnO_4$ stain (undesired).

2.6.3.5. (*R*,4*Z*,6*E*)-*N*-((2*R*,3*S*)-2-((*tert*-butyldimethylsilyl)oxy)-3-methyl-4-oxo-4-(((*E*)-4-(4,4,5,5-tetramethyl-1,3,2-dioxaborolan-2-yl)but-3-en-1-yl)amino)butyl)-3-hydroxy-4-(trifluoromethyl)tetradeca-4,6-dienamide (2.S38)

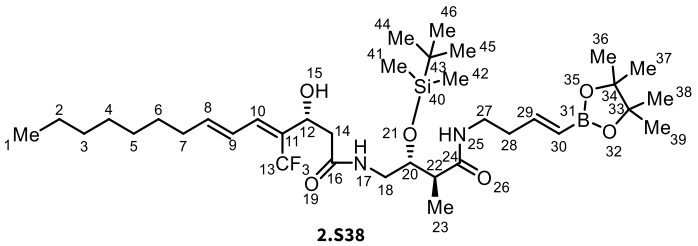

2.S38

Chemical Formula: $C_{36}H_{64}BF_3N_2O_6Si$

(*R*,4*Z*,6*E*)-*N*-((2*R*,3*S*)-2-((*tert*-butyldimethylsilyl)oxy)-3-methyl-4-oxo-4-(((*E*)-4-(4,4,5,5-tetramethyl-1,3,2-dioxaborolan-2-yl)but-3-en-1-yl)amino)butyl)-3-hydroxy-4-(trifluoromethyl)tetradeca-4,6-dienamide (**2.S38**) was synthesised according to the general procedure outlined in chapter 2.5.2.15. on 0.494 mmol scale to yield **2.S38** (217 mg, 0.303 mmol, 61%) as a yellow foam.

^{1}H-NMR (600MHz, $CDCl_3$): δ 6.67 (d, *J* = 116. Hz, 1H, **H_{10}**), 6.55 (dt, *J* = 17.9, 6.5 Hz, 1H, **H_{29}**), 6.44 (app. t, *J* = 12.6 Hz, 1H, **H_9**), 6.29 (br. s. 1H, **H_{NH17}**), 6.08 (t, *J* = 5.4 Hz, 1H, **H_{NH25}**), 6.06-5.97 (m, 1H, **H_8**), 5.52 (d, *J* = 18.0 Hz, 1H, **H_{30}**), 4.73 (d, *J* = 8.9 Hz, 1H, **H_{20}**), 3.91-3.87 (m, 1H, **H_{14}**), 3.71-3.65 (m, 1H, **H_{15}**), 3.48-3.36 (m, 2H, **$H_{18,29}$**), 3.31-3.24 (m, 1H, **H_{29}**), 3.00-2.94 (m 1H, **H_{14}**), 2.56 (dd, *J* = 15.4, 2.5 Hz, 1H, **H_{28}**), 2.42-2.32 (m, 4H, **$H_{18,22,28}$**), 2.16 (q, *J* = 7.1 Hz, 2H, **H_7**), 1.43-1.35 (m, 2H, **H_6**), 1.33-1.22 (m, 20H, **$H_{2\text{-}5,36\text{-}39}$**), 1.14 (t, *J* = 7.2 Hz, 3H, **H_{23}**), 0.92-0.83 (m, 12H, **$H_{1,44\text{-}46}$**), 0.17-0.02 (m, 6H, **$H_{41,42}$**) ppm.

^{13}C-NMR (151MHz, $CDCl_3$): δ 174.4 (**C_{24}**), 171.8 (**C_{16}**), 150.3 (**C_{29}**), 144.6 (**C_8**), 135.6 (d, *J* = 3.3 Hz, **C_{10}**), 126.8 (q, *J* = 27.9 Hz, **C_{11}**), 124.5 (**C_9**), 124.3 (q, *J* = 275.4 Hz, **C_{13}**), 121.6 (**C_{30}**, *deduced from HSQC*), 83.4 (2C, **$C_{33,34}$**), 72.0 (**C_{20}**), 68.3, 66.8 (q, *J* = 3.0 Hz, **C_{12}**), 42.9 (**C_{14}**), 42.3 (**C_{28}**), 38.0 (**C_{29}**), 35.7 (**C_{22}**), 33.1 (**C_7**), 31.9 (**$C_{2\text{-}5}$**), 29.3 (**$C_{2\text{-}5}$**),

29.2 (**C$_{2\text{-}5}$**), 29.0 (**C$_6$**), 26.0 (**C$_{2\text{-}5}$**), 25.0 (3C, **C$_{44\text{-}46}$**), 24.92 (2C, **C$_{36\text{-}39}$**), 24.91 (2C, **C$_{36\text{-}39}$**), 22.8 (**C$_{43}$**), 15.2 (**C$_{23}$**), 14.2 (**C$_1$**), −4.38 (**C$_{41}$**), −4.81 (**C$_{42}$**) ppm.

^{19}F-NMR (565MHz, $CDCl_3$): δ −57.97 (s, **F$_{13}$**) ppm.

HRMS (ESI+): exact mass calculated for $[M+Na]^+$ ($C_{36}H_{64}BF_3N_2O_6SiNa^+$) required *m/z* 739.4477, found *m/z* 739.4455.

TLC: R_f (30% *i*PrOH in heptane) = 0.80, $KMnO_4$ stain.

2.6.4. Synthesis of sc-FR

2.6.4.1. Ethyl (2*E*,4*E*)-2-methylhexa-2,4-dienoate (2.S39)

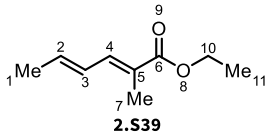

2.S39

Chemical Formula: $C_9H_{14}O_2$

Ethyl (2*E*,4*E*)-2-methylhexa-2,4-dienoate (**2.S39**) was synthesised according to the general procedure outlined in chapter 2.5.2.1. on 18.2 mmol scale to yield **2.S39** (2.25 g, 14.6 mmol, 81%) as a colourless oil.

^{1}H-NMR (600MHz, $CDCl_3$): δ 7.15 (d, *J* = 11.3 Hz, 1H, **H_4**), 6.36 (ddq, *J* = 14.6, 11.3 ,1.6 Hz, 1H, **H_3**). 6.12-6.06 (m, 1H, **H_2**), 4.20 (q, *J* = 7.1 Hz, 2H, **H_{10}**), 1.92 (s, 3H, **H_7**), 1.87 (d, *J* = 6.8 Hz, 3H, **H_1**), 1.30 (t, *J* = 7.1 Hz, 3H, **H_{11}**) ppm.

^{13}C-NMR (151MHz, $CDCl_3$): δ 168.9 (**C_6**), 138.6 (**C_4**), 137.7 (**C_2**), 127.6 (**C_3**), 125.1 (**C_5**), 60.6 (**C_{10}**), 19.0 (**C_1**), 14.5 (**C_{11}**), 12.7 (**C_7**) ppm.

HRMS (ESI+): exact mass calculated for $[M+Na]^+$ ($C_9H_{14}O_2Na^+$) required *m/z* 177.0892, found *m/z* 177.0894.

FT-IR (neat) ν_{max}: 2983, 2957, 2927, 2853, 1740, 1702, 1642, 1444, 1390, 1367, 1290, 1230, 1167, 1101, 968, 745, 732 cm^{-1}.

TLC: R_f (20% EtOAc in heptane) = 0.68, $KMnO_4$ stain.

2.6.4.2. (2*E*,4*E*)-2-methylhexa-2,4-dien-1-ol (2.S40)

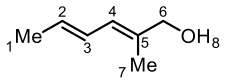

2.S40

Chemical Formula: C_9H_{18}

(2*E*,4*E*)-2-methylhexa-2,4-dien-1-ol (**2.S40**) was synthesised according to the general procedure outlined in chapter 2.5.2.2. on 20.0 mmol scale to yield **2.S40** (2.21 g, 19.7 mmol, 99%) as a colourless oil.

All spectroscopic data are in accordance with the reported literature.[312]

2.6.4.3. (2*E*,4*E*)-2-methylhexa-2,4-dienal (2.131)

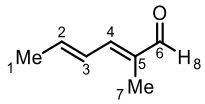

2.131

Chemical Formula: $C_7H_{10}O$

(2*E*,4*E*)-2-methylhexa-2,4-dienal (**2.131**) was synthesised according to the general procedure outlined in chapter 2.5.2.3. on 10.0 mmol scale to yield **2.131** (841 mg, 7.63 mmol, 76%) as a colourless oil.

All spectroscopic data are in accordance with the reported literature.[313]

2.6.4.4. (*R*,4*E*,6*E*)-1-((*S*)-4-benzyl-2-thioxothiazolidin-3-yl)-3-hydroxy-4-methylocta-4,6-dien-1-one (2.132)

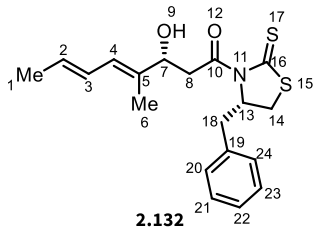

2.132

Chemical Formula: $C_{19}H_{23}NO_2S_2$

(*R*,4*E*,6*E*)-1-((*S*)-4-benzyl-2-thioxothiazolidin-3-yl)-3-hydroxy-4-methylocta-4,6-dien-1-one (**2.132**) was synthesised according to the general procedure outlined in chapter 2.5.2.5. on 10.0 mmol scale to yield **2.132** (841 mg, 7.63 mmol, 76%) as a yellow oil.

^{1}H-NMR (600MHz, $CDCl_3$): δ 7.37-7.34 (m, 2H, **$H_{20\&24}$**), 7.30-7.27 (d, *J* = 7.3 Hz, 3H, **$H_{21\text{-}23}$**), 6.27 (ddd, *J* = 14.9, 10.9, 1.6 Hz, 1H, **H_3**), 6.10 (d, *J* = 11.0 Hz, 1H, **H_4**), 5.74 (dq, *J* = 13.4, 6.6 Hz, 1H, **H_2**), 5.38 (ddd, *J* = 10.8, 7.1, 4.0 Hz, 1H, **H_{13}**), 4.63 (d, *J* = 9.6 Hz, 1H, **H_7**), 3.56 (dd, *J* = 17.4, 2.6 Hz, 1H, **H_8**), 3.44-3.39 (m, 2H, **H** ppm.

^{13}C-NMR (151MHz, $CDCl_3$): δ 201.5 (**C_{16}**), 173.0 (**C_{10}**), 136.6 (**C_{19}**), 135.0 (**C_5**), 130.5 (**C_2**), 129.6 (**$C_{21\&23}$**), 129.1 (**$C_{20\&24}$**), 127.4 (**C_{22}**), 127.3 (**C_3**), 125.8 (**C_4**), 72.9 (**C_7**), 68.6 (**C_{13}**), 44.5 (**C_8**), 37.0 (**C_{18}**), 32.3 (**C_{14}**), 18.6 (**C_1**), 13.0 (**C_6**) ppm.

HRMS (ESI+): exact mass calculated for $[M+Na]^+$ ($C_{19}H_{23}NO_2S_2Na^+$) required *m/z* 384.1062, found *m/z* 384.1061.

FT-IR (neat) ν_{max}: 3510, 3474, 3025, 2924, 2852, 1693, 1495, 1453, 1437, 1342, 1318, 1292, 1257, 1227, 1191, 1163, 1136, 1092, 1043, 964, 894, 748, 723, 702, 620, 565, 555, 510, 482, 466 cm^{-1}.

[a]$_D^{20}$ = +59.2° (c = 1.00, $CHCl_3$).

2.6.4.5. (*R*,4*E*,6*E*)-*N*-((2*R*,3*S*)-2-((*tert*-butyldimethylsilyl)oxy)-3-methyl-4-oxo-4-(((*E*)-4-(4,4,5,5-tetramethyl-1,3,2-dioxaborolan-2-yl)but-3-en-1-yl)amino)butyl)-3-hydroxy-4-methylocta-4,6-dienamide (2.S41)

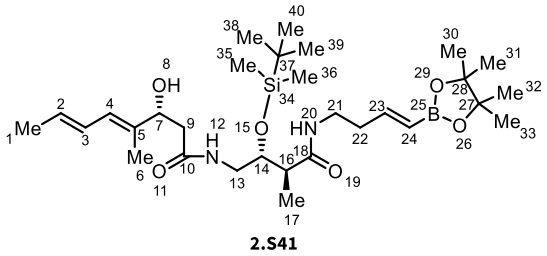

2.S41

Chemical Formula: $C_{30}H_{55}BN_2O_6Si$

(*R*,4*E*,6*E*)-*N*-((2*R*,3*S*)-2-((*tert*-butyldimethylsilyl)oxy)-3-methyl-4-oxo-4-(((*E*)-4-(4,4,5,5-tetramethyl-1,3,2-dioxaborolan-2-yl)but-3-en-1-yl)amino)butyl)-3-hydroxy-4-methylocta-4,6-dienamide (**2.S41**) was synthesised according to the general procedure outlined in chapter 2.5.2.15. on 1.82 mmol scale to yield **2.S41** (557 mg, 0.963 mmol, 53%) as a colourless foam.

^{1}H-NMR (600MHz, $CDCl_3$): δ 6.55 (dt, *J* = 17.9, 6.6 Hz, 1H, **H_{24}**), 6.42-6.40 (m, 1H, **H_{NH12}**), 6.25 (ddd, *J* = 14.9, 10.9, 1.5 Hz, 1H, **H_3**), 6.12 (t, *J* = 5.4 Hz, 1H, **H_{NH20}**), 6.07 (d, *J* = 10.8 Hz, 1H, **H_4**), 5.71 (dq, *J* = 13.6, 6.7 Hz, 1H, **H_2**), 5.52 (d, *J* = 18.0 Hz, 1H, **H_{23}**), 4.43 (d, *J* = 8.8 Hz, 1H, **H_7**), 3.90-3.86 (m, 1H, **H_{14}**), 3.72 (ddd *J* = 13.7, 7.6, 4.2 Hz, 1H, **H_{13}**), 3.49 (d, *J* = 2.7 Hz, 1H, **H_8**), 3.44 (td, *J* = 13.4, 6.7 Hz, 1H, **H_{22}**), 3.27 (dt, *J* = 12.0, 6.5 Hz, 1H, **H_{22}**), 2.93 (ddd, *J* = 13.5, 7.5, 4.4 Hz, 1H, **H_{13}**), 2.47-2.32 (m, 5H, **$H_{9/16/21}$**), 1.78 (d, *J* = 6.6 Hz, 3H, **H_1**), 1.74 (s, 3H, **H_6**), 1.25 (s, 12H, **H_{30-33}**), 1.14-1.13 (d, *J* = 7.2 Hz, 3H, **H_{17}**), 0.90 (s, 9H, **H_{38-40}**), 0.15-0.07 (m, 6H, **$H_{35\&36}$**) ppm.

^{13}C-NMR (151MHz, $CDCl_3$): δ 174.4 (**C_{18}**), 172.1 (**C_{10}**), 150.3 (**C_{24}**), 135.2 (**C_5**), 130.1 (**C_2**), 127.1 (**C_3**), 125.4 (**C_4**), 121.6 (**C_{23}**, *deducted from HSQC*), 83.3 (2C, **$C_{27\&28}$**), 73.5 (**C_7**), 72.0 (**C_{14}**), 44.7 (**C_{16}**), 42.8 (**C_{13}**), 41.5 (**C_9**), 37.8 (**C_{22}**), 35.6 (**C_{21}**), 25.9 (3C, **C_{38-40}**), 25.0 (**C_{37}**), 24.9 (2C, **C_{30-33}**), 24.8 (2C, **C_{30-33}**), 18.4 (**C_1**), 15.2 (**C_{17}**), 12.6 (**C_6**), −4.54 (**C_{35}**), −5.00 (**C_{36}**) ppm.

HRMS (ESI+): exact mass calculated for $[M+Na]^+$ ($C_{30}H_{55}BN_2O_6SiNa^+$) required *m/z* 601.3820, found *m/z* 601.3829.

FT-IR (neat) ν_{max}: 3309, 2976, 2953, 2929, 2884, 2856, 1642, 1541, 1471, 1462, 1446, 1397, 1389, 1360, 1322, 1255, 1144, 1102, 1028, 1004, 967, 937, 884, 837, 812, 778, 679, 666, 641, 623 cm^{-1}.

$[a]_D^{20}$ = +30.1° (c = 1.00, $CHCl_3$).

TLC: R_f (30% *i*PrOH in heptane) = 0.85, $KMnO_4$ or PMA stain.

2.6.4.6. (*R*,4*E*,6*E*)-1-(((2*R*,3*S*)-2-((*tert*-butyldimethylsilyl)oxy)-3-methyl-4-oxo-4-(((*E*)-4-(4,4,5,5-tetramethyl-1,3,2-dioxaborolan-2-yl)but-3-en-1-yl)amino)butyl)amino)-4-methyl-1-oxoocta-4,6-dien-3-yl (1*R*,4*R*)-4-chlorocyclobut-2-ene-1-carboxylate (2.S42)

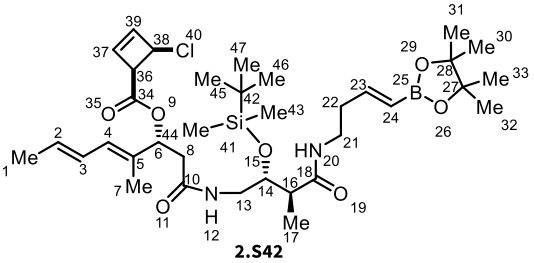

2.S42

Chemical Formula: $C_{35}H_{58}BClN_2O_7Si$

(*R*,4*E*,6*E*)-1-(((2*R*,3*S*)-2-((*tert*-butyldimethylsilyl)oxy)-3-methyl-4-oxo-4-(((*E*)-4-(4,4,5,5-tetramethyl-1,3,2-dioxaborolan-2-yl)but-3-en-1-yl)amino)butyl)amino)-4-methyl-1-oxoocta-4,6-dien-3-yl (1*R*,4*R*)-4-chlorocyclobut-2-ene-1-carboxylate (**2.S42**) was synthesised according to the general procedure outlined in chapter 2.5.2.17. on 0.200 mmol scale to yield **2.S42** (54.0 mg, 77.9 µmol, 39%) as a colourless foam.

^{1}H-NMR (600MHz, $CDCl_3$): δ 6.55 (dt, *J* = 18.0, 6.5 Hz, 1H, **H_{23}**), 6.29-6.24 (m, 2H, **$H_{37,39}$**), 6.22-6.17 (m, 2H, **$H_{3,NH12}$**), 6.19-6.15 (m, 1H, **H_{NH20}**), 6.12 (d, *J* = 11.0 Hz, 1H, **H_4**), 5.74 (dq, *J* = 13.3, 6.6 Hz, 1H, **H_2**), 5.63 (dd, *J* = 7.5, 5.9 Hz, 1H, **H_6**), 5.51 (dt, *J* = 17.9, 1.3 Hz, 1H, **H_{24}**), 5.08 (d, *J* = 4.3 Hz, 1H, **H_{36}**), 4.07 (dd, *J* = 4.3, 0.7 Hz, 1H, **H_{38}**), 3.82-3.79 (m, 1H, **H_{14}**), 3.79-3.74 (m, 1H, **H_{13}**), 3.42 (td, *J* = 13.3, 6.9 Hz, 1H, **H_{21}**), 3.27 (qd, *J* = 12.3, 6.7 Hz, 1H, **H_{21}**), 2.82-2.76 (m, 1H, **H_{13}**), 2.67 (dd, *J* = 14.4, 7.8 Hz, 1H, **H_8**), 2.50 (dd, *J* = 14.3, 5.7 Hz, 1H, **H_8**), 2.36 (m, 3H, **$H_{16,22}$**), 1.76 (d, *J* = 7.9 Hz, 6H, **$H_{1,7}$**), 1.25 (s, 12H, **H_{30-33}**), 1.10 (d, *J* = 7.2 Hz, 3H, **H_{17}**), 0.90 (s, 9H, **H_{45-47}**), 0.15 (s, 3H, **H_{43}**), 0.08 (s, 3H, **H_{44}**) ppm.

^{13}C-NMR (151MHz, $CDCl_3$): δ 174.7 (**C_{18}**), 169.3 (**C_{10}**), 168.8 (**C_{34}**), 150.3 (**C_{23}**), 140.6 (**C_{37}**), 136.6 (**C_{39}**), 131.5 (**C_2**), 130.7 (**C_5**), 128.9 (**C_4**), 127.0 (**C_3**), 121.4 (**C_{24}**, *deduced from HSQC*), 83.4 (2C, **$C_{27,28}$**), 77.0 (**C_6**), 72.1 (**C_{14}**), 56.4 (**C_{36}**), 54.0 (**C_{38}**), 44.5 (**C_{16}**), 43.0 (**C_{13}**), 40.9 (**C_8**), 38.0 (**C_{21}**), 35.8 (**C_{22}**), 26.0 (3C, **$C_{45\text{-}47}$**), 24.9 (4C, **$C_{30\text{-}33}$**), 18.6 (**C_1**), 18.1 (**C_{42}**), 15.5 (**C_{17}**), 12.7 (**C_7**), −4.3 (**C_{43}**), −4.9 (**C_{44}**) ppm.

HRMS (ESI+): exact mass calculated for $[M+Na]^+$ ($C_{35}H_{58}BClN_2O_7SiNa^+$) required *m/z* 715.3692, found *m/z* 715.3695.

FT-IR (neat) ν_{max}: 3345, 2930, 2857, 1733, 1642, 1536, 1470, 1358, 1322, 1288, 1257, 1234, 1168, 1141, 908, 727 cm^{-1}.

$[a]_D^{20}$ = +16.6° (c = 1.30, $CHCl_3$).

TLC: alcohol **2.S41**: R_f (60% EtOAc in heptanes) = 0.30; PMA stain;

trans$_1$-**2.S42**: R_f (60% EtOAc in heptanes) = 0.66; PMA stain;

trans$_2$-**2.S42**: R_f (60% EtOAc in heptanes) = 0.57; PMA stain;

cis$_1$-**2.S42**: R_f (60% EtOAc in heptanes) = 0.52; PMA stain;

cis$_2$-**2.S42**: R_f (60% EtOAc in heptanes) = 0.48; PMA stain.

2.6.4.7. (2*R*,7*R*,8*S*,13*E*,15*E*,17*E*)-7-((*tert*-butyldimethylsilyl)oxy)-2-((2*E*,4*E*)-hexa-2,4-dien-2-yl)-8-methyl-1-oxa-5,10-diazacyclononadeca-13,15,17-triene-4,9,19-trione (2.S43)

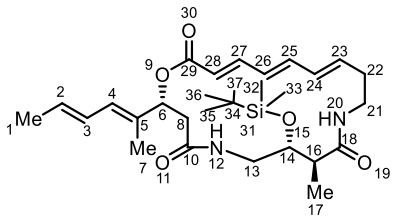

2.S43
Chemical Formula: $C_{29}H_{46}N_2O_5Si$

(2*R*,7*R*,8*S*,13*E*,15*E*,17*E*)-7-((*tert*-butyldimethylsilyl)oxy)-2-((2*E*,4*E*)-hexa-2,4-dien-2-yl)-8-methyl-1-oxa-5,10-diazacyclononadeca-13,15,17-triene-4,9,19-trione (**2.S43**) was synthesised according to the general procedure outlined in chapter 2.5.2.18. on 33.0 µmol scale to yield **2.S43** (10.6 mg, 20.0 µmol, 61%) as a colourless foam.

^{1}H-NMR (700MHz, $CDCl_3$): δ 7.25 (dd, *J* = 15.1, 10.9 Hz, 1H, **H_{27}**), 6.45 (dd, *J* = 14.9, 10.8 Hz, 1H, **H_{25}**), 6.25 (ddd, *J* = 15.0, 11.0, 1.5 Hz, 1H, **H_3**), 6.16 (dd, *J* = 14.9, 11.2 Hz, 1H, **H_{26}**), 6.12-6.07 (m, 2H, **$H_{4,24}$**), 6.02 (d, *J* = 10.1 Hz, 1H, **H_{NH12}**), 5.90 (ddd, *J* = 14.6, 10.9, 3.4 Hz, 1H, **H_{23}**), 5.86 (d, *J* = 5.4 Hz, 1H, **H_{NH20}**), 5.75 (dd, *J* = 15.0, 6.8 Hz, 1H, **H_2**), 5.71 (d, *J* = 15.4 Hz, 1H, **H_{28}**), 5.62 (dd, *J* = 11.2, 3.2 Hz, 1H, **H_6**), 4.13-4.07 (m, 2H, **$H_{13,14}$**), 4.00 (bs, 1H, **H_{13}**), 3.52-3.40 (m, 2H, **H_{21}**), 2.96 (m, 1H, **H_{22}**), 2.55-2.50 (m, 1H, **H_{22}**), 2.47 (ddd, *J* = 14.3, 7.2, 3.0 Hz, 1H, **H_8**), 2.45-2.36 (m, 2H, **$H_{8,16}$**), 1.79 (d, *J* = 5.6 Hz, 6H, **$H_{1,7}$**), 1.13 (d, *J* = 7.9 Hz, 3H, **H_{17}**), 0.87 (s, 9H, **$H_{35\text{-}37}$**), 0.08 (s, 3H, **H_{32}**), 0.05 (s, 3H, **H_{33}**) ppm.

^{13}C-NMR (176MHz, $CDCl_3$): δ 174.2 (**C_{18}**), 169.9 (**C_{10}**), 166.3 (**C_{29}**), 146.6 (**C_{27}**), 143.2 (**C_{25}**), 138.8 (**C_{23}**), 132.0 (**C_5**), 131.6 (**C_{24}**), 131.0 (**C_2**), 127.6 (**C_{26}**), 127.1 (**C_3**), 126.4 (**C_4**), 119.6 (**C_{28}**), 76.4 (**C_6**), 72.4 (**C_{13}**), 71.3 (**C_{21}**), 45.3 (**C_8**), 43.0 (**C_{16}**), 42.3 (**C_{22}**), 37.5 (**C_{14}**), 18.7 (**C_{17}**), 18.6 (**C_1**), 18.0 (**C_{34}**), 14.4 (3C, **$C_{35\text{-}37}$**), 13.3 (**C_7**), −4.5 (**C_{32}**), −4.8 (**C_{33}**) ppm.

HRMS (ESI+): exact mass calculated for $[M+Na]^+$ ($C_{29}H_{46}N_2O_5SiNa^+$) required *m/z* 553.3074, found *m/z* 553.3065.

FT-IR (neat) ν_{max}: 3385, 2955, 2927, 2854, 1712, 1646, 1552, 1540, 1467, 1437, 1389, 1361, 1259, 1240, 1218, 1094, 1052, 1021, 985, 965, 873, 838 cm^{-1}.

$[a]_D^{20}$ = −142° (c = 0.45, $CHCl_3$).

TLC: R_f (60% EtOAc in heptanes) = 0.30; $KMnO_4$ stain.

2.6.4.8. (2*R*,7*R*,8*S*,13*E*,15*E*,17*E*)-2-((2*E*,4*E*)-hexa-2,4-dien-2-yl)-7-hydroxy-8-methyl-1-oxa-5,10-diazacyclononadeca-13,15,17-triene-4,9,19-trione, sc-FR (2.113)

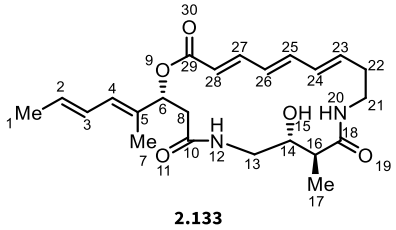

2.133

Chemical Formula: $C_{23}H_{32}N_2O_5$

(2*R*,7*R*,8*S*,13*E*,15*E*,17*E*)-2-((2*E*,4*E*)-hexa-2,4-dien-2-yl)-7-hydroxy-8-methyl-1-oxa-5,10-diazacyclo-nonadeca-13,15,17-triene-4,9,19-trione (**2.133**) was synthesised according to the general procedure outlined in chapter 2.5.2.19. on 20.0 µmol scale to yield **2.133** (5.40 mg, 13.0 µmol, 65%) as a white solid.

^{1}H-NMR (600MHz, $CDCl_3$): δ 7.29-7.23 (m, 1H, $\mathbf{H_{27}}$), 6.51 (dd, *J* = 14.9, 10.8 Hz, 1H, $\mathbf{H_{25}}$), 6.22 (ddd, *J* = 25.9, 15.0, 9.7 Hz, 3H, $\mathbf{H_{NH+3+26}}$), 6.13 (d, *J* = 10.9 Hz, 1H, $\mathbf{H_4}$), 6.07 (dd, *J* = 14.9, 11.2 Hz, 1H, $\mathbf{H_{24}}$), 5.81-5.64 (m, 5H, $\mathbf{H_{NH+2+6+23+28}}$), 4.13 (ddd, *J* = 23.5, 13.4, 5.1 Hz, 1H, $\mathbf{H_{14}}$), 3.82-3.76 (m, 1H, $\mathbf{H_{21}}$), 3.36-3.30 (m, 1H, $\mathbf{H_{13}}$), 3.01 (d, *J* = 15.0 Hz, 1H, $\mathbf{H_{13}}$), 2.66-2.47 (m, 4H, $\mathbf{H_{8+21+22}}$), 2.29-2.18 (m, 2H, $\mathbf{H_{8+16}}$), 1.78 (app. d, *J* = 7.4 Hz, 6H, $\mathbf{H_{1+7}}$), 0.98 (d, *J* = 7.1 Hz, 3H, $\mathbf{H_{17}}$) ppm.

^{13}C-NMR (151MHz, $CDCl_3$): δ 176.0 ($\mathbf{C_{18}}$), 169.4 ($\mathbf{C_{10}}$), 165.4 ($\mathbf{C_{29}}$), 144.6 ($\mathbf{C_{27}}$), 140.8 ($\mathbf{C_{25}}$), 136.0, 133.0, 131.8 ($\mathbf{C_5}$), 130.9, 128.7, 127.1, 126.6, 121.3, 76.1 ($\mathbf{C_6}$),71.6 ($\mathbf{C_{14}}$), 44.1 ($\mathbf{C_{13}}$), 43.1 ($\mathbf{C_{16}}$), 42.0, 36.9 ($\mathbf{C_{21}}$), 34.6, 18.6 ($\mathbf{C_1}$), 13.1 ($\mathbf{C_7}$), 11.1 ($\mathbf{C_{17}}$) ppm.

HRMS (ESI+): exact mass calculated for $[M+Na]^+$ ($C_{23}H_{32}N_2O_5Na^+$) required *m/z* 439.2209, found *m/z* 439.2206.

FT-IR (neat) ν_{max}: 2957, 2922, 2852, 1709, 1648, 1639, 1613, 1552, 1537, 1465, 1435, 1377, 1338, 1299, 1259, 1233, 1214, 1101, 1062, 1008, 964, 927, 884, 836 cm^{-1}.

$[a]_D^{20}$ = −10.0° (c = 0.100, $CHCl_3$).

TLC: R_f (10% MeOH in $CHCl_3$) = 0.53; $KMnO_4$ stain.

2.6.5. Synthesis of Cy-FR

2.6.5.1. Methyl (2*E*,4*E*)-5-cyclohexyl-2-methylpenta-2,4-dienoate (2.S44)

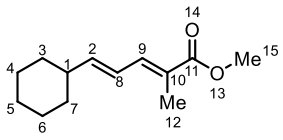

2.S44
Chemical Formula: $C_{13}H_{20}O_2$

(*E*)-3-cyclohexylacrylaldehyde (3.41 g, 24.7 mmol, 1.00 eq) and methyl 2-(triphenyl-λ^5-phosphaneylidene)propanoate (25.8 g, 74.1 mmol, 3.00 eq) were dissolved in toluene (0.5 M) and the resulting mixture was heated to reflux for 18 h. Afterwards, the reaction mixture was concentrated and filtered through a short pad of silica, which was washed with 20%EtOAc in heptane. The filtrate was concentrated and the resulting crude material was used without further purification in the next step.

2.6.5.2. (2*E*,4*E*)-5-cyclohexyl-2-methylpenta-2,4-dien-1-ol (2.S45)

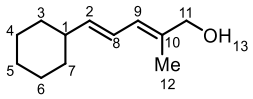

2.S45
Chemical Formula: $C_{12}H_{20}O$

(2*E*,4*E*)-5-cyclohexyl-2-methylpenta-2,4-dien-1-ol (**2.S45**) was synthesised according to the general procedure outlined in chapter 2.5.2.2. on 14.8 mmol scale to yield **2.S45** (821 mg, 4.55 mmol, 31% over two steps) as a colourless oil.

^{1}H-NMR (600MHz, $CDCl_3$): δ 6.21 (ddd, *J* = 15.2, 10.8, 1.0 Hz, 1H, **H_8**), 5.99 (d, *J* = 10.8 Hz, 1H, **H_9**), 5.64 (dd, *J* = 15.2, 7.1 Hz, 1H, **H_2**), 4.03 (s, 2H, **H_{11}**), 2.03-1.99 (m, 1H, **H_1**), 1.76 (s, 3H, **H_{12}**), 1.73-1.70 (m, 4H, **$H_{3\text{-}7}$**), 1.66-1.62 (m, 1H, **$H_{3\text{-}7}$**), 1.30-1.26 (m, 1H, **$H_{3\text{-}7}$**), 1.19-1.06 (m, 4H, **$H_{3\text{-}7}$**) ppm.

^{13}C-NMR (151MHz, $CDCl_3$): δ 141.1 (**C_2**), 135.0 (**C_{10}**), 125.7 (**C_9**), 123.4 (**C_8**), 68.8 (**C_{11}**), 41.2 (**C_1**), 33.1 (2C, **$C_{3\text{-}7}$**), 26.3 (**$C_{3\text{-}7}$**), 26.1 (**$C_{3\text{-}7}$**), 21.1 (**$C_{3\text{-}7}$**), 14.3 (**C_{12}**) ppm.

HRMS (ESI−): exact mass calculated for $[M]^-$ ($C_{12}H_{19}O^-$) required *m/z* 179.1441, found *m/z* 179.1429.

FT-IR (neat) ν_{max}: 3307, 3023, 2921, 2850, 1447, 1386, 1349, 1302, 1259, 1222, 1066, 1005, 966, 892, 749, 667, 624 cm^{-1}.

TLC: R_f (20% EtOAc in heptane) = 0.34; $KMnO_4$ stain.

2.6.5.3. (2*E*,4*E*)-5-cyclohexyl-2-methylpenta-2,4-dienal (2.129)

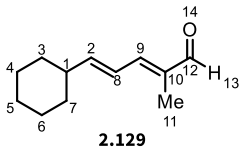

2.129

Chemical Formula: $C_{12}H_{18}O$

(2*E*,4*E*)-5-cyclohexyl-2-methylpenta-2,4-dienal (**2.129**) was synthesised according to the general procedure outlined in chapter 2.5.2.3. on 3.00 mmol scale to yield **2.129** (408 mg, 2.29 mmol, 76%) as a colourless oil.

^{1}H-NMR (600MHz, $CDCl_3$): δ 9.41 (s, 1H, **H_{13}**), 6.81 (d, *J* = 11.1 Hz, 1H, **H_9**), 6.47 (ddd, *J* = 15.2, 11.1, 1.2 Hz, 1H, **H_8**), 6.18 (dd, *J* = 15.2, 7.1 Hz, 1H, **H_2**), 2.16 (dtd, *J* = 14.2, 7.3, 3.6 Hz, 1H, **H_1**), 1.82 (d, *J* = 0.8 Hz, 3H, **H_{11}**), 1.80-1.74 (m, 4H, **H_{4+6}**), 1.69-1.67 (m, 1H, **H_5**), 1.32-1.27 (m, 2H, **H_{5+7}**), 1.22-1-13 (m, 3H, **H_{3+7}**) ppm.

^{13}C-NMR (151MHz, $CDCl_3$): δ 195.2 (**C_{12}**), 151.4 (**C_2**), 149.9 (**C_9**), 136.2 (**C_{10}**), 123.5 (**C_8**), 41.7 (**C_1**), 32.4 (2C, **C_{3-7}**), 26.1 (2C, **C_{3-7}**), 25.9 (**C_{3-7}**), 9.52 (**C_{11}**) ppm.

HRMS (ESI+): exact mass calculated for $[M+Na]^+$ ($C_{12}H_{18}ONa^+$) required *m/z* 201.1250, found *m/z* 201.1248.

FT-IR (neat) ν_{max}: 2922, 2850, 1674, 1630, 1447, 1405, 1379, 1355, 1328, 1260, 1223, 1202, 1173, 1148, 1128, 1098, 1009, 993, 964, 898, 834, 792, 774, 687, 563, 528, 490, 452, 441, 426 cm^{-1}.

TLC: R_f (20% EtOAc in heptane) = 0.75; $KMnO_4$ stain.

2.6.5.4. (*R*,4*E*,6*E*)-1-((*S*)-4-benzyl-2-thioxothiazolidin-3-yl)-7-cyclohexyl-3-hydroxy-4-methylhepta-4,6-dien-1-one (2.130)

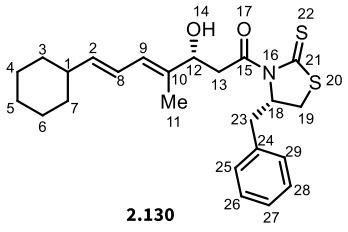

2.130

Chemical Formula: $C_{24}H_{31}NO_2S_2$

(*R*,4*E*,6*E*)-1-((*S*)-4-benzyl-2-thioxothiazolidin-3-yl)-7-cyclohexyl-3-hydroxy-4-methylhepta-4,6-dien-1-one (**2.130**) was synthesised according to the general procedure outlined in chapter 2.5.2.5. on 3.94 mmol scale to yield **2.130** (504 mg, 1.17 mmol, 30%) as a yellow oil.

^{1}H-NMR (600MHz, $CDCl_3$): δ 7.37-7.34 (m, 2H, $\mathbf{H_{25+29}}$), 7.30-7.27 (m, 3H, $\mathbf{H_{26-28}}$), 6.22 (ddd, *J* = 15.1, 10.8, 1.1 Hz, 1H, $\mathbf{H_8}$), 6.10 (bd, *J* = 10.9 Hz, 1H, $\mathbf{H_9}$), 5.68 (dd, *J* = 15.1, 7.1 Hz, 1H, $\mathbf{H_2}$), 5.38 (ddd, *J* = 10.7, 7.0, 4.0 Hz, 1H, $\mathbf{H_{18}}$), 4.64 (dt, *J* = 10.0, 2.8 Hz, 1H, $\mathbf{H_{12}}$), 3.55 (dd, *J* = 17.2, 2.6 Hz, 1H, $\mathbf{H_{13}}$), 3.43 (dd, *J* = 17.4, 9.6 Hz, 1H, $\mathbf{H_{13}}$), 3.42-3.39 (m, 1H, $\mathbf{H_{19}}$), 3.25 (dd, *J* = 13.2, 3.8 Hz, 1H, $\mathbf{H_{23}}$), 3.05 (dd, *J* = 13.2, 10.5 Hz, 1H, $\mathbf{H_{23}}$), 2.90 (d, *J* = 11.5 Hz, 1H, $\mathbf{H_{19}}$), 2.50 (d, *J* = 3.6 Hz, 1H, $\mathbf{H_{OH14}}$), 2.06-2.01 (m, 1H, $\mathbf{H_1}$), 1.79 (s, 3H, $\mathbf{H_{11}}$), 1.73 (bd, *J* = 10.5 Hz, 4H, $\mathbf{H_{3-7}}$), 1.65 (d, *J* = 12.8 Hz, 1H, $\mathbf{H_5}$), 1.31-1.06 (m, 5H, $\mathbf{H_{3-7}}$) ppm.

^{13}C-NMR (151MHz, $CDCl_3$): δ 201.5 ($\mathbf{C_{21}}$), 173.0 ($\mathbf{C_{15}}$), 142.0 ($\mathbf{C_2}$), 136.6 ($\mathbf{C_{24}}$), 135.4 ($\mathbf{C_{10}}$), 129.6 (2C, $\mathbf{C_{26/28}}$), 129.1 (2C, $\mathbf{C_{25/29}}$), 127.4 ($\mathbf{C_{27}}$), 126.2 ($\mathbf{C_9}$), 123.3 ($\mathbf{C_8}$), 72.9 ($\mathbf{C_{12}}$), 68.7 ($\mathbf{C_{18}}$), 44.5 ($\mathbf{C_{13}}$), 41.3 ($\mathbf{C_1}$), 37.0 ($\mathbf{C_{23}}$), 33.1 ($\mathbf{C_{3-7}}$), 32.3 ($\mathbf{C_{19}}$), 26.3 (2C, $\mathbf{C_{3-7}}$), 26.1 (2C, $\mathbf{C_{3-7}}$), 13.1 ($\mathbf{C_{11}}$) ppm.

HRMS (ESI+): exact mass calculated for $[M+Na]^+$ ($C_{24}H_{31}NO_2S_2Na^+$) required *m/z* 452.1688, found *m/z* 452.1694.

FT-IR (neat) ν_{max}: 2922, 2850, 2362, 2335, 1692, 1633, 1495, 1448, 1342, 1318, 1292, 1259, 1226, 1191, 1163, 1137, 1075, 1043, 1012, 966, 894, 748, 724, 701, 668, 580, 521, 511, 478, 418 cm^{-1}.

$[a]_D^{20}$ = +8.20° (c = 1.00, $CHCl_3$).

TLC: R_f (20% EtOAc in heptane) = 0.20; $KMnO_4$ stain.

2.6.5.5. (*R*,4*E*,6*E*)-*N*-((2*R*,3*S*)-2-((*tert*-butyldimethylsilyl)oxy)-3-methyl-4-oxo-4-(((*E*)-4-(4,4,5,5-tetramethyl-1,3,2-dioxaborolan-2-yl)but-3-en-1-yl)amino)butyl)-7-cyclohexyl-3-hydroxy-4-methylhepta-4,6-dienamide (2.S46)

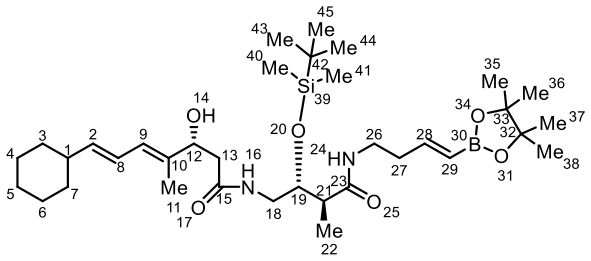

2.S46

Chemical Formula: $C_{35}H_{63}BN_2O_6Si$

(*R*,4*E*,6*E*)-*N*-((2*R*,3*S*)-2-((*tert*-butyldimethylsilyl)oxy)-3-methyl-4-oxo-4-(((*E*)-4-(4,4,5,5-tetramethyl-1,3,2-dioxaborolan-2-yl)but-3-en-1-yl)amino)butyl)-7-cyclohexyl-3-hydroxy-4-methylhepta-4,6-dienamide (**2.S46**) was synthesised according to the general procedure outlined in chapter 2.5.2.15. on 0.97 mmol scale to yield **2.S46** (364 mg, 0.563 mmol, 58%) as a colourless foam.

^{1}H-NMR (600MHz, $CDCl_3$): δ 6.55 (dt, *J* = 18.0, 6.5 Hz, 1H, **H_{29}**), 6.44 (dd, *J* = 7.1, 4.3 Hz, 1H, **H_{NH16}**), 6.19 (ddd, *J* = 15.2, 10.8, 1.0 Hz, 1H, **H_8**), 6.14 (t, *J* = 5.5 Hz, 1H, **H_{NH24}**), 6.07 (d, *J* = 10.8 Hz, 1H, **H_9**), 5.65 (dd, *J* = 15.1, 7.0 Hz, 1H, **H_2**), 5.52 (d, *J* = 18.0 Hz, 1H, **H_{28}**), 4.43 (dd, *J* = 8.9, 3.0 Hz, 1H, **H_{12}**), 3.88 (dt, *J* = 7.7, 4.4 Hz, 1H, **H_{19}**), 3.72 (ddd, *J* = 13.7, 7.7, 4.2 Hz, 1H, **H_{18}**), 3.47-3-42 (m, 1H, **H_{27}**), 3.30-3.24 (m, 1H, **H_{27}**), 2.93 (ddd, *J* = 13.6, 7.6, 4.5 Hz, 1H, **H_{18}**), 2.44-2.34 (m, 5H, **$H_{13/21/26}$**), 2.05-1.99 (m, 1H, **H_1**), 1.75-1.71 (m, 7H, **$H_{3\text{-}7/11}$**), 1.27-1.25 (m, 15H, **$H_{3\text{-}7,35\text{-}38}$**), 1.16-1-06 (m, 3H, **$H_{3\text{-}7}$**), 1.14 (d, *J* = 7.2 Hz, 3H, **H_{22}**), 0.92-0.88 (m, 9H, **$H_{43\text{-}45}$**), 0.17-0.07 (m, 6H, **H_{40+41}**) ppm.

^{13}C-NMR (151MHz, $CDCl_3$): δ 174.6 (**C_{23}**), 172.3 (**C_{15}**), 150.4 (**C_{29}**), 141.8 (**C_2**), 135.7 (**C_{10}**), 126.0 (**C_9**), 123.3 (**C_8**), 121.7 (**C_{28}**, *deducted from HSQC*), 83.4 (2C, **$C_{32/33}$**), 73.7 (**C_{12}**), 72.2 (**C_{19}**), 44.8 (**C_{21}**), 43.0 (**C_{18}**), 41.6 (**C_{13}**), 41.3 (**C_1**), 38.0 (**C_{27}**), 35.8 (**C_{26}**), 33.1 (2C, **$C_{3\text{-}7}$**), 26.3 (2C, **$C_{35\text{-}38}$**), 26.1 (3C, **$C_{43\text{-}45}$**), 26.0 (3C, **$C_{3\text{-}7}$**), 25.0 (**$C_{35\text{-}38}$**), 24.9 (**$C_{35\text{-}38}$**), 18.1 (**C_{42}**), 15.4 (**C_{22}**), 12.8 (**C_{11}**), −4.4 (**C_{40}**), −4.8 (**C_{41}**) ppm.

HRMS (ESI+): exact mass calculated for $[M+Na]^+$ ($C_{35}H_{63}BN_2O_6SiNa^+$) required *m/z* 669.4441, found *m/z* 669.4450.

FT-IR (neat) ν_{max}: 3335, 3307, 2976, 2927, 2854, 2361, 2340, 1643, 1540, 1471, 1448, 1397, 1389, 1360, 1322, 1257, 1144, 1102, 1042, 1023, 1003, 967, 836, 812, 778, 749, 681, 667, 655, 579 cm^{-1}.

$[a]_D^{20}$ = +27.6° (c = 1.00, $CHCl_3$).

TLC: R_f (30% *i*PrOH in heptane) = 0.75; $KMnO_4$ or PMA stain.

2.6.5.6. (*R*,4*E*,6*E*)-1-(((2*R*,3*S*)-2-((*tert*-butyldimethylsilyl)oxy)-3-methyl-4-oxo-4-(((*E*)-4-(4,4,5,5-tetramethyl-1,3,2-dioxaborolan-2-yl)but-3-en-1-yl)amino)butyl)amino)-7-cyclohexyl-4-methyl-1-oxohepta-4,6-dien-3-yl (1*R*,4*R*)-4-chlorocyclobut-2-ene-1-carboxylate (2.S47)

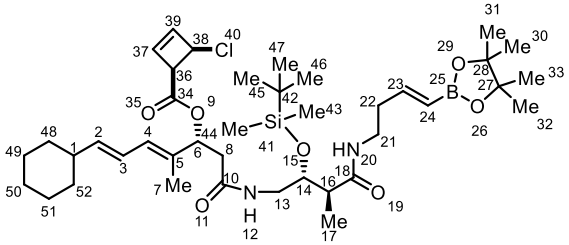

2.S47

Chemical Formula: $C_{40}H_{66}BClN_2O_7Si$

(*R*,4*E*,6*E*)-1-(((2*R*,3*S*)-2-((*tert*-butyldimethylsilyl)oxy)-3-methyl-4-oxo-4-(((*E*)-4-(4,4,5,5-tetramethyl-1,3,2-dioxaborolan-2-yl)but-3-en-1-yl)amino)butyl)amino)-7-cyclohexyl-4-methyl-1-oxohepta-4,6-dien-3-yl (1*R*,4*R*)-4-chlorocyclobut-2-ene-1-carboxylate (**2.S47**) was synthesised according to the general procedure outlined in chapter 2.5.2.17. on 79.0 µmol scale to yield **2.S47** (26.3 mg, 34.5 µmol, 44%) as a colourless foam.

^{1}H-NMR (600MHz, $CDCl_3$): δ 6.55 (dt, *J* = 17.9, 6.4 Hz, 1H, **H_{23}**), 6.29-6.23 (m, 2H, **H_{37+39}**), 6.17 (t, *J* = 5.7 Hz, 1H, **H_{20}**), 6.16-6.09 (m, 3H, **H_{3+4+12}**), 5.69-5.65 (m ,1H, **H_2**), 5.63 (dd, *J* = 7.8, 5.4 Hz, 1H, **H_6**), 5.51 (d, *J* = 18.0 Hz, 1H, **H_{24}**), 5.08 (d, *J* = 4.2 Hz, 1H, **H_{36}**), 4.08 (d, *J* = 4.3 Hz, 1H, **H_{38}**), 3.83-3.80 (m, 1H, **H_{13}**), 3.75 (ddd, *J* = 13.4, 8.0, 4.0 Hz, 1H, **H_{13}**), 3.45-3.39 (m, 1H, **H_{21}**), 3.27 (td, *J* = 12.5, 6.7 Hz, 1H, **H_{21}**), 2.81 (ddd, *J* = 13.5, 7.7, 4.2 Hz, 1H, **H_{14}**), 2.66 (dd, *J* = 14.5, 7.9 Hz, 1H, **H_8**), 2.50 (dd, *J* = 14.5, 5.3 Hz, 1H, **H_8**), 2.38-2.33 (m, 3H, **H_{16+22}**), 2.03-1.97 (m, 1H, **H_1**), 1.77 (s, 3H, **H_7**), 1.70 (s, 5H, **H_{48-51}**), 1.64 (d, *J* = 12.6 Hz, 1H, **H_{50}**), 1.25 (s, 12H, **H_{30-33}**),

1.14 (d, *J* = 6.4 Hz, 2H, **H$_{48\text{-}52}$**), 1.10 (d+m, *J* = 7.1 Hz, 5H, **H$_{17,48\text{-}52}$**), 0.90 (s, 9H, **H$_{45\text{-}47}$**), 0.14 (s, 3H, **H$_{43}$**), 0.08 (s, 3H, **H$_{44}$**) ppm.

^{13}C-NMR (151MHz, $CDCl_3$): δ 174.5 (**C$_{18}$**), 169.3 (**C$_{10}$**), 168.8 (**C$_{34}$**), 150.4 (**C$_{23}$**), 142.9 (**C$_{2}$**), 140.6 (**C$_{37}$**), 136.7 (**C$_{39}$**), 130.9 (**C$_{5}$**), 129.2 (**C$_{4}$**), 122.9 (**C$_{3}$**), 121.7 (**C$_{24}$**, *deduced from HSQC*), 83.6 (2C, **C$_{27,28}$**), 77.0 (**C$_{6}$**), 72.1 (**C$_{13}$**), 56.4 (**C$_{36}$**), 54.1 (**C$_{38}$**), 44.6 (**C$_{16}$**), 43.0 (**C$_{14}$**), 41.3 (**C$_{1}$**), 40.9 (**C$_{8}$**), 38.0 (**C$_{21}$**), 35.9 (**C$_{22}$**), 33.0 (**C$_{48\text{-}52}$**), 32.9 (**C$_{48\text{-}52}$**), 26.3 (**C$_{48\text{-}52}$**), 26.1 (**C$_{48\text{-}52}$**), 26.0 (3C, **C$_{45\text{-}47}$**), 25.9 (**C$_{48\text{-}52}$**), 24.94 (4C, **C$_{30\text{-}33}$**), 18.1 (**C$_{42}$**), 15.5 (**C$_{17}$**), 12.8 (**C$_{7}$**), −4.3 (**C$_{43}$**), −4.9 (**C$_{44}$**) ppm.

HRMS (ESI+): exact mass calculated for $[M+Na]^+$ ($C_{40}H_{66}BClN_2O_7SiNa^+$) required *m/z* 783.4319, found *m/z* 783.4324.

TLC: alcohol **2.S46**: R_f (60% EtOAc in heptane) = 0.15; PMA stain;

trans$_1$-**2.S47**: R_f (60% EtOAc in heptane) = 0.35; PMA stain;

trans$_2$-**2.S47**: R_f (60% EtOAc in heptane) = 0.30; PMA stain;

cis$_1$-**2.S47**: R_f (60% EtOAc in heptane) = 0.25; PMA stain;

cis$_2$-**2.S47**: R_f (60% EtOAc in heptane) = 0.20; PMA stain.

2.6.5.7. (2*R*,7*R*,8*S*,13*E*,15*E*,17*E*)-7-((*tert*-butyldimethylsilyl)oxy)-2-((2*E*,4*E*)-5-cyclohexylpenta-2,4-dien-2-yl)-8-methyl-1-oxa-5,10-diazacyclononadeca-13,15,17-triene-4,9,19-trione (2.S48)

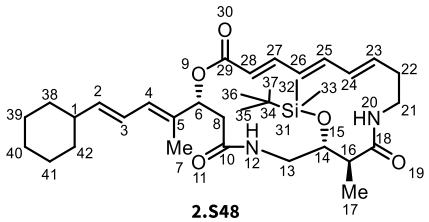

2.S48

Chemical Formula: $C_{34}H_{54}N_2O_5Si$

(2*R*,7*R*,8*S*,13*E*,15*E*,17*E*)-7-((*tert*-butyldimethylsilyl)oxy)-2-((2*E*,4*E*)-5-cyclohexylpenta-2,4-dien-2-yl)-8-methyl-1-oxa-5,10-diazacyclononadeca-13,15,17-triene-4,9,19-trione (**2.S48**) was synthesised according to the general procedure outlined in chapter 2.5.2.18. on 15.8 µmol scale to yield **2.S48** (8.30 mg, 13.9 µmol, 88%) as a colourless foam.

^{1}H-NMR (700MHz, $CDCl_3$): δ 7.29-7.23 (m, 1H, $\mathbf{H_{27}}$), 6.45 (dd, *J* = 14.9, 10.9 Hz, 1H, $\mathbf{H_{25}}$), 6.22-6.17 (m, 1H, $\mathbf{H_3}$), 6.15 (dd, *J* = 13.2, 9.5 Hz, 1H, $\mathbf{H_{26}}$), 6.14-6.07 (m, 3H, $\mathbf{H_{4+20+24}}$), 6.02 (bs, 1H, $\mathbf{H_{12}}$), 5.90 (ddd, *J* = 14.7, 10.9, 3.4 Hz, 1H, $\mathbf{H_{23}}$), 5.71 (d, *J* = 15.6 Hz, 1H, $\mathbf{H_{28}}$), 5.69 (dd, *J* = 15.3, 6.9 Hz, 1H, $\mathbf{H_2}$), 5.62 (dd, *J* = 11.1, 3.2 Hz, 1H, $\mathbf{H_6}$), 4.11-4.04 (m, 1H, $\mathbf{H_{21}}$), 3.51-3.40 (m, 2H, $\mathbf{H_{13}}$), 2.96 (bd, *J* = 13.9 Hz, 1H, $\mathbf{H_{21}}$), 2.56-2.36 (m, 4H, $\mathbf{H_{14+16+22}}$), 2.23-2.15 (m, 1H, $\mathbf{H_{22}}$), 2.05-1.99 (m, 1H, $\mathbf{H_1}$), 1.79 (s, 3H, $\mathbf{H_7}$), 1.72 (bd, *J* = 10.2 Hz, 4H, $\mathbf{H_{38\text{-}42}}$), 1.68-1.63 (m, 2H, $\mathbf{H_{38\text{-}42}}$), 1.25 (s, 3H, $\mathbf{H_{38\text{-}42}}$), 1.14 (dd, *J* = 6.9, 3.4 Hz, 3H, $\mathbf{H_{17}}$), 1.12-1.05 (m, 2H, $\mathbf{H_{38\text{-}42}}$), 0.87 (s, 9H, $\mathbf{H_{35\text{-}37}}$), 0.09 (s, 3H, $\mathbf{H_{32}}$), 0.06 (s, 3H, $\mathbf{H_{33}}$) ppm.

^{13}C-NMR (176MHz, $CDCl_3$): δ 176.6 ($\mathbf{C_{18}}$), 174.4 ($\mathbf{C_{10}}$) 170.0 ($\mathbf{C_{29}}$), 166.4 ($\mathbf{C_{28}}$), 146.7 ($\mathbf{C_{27}}$), 143.2 ($\mathbf{C_{25}}$), 142.4 ($\mathbf{C_2}$), 138.7 ($\mathbf{C_{23}}$), 132.3 ($\mathbf{C_{24}}$), 131.6 ($\mathbf{C_5}$), 127.7 ($\mathbf{C_{26}}$), 126.8 ($\mathbf{C_{20}}$), 123.1 ($\mathbf{C_3}$), 119.5 ($\mathbf{C_4}$), 76.4 ($\mathbf{C_6}$), 72.4 ($\mathbf{C_{13}}$), 45.2 ($\mathbf{C_{16}}$), 43.1 ($\mathbf{C_{14}}$), 42.2 ($\mathbf{C_{21}}$), 41.3 ($\mathbf{C_{22}}$), 37.5 ($\mathbf{C_{38\text{-}42}}$), 34.4 ($\mathbf{C_{38\text{-}42}}$), 33.9 ($\mathbf{C_{38\text{-}42}}$), 29.9 ($\mathbf{C_1}$), 25.9 ($\mathbf{C_{38\text{-}42}}$), 19.4 ($\mathbf{C_{38\text{-}42}}$), 18.7 ($\mathbf{C_{17}}$), 18.0 ($\mathbf{C_{34}}$), 14.3 (3C, $\mathbf{C_{35\text{-}37}}$), 13.4 ($\mathbf{C_7}$), −4.5 ($\mathbf{C_{32}}$), −4.8 ($\mathbf{C_{33}}$) ppm.

HRMS (ESI+): exact mass calculated for $[M+Na]^+$ ($C_{34}H_{54}N_2O_5SiNa^+$) required *m/z* 621.3700, found *m/z* 621.3685.

FT-IR (neat) ν_{max}: 2957, 2925, 2853, 1712, 1651, 1614, 1538, 1467, 1378, 1361, 1256, 1228, 1218, 1186, 1144, 1101, 1009, 966, 837, 776, 751 cm^{-1}.

$[a]_D^{20}$ = −85.9° (c = 0.300, $CHCl_3$).

TLC: R_f (60% EtOAc in heptanes) = 0.25; $KMnO_4$ or PMA stain.

2.6.5.8. (2*R*,7*R*,8*S*,13*E*,15*E*,17*E*)-2-((2*E*,4*E*)-5-cyclohexylpenta-2,4-dien-2-yl)-7-hydroxy-8-methyl-1-oxa-5,10-diazacyclononadeca-13,15,17-triene-4,9,19-trione, Cy-FR (2.115)

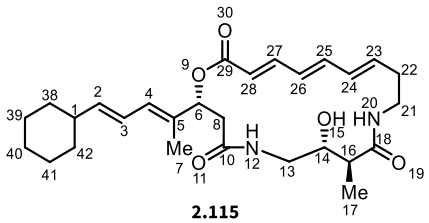

2.115

Chemical Formula: $C_{28}H_{40}N_2O_5$

Cy-FR (**2.115**) was synthesised according to the general procedure outlined in chapter 2.5.2.19. on 17.9 µmol scale to yield **2.115** (6.30 mg, 13.0 µmol, 73%) as a white solid.

^{1}H-NMR (700MHz, $CDCl_3$): δ 7.28-7.25 (m, 1H, $\mathbf{H_{27}}$), 6.50 (dd, *J* = 14.8, 10.8 Hz, 1H, $\mathbf{H_{24}}$), 6.26 (d, *J* = 8.5 Hz, 1H, $\mathbf{H_{NH12}}$), 6.21-6.16 (m, 2H, $\mathbf{H_{3+26}}$), 6.12 (d, *J* = 10.8 Hz, 1H, $\mathbf{H_4}$), 6.07 (dd, *J* = 14.6, 11.2 Hz, 1H, $\mathbf{H_{25}}$), 5.96 (bs, 1H, $\mathbf{H_{NH20}}$), 5.81-5.74 (m, 1H, $\mathbf{H_{23}}$), 5.76 (d, *J* = 15.4 Hz, 1H, $\mathbf{H_{28}}$), 5.71-5.65 (m, 3H, $\mathbf{H_{2,6,14}}$), 4.14 (tdd, *J* = 13.6, 10.4, 5.1 Hz, 1H, $\mathbf{H_{21}}$), 3.83-3.78 (m, 1H, $\mathbf{H_{13}}$), 3.33 (td, *J* = 10.5, 2.9 Hz, 1H, $\mathbf{H_{13}}$), 3.04-2.98 (m, 1H, $\mathbf{H_{21}}$), 2.65-2.61 (m, 1H, $\mathbf{H_{14}}$), 2.61-2.56 (m, 1H, $\mathbf{H_{22}}$), 2.56 (dd, *J* = 14.0, 3.2, Hz, 1H, $\mathbf{H_8}$), 2.50 (dd, *J* = 13.8, 11.4 Hz, 1H, $\mathbf{H_8}$), 2.29-2.23 (m, 1H, $\mathbf{H_{15}}$), 2.23-2.17 (m, 1H, $\mathbf{H_{22}}$), 2.06-2.00 (m, 1H, $\mathbf{H_1}$), 1.79 (s, 3H, $\mathbf{H_7}$), 1.72 (d, *J* = 10.5 Hz, 1H, $\mathbf{H_{39,41}}$), 1.64 (dt, *J* = 15.1, 7.5 Hz, 3H, $\mathbf{H_{39,41}}$), 1.34-1.25 (m, 4H, $\mathbf{H_{38,40,42}}$), 1.12-1.05 (m, 2H, $\mathbf{H_{38,42}}$), 0.98 (d, *J* = 7.1 Hz, 3H, $\mathbf{H_{17}}$) ppm.

^{13}C-NMR (176MHz, $CDCl_3$): δ 176.0 ($\mathbf{C_{18}}$), 169.4 ($\mathbf{C_{10}}$), 165.4 ($\mathbf{C_{29}}$), 144.5 ($\mathbf{C_{27}}$), 142.4 ($\mathbf{C_2}$), 140.8 ($\mathbf{C_{24}}$), 136.0 ($\mathbf{C_{23}}$), 133.0 ($\mathbf{C_{25}}$), 132.2 ($\mathbf{C_5}$), 128.7 ($\mathbf{C_{26}}$), 127.0 ($\mathbf{C_4}$), 123.1 ($\mathbf{C_3}$), 121.3 ($\mathbf{C_{28}}$), 76.1 ($\mathbf{C_6}$), 71.6 ($\mathbf{C_{13}}$), 44.1 ($\mathbf{C_{14}}$), 43.1 ($\mathbf{C_{16}}$), 42.0 ($\mathbf{C_8}$), 41.3 ($\mathbf{C_1}$), 36.9 ($\mathbf{C_{21}}$), 34.6 ($\mathbf{C_{22}}$), 32.1 ($\mathbf{C_{38/40/42}}$), 29.9 ($\mathbf{C_{38/40/42}}$), 26.1 ($\mathbf{C_{39/41}}$), 24.9 ($\mathbf{C_{39/41}}$), 22.9 ($\mathbf{C_{38/40/42}}$), 13.3 ($\mathbf{C_7}$), 11.1 ($\mathbf{C_{17}}$) ppm.

HRMS (ESI+): exact mass calculated for $[M+Na]^+$ ($C_{28}H_{40}N_2O_5Na^+$) required *m/z* 507.2835, found *m/z* 507.2838.

FT-IR (neat) ν_{max}: 3020, 2961, 2923, 2852, 2359, 1705, 1643, 1630, 1613, 1540, 1249, 1229, 1218, 1005, 767, 755 cm^{-1}.

$[a]_D^{20}$ = −242° (c = 0.050, $CHCl_3$).

TLC: R_f (10% MeOH in $CHCl_3$) = 0.50; $KMnO_4$ stain.

2.6.6. Synthesis of EZE-FR252921

2.6.6.1. (2*R*,7*R*,8*S*,13*E*,15*Z*,17*E*)-2-((2*E*,4*E*)-dodeca-2,4-dien-2-yl)-7-hydroxy-8-methyl-1-oxa-5,10-diazacyclononadeca-13,15,17-triene-4,9,19-trione, EZE-FR252921 (2.136)

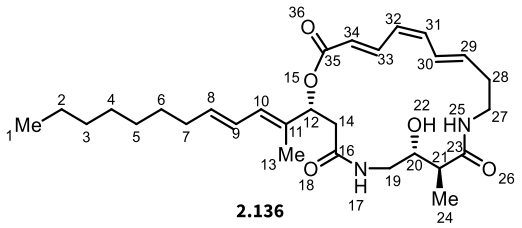

2.136

Chemical Formula: $C_{29}H_{44}N_2O_5$

EZE-FR252921 (**2.136**) was synthesised according to the general procedure outlined in chapter 2.5.2.19. on 7.30 µmol scale to yield **2.136** (0.800 mg, 1.60 µmol, 22%) as a white solid.

^{1}H-NMR (600MHz, $CDCl_3$): δ 7.73 (ddd, *J* = 15.3, 11.8, 0.7 Hz, 1H, **H_{33}**), 6.64 (dd, *J* = 15.1, 11.5 Hz, 1H, **H_{30}**), 6.36 (t, *J* = 5.6 Hz, 1H, **H_{NH25}**), 6.31 (app. t, *J* = 10.9 Hz, 1H, **H_{31}**), 6.24-6.16 (m, 2H, **H_{9+NH17}**), 6.11 (d, *J* = 10.9 Hz, 1H, **H_{10}**), 6.04 (app. t, *J* = 11.2 Hz, 1H, **H_{32}**), 5.91 (ddd, *J* = 15.1, 8.5, 6.2 Hz, 1H, **H_{29}**), 5.83 (d, *J* = 15.3 Hz, 1H, **H_{34}**), 5.76-5.70 (m, 1H, **H_8**), 5.50 (dd, *J* = 8.7, 3.3 Hz, 1H, **H_{12}**), 3.74 (tdd, *J* = 8.3, 4.5, 2.3 Hz, 1H, **H_{20}**), 3.59-3.54 (m, 1H, **H_{19}**), 3.50 (ddd, *J* = 13.9, 5.7, 4.4 Hz, 1H, **H_{27}**), 3.34-3.24 (m, 2H, **H_{19+27}**), 3.10 (d, *J* = 4.5 Hz, 1H, **H_{OH22}**), 2.71 (dd, *J* = 14.9, 8.8 Hz, 1H, **H_{14}**), 2.62 (dd, *J* = 14.8, 3.5 Hz, 1H, **H_{14}**), 2.48-2.43 (m, 1H, **H_{28}**), 2.38 (p, *J* = 7.1 Hz, 1H, **H_{21}**), 2.32-2.25 (m, 1H, **H_{28}**), 2.10 (q, *J* = 7.2 Hz, 2H, **H_7**), 1.79 (s, 3H, **H_{13}**), 1.41-1.35 (m, 2H, **H_6**), 1.41-1.35 (m, 8H, **$H_{2\text{-}5}$**), 1.16 (d, *J* = 7.1 Hz, 3H, **H_{24}**), 0.88 (t, *J* = 7.0 Hz, 3H, **H_1**) ppm.

^{13}C-NMR (151MHz, $CDCl_3$): 176.6 (**$C_{16/23}$**), 174.6 (**$C_{16/23}$**), 165.4 (**C_{25}**), 139.3 (**C_{33}**), 137.2 (**C_{olefin}**), 137.0 (**C_8**), 136.1 (**C_{olefin}**), 131.6 (**C_{olefin}**), 128.2 (**C_{30}**), 127.8 (**C_{olefin}**), 126.8 (**C_{olefin}**), 125.8 (**C_{olefin}**), 125.5 (**C_{olefin}**), 121.5 (**C_{34}**), 75.3 (**C_{12}**), 72.4 (**C_{20}**), 44.9 (**C_{21}**), 43.6 (**C_{27}**), 41.1 (**C_{14}**), 37.9 (**C_{19}**), 33.2 (**C_7**), 33.0 (**C_{28}**), 32.0 (**$C_{2\text{-}5}$**), 29.5 (**$C_{2\text{-}5}$**), 29.4 (**$C_{2\text{-}5}$**), 29.3 (**$C_{2\text{-}5}$**), 14.6 (**C_{24}**), 14.3 (**C_1**), 13.5 (**C_{13}**) ppm.

HRMS (ESI+): exact mass calculated for $[M+Na]^+$ ($C_{29}H_{44}N_2O_5Na^+$) required *m/z* 523.3148, found *m/z* 523.3143.

FT-IR (neat) ν_{max}: 3324, 3305, 2922, 2851, 1709, 1692, 1641, 1547, 1536, 1241, 1217, 969, 760 cm^{-1}.

TLC: R_f (10% MeOH in $CHCl_3$) = 0.50; $KMnO_4$ stain.

2.6.7. Synthesis of Trilactam-FR252921 precursors

2.6.7.1. Diethyl (*syn*-1-(5-(1-hydroxyethyl)-4,5-dihydroisoxazol-3-yl)ethyl)phosphonate (2.167)

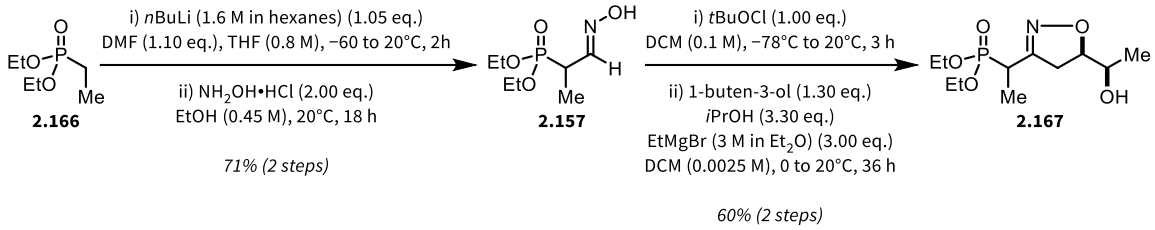

To a solution of Diethyl elthylphosphonate (**2.166**) (3.25 mL, 20.0 mmol, 1.00 eq.) in THF (0.8 M) at −60°C was added *n*BuLi (1.6 M in hexanes) (13.1 mL, 21.0 mmol, 1.05 eq.) and the resulting mixture was stirred at −60°C for 15 min before DMF (1.70 mL, 22.0 mmol, 1.10 eq.) was added. The reaction mixture was subsequently allowed to slowly warm to 20°C over the course of two hours to give a clear solution. The reaction was quenched by addition of 2 M HCl (21.0 mL, 42.0 mmol, 2.10 eq.) followed by addition of 0.100 mL of a sat. aq. solution of $Na_2S_2O_3$. The layers were separated and the aqueous layer was extracted with DCM (3 x 15.0 mL) and the combined organic layers were washed with brine (1 x 15.0 mL), dried over Na_2SO_4, the solids were filtered off and the solvents were removed *in vacuo* to provide the product diethyl (1-oxopropan-2-yl)phosphonate which was used in the next step without further purification.

To a solution of diethyl (1-oxopropan-2-yl)phosphonate (3.88 g, 20.0 mmol, 1.00 eq.) in EtOH (0.45 M) at 20°C was added a solution of $NH_2OH \cdot HCl$ (2.78 g, 40.0 mmol, 2.00 eq.) in water (2 M). The resulting reaction mixture was stirred at 20°C for 18 h before being diluted with water and DCM. The layers were separated and the aqueous layer was extracted with DCM (5 x 20.0 mL). The combined organic layers were washed with brine (1 x 20.0 mL), dried over Na_2SO_4, the solids were filtered off and the solvents were removed *in vacuo* to yield the crude product. The crude material was purified by flash column chromatography (SiO_2, EtOAc/heptane) to yield diethyl (*E*)-(1-(hydroxyimino)propan-2-yl)phosphonate (**2.157**) (2.93 g, 14.1 mmol, 71% over two steps) as a yellow oil.

All spectroscopic data are in accordance with the reported literature.[314]

To a solution of oxime **2.157** (1.05 g, 5.00 mmol, 1.00 eq.) in DCM (0.1 M) at −78°C was dropwise added *t*BuOCl (543 mg, 5.00 mmol, 1.00 eq.) to yield a clear blue solution. The reaction mixture was stirred at −78°C for 60 min before being allowed to slowly warm to room temperature over a span of 90 min. The resulting solution containing diethyl (*Z*)-(1-chloro-1-(hydroxyimino)propan-2-yl)phosphonate (**2.165**) was used in the next step immediately.

To a solution of 1-buten-3-ol (0.563 mL, 6.50 mmol, 1.30 eq.) and *i*PrOH (1.26 mL, 16.5 mmol, 3.30 eq.) in DCM (0.025 M relative to diethyl (*Z*)-(1-chloro-1-(hydroxyimino)propan-2-yl)phosphonate (1.00 eq.)) at 0°C was added EtMgBr (3 M in Et_2O) (5.36 mL, 15.0 mmol, 3.00 eq.) and the resulting mixture was stirred at 0°C for 30 min. Afterwards, the previously prepared solution of diethyl (Z)-(1-chloro-1-(hydroxyimino)propan-2-yl)phosphonate (**2.165**) (1.22 g, 5.00 mmol, 1.00 eq) in DCM (0.1 M) was added at 0°C. The resulting reaction mixture was allowed to warm to 20°C and was subsequently stirred for 36 h. After the reaction time had elapsed, the reaction was quenched by addition of a sat. aq. solution of NH_4Cl (75% of reaction solvent volume) and water (25% of reaction solvent volume) and the layers were separated. The aqueous layer was extracted with EtOAc (3 x 100 mL) and the combined organic layers were washed with brine (1 x 50.0 mL), dried over Na_2SO_4, the solids were filtered off and the solvents were removed *in vacuo* to yield the crude product. The crude material was purified by flash column chromatography (SiO_2, acetone/EtOAc) to yield diethyl (*syn*-1-(5-(1-hydroxyethyl)-4,5-dihydroisoxazol-3-yl)ethyl)phosphonate (**2.167**) (842 mg, 3.01 mmol, 60% over two steps) as a colourless oil.

All spectroscopic data are in accordance with the reported literature.[208,314]

TLC: R_f (15% acetone in EtOAc) = 0.15; $KMnO_4$ stain.

2.6.7.2. ((*2E*,*4E*)-Dodeca-2,4-dien-2-yl)-4,5-dihydroisoxazol-5-yl)ethan-1-ol (2.168)

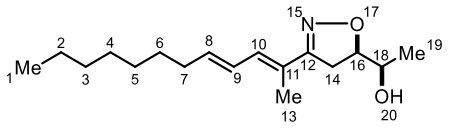

2.168

Chemical Formula: $C_{17}H_{29}NO_2$

To a solution of phosphonate **2.167** (637 mg, 2.28 mmol, 1.00 eq.) in THF (0.1 M) at 0°C was added NaH (60 wt% in paraffin) (228 mg, 5.70 mmol, 2.50 eq.) and the resulting mixture was stirred for 15 min at 0°C. To the thusly formed solution of phosphor ylide was added dropwise *trans*-2-decanal (0.660 mL, 555 mg, 3.42 mmol, 1.50 eq.) at 0°C. After the addition of *trans*-2-decanal was completed, the reaction was allowed to warm to room temperature and was stirred for 18 h or until the starting material had been consumed (as indicated by TLC analysis). The reaction mixture was quenched through careful addition of a sat. aq. solution of NH_4Cl and the layers were separated. The aqueous layer was extracted with EtOAc (3 x 25.0 mL) and the combined organic layers were washed with brine (1 x 25.0 mL) before being dried over Na_2SO_4. The solids were filtered off and the solvents were evaporated to provide crude **2.168**. The crude product was subsequently purified by flash column chromatography (SiO_2, 0 to 40% EtOAc in heptanes) to provide **2.168** (547 mg, 1.96 mmol, 86%) as an orange oil.

^{1}H-NMR (600MHz, $CDCl_3$): δ 6.42-6.39 (m, 1H, **H_9**), 6.21 (d, *J* = 10.9 Hz, 1H, **H_{10}**), 5.93-5.87 (m, 1H, **H_8**; expected dt, *J* = 15.0, 7.1 Hz), 4.45 (ddd, *J* = 10.7, 7.2, 6.0 Hz, 1H, **H_{16}**), 3.71 (p, *J* = 6.2 Hz, 1H, **H_{18}**), 3.16 (dd, *J* = 16.2, 10.7 Hz, 1H, **H_{14}**), 2.92 (dd, *J* = 16.2, 7.3 Hz, 1H, **H_{14}**), 2.17 (dd, *J* = 14.5, 7.2 Hz, 2H, **H_7**), 2.04 (s, 3H, **H_{13}**), 1.45-1.39 (m, 2H, **H_6**), 1.33-1.28 (m, 8H, **$H_{2\text{-}5}$**), 1.24 (d, *J* = 6.4 Hz, 3H, **H_{19}**), 0.88 (t, *J* = 7.0 Hz, 3H, **H_1**) ppm.

^{13}C-NMR (151MHz, $CDCl_3$): δ 160.4 (**C_{12}**), 140.1 (**C_8**), 133.7 (**C_{10}**), 126.0 (**C_9**), 125.4 (**C_{11}**), 85.0 (**C_{16}**), 69.4 (**C_{18}**), 36.5 (**C_{14}**), 33.4 (**C_7**), 32.0 (**C_5**), 29.32 (**C_6**), 29.28 (2C, **$C_{3,4}$**), 22.8 (**C_2**), 19.0 (**C_{19}**), 14.2 (**C_1**), 13.3 (**C_{13}**) ppm.

HRMS (ESI+): exact mass calculated for $[M+Na]^+$ ($C_{17}H_{29}NO_2Na^+$) required *m/z* 302.2096, found *m/z* 302.2094.

FT-IR (neat) ν_{max}: 3401, 2923, 2853, 1637, 1457, 1375, 963, 907, 736 cm^{-1}.

TLC: R_f (30% EtOAc in heptane) = 0.33; $KMnO_4$ stain.

2.6.7.3. Diethyl (*E*)-dec-2-en-1-ylphosphonate (2.177)

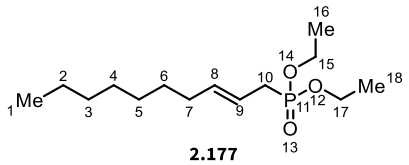

2.177

Chemical Formula: $C_{14}H_{29}O_3P$

To (*E*)-1-bromodec-2-ene (1.95 g, 8.90 mmol, 1.00 eq.) was added triethylphosphite (7.40 g, 44.6 mmol, 5.00 eq.) and the resulting reaction mixture was stirred and heated to reflux for 16 h. After the starting material had been consumed (as indicated by TLC analysis), triethylphosphite was removed under reduced pressure and the crude phosphonate was further purified by Kugelrohr distillation (4 bulbs, 145°C, 10 mBar) to yield **2.177** (1.21 g, 2.80 mmol, 31%) as a colourless oil. (*Nota bene: overall purification attempts: 3 columns and 4 Kugelrohr distillations*).

^{1}H-NMR (600MHz, $CDCl_3$): δ 5.64-5.56 (m, 1H, **H_8**), 5.39 (dq, *J* = 14.6, 7.1 Hz, 1H, **H_9**), 4.14-4.04 (m, 4H, **H_{15+17}**), 2.54 (dd, *J* = 21.4, 7.3 Hz, 2H, **H_{10}**), 2.05-2.00 (m, 2H, **H_7**), 1.38-1.33 (m, 2H, **H_6**), 1.31 (t, *J* = 7.1 Hz, 6H, **H_{16+18}**), 1.29-1.25 (m, 8H, **H_{2-5}**), 0.88 (t, *J* = 7.0 Hz, 3H, **H_1**) ppm.

^{13}C-NMR (151MHz, $CDCl_3$): δ 136.5 (d, *J* = 14.3 Hz, **C_8**), 118.5 (d, *J* = 11.1 Hz, **C_9**), 61.9 (d, *J* = 6.7 Hz, 2C, **C_{15+17}**), 32.8 (d, *J* = 2.0 Hz, **C_7**), 32.0 (2C, **C_{2-5}**, **$_{2-5}$**), 30.6 (d, *J* = 139.6 Hz, **C_{10}**), 29.33 (d, *J* = 3.3 Hz, **C_{2-5}**), 29.26 (d, *J* = 9.9 Hz, **C_{2-5}**), 22.8 (**C_{2-5}**), 16.62 (**C_{16}**), 16.58 (**C_{18}**), 14.2 (**C_1** ppm.

^{31}P-NMR (162MHz, $CDCl_3$): δ 28.1 ppm.

HRMS (ESI+): exact mass calculated for $[M+Na]^+$ ($C_{14}H_{29}O_3PNa^+$) required *m/z* 299.1752, found *m/z* 299.1748.

FT-IR (neat) ν_{max}: 3483, 2957, 2924, 2854, 1459, 1443, 1392, 1367, 1251, 1163, 1097, 1024, 960, 833, 781, 722, 665, 530, 445, 429 cm^{-1}.

TLC: R_f (100% EtOAc) = 0.55; PMA stain.

2.6.7.4. (*E*)-Dec-2-en-1-yltriphenylphosphonium bromide (2.178)

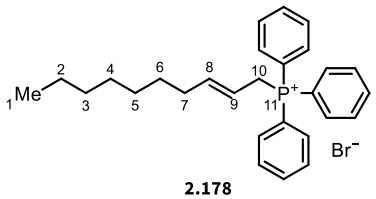

2.178

Chemical Formula: $C_{28}H_{34}BrP$

To (*E*)-1-bromodec-2-ene (2.26 g, 10.3 mmol, 1.00 eq.) in toluene (0.5 M) was added triphenylphosphine (2.70 g, 10.3 mmol, 1.00 eq.) and the resulting mixture was stirred and heated to reflux for 18 h. Afterwards, the reaction mixture was cooled to 0°C to precipitate the phosphonium salt. The crude product was filtered and washed with cold toluene and subsequently dried under vacuum to yield **2.178** (3.40 g, 7.06 mmol, 69%) as an off-white waxy solid.

All spectroscopic data are in accordance with the reported literature.[315]

^{1}H-NMR (600MHz, $CDCl_3$): δ 7.86-7.81 (m, 6H, $\mathbf{H_{o\text{-}Ar}}$), 7.80-7.75 (m, 3H, $\mathbf{H_{p\text{-}Ar}}$), 7.70-7.65 (m, 6H, $\mathbf{H_{m\text{-}Ar}}$), 5.95-5.87 (m, 1H, $\mathbf{H_8}$), 5.28-5.22 (m, 1H, $\mathbf{H_9}$), 4.72 (dd, *J* = 14.7, 7.3 Hz, 2H, $\mathbf{H_{10}}$), 1.95-1.89 (m, 2H, $\mathbf{H_7}$), 1.27 1.13 (m, 8H, $\mathbf{H_{2\text{-}6}}$), 1.10-1.04 (m, 2H, $\mathbf{H_{2\text{-}6}}$), 0.85 (t, *J* = 7.3 Hz, 3H, $\mathbf{H_1}$) ppm.

^{13}C-NMR (151MHz, $CDCl_3$): δ 143.3 (d, *J* = 13.3 Hz, $\mathbf{C_8}$), 135.0 (d, *J* = 3.0 Hz, 3C, $\mathbf{C_{p\text{-}Ar}}$), 134.1 (d, *J* = 9.7 Hz, 6C, $\mathbf{C_{m\text{-}Ar}}$), 130.4 (d, *J* = 12.5 Hz, 6C, $\mathbf{C_{o\text{-}Ar}}$), 118.7 ($\mathbf{C_{i\text{-}Ar}}$), 118.2 (2C, $\mathbf{C_{i\text{-}Ar}}$), 113.8 (d, *J* = 9.9 Hz, $\mathbf{C_9}$), 33.0 (d, *J* = 2.6 Hz, $\mathbf{C_7}$), 31.9 ($\mathbf{C_{2\text{-}6}}$), 29.1 (2C, $\mathbf{C_{2\text{-}6}}$), 28.8 (d, *J* = 3.6 Hz, $\mathbf{C_{2\text{-}6}}$), 28.1 (d, *J* = 48.9 Hz, $\mathbf{C_{10}}$), 22.7 ($\mathbf{C_{2\text{-}6}}$), 14.2 ($\mathbf{C_1}$) ppm.

^{31}P-NMR (243MHz, $CDCl_3$): δ 21.4 ppm.

HRMS (ESI+): exact mass calculated for $[M]^+$ ($C_{28}H_{34}P^+$) required *m/z* 401.2398, found *m/z* 401.2392.

FT-IR (neat) ν_{max}: 3408, 3386, 3362, 3054, 3009, 2953, 2924, 2853, 1667, 1587, 1484, 1463, 1437, 1403, 1188, 1161, 1112, 996, 973, 743, 722, 690, 542, 508, 489, 458, 442, 431, 416 cm^{-1}.

2.6.7.5. *tert*-Butyl (*R*)-(1-((*tert*-butyldimethylsilyl)oxy)-4-oxopentan-3-yl)carbamate (2.173)

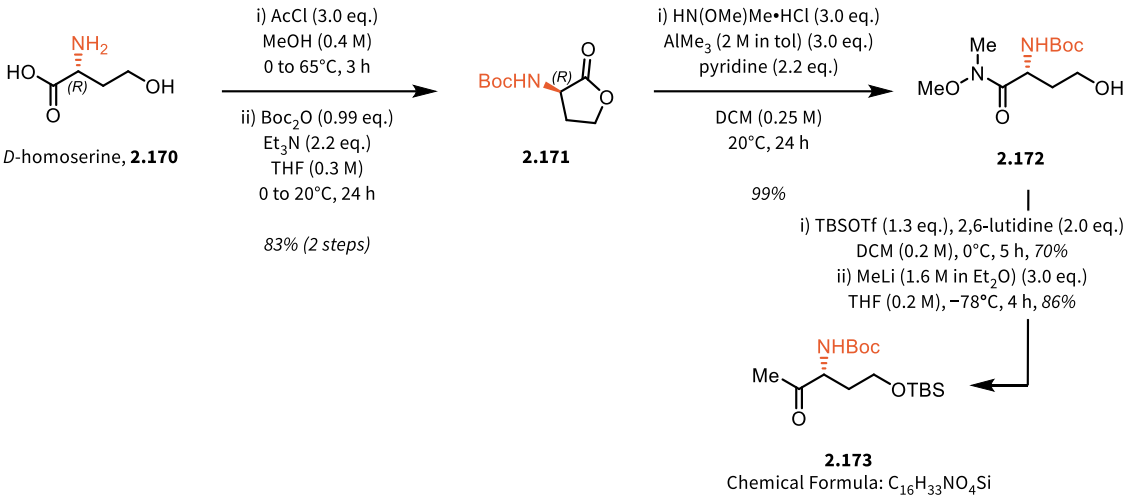

tert-Butyl (*R*)-(1-((*tert*-butyldimethylsilyl)oxy)-4-oxopentan-3-yl)carbamate (**2.173**) was prepared using a modified procedure from the literature.[316]

A flame-dried Schlenk-flask under Argon was charged with MeOH (75.0 mL, 0.4 M) and cooled to 0°C. To the cold MeOH was added AcCl (6.40 mL, 90.0 mmol, 3.00 eq.) and the resulting mixture was stirred at 0°C for 15 min. Afterwards, D-homoserine (**2.170**) (3.57 g, 30.0 mmol, 1.00 eq.) was added in one portion and the resulting mixture was slowly heated to 65°C. Reflux and stirring was maintained for 2 h before the reaction mixture was cooled to 20°C. The solvent was removed under reduced pressure to yield the crude homoserine lactone hydrochloride, which was used in the next step without further purification.

Crude homoserine lactone (4.13 g, 30.0 mmol, 1.00 eq.) was dissolved in THF (0.3 M) at 20°C and Et_3N (9.20 mL, 66.0 mmol, 2.20 eq.) was added. The resulting white suspension was cooled to 0°C before a solution of Boc_2O (6.48 g, 29.7 mmol, 0.990 eq.) in THF (0.6 M) was slowly added dropwise. After the addition was completed, stirring was maintained for additional 10 min at 0°C before the reaction was warmed to 20°C and stirring was continued at 20°C for 24 h. After the reaction time had elapsed, the solvents were removed *in vacuo* and the remaining residue was redissolved in Et_2O (100 mL) and sat. aq. $NaHCO_3$ solution (100 mL). The layers were separated and the aqueous layer was extracted with Et_2O (3 x 70.0 mL). The combined organic layers were dried over Na_2SO_4, the solids were filtered off and the

solvents were removed under reduced pressure to yield crude *N*-Boc homoserine lactone **2.171**. The crude product was purified by flash column chromatography (SiO_2, EtOAc/heptane) to yield **2.171** (5.34 g, 24.8 mmol, 83%) as a white solid.

All spectroscopic data are in accordance with the reported literature.[316]

TLC: R_f (60% EtOAc in heptane) = 0.60; $KMnO_4$ stain.

To a solution of *N*,*O*-dimethylhydroxylamine hydrochloride (7.26 g, 74.4 mmol, 3.00 eq.) in DCM (1 M relative to *N*,*O*-dimethylhydroxylamine, 74.4 mL) was added pyridine (4.41 mL, 54.6 mmol, 2.20 eq.) followed by slow, careful addition of $AlMe_3$ (2 M in toluene) (37.2 mL, 74.4 mmol, 3.00 eq.) (*gas evolution*). The resulting mixture was stirred additional 15 min upon completion of addition of $AlMe_3$ at 20°C before a solution of *N*-Boc-homoserine lactone (**2.171**) (5.34 g, 24.8 mmol, 1.00 eq.) in DCM (1 M, overall concentration 0.25 M) was added dropwise. The resulting mixture was stirred at 20°C for 24 h or until the starting material had been consumed (as indicated by TLC analysis). Subsequently, the reaction mixture was cooled to 0°C prior to the addition of a small amount of a sat. aq. solution of Rochelle salt until gas evolution ceased. The quenched reaction mixture was diluted with a sat. aq. solution of Rochelle salt solution and EtOAc and the layers were separated. The aqueous layer was extracted with EtOAc (3 x 100 mL) and the combined organic layers were dried over Na_2SO_4, the solids were filtered off and the solvents were removed *in vacuo* to provide the crude weinreb amide **2.172**. The crude product was purified by flash column chromatography (SiO_2, EtOAc/heptane) to yield **2.172** (6.44 g, 24.5 mmol, 99%) as a colourless oil.

All spectroscopic data are in accordance with the reported literature.[316]

TLC: R_f (70% EtOAc in heptane) = 0.30; $KMnO_4$ stain.

Weinreb amide **2.172** was protected following the general procedure outlined in chapter 2.5.2.11 on 24.5 mmol scale to yield TBS-protected *tert*-butyl (*R*)-(4-hydroxy-1-(methoxy(methyl)amino)-1-oxobutan-2-yl)carbamate (6.48 g, 17.2 mmol, 70%) as a colourless oil.

All spectroscopic data are in accordance with the reported literature.[316]

TLC: R_f (30% EtOAc in heptane) = 0.31; $KMnO_4$ stain.

To a solution of TBS-protected *tert*-butyl (*R*)-(4-hydroxy-1-(methoxy(methyl)amino)-1-oxobutan-2-yl)carbamate (753 mg, 2.00 mmol, 1.00 eq.) in THF (0.4 M) at −78°C was carefully added MeLi (1.6 M in Et_2O) (3.75 mL, 6.00 mmol, 3.00 eq.) (*gas evolution*) and the resulting reaction mixture was stirred at −78°C for 4 h or until the starting material had been consumed (as indicated by TLC analysis). Afterwards, the reaction was quenched at −78°C by addition of a sat. aq. solution of NH_4Cl (50% reaction solvent volume) and the quenched reaction mixture was warmed to 20°C. Water was added to dissolve the white residue and the layers were separated. The aqueous layer was extracted with Et_2O (5 x reaction solvent amount) and the combined organic layers were dried over Na_2SO_4, the solids were filtered off and the solvents were removed under reduced pressure to yield crude methyl ketone **2.173**. The crude product was purified by flash column chromatography (SiO_2, EtOAc/heptane) to yield **2.173** (572 mg, 1.73 mmol, 83%) as a colourless oil.

All spectroscopic data are in accordance with the reported literature.[316]

TLC: R_f (20% EtOAc in heptane) = 0.56; $KMnO_4$ stain.

2.6.7.6. *tert*-Butyl ((*R*,4*E*,6*E*)-1-((*tert*-butyldimethylsilyl)oxy)-4-methyltetradeca-4,6-dien-3-yl)carbamate (2.174)

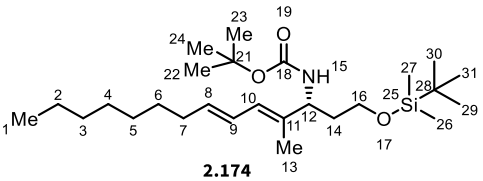

2.174

Chemical Formula: $C_{26}H_{51}NO_3Si$

To a suspension of Wittig salt **2.178** (3.27 g, 6.80 mmol, 2.00 eq.) in THF (0.15 M) at 0°C was added *n*BuLi (2.5 M in hexanes) (2.72 mL, 6.80 mmol, 2.00 eq.) and the resulting deep red mixture was stirred at 0°C for 30 min during which the colour lightened to yellow. To the activated ylide solution was subsequently added a solution of methylketone **2.173** (1.13 g, 3.40 mmol, 1.00 eq.) in THF (0.15 M) at 0°C. The reaction mixture was then stirred for 16 h, during which time it was allowed to warm to 20°C. After the starting material had been consumed (as indicated by TLC analysis), the reaction was quenched by addition of a

sat. aq. solution of NH_4Cl (20.0 mL) and the layers were separated. The aqueous layer was extracted with DCM (3 x 20.0 mL) and the combined organic layers were washed with brine (1 x 20.0 mL). The combined organic layers were dried over Na_2SO_4 and the solids were filtered off. The solvents were removed *in vacuo* and the crude product was purified by flash column chromatography (SiO_2, EtOAc/heptane) to afford **2.174** (1.03 g, 3.40 mmol, 67%) as a colourless oil.

^{1}H-NMR (400MHz, $CDCl_3$): δ 6.22 (dd, *J* = 15.0, 10.8 Hz, 1H, **H_9**), 5.95 (d, *J* = 10.8 Hz, 1H, **H_{10}**), 5.69-5.58 (m, 1H, **H_8**), 5.54 (bs, 1H, **H_{15}**), 4.26-4.00 (b, 1H, **H_{12}**), 3.72-3.57 (m, 2H, **H_{16}**), 2.09 (dd, *J* = 13.9, 6.8 Hz, 2H, **H_7**), 1.86-1.75 (b, 1H, **H_{14}**), 1.70 (s, 4H, **H_{13+14}**), 1.43 (s, 9H, **H_{22-24}**), 1.40-1.34 (m, 2H, **H_6**), 1.27 (b, 8H, **H_{2-5}**), 0.91 (s, 9H, **H_{29-31}**), 0.88 (t, *J* = 6.9 Hz, 3H, **H_1**), 0.04 (s, 6H, **H_{26+27}**) ppm.

TLC: R_f (20% EtOAc in heptane) = 0.62; $KMnO_4$ stain.

2.6.7.7. *tert*-butyl ((*R*,4*E*,6*E*)-1-hydroxy-4-methyltetradeca-4,6-dien-3-yl)carbamate (2.175)

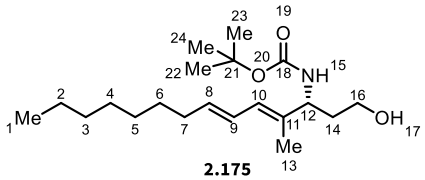

2.175

Chemical Formula: $C_{20}H_{37}NO_3$

To a solution of TBS-protected alcohol **2.174** (454 mg, 1.00 mmol, 1.00 eq.) in THF (0.2 M) at 0°C was added TBAF (1 M in THF) (1.10 mL, 1.10 mmol, 1.10 eq.) dropwise., upon which the reaction colour turned from colourless to yellow/brown. Afterwards, the reaction was stirred at 0°C for 2 h or until the starting material had been consumed (as indicated by TLC analysis). The reaction was quenched by addition of a sat. aq. solution of NH_4Cl (5.00 mL) and the layers were separated. The aqueous layer was extracted with DCM (4 x 5.00mL) and the combined organic layers were washed with brine (1 x 5.00 mL). The organic layers were dried over Na_2SO_4, the solids were filtered off and the solvents were removed *in vacuo*. The crude alcohol was subsequently purified by flash column chromatography (SiO_2, EtOAc/heptane) to afford pure alcohol **2.175** (245 mg, 0.722 mmol, 72%) as a colourless oil which solidified upon cooling to 4°C.

^{1}H-NMR (600MHz, $CDCl_3$): δ 6.21 (ddt, *J* = 14.8, 10.6, 1,2 Hz, 1H, **H_9**), 5.97 (d, *J* = 10.6 Hz, 1H, **H_{10}**), 5.74-5.64 (m, 1H, **H_8**), 4.67 (bd, *J* = 7.7 Hz, 1H, **H_{15}**), 4.23 (bs, 1H, **H_{15}**), 3.71-3.62 (m, 2H, **H_{16}**), 2.94 (b, 1H, **H_{17}**), 2.09 (q,

J = 7.2 Hz, 2H, **H$_7$**), 1.92-1.85 (m, 1H, **H$_{14}$**), 1.76 (s, 3H, **H$_{13}$**), 1.55 (b, 1H, **H$_{14}$**), 1.44 (s, 9H, **H$_{22\text{-}24}$**), 1.40-1.36 (m, 2H, **H$_6$**), 1.33-1.22 (m, 8H, **H$_{2\text{-}5}$**), 0.88 (t, *J* = 7.0 Hz, 3H, **H$_1$**) ppm.

^{13}C-NMR (151MHz, $CDCl_3$): δ 156.7 (**C$_{18}$**), 135.8 (**C$_8$**), 134.2 (**C$_{11}$**), 125.9 (**C$_9$**), 125.8 (**C$_{10}$**), 80.0 (**C$_{21}$**), 59.3 (**C$_{16}$**), 53.8 (**C$_{12}$**), 36.8 (**C$_{14}$**), 33.1 (**C$_6$**), 32.0 (**C$_{2\text{-}5}$**), 29.6 (**C$_{2\text{-}5}$**), 29.4 (**C$_{2\text{-}5}$**), 29.3 (**C$_{2\text{-}5}$**), 28.5 (3C, **C$_{22\text{-}24}$**), 22.8 (**C$_{2\text{-}5}$**), 14.6 (**C$_{13}$**), 14.3 (**C$_1$**) ppm.

HRMS (ESI+): exact mass calculated for $[M+Na]^+$ ($C_{20}H_{37}NO_3Na^+$) required *m/z* 362.2671, found *m/z* 362.2661.

FT-IR (neat) ν_{max}: 3347, 2956, 2924, 2854, 1689, 1503, 1455, 1390, 1365, 1248, 1169, 1052, 963, 873, 757, 722, 667 cm^{-1}.

TLC: R_f (50% EtOAc in heptane) = 0.51; $KMnO_4$ stain;

R_f (50% EtOAc in heptane) = 0.95, $KMnO_4$ stain (starting material).

2.6.7.8. (*R*,4*E*,6*E*)-3-((*tert*-butoxycarbonyl)amino)-4-methyltetradeca-4,6-dienoic acid (2.S49)

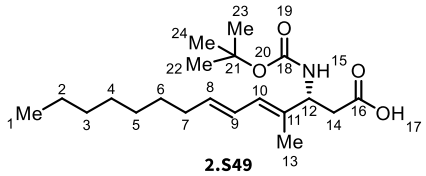

2.S49

Chemical Formula: $C_{20}H_{35}NO_4$

To a solution of primary alcohol **2.175** (197 mg, 0.580 mmol, 1.00 eq.) in acetone (0.1 M) at 0°C was added Jones reagent (CrO_3, 2.5 M in H_2SO_4) (0.510 mL, 1.28 mmol, 2.20 eq.) and the resulting dark red solution was stirred at 0°C for 1 h or until the starting material had been consumed (as indicated by TLC analysis). Afterwards, the reaction was diluted with Et_2O and water at 0°C and pH was controlled (pH = 2-3). The layers were separated and the aqueous layer was extracted with Et_2O (3 x 5.00 mL). The combined organic layers were washed with water (1 x 5.00 mL) and brine (1 x 5.00 mL). The combined organic layers were dried over Na_2SO_4, the solids were filtered off and the solvents were removed *in vacuo* to yield crude carboxylic acid **2.S49**, which was used in the next step without further purification.

HRMS (ESI+): exact mass calculated for $[M+Na]^+$ ($C_{20}H_{35}NO_4Na^+$) required *m/z* 376.2464, found *m/z* 376.2458.

TLC: R_f (50% EtOAc in heptane) = 0.25; $KMnO_4$ stain;

R_f (50% EtOAc in heptane) = 0.51, $KMnO_4$ stain (starting material).

2.6.7.9. *tert*-Butyl ((*R*,4*E*,6*E*)-1-(((2*R*,3*S*)-2-((*tert*-butyldimethylsilyl)oxy)-3-methyl-4-oxo-4-(((*E*)-4-(4,4,5,5-tetramethyl-1,3,2-dioxaborolan-2-yl)but-3-en-1-yl)amino)butyl)amino)-4-methyl-1-oxotetradeca-4,6-dien-3-yl)carbamate (2.176)

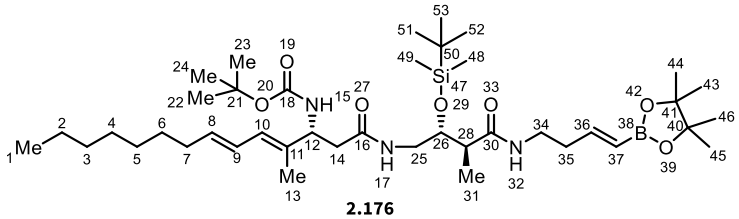

2.176

Chemical Formula: $C_{41}H_{76}BN_3O_7Si$

To a solution of carboxylic acid **2.S49** (205 mg, 0.580 mmol, 1.00 eq.) and FR core amine **2.095** (297 mg, 0.696 mmol, 1.20 eq.) in DCM (0.1 M) at 0°C was added Et_3N (0.243 mL, 1.74 mmol, 3.00 eq.) and HATU (270 mg, 0.696 mmol, 1.20 eq.). The resulting reaction was mixture allowed to warm to room temperature and was stirred for 18 h or until the starting materials had been consumed (as indicated by TLC analysis). Afterwards, the reaction was quenched by addition of 1 M aqueous HCl (5.00 mL) and the layers were separated. The aqueous layer was extracted with DCM (3 x 5.00 mL) and the combined organic layers were washed with brine (1 x 5.00 mL). The organic layers were dried over Na_2SO_4, the solids were filtered off, the solvents were removed under reduced pressure and the crude product was purified by flash column chromatograph (SiO_2, 3:1EtOAc/EtOH in heptane) to afford **2.176** (34 mg, 44.6 µmol, 8%) as a yellow foam. Analysis and assignment of signals is impeded due to the presence of rotamers.

^{1}H-NMR (700MHz, $CDCl_3$): δ 6.55 (dt, *J* = 18.0, 6.5 Hz, 1H, **H_{36}**), 6.23-6.17 (m, 3H, **$H_{9+NH32+NH15}$**), 5.95 (d, *J* = 10.4 Hz, 1H, **H_{10}**), 5.71-5.64 (m, 1H, **H_8**), 5.51 (ddd, *J* = 18.0, 3.3, 1.5 Hz, 1H, **H_{37}**), 4.33 (b, 1H, **H_{NH17}**), 3.89 (dt, *J* = 8.0, 4.4 Hz, 0.5H, **H_{26}**), 3.88-3.83 (m, 1H, **H_{25}**), 3.76-3.73 (m, 0.5H, **H_{14}**), 3.73-3.69 (m, 0.5H, **H_{26}**), 3.48-3.40 (m, 1H, **H_{34}**), 3.30-3.21 (m, 1H, **H_{34}**), 2.88 (ddd, *J* = 13.6, 7.7, 4.5 Hz, 0.5H, **H_{14}**), 2.85-2.82 (bm, 0.5H, **H_x**), 2.50-2.46 (m, 1H, **H_{14}**), 2.43-2.38 (m, 1.5H, **H_x**), 2.38-2.33 (m, 4H, **$H_{25+28+35}$**), 2.16 (td, *J* = 7.4, 3.2 Hz, 1H,

$\mathbf{H_x}$), 2.10-2.05 (m, 2H, $\mathbf{H_7}$), 1.73 (s, 3H, $\mathbf{H_{13}}$), 1.61 (s, 6H, $\mathbf{H_x}$), 1.42 (s, 9H, $\mathbf{H_{22\text{-}24}}$), 1.40-1.34 (m, 2H, $\mathbf{H_6}$), 1.33-1.21 (m, 29H, $\mathbf{H_{2\text{-}5,\ 43\text{-}46,\ 51\text{-}53}}$) 1.09 (d, *J* = 7.2 Hz, 3H, $\mathbf{H_{31}}$), 0.92-0.77 (m, 6H, $\mathbf{H_{48+49}}$) ppm.

^{13}C-NMR (176MHz, $CDCl_3$): δ 174.60 ($\mathbf{C_{30}}$), 174.55 ($\mathbf{C_{16}}$), 173.55 ($\mathbf{C_x}$), 155.5 ($\mathbf{C_{18}}$), 150.4 ($\mathbf{C_{36}}$), 135.8 ($\mathbf{C_8}$), 133.6 ($\mathbf{C_{11}}$), 125.9 (2C, $\mathbf{C_{9+10}}$), 121.4 ($\mathbf{C_{37}}$; *deduced from HSQC*), 83.38 ($\mathbf{C_{40}}$), 83.36 ($\mathbf{C_{41}}$), 72.2 ($\mathbf{C_{25}}$), 72.0 ($\mathbf{C_{26}}$), 44.9 ($\mathbf{C_x}$), 44.6 ($\mathbf{C_{28}}$), 43.1 ($\mathbf{C_x}$), 42.6 ($\mathbf{C_{14}}$), 40.7 ($\mathbf{C_x}$), 38.1 ($\mathbf{C_q}$), 38.0 ($\mathbf{C_{34}}$), 37.9 ($\mathbf{C_x}$), 36.8 ($\mathbf{C_x}$), 35.9 ($\mathbf{C_{q?}}$), 35.8 ($\mathbf{C_{35}}$), 33.2 ($\mathbf{C_7}$), 32.0 ($\mathbf{C_{2\text{-}5,\ 43\text{-}46,\ 51\text{-}53}}$), 31.8 ($\mathbf{C_{2\text{-}5,\ 43\text{-}46,\ 51\text{-}53}}$), 29.85 ($\mathbf{C_{2\text{-}5,\ 43\text{-}46,\ 51\text{-}53}}$), 29.56 ($\mathbf{C_{2\text{-}5,\ 43\text{-}46,\ 51\text{-}53}}$), 29.42 ($\mathbf{C_{2\text{-}5,\ 43\text{-}46,\ 51\text{-}53}}$), 29.38 ($\mathbf{C_{2\text{-}5,\ 43\text{-}46,\ 51\text{-}53}}$), 29.33 ($\mathbf{C_{2\text{-}5,\ 43\text{-}46,\ 51\text{-}53}}$), 29.15 ($\mathbf{C_{2\text{-}5,\ 43\text{-}46,\ 51\text{-}53}}$), 28.6 ($\mathbf{C_{22\text{-}24}}$), 26.04 ($\mathbf{C_{2\text{-}5,\ 43\text{-}46,\ 51\text{-}53}}$), 26.02 ($\mathbf{C_{2\text{-}5,\ 43\text{-}46,\ 51\text{-}53}}$), 25.8 ($\mathbf{C_{50}}$), 24.98 ($\mathbf{C_{2\text{-}5,\ 43\text{-}46,\ 51\text{-}53}}$), 24.93 ($\mathbf{C_{2\text{-}5,\ 43\text{-}46,\ 51\text{-}53}}$), 22.81 ($\mathbf{C_{2\text{-}5,\ 43\text{-}46,\ 51\text{-}53}}$), 22.75 ($\mathbf{C_{2\text{-}5,\ 43\text{-}46,\ 51\text{-}53}}$), 18.1 ($\mathbf{C_q}$), 15.6 ($\mathbf{C_{31}}$), 15.2 ($\mathbf{C_{31?}}$), 14.25 ($\mathbf{C_1}$), 14.22 ($\mathbf{C_{13}}$), −4.34 ($\mathbf{C_{48+49}}$), −4.38 ($\mathbf{C_{48+49}}$), −4.80 ($\mathbf{C_{48+49}}$), −4.87 ($\mathbf{C_{48+49}}$) ppm.

HRMS (ESI+): exact mass calculated for $[M+Na]^+$ ($C_{41}H_{76}BN_3O_7SiNa^+$) required *m/z* 784.5443, found *m/z* 784.5445.

FT-IR (neat) ν_{max}: 3306, 2976, 2954, 2927, 2855, 1642, 1536, 1462, 1390, 1362, 1323, 1251, 1217, 1167, 1145, 1100, 1049, 1026, 1004, 968, 848, 837, 808, 776, 667 cm^{-1}.

TLC: R_f (40% 3:1EtOAc/EtOH in heptane) = 0.61; $KMnO_4$ stain.

2.6.8. Synthesis of OMe-FR252921

2.6.8.1. (2*S*,3*R*)-4-azido-3-methoxy-2-methylbutanoic acid (2.184)

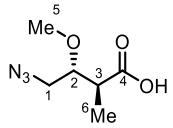

2.184

Chemical Formula: $C_6H_{11}N_3O_3$

To a solution of ethyl (*2S*,*3R*)-4-azido-3-methoxy-2-methylbutanoate (**2.183**) (1.06 g, 5.00 mmol, 1.00 eq.) in DCE (0.2 M) was added Me_3SnOH (4.52 g, 25.0 mmol, 5.00 eq.) and the resulting mixture was heated to 80°C for 72 h. Afterwards, the reaction was allowed to cool to room temperature and the solvents were removed under reduced pressure. The concentrated crude material was dissolved in EtOAc (50.0 mL) and was washed with 5% HCl (3 x 50.0 mL), water (1 x 50.0 mL) and brine (1 x 50.0 mL). The organic layer was

dried over Na_2SO_4, the solids were filtered off and the solvents were removed *in vacuo* to yield carboxylic acid **2.184** amenable to be used without further purification.

^{1}H-NMR (400MHz, $CDCl_3$): δ 3.58 (ddd, *J* = 7.2, 5.6, 3.4 Hz, 1H, **H_2**), 3.54-3.45 (m, 4H, **H_{1+5}**), 3.30 (dd, *J* = 13.2, 5.5 Hz, 1H, **H_1**), 2.85 (p, *J* = 7.2 Hz, 1H, **H_3**), 1.19 (d, *J* = 7.2 Hz, 3H, **H_6**) ppm.

HRMS (ESI+): exact mass calculated for $[M+Na]^+$ ($C_6H_{11}N_3O_3Na^+$) required *m/z* 196.0698, found *m/z* 196.0690.

2.6.9. Synthesis of Bioiso-FR252921

2.6.9.1. (*R*,4*E*,6*E*)-1-((*S*)-4-benzyl-2-thioxothiazolidin-3-yl)-3-((*tert*-butyldimethylsilyl)oxy)-4-methyltetradeca-4,6-dien-1-one (2.189)

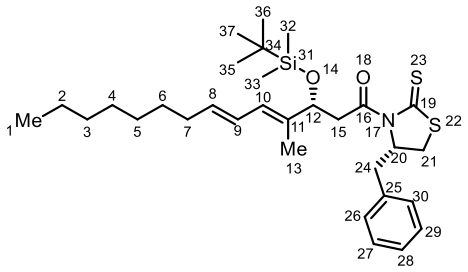

2.189

Chemical Formula: $C_{31}H_{49}NO_2S_2Si$

(*R*,4*E*,6*E*)-1-((*S*)-4-benzyl-2-thioxothiazolidin-3-yl)-3-((*tert*-butyldimethylsilyl)oxy)-4-methyltetradeca-4,6-dien-1-one (**2.189**) was synthesised according to the general procedure outlined in chapter 2.5.2.11. on 2.00 mmol scale to yield **2.189** (883 mg, 1.58 mmol, 79%) as a yellow oil.

^{1}H-NMR (600MHz, $CDCl_3$): δ 7.35 (t, *J* = 7.4 Hz, 2H, **$H_{26,30}$**), 7.29 (d, *J* = 7.5 Hz, 3H, **H_{27-29}**), 6.20 (dd, *J* = 15.0, 10.8 Hz, 1H, **H_9**), 5.98 (d, *J* = 10.8 Hz, 1H, **H_{10}**), 5.66 (dt, *J* = 15.1, 7.5 Hz, 1H, **H_8**), 5.19 (ddd, *J* = 10.6, 6.9, 3.6 Hz, 1H, **H_{20}**), 4.70 (dd, *J* = 9.1, 3.5 Hz, 1H, **H_{12}**), 3.91 (dd, *J* = 15.8, 9.2 Hz, 1H, **H_{15}**), 3.32 (dd, *J* = 11.3, 7.1 Hz, 1H, **H_{21}**), 3.26 (dd, *J* = 13.2, 2.4 Hz, 1H, **H_{24}**), 3.03 (dd, *J* = 13.1, 10.9 Hz, 1H, **H_{24}**), 2.95 (dd, *J* = 15.8, 3.6 Hz, 1H, **H_{21}**), 2.87 (d, *J* = 11.5 Hz, 1H, **H_{15}**), 2.09 (q, *J* = 7.2 Hz, 2H, **H_7**), 1.73 (s, 3H, **H_{13}**), 1.38-1.36 (m, 2H, **H_6**), 1.32-1.27 (m, 8H, **H_{2-5}**), 0.89-0.84 (m, 12H, **$H_{1,35-37}$**), 0.06 (s, 3H, **H_{32}**), 0.01 (s, 3H, **H_{33}**) ppm.

^{13}C-NMR (151MHz, $CDCl_3$): δ 201.3 (**C_{22}**), 172.1 (**C_{16}**), 136.8 (**C_{11}**), 136.6 (**C_{25}**), 135.6 (**C_8**), 129.6 (2C, **$C_{27,29}$**), 129.1 (2C, **$C_{26.30}$**), 127.3 (**C_{28}**), 126.1 (**C_{10}**), 126.0 (**C_9**), 75.3 (**C_{12}**), 69.1 (**C_{20}**), 45.5 (**C_{15}**), 36.7 (**C_{24}**), 33.1 (**C_7**), 32.4 (**C_{21}**),

32.0 (**C$_2$**), 29.5 (**C$_6$**), 29.4 (**C$_{3\text{-}5}$**), 29.3 (**C$_{3\text{-}5}$**), 25.9 (3C, **C$_{35\text{-}37}$**), 22.8 (**C$_{3\text{-}5}$**), 18.2 (**C$_{34}$**), 14.2 (**C$_1$**), 12.1 (**C$_{13}$**), −4.6 (**C$_{32}$**), −5.0 (**C$_{33}$**) ppm.

HRMS (ESI+): exact mass calculated for $[M+Na]^+$ ($C_{31}H_{49}NO_2S_2SiNa^+$) required *m/z* 582.2872, found *m/z* 582.2862.

FT-IR (neat) ν_{max}: 3027, 2953, 2925, 2854, 1698, 1496, 1455, 1438, 1359, 1340, 1283, 1251, 1225, 1190, 1161, 1136, 1076, 1039, 1006, 965, 941, 894, 835, 811, 776, 744, 701, 666, 610, 561, 548, 508, 483 cm^{-1}.

TLC: R_f (20% EtOAc in heptane) = 0.90; $KMnO_4$ stain.

2.6.9.2. (*R*,4*E*,6*E*)-3-((*tert*-butyldimethylsilyl)oxy)-4-methyltetradeca-4,6-dienal (2.190)

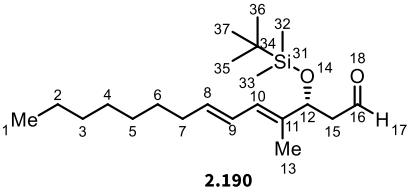

2.190

Chemical Formula: $C_{21}H_{40}O_2Si$

To a solution of TBS-aldol product **2.189** (1.71 g, 3.05 mmol, 1.00 eq.) in Et_2O (0.1 M) at −78°C was added dropwise over five minutes DIBAL-H (1 M in toluene) (3.08 mL, 3.08 mmol, 1.01 eq.). The resulting mixture was stirred at −78°C for 60 min or until full conversion of the starting material was observed (as indicated by ^{1}H-NMR or TLC analysis). After the starting material had been consumed, the reaction was quenched by addition of 0.200 mL of water. The resulting mixture was stirred at −78°C for 5 min before being allowed to warm to 20°C. Afterwards, $MgSO_4$ was added and the reaction mixture was stirred until an opaque gel formed. The opaque gel was then filtered through a short pad of Celite® and the filter cake was washed with Et_2O. The filtrate was concentrated under reduced pressure and the crude product was purified by flash column chromatography (SiO_2, EtOAc/heptane or Et_2O/pentane) to afford **2.190** (897 mg, 2.54 mmol, 83%) as a colourless oil.

^{1}H-NMR (600MHz, $CDCl_3$): δ 9.75 (t, *J* = 2.5 Hz, 1H, **H$_{17}$**), 6.19 (dd, *J* = 15.0, 10.9 Hz, 1H, **H$_9$**), 6.01 (d, *J* = 10.8 Hz, 1H, **H$_{10}$**), 5.68 (dt, *J* = 14.9, 7.4 Hz, 1H, **H$_8$**), 4.55 (dd, *J* = 8.2, 4.1 Hz, 1H, **H$_{12}$**), 2.67 (ddd, *J* = 15.4, 8.3, 2.9 Hz, 1H, **H$_{15}$**), 2.42 (ddd, *J* = 15.4, 4.1, 2.0 Hz, 1H, **H$_{15}$**), 2.10 (q, *J* = 7.2 Hz, 2H, **H$_7$**), 1.71 (s, 3H, **H$_{13}$**),

1.40-1.37 (m, 2H, **H$_6$**), 1.31-1.27 (m, 8H, **H$_{2\text{-}5}$**), 0.89-0.87 (m, 12H, **H$_{1,35\text{-}37}$**), 0.05 (s, 3H, **H$_{32}$**), 0.00 (s, 3H, **H$_{33}$**) ppm.

^{13}C-NMR (151MHz, $CDCl_3$): δ 202.1 (**C$_{16}$**), 135.9 (**C$_8$**), 135.8 (**C$_{11}$**), 126.1 (**C$_{10}$**), 125.7 (**C$_9$**), 73.8 (**C$_{12}$**), 50.2 (**C$_{15}$**), 33.2 (**C$_7$**), 32.0 (**C$_2$**), 29.5 (**C$_6$**), 29.4 (**C$_{3\text{-}5}$**), 29.3 (**C$_{3\text{-}5}$**), 25.9 (3C, **C$_{35\text{-}37}$**), 22.8 (**C$_{3\text{-}5}$**), 18.2(**C$_{34}$**), 14.2 (**C$_1$**), 12.1 (**C$_{13}$**), −4.5 (**C$_{32}$**), −5.1 (**C$_{33}$**) ppm.

FT-IR (neat) ν_{max}: 2954, 2923, 2853, 1728, 1681, 1599, 1461, 1377, 1252, 1075, 1002, 965,836, 776, 740, 669 cm^{-1}.

$[a]_D^{20}$ = +2.13° (c = 1.00, $CHCl_3$).

TLC: R_f (10% EtOAc in heptane) = 0.65; $KMnO_4$ stain.

2.6.9.3. *tert*-butyldimethyl(((*R*,5*E*,7*E*)-5-methylpentadeca-5,7-dien-1-yn-4-yl)oxy)silane (2.S50)

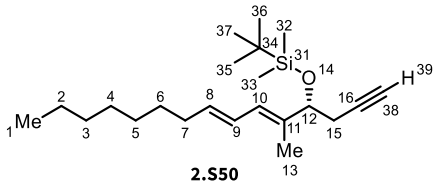

2.S50

Chemical Formula: $C_{22}H_{40}OSi$

To a solution of aldehyde **2.190** (896 mg, 2.54 mmol, 1.00 eq.) in MeOH (0.1 M) at 0°C was added dimethyl-(1-diazo-2-oxopropyl)phosphonate (Bestmann-Ohira reagent, 10 wt% in MeCN) (9.15 mL, 3.81 mmol, 1.50 eq.) and K_2CO_3 (1.05 g, 7.62 mmol, 3.00 eq.). The resulting mixture was stirred at 0°C for 3 h before being diluted with Et_2O (25.0 mL) and water (25.0 mL). The layers were separated and the aqueous layer was extracted with Et_2O (3 x 25.0 mL) and the combined organic layers were washed with brine (1 x 25.0 mL). The combined organic layers were dried over Na_2SO_4, the solids were filtered off and the solvents were removed under reduced pressure. The crude product was purified by flash column chromatography (SiO_2, EtOAc/heptane) to afford **2.S50** (526 mg, 1.51 mmol, 59%) as a colourless oil.

^{1}H-NMR (600MHz, $CDCl_3$): δ 6.21 (dd, *J* = 15.0, 10.9 Hz, 1H, **H$_9$**), 5.97 (d, *J* = 10.8 Hz, 1H, **H$_{10}$**), 5.67 (dt, *J* = 15.0, 7.5 Hz, 1H, **H$_8$**), 4.18 (t, *J* = 6.5 Hz, 1H, **H$_{12}$**) 2.40 (ddd, *J* = 16.6, 7.2, 2.6 Hz, 1H, **H$_{15}$**), 2.35 (ddd,

J = 16.6, 6.0, 2.6 Hz, 1H, **H$_{15}$**), 2.10 (q, *J* = 7.2 Hz, 2H, **H$_7$**), 1.94 (t, *J* = 2.6 Hz, 1H, **H$_{39}$**),1.69 (s, 3H, **H$_{13}$**), 1.30-1.37 (m, 2H, **H$_6$**), 1.31-1.26 (m, 8H, **H$_{2\text{-}5}$**), 0.90-0.84 (m, 12H, **H$_{1,35\text{-}37}$**), 0.07 (s, 3H, **H$_{32}$**), 0.01 (s, 3H, **H$_{33}$**) ppm.

^{13}C-NMR (151MHz, $CDCl_3$): δ 136.1 (**C$_{11}$**), 135.3 (**C$_8$**), 126.3 (**C$_{10}$**), 125.9 (**C$_9$**), 82.1 (**C$_{16}$**), 77.2 (**C$_{12}$**), 69.8 (**C$_{38}$**), 33.2 (**C$_7$**), 32.0 (**C$_2$**), 29.9 (**C$_6$**), 29.5 (**C$_{3\text{-}5}$**), 29.4 (**C$_{3\text{-}5}$**), 27.2 (**C$_{15}$**), 25.9 (3C, **C$_{35\text{-}37}$**), 22.8 (**C$_{3\text{-}5}$**), 18.4 (**C$_{34}$**), 14.3 (**C$_1$**), 11.7 (**C$_{13}$**), −4.6 (**C$_{32}$**), −4.8 (**C$_{33}$**) ppm.

HRMS (ESI+): exact mass calculated for $[M+Na]^+$ ($C_{22}H_{40}OSiNa^+$) required *m/z* 371.2746, found *m/z* 371.2739.

FT-IR (neat) ν$_{max}$: 3314,2954, 2925, 2854, 1713, 1683, 1462, 1361, 1251, 1221, 1073, 1006, 965, 936, 890, 836, 810, 776, 739, 668, 635 cm^{-1}.

[a]$_D^{20}$ = −7.35° (c = 1.00, $CHCl_3$).

TLC: R_f (10% Et_2O in pentane) = 0.87; $KMnO_4$ stain.

2.6.9.4. (*R*,5*E*,7*E*)-5-methylpentadeca-5,7-dien-1-yn-4-ol (2.192)

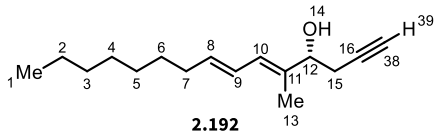

2.192

Chemical Formula: $C_{16}H_{26}O$

(*R*,5*E*,7*E*)-5-methylpentadeca-5,7-dien-1-yn-4-ol (**2.192**) was synthesised according to the general procedure outlined in chapter 2.5.2.19. on 0.220 mmol scale in THF (0.2 M) to yield **2.192** (45.0 mg, 0.192 mmol, 87%) as a colourless oil.

^{1}H-NMR (600MHz, $CDCl_3$): δ 6.23 (ddt, *J* = 14.9, 10.8, 1.4 Hz, 1H, **H$_9$**), 6.08 (d, *J* = 10.9 Hz, 1H, **H$_{10}$**), 5.75-5.71 (m, 1H, **H$_8$**), 4.23 (t, *J* = 6.4 Hz, 1H, **H$_{12}$**), 2.48 (dd, *J* = 6.4, 2.6 Hz, 2H, **H$_{15}$**), 2.11 (q, *J* = 7.1 Hz, 2H, **H$_7$**), 2.05 (t, *J* = 2.6 Hz, 1H, **H$_{39}$**), 1.95 (b, 1H, **H$_{14}$**), 1.75 (d, *J* = 0.7 Hz, 3H, **H$_{13}$**), 1.39-1.38 (m, 2H, **H$_6$**), 1.30-1.26 (m, 8H, **H$_{2\text{-}5}$**), 0.91 (s, 3H, **H$_1$**) ppm.

^{13}C-NMR (151MHz, $CDCl_3$): δ 136.4 (**C$_8$**), 135.0 (**C$_{11}$**), 126.6 (**C$_{10}$**), 125.7 (**C$_9$**), 81.0 (**C$_{16}$**), 75.4 (**C$_{12}$**), 70.8 (**C$_{38}$**), 33.2 (**C$_7$**), 32.0 (**C$_{2\text{-}5}$**), 29.5 (**C$_{2\text{-}5}$**), 29.34 (**C$_6$**), 29.32 (**C$_{2\text{-}5}$**), 26.1 (**C$_{14}$**), 22.8 (**C$_{2\text{-}5}$**), 14.2 (**C$_1$**), 12.4 (**C$_{13}$**) ppm.

HRMS (ESI+): exact mass calculated for $[M+Na]^+$ ($C_{16}H_{26}ONa^+$) required *m/z* 257.1881, found *m/z* 257.1874.

FT-IR (neat) ν$_{max}$: 3312, 2923, 2853, 1462, 1378, 1252, 1016, 964, 630 cm^{-1}.

TLC: R_f (5% Et_2O in pentane) = 0.50; $KMnO_4$ stain.

2.6.9.5. (2*S*,3*R*)-3-((*tert*-butyldimethylsilyl)oxy)-4-(4-((*R*,3*E*,5*E*)-2-hydroxy-3-methyltrideca-3,5-dien-1-yl)-1*H*-1,2,3-triazol-1-yl)-2-methyl-*N*-((*E*)-4-(4,4,5,5-tetramethyl-1,3,2-dioxaborolan-2-yl)but-3-en-1-yl)butanamide (2.194)

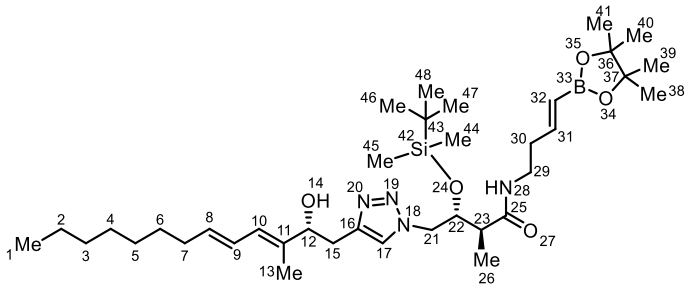

2.194
Chemical Formula: $C_{37}H_{67}BN_4O_5Si$

To a solution of FR core azide **2.193** (103 mg, 0.192 mmol, 1.00 eq.) in THF (0.15 M) at 20°C was added alkyne **2.192** (45.0 mg, 0.192 mmol, 1.00 eq.), followed by addition of DIPEA (66.9 µL, 0.384 mmol, 2.00 eq.) and CuI (36.8 mg, 0.192 mmol, 1.00 eq.). The resulting cloudy reaction mixture was stirred at 20°C for 22 h. Afterwards, the solvents were removed *in vacuo* and the resulting crude product was purified by flash column chromatography (SiO_2, 10 mL/0.1mmol C_v, MeOH in DCM gradient, 0% (1 C_v) → 1% (1 C_v) → 2% (2 C_v) → 4% (2 C_v) → 7% (2 C_v) → 10% (2 C_v)) to afford **2.194** (104 mg, 0.151 mmol, 79%) as a white foam.

^{1}H-NMR (600MHz, $CDCl_3$): δ 7.53 (s, 1H, **H_{17}**), 6.55 (dt, *J* = 18.0, 6.5 Hz, 1H, **H_{31}**), 6.23 (dd, *J* = 15.0, 10.9 Hz, 1H, **H_9**), 6.07 (d, *J* = 10.7 Hz, 1H, **H_{10}**), 5.95 (t, *J* = 5.3 Hz, 1H, **H_{28}**), 5.72-5.64 (m, 1H, **H_8**), 5.52 (d, *J* = 18.0 Hz, 1H, **H_{32}**), 4.51 (dd, *J* = 14.0, 4.9 Hz, 1H, **H_{21}**), 4.38 (d, *J* = 8.1 Hz, 1H, **H_{12}**), 4.32 (dd, *J* = 14.0, 5.7 Hz, 1H, **H_{21}**), 4.24 (dd, *J* = 10.4, 5.2 Hz, 1H, **H_{22}**), 3.48 (dt, *J* = 13.5, 6.7 Hz, 1H, **H_{29}**), 3.24 (td, *J* = 12.1, 6.5 Hz, 1H, **H_{29}**), 2.97 (dd, *J* = 15.0, 3.8 Hz, 1H, **H_{15}**), 2.94-2.87 (m, 2H, **$H_{14,15}$**), 2.42-2.29 (m, 2H, **H_{30}**), 2.09 (q, *J* = 7.1 Hz, 3H, **$H_{7,23}$**), 1.81 (s, 3H, **H_{13}**), 1.41-1.36 (m, 2H, **H_6**), 1.31-1.24 (m, 20H, **$H_{2\text{-}5,38\text{-}40}$**), 1.18 (d, *J* = 7.1 Hz, 3H, **H_{26}**), 0.90 (s, 12H, **$H_{1,46\text{-}48}$**), 0.08 (s, 3H, **H_{44}**), 0.01 (s, 3H, **H_{45}**) ppm.

^{13}C-NMR (151MHz, $CDCl_3$): δ 173.4 (**C_{25}**), 150.4 (**C_{31}**), 145.0 (**C_{16}**), 136.1 (**C_{11}**), 135.6 (**C_8**), 126.0 (**C_9**), 125.8 (**C_{10}**), 123.9 (**C_{17}**), 121.9 (**C_{32}**, *deduced from HSQC*), 83.4 (2C, **$C_{36,37}$**), 76.1 (**C_{12}**), 73.0 (**C_{22}**), 53.5 (**C_{21}**), 44.9 (**C_{23}**), 38.0

(**C$_{29}$**), 35.8 (**C$_{30}$**), 33.2 (**C$_{7}$**), 32.0 (**C$_{5}$**), 31.9 (**C$_{15}$**), 29.6 (**C$_{6}$**), 29.4 (**C$_{2\text{-}4,38\text{-}41}$**), 29.3 (**C$_{2\text{-}4,38\text{-}41}$**), 26.0 (**C$_{1,46\text{-}48}$**), 25.0 (2C, **C$_{2\text{-}4,38\text{-}41}$**), 24.92 (**C$_{2\text{-}4,38\text{-}41}$**), 24.91 (**C$_{2\text{-}4,38\text{-}41}$**), 22.8 (**C$_{2\text{-}4,38\text{-}41}$**), 18.1 (**C$_{43}$**), 14.9 (**C$_{26}$**), 14.3 (3C, **C$_{1,46\text{-}48}$**), 12.9 (**C$_{13}$**), −4.64 (**C$_{44}$**), −4.83 (**C$_{45}$**) ppm.

HRMS (ESI+): exact mass calculated for $[M+Na]^+$ ($C_{37}H_{67}N_4O_5BSiNa^+$) required *m/z* 709.4871, found *m/z* 709.4870.

FT-IR (neat) ν_{max}: 2978, 2956, 2927, 2855, 1657, 1640, 1552, 1545, 1468, 1460, 1431, 1400, 1359, 1320, 1256, 1216, 1144, 1111, 1085, 1050, 1006, 992, 967, 941, 848, 834, 811, 779, 759 cm^{-1}.

$[a]_D^{20}$ = +10.7° (c = 0.45, $CHCl_3$).

TLC: R_f (10% MeOH in DCM) = 0.88; PMA stain.

2.6.9.6. (*R*,3*E*,5*E*)-1-(1-((2*R*,3*S*)-2-((*tert*-butyldimethylsilyl)oxy)-3-methyl-4-oxo-4-(((*E*)-4-(4,4,5,5-tetramethyl-1,3,2-dioxaborolan-2-yl)but-3-en-1-yl)amino)butyl)-1*H*-1,2,3-triazol-4-yl)-3-methyltrideca-3,5-dien-2-yl (1*R*,4*R*)-4-chlorocyclobut-2-ene-1-carboxylate (2.S51)

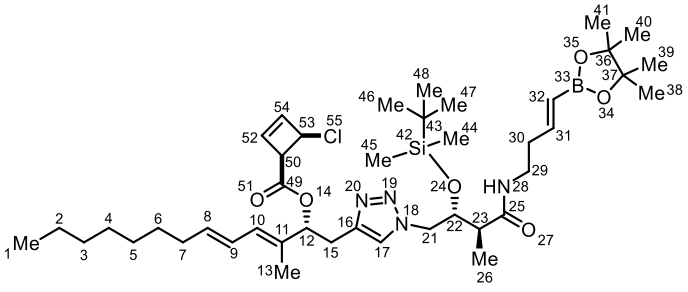

2.S51
Chemical Formula: $C_{42}H_{70}BClN_4O_6Si$

(*R*,3*E*,5*E*)-1-(1-((2*R*,3*S*)-2-((*tert*-butyldimethylsilyl)oxy)-3-methyl-4-oxo-4-(((*E*)-4-(4,4,5,5-tetramethyl-1,3,2-dioxaborolan-2-yl)but-3-en-1-yl)amino)butyl)-1*H*-1,2,3-triazol-4-yl)-3-methyltrideca-3,5-dien-2-yl (1*R*,4*R*)-4-chlorocyclobut-2-ene-1-carboxylate (**2.S51**) was synthesised according to the general procedure outlined in chapter 2.5.2.17. on 0.141 mmol scale to yield **2.S51** (65.2 mg, 92.0 µmol, 65%) as a colourless foam.

^{1}H-NMR (700MHz, $CDCl_3$): δ 7.60 (s, 1H, **H$_{17}$**), 6.54 (dt, *J* = 17.9, 6.5 Hz, 1H, **H$_{31}$**), 6.31 (t, *J* = 5.5 Hz, 1H, **H$_{28}$**), 6.23 (d, *J* = 2.3 Hz, 1H, **H$_{52}$**), 6.18-6.16 (m, 2H, **H$_{9,54}$**), 6.09 (d, *J* = 10.8 Hz, 1H, **H$_{10}$**), 5.75-5.69 (m, 1H, **H$_{8}$**), 5.52

(dd, *J* = 9.1, 4.4 Hz, 1H, **H$_{12}$**), 5.49 (d, *J* = 18.0 Hz, 1H, **H$_{32}$**), 5.05 (d, *J* = 4.3 Hz, 1H, **H$_{50}$**), 4.61 (dd, *J* = 14.2, 3.8 Hz, 1H, **H$_{21}$**), 4.23 (dd, *J* = 14.2, 4.6 Hz, 1H, **H$_{21}$**), 4.17 (dt, *J* = 8.2, 4.2 Hz, 1H, **H$_{22}$**), 4.07 (d, *J* = 4.2 Hz, 1H, **H$_{53}$**), 3.47 (dd, *J* = 13.6, 6.5 Hz, 1H, **H$_{29}$**), 3.22 (dd, *J* = 14.9, 9.3 Hz, 1H, **H$_{15}$**), 3.14 (dt, *J* = 13.2, 7.0 Hz, 1H, **H$_{29}$**), 3.04 (dd, *J* = 14.9, 4.4 Hz, 1H, **H$_{15}$**), 2.34 (ddd, *J* = 7.5, 3.5, 1.6 Hz, 2H, **H$_{30}$**), 2.09 (dd, *J* = 13.7, 6.5 Hz, 2H, **H$_{7}$**), 1.83 (m, 4H, **H$_{13,23}$**), 1.39-1.35 (m, 2H, **H$_{6}$**), 1.28-1.24 (m, 20H, **H$_{2\text{-}5,38\text{-}41}$**), 1.11 (d, *J* = 7.0 Hz, 3H, **H$_{26}$**), 0.92 (s, 9H, **H$_{46\text{-}48}$**), 0.88 (t, *J* = 7.1 Hz, 3H, **H$_{1}$**), 0.10 (s, 3H, **H$_{44}$**), 0.08 (s, 3H, **H$_{45}$**) ppm.

^{13}C-NMR (176MHz, $CDCl_3$): δ 173.6 (**C$_{25}$**), 150.5 (**C$_{31}$**), 143.6 (**C$_{16}$**), 140.7 (**C$_{52}$**), 137.0 (**C$_{8}$**), 136.6 (**C$_{54}$**), 131.5 (**C$_{11}$**), 128.8 (**C$_{10}$**), 126.0 (**C$_{9}$**), 123.9 (**C$_{17}$**), 121.8 (**C$_{32}$**, *deduced from HSQCs*), 83.3 (2C, **C$_{36,37}$**), 79.5 (**C$_{12}$**), 73.0 (**C$_{22}$**), 56.2 (**C$_{50}$**), 54.1 (**C$_{53}$**), 53.5 (**C$_{21}$**), 44.1 (**C$_{23}$**), 38.2 (**C$_{29}$**), 35.7 (**C$_{30}$**), 33.2 (**C$_{7}$**), 32.0 (**C$_{2}$**), 30.2 (**C$_{15}$**), 29.47 (**C$_{x}$**), 29.37 (**C$_{x}$**), 29.31 (**C$_{6}$**), 26.0 (4C, **C$_{38\text{-}41}$**), 24.9 (2C, **C$_{4,5}$**), 22.8 (**C$_{3}$**), 18.1 (**C$_{43}$**), 14.8 (**C$_{26}$**), 14.3 (3C, **C$_{46\text{-}48}$**), 12.9 (**C$_{13}$**), −4.4 (**C$_{44}$**), −5.0 (**C$_{45}$**) ppm.

HRMS (ESI+): exact mass calculated for $[M+Na]^+$ ($C_{42}H_{70}N_4O_6BSiClNa^+$) required *m/z* 823.4744, found *m/z* 823.4742.

TLC: *cis$_1$*-**2.S51**: R_f (60% EtOAc in heptane) = 0.36; $KMnO_4$ stain;

cis$_2$-**2.S51**: R_f (60% EtOAc in heptane) = 0.28; $KMnO_4$ stain.

2.6.9.7. (14*Z*,3*R*,6*E*,8*E*,10*E*,16*S*,17*R*)-17-((*tert*-butyldimethylsilyl)oxy)-3-((2*E*,4*E*)-dodeca-2,4-dien-2-yl)-16-methyl-11*H*-4-oxa-14-aza-1(4,1)-triazolacyclooctadecaphane-6,8,10-triene-5,15-dione (2.S52)

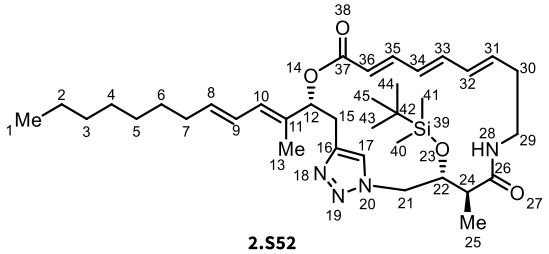

2.S52

Chemical Formula: $C_{36}H_{58}N_4O_4Si$

(14*Z*,3*R*,6*E*,8*E*,10*E*,16*S*,17*R*)-17-((*tert*-butyldimethylsilyl)oxy)-3-((2*E*,4*E*)-dodeca-2,4-dien-2-yl)-16-methyl-11*H*-4-oxa-14-aza-1(4,1)-triazolacyclooctadecaphane-6,8,10-triene-5,15-dione (**2.S52**) was synthesised

according to the general procedure outlined in chapter 2.5.2.18. on 50.0 µmol scale to yield **2.S52** (21.2 mg, 33.2 µmol, 66%) as a colourless foam.

^{1}H-NMR (600MHz, $CDCl_3$): δ 7.24 (s, 1H, $\mathbf{H_{17}}$), 6.69 (dd, *J* = 15.3, 11.3 Hz, 1H, $\mathbf{H_{35}}$), 6.41 (dd, *J* = 14.9, 10.6 Hz, 1H, $\mathbf{H_{32}}$), 6.26 (dd, *J* = 14.9, 10.8 Hz, 1H, $\mathbf{H_{9}}$), 6.16 (d, *J* = 10.8 Hz, 1H, $\mathbf{H_{10}}$), 6.14-6.08 (m, 1H, $\mathbf{H_{33}}$), 6.04 (dd, *J* = 15.0, 11.5 Hz, 1H, $\mathbf{H_{34}}$), 6.03-5.97 (m, 1H, $\mathbf{H_{31}}$), 5.83 (dd, *J* = 8.6, 4.1 Hz, 1H, $\mathbf{H_{NH28}}$), 5.78-5.71 (m, 1H, $\mathbf{H_{8}}$), 5.51 (dd, *J* = 9.1, 5.3 Hz, 1H, $\mathbf{H_{12}}$), 5.49 (d, *J* = 15.5 Hz, 1H, $\mathbf{H_{36}}$), 4.63 (ddd, *J* = 9.6, 3.7, 2.8 Hz, 1H, $\mathbf{H_{22}}$), 4.04-3.88 (m, 4H, $\mathbf{H_{21,29}}$), 3.14-3.08 (m, 2H, $\mathbf{H_{15}}$), 2.61 (qd, *J* = 7.2, 4.0 Hz, 1H, $\mathbf{H_{24}}$); 2.54 (bd, *J* = 14.2 Hz, 1H, $\mathbf{H_{30}}$), 2.28-2.20 (m, 1H, $\mathbf{H_{30}}$); 2.14-2.08 (m, 2H, $\mathbf{H_{7}}$), 1.87 (s, 3H, $\mathbf{H_{13}}$), 1.41-1.35 (m, 2H, $\mathbf{H_{6}}$), 1.31-1.25 (m, 8H, $\mathbf{H_{2\text{-}5}}$), 1.21 (d, *J* = 7.3 Hz, 3H, $\mathbf{H_{25}}$), 0.92 (t, *J* = 7.4 Hz, 3H, $\mathbf{H_{1}}$), 0.78 (s, 9H, $\mathbf{H_{43\text{-}45}}$), −0.07 (s, 3H, $\mathbf{H_{40}}$), −0.41 (s, 3H, $\mathbf{H_{41}}$) ppm.

^{13}C-NMR (151MHz, $CDCl_3$): δ 172.5 ($\mathbf{C_{26}}$), 166.2 ($\mathbf{C_{37}}$), 145.6 ($\mathbf{C_{35}}$), 144.0 ($\mathbf{C_{16}}$), 141.8 ($\mathbf{C_{32}}$), 138.6 ($\mathbf{C_{9}}$), 136.4 ($\mathbf{C_{8}}$), 132.8 ($\mathbf{C_{11}}$), 131.4 ($\mathbf{C_{33}}$), 127.5 ($\mathbf{C_{34}}$), 126.6 ($\mathbf{C_{10}}$), 125.8 ($\mathbf{C_{31}}$), 123.5 ($\mathbf{C_{17}}$), 120.0 ($\mathbf{C_{36}}$), 78.1 ($\mathbf{C_{12}}$), 76.4 ($\mathbf{C_{15}}$), 71.8 ($\mathbf{C_{22}}$), 53.2 ($\mathbf{C_{21}}$), 45.8 ($\mathbf{C_{24}}$), 37.8 ($\mathbf{C_{29}}$), 34.5 ($\mathbf{C_{30}}$), 33.18 ($\mathbf{C_{7}}$), 33.15 ($\mathbf{C_{6}}$), 32.0 ($\mathbf{C_{2\text{-}5}}$), 29.5 ($\mathbf{C_{2\text{-}5}}$), 29.3 ($\mathbf{C_{2\text{-}5}}$), 25.8 ($\mathbf{C_{42}}$), 25.0 ($\mathbf{C_{2\text{-}5}}$), 14.3 (3C, $\mathbf{C_{43\text{-}45}}$), 13.3 (2C, $\mathbf{C_{1+13}}$), 10.0 ($\mathbf{C_{25}}$), −5.1 ($\mathbf{C_{40}}$), −5.5 ($\mathbf{C_{41}}$) ppm.

HRMS (ESI+): exact mass calculated for $[M+Na]^+$ ($C_{36}H_{58}N_4O_4SiNa^+$) required *m/z* 661.4125, found *m/z* 661.4119.

FT-IR (neat) ν_{max}: 2956, 2925, 2854, 1710, 1654, 1640, 1616, 1533, 1528, 1467, 1462, 1432, 1387, 1360, 1298, 1249, 1234, 1216, 1144, 1111, 1080, 1051, 1007, 965, 939, 886, 837, 830, 809 cm^{-1}.

$[a]_D^{20}$ = −13.9° (c = 0.054, $CHCl_3$).

TLC: R_f (60% EtOAc in heptane) = 0.30; $KMnO_4$ stain.

2.6.9.8. (1^4*Z*,3*R*,6*E*,8*E*,10*E*,16*S*,17*R*)-3-((2*E*,4*E*)-dodeca-2,4-dien-2-yl)-17-hydroxy-16-methyl-1^1*H*-4-oxa-14-aza-1(4,1)-triazolacyclooctadecaphane-6,8,10-triene-5,15-dione, Bioiso-FR252921 (2.188)

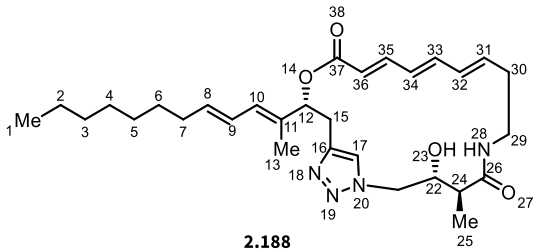

2.188
Chemical Formula: $C_{30}H_{44}N_4O_4$

Bioiso-FR252921 (**2.188**) was synthesised according to the general procedure outlined in chapter 2.5.2.19. on 24.0 µmol scale to yield **2.188** (10.1 mg, 19.2 µmol, 80%) as a white solid.

^{1}H-NMR (700MHz, $CDCl_3$): δ 7.54 (s, 1H, **H_{17}**), 6.99 (dd, *J* = 15.3, 11.3 Hz, 1H, **H_{25}**), 6.43 (dd, 15.0, 10.7 Hz, 1H, **H_{33}**), 6.25 (dd, *J* = 14.9, 10.9 Hz, 1H, **H_9**), 6.17 (d, *J* = 10.8 Hz, 1H, **H_{10}**), 6.15 (dd, *J* = 15.0, 11.3 Hz, 1H,**H_{34}**), 6.09 (dd, *J* = 15.1, 10.7 Hz, 1H, **H_{32}**), 5.87 (dt, *J* = 15.0, 7.5 Hz, 1H, **H_{31}**), 5.75 (dd, *J* = 14.6, 7.2 Hz, 1H, **H_8**), 5,71 (d, *J* = 15.3 Hz, 1H, **H_{36}**), 5.66 (t, *J* = 6.5 Hz, 1H, **H_{28}**), 5.48 (dd, *J* = 10.8, 3.2 Hz, 1H, **H_{12}**), 4.61 (d, *J* = 13.5 Hz, 1H, **H_{21}**), 3.99 (dd, *J* = 13.7, 10.5 Hz, 1H, **H_{21}**), 3.95-3.89 (m, 1H, **H_{22}**), 3.59-3.52 (m, 1H, **H_{29}**), 3.47 (dtd, *J* = 11.6, 6.7, 5.0 Hz, 1H, **H_{29}**), 3.41 (d, *J* = 3.3 Hz, 1H, **H_{23}**), 3.12 (dd, *J* = 14.8, 3.5 Hz, 1H, **H_{15}**), 3.04 (dd, *J* = 14.9, 10.9 Hz, 1H, **H_{15}**), 2.40-2.29 (m, 3H, **$H_{24,30}$**), 2.11 (q, *J* = 7.2 Hz, 2H, **H_7**), 1.85 (s, 3H, **H_{13}**), 1.41-1.36 (m, 2H, **H_6**), 1.33-1.26 (m, 8H, **$H_{2\text{-}5}$**), 1.22 (d, *J* = 7.0 Hz, 3H, **H_{25}**), 0.88 (t, *J* = 7.0 Hz, 3H, **H_1**) ppm.

^{13}C-NMR (176MHz, $CDCl_3$): δ 174.3 (**C_{26}**), 166.0 (**C_{37}**), 144.5 (**C_{35}**), 143.7 (**C_{16}**), 140.4 (**C_{33}**), 136.6 (**C_{31}**), 136.5 (**C_8**), 132.6 (**C_{11}**), 132.0 (**C_{32}**), 128.8 (**C_{34}**), 126.9 (**C_{10}**), 125.7 (**C_9**), 124.7 (**C_{17}**), 120.9 (**C_{36}**), 77.6 (**C_{12}**), 72.4 (**C_{22}**), 54.5 (**C_{21}**), 45.5 (**C_{24}**), 38.1 (**C_{29}**), 34.4 (**C_{30}**), 33.2 (**C_7**), 32.0 (**C_6**), 30.7 (**C_{15}**), 29.9 (**$C_{2\text{-}5}$**), 29.5 (**$C_{2\text{-}5}$**), 29.3 (**$C_{2\text{-}5}$**), 22.8 (**$C_{2\text{-}5}$**), 14.26 (**C_1**), 14.24 (**C_{25}**), 13.3 (**C_{13}**) ppm.

HRMS (ESI+): exact mass calculated for $[M+Na]^+$ ($C_{30}H_{44}N_4O_4Na^+$) required *m/z* 547.3260, found *m/z* 547.3265.

FT-IR (neat) ν_{max}: 3348, 2959, 2921, 2851, 1710, 1685, 1658, 1616, 1588, 1519, 1466, 1430, 1356, 1332, 1297, 1271, 1261, 1237, 1217, 1196, 1172, 1136, 1100, 1053, 1021, 998, 960, 878, 839, 795, 759, 720, 671, 616 cm^{-1}.

$[a]_D^{20}$ = −1.08° (c = 0.012, $CHCl_3$).

TLC: R_f (10% MeOH in $CHCl_3$) = 0.50; $KMnO_4$ stain.

2.7. Synthesis of Macrocyclisation Models

2.7.1. Synthesis of the 19-membered Macrocycle Model Precursor

2.7.1.1. Tridec-2-yn-1-ol (2.S53)

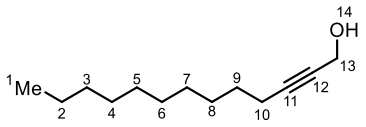

2.S53

Chemical Formula: $C_{13}H_{24}O$

Tridec-2-yn-1-ol (**2.S53**) was synthesised according to the general procedure outlined in chapter 2.5.2.20. on 20.0 mmol scale to yield **2.S53** (3.93 g, 20.0 mmol, quantitative) as a colourless oil.

^{1}H-NMR (600MHz, $CDCl_3$): δ 4.25 (s, 2H, **H_{13}**), 2.20 (t, *J* = 7.1 Hz, 2H, **H_{10}**), 1.72 (bs, 1H, **H_{14}**), 1.53-1.48 (m, 2H, **H_9**), 1.39-1.33 (m, 2H, **H_8**), 1.29-1.22 (m, 12H, **H_{2-7}**), 0.87 (t, *J* = 6.9 Hz, 3H, **H_1**) ppm.

^{13}C-NMR (151MHz, $CDCl_3$): δ 86.8 (**C_{11}**), 78.4 (**C_{12}**), 51.5 (**C_{13}**), 32.0 (**C_{2-8}**), 29.71 (**C_{2-8}**), 29.65 (**C_{2-8}**), 29.44 (**C_{2-8}**), 29.27 (**C_{2-8}**), 29.01 (**C_{2-8}**), 28.75 (**C_9**), 22.8 (**C_{2-8}**), 18.9 (**C_{10}**), 14.2 (**C_1**) ppm.

FT-IR (neat) ν_{max}: 3309, 2922., 2853, 1464, 1377, 1137, 1010, 721, 558 cm^{-1}.

2.7.1.2. Tridec-12-yn-1-ol (2.S54)

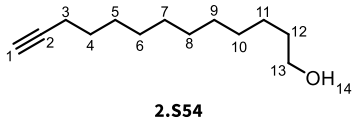

2.S54

Chemical Formula: $C_{13}H_{24}O$

Tridec-12-yn-1-ol (**2.S54**) was synthesised according to the general procedure outlined in chapter 2.5.2.21. on 5.28 mmol scale to yield **2.S54** (693 mg, 3.53 mmol, 67%) as a colourless oil.

^{1}H-NMR (400MHz, $CDCl_3$): δ 3.64 (dd, *J* = 11.7, 5.9 Hz, 2H, **H_{13}**), 2.18 (t, *J* = 6.6 Hz, 2H, **H_3**), 1.93 (t, *J* = 2.6 Hz, 1H, **H_1**), 1.61-1.47 (m, 4H, **$H_{11,12}$**), 1.43-1.24 (m, 14H, **H_{4-11}**), 1.20 (t, *J* = 4.9 Hz, 1H, **H_{14}**) ppm.

^{13}C-NMR (101MHz, $CDCl_3$): δ 85.0 (**C_2**), 68." (**C_1**), 63.2 (**C_{13}**), 33.0 (**C_{3-12}**), 29.7 (**C_{3-12}**), 29.7 (**C_{3-12}**), 29.6 (**C_{3-12}**), 29.6 (**C_{3-12}**), 29.2 (**C_{3-12}**), 28.9 (**C_{3-12}**), 28.6 (**C_{3-12}**), 25.9 (**C_{3-12}**), 18.5 (**C_{3-12}**) ppm.

FT-IR (neat) ν_{max}: 3309, 2922., 2853, 1464, 1377, 1137, 1010, 721, 558 cm^{-1}.

2.7.1.3. (*E*)-13-(4,4,5,5-tetramethyl-1,3,2-dioxaborolan-2-yl)tridec-12-en-1-ol (2.S55)

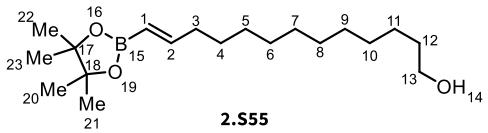

2.S55

Chemical Formula: $C_{19}H_{37}BO_3$

(*E*)-13-(4,4,5,5-tetramethyl-1,3,2-dioxaborolan-2-yl)tridec-12-en-1-ol (**2.S55**) was synthesised according to the general procedure outlined in chapter 2.5.2.22. on 5.24 mmol scale to yield **2.S55** (1.19 g, 3.68 mmol, 70%) as a colourless oil.

^{1}H-NMR (400MHz, $CDCl_3$): δ 6.63 (dt, *J* = 17.9, 6.4 Hz, 1H, **H_2**), 5.42 (d, *J* = 18.0 Hz, 1H, **H_1**), 3.63 (t, *J* = 6.6 Hz, 3H, **$H_{13,14}$**), 2.18-2.09 (m, 2H, **H_3**), 1.61-1.49 (m, 4H, **$H_{4,12}$**). 1.44-1.17 (m, 26H, **$H_{5\text{-}11,20\text{-}23}$**) ppm.

HRMS (ESI+): exact mass calculated for $[M]^+$ ($C_{19}H_{37}BO_3^+$) required *m/z* 347.2733; found *m/z* 347.2731.

FT-IR (neat) ν_{max}: 3362, 2978, 2924, 2853, 1638, 1464, 1398, 1361, 1317, 1270, 1215, 1144, 1103, 1056, 998, 970, 897, 850, 733, 647, 578, 523, 446 cm^{-1}.

2.7.1.4. (*E*)-13-(4,4,5,5-tetramethyl-1,3,2-dioxaborolan-2-yl)tridec-12-en-1-yl 4-chlorocyclobut-2-ene-1-carboxylate (2.S56)

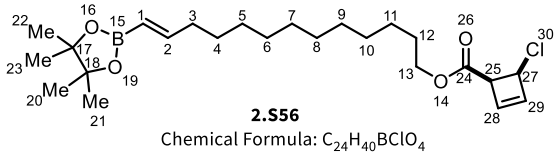

2.S56

Chemical Formula: $C_{24}H_{40}BClO_4$

(*E*)-13-(4,4,5,5-tetramethyl-1,3,2-dioxaborolan-2-yl)tridec-12-en-1-yl 4-chlorocyclobut-2-ene-1-carboxylate (**2.S56**) was synthesised according to the general procedure outlined in chapter 2.5.2.17. on 0.500 mmol scale to yield **2.S56** (187 mg, 0.426 mmol, 61%) as a colourless oil.

^{1}H-NMR (600MHz, $CDCl_3$): δ 6.62 (dt, *J* = 17.9, 6.4 Hz, 1H, **H_2**), 6.26 (dd, *J* = 8.0, 2.6 Hz, 2H, **$H_{28/29}$**), 5.41 (d, *J* = 16.6, 1.3 Hz, 1H, **H_1**), 5.08 (d, *J* = 4.2 Hz, 1H, **H_{25}**), 4.20-4.09 (m, 2H, **H_{13}**), 4.06 (d, *J* = 4.2 Hz, 1H, **H_{27}**), 2.19-2.07 (m, 2H, **H_3**), 1.69-1.63 (m, 2H, **H_{12}**), 1.49-1.21 (m, 28H, **$H_{4\text{-}11,\ 20\text{-}23}$**) ppm.

^{13}C-NMR (151MHz, $CDCl_3$): δ 170.1 (**C_{24}**), 155.0 (**C_2**), 140.4 (**$C_{28/29}$**), 136.7 (**$C_{28/29}$**), 118.1 (**C_1**, *deduced from HSQC*), 83.1 (2C, **$C_{17,18}$**), 65.4 (**C_{13}**), 56.4 (**C_{25}**), 54.1 (**C_{27}**), 36.0 (**C_3**), 29.7 (**$C_{4\text{-}12}$**), 29.7 (**$C_{4\text{-}12}$**), 29.6 (**$C_{4\text{-}12}$**), 29.6 (**$C_{4\text{-}12}$**), 29.4 (**$C_{4\text{-}12}$**), 29.3 (**$C_{4\text{-}12}$**), 28.7 (**$C_{4\text{-}12}$**), 28.4 (**$C_{4\text{-}12}$**), 26.0 (**$C_{4\text{-}12}$**), 24.9 (4C, **$C_{20\text{-}23}$**) ppm.

HRMS (ESI+): exact mass calculated for $[M+Na]^+$ ($C_{24}H_{40}BClO_4Na^+$) required *m/z* 461.2606; found *m/z* 461.2597.

FT-IR (neat) ν_{max}: 2926, 2854, 1738, 1638, 1466, 1397, 1362, 1331, 1289, 1268, 1234, 1177, 1145, 1119, 1048, 999, 971, 913, 850, 773, 736 cm^{-1}.

2.7.2. Synthesis of the 20-membered Macrocycle Model Precursor

2.7.2.1. Tetradec-2-yn-1-ol (2.S57)

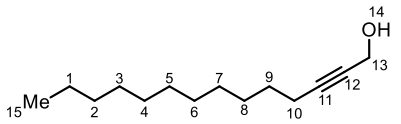

2.S57
Chemical Formula: $C_{14}H_{26}O$

Tetradec-2-yn-1-ol (**2.S57**) was synthesised according to the general procedure outlined in chapter 2.5.2.20. on 5.00 mmol scale to yield **2.S57** (1.05 g, 5.00 mmol, quantitative) as a colourless oil.

^{1}H-NMR (600MHz, $CDCl_3$): δ 4.28-4.21 (m, 2H, **H_{13}**), 2.21 (tt, *J* = 7.3, 2.2 Hz, 2H, **H_{10}**), 1.61-1.16 (m, 18H, **H_{1-9}**), 0.88 (t, *J* = 6.8 Hz, 3H, **H_{15}**) ppm.

^{13}C-NMR (151MHz, $CDCl_3$): δ 86.9 (**C_{11}**), 78.4 (**C_{12}**), 51.6 (**C_{13}**), 32.1 (**C_{1-9}**), 29.8 (2C, **C_{1-9}**), 29.7 (**C_{1-9}**), 29.5 (**C_{1-9}**), 29.3 (**C_{1-9}**), 29.0 (**C_{1-9}**), 28.8 (**C_{1-9}**), 22.8 (**C_{1-9}**), 18.9 (**C_{10}**), 14.2 (**C_{15}**) ppm.

HRMS (ESI+): exact mass calculated for $[M+H]^+$ ($C_{14}H_{27}O^+$) required *m/z* 211.2062; found *m/z* 211.2056.

FT-IR (neat) ν_{max}: 3285, 2916, 2848, 1472, 1461, 1070, 1056, 1042, 1026, 1005, 730, 719, 682, 665, 652, 629, 535 cm^{-1}.

2.7.2.2. Tetradec-13-yn-1-ol (2.S58)

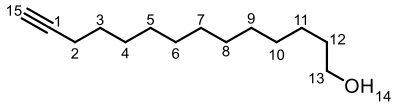

2.S58
Chemical Formula: $C_{14}H_{26}O$

Tetradec-13-yn-1-ol (**2.S58**) was synthesised according to the general procedure outlined in chapter 2.5.2.21. on 5.33 mmol scale to yield **2.S58** (576 mg, 2.74 mmol, 51%) as a colourless oil.

^{1}H-NMR (400MHz, $CDCl_3$): δ 3.64 (dd, *J* = 11.0, 6.4 Hz, 2H, **H_{13}**), 2.18 (td, *J* = 7.1, 2.6 Hz, 2H, **H_2**), 1.94 (t, *J* = 2.6 Hz, 1H, **H_{15}**), 1.62-1.44 (m, 6H, **$H_{3,11,12}$**), 1.43-1.24 (m, 14H, **H_{4-10}**), 1.18 (t, *J* = 4.9 Hz, 1H, **H_{14}**) ppm.

^{13}C-NMR (101MHz, $CDCl_3$): δ 85.0 (**C_1**), 68.2 (**C_{15}**), 63.3 (**C_{13}**), 33.0 (**C_{2-12}**), 29.7 (2C, **C_{2-12}**), 29.7 (**C_{2-12}**), 29.6 (**C_{2-12}**), 29.6 (**C_{2-12}**), 29.2 (**C_{2-12}**), 28.9 (**C_{2-12}**), 28.6 (**C_{2-12}**), 25.9 (**C_{2-12}**), 18.5 (**C_{2-12}**) ppm.

FT-IR (neat) ν_{max}: 3285, 2916, 2848, 1472, 1461, 1070, 1056, 1042, 1026, 1005, 730, 719, 682, 665, 652, 629, 535 cm^{-1}.

2.7.2.3. (*E*)-14-(4,4,5,5-tetramethyl-1,3,2-dioxaborolan-2-yl)tetradec-13-en-1-ol (2.S59)

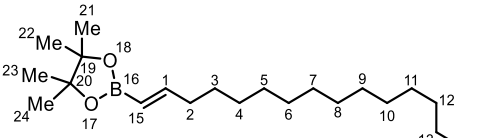

2.S59

Chemical Formula: $C_{20}H_{39}BO_3$

(*E*)-14-(4,4,5,5-tetramethyl-1,3,2-dioxaborolan-2-yl)tetradec-13-en-1-ol (**2.S59**) was synthesised according to the general procedure outlined in chapter 2.5.2.22. on 2.74 mmol scale to yield **2.S59** (740 mg, 2.19 mmol, 80%) as a colourless oil.

^{1}H-NMR (400MHz, $CDCl_3$): δ 6.63 (dt, *J* = 18.0, 6.4 Hz, 1H, **H_1**), 5.42 (dt, *J* = 17.9, 1.5 Hz, 1H, **H_{15}**), 3.64 (t, *J* = 5.5 Hz, 2H, **H_{13}**), 2.14 (td, *J* = 8.0, 1.5 Hz, 2H, **H_2**), 1.61-1.52 (m, 2H, **H_{12}**), 1.43-1.19 (m, 30H, **$H_{3\text{-}11,21\text{-}24}$**) ppm.

^{13}C-NMR (101MHz, $CDCl_3$): δ 155.0 (**C_1**), 118.1 (**C_{15}**, *deduced from HSQC*), 83.1 (2C, **$C_{19,20}$**), 63.3 (**C_{13}**), 36.0 (**C_2**), 33.0 (**C_{12}**), 29.8 (**$C_{3\text{-}11}$**), 29.7 (**$C_{3\text{-}11}$**), 29.7 (**$C_{3\text{-}11}$**), 29.7 (**$C_{3\text{-}11}$**), 29.6 (**$C_{3\text{-}11}$**), 29.6 (**$C_{3\text{-}11}$**), 29.4 (**$C_{3\text{-}11}$**), 28.4 (**$C_{3\text{-}11}$**), 25.9 (**$C_{3\text{-}11}$**), 24.9 (4C, **$C_{21\text{-}24}$**) ppm.

HRMS (ESI+): exact mass calculated for $[M+Na]^+$ ($C_{20}H_{39}BO_3Na^+$) required *m/z* 361.2890; found *m/z* 361.2884.

FT-IR (neat) ν_{max}: 3428, 2978, 2924, 2853, 1638, 1465, 1398, 1361, 1318, 1271, 1215, 1145, 1104, 1056, 997, 970, 910, 850, 735, 648, 578 cm^{-1}.

2.7.2.4. (*E*)-14-(4,4,5,5-tetramethyl-1,3,2-dioxaborolan-2-yl)tetradec-13-en-1-yl 4-chlorocyclobut-2-ene-1-carboxylate (2.S60)

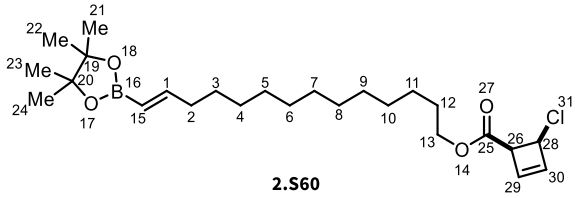

2.S60
Chemical Formula: $C_{25}H_{42}BClO_4$

(*E*)-14-(4,4,5,5-tetramethyl-1,3,2-dioxaborolan-2-yl)tetradec-13-en-1-yl 4-chlorocyclobut-2-ene-1-carboxylate (**2.S60**) was synthesised according to the general procedure outlined in chapter 2.5.2.17. on 0.700 mmol scale to yield **2.S60** (122 mg, 0.269 mmol, 39%) as a colourless oil.

^{1}H-NMR (600MHz, $CDCl_3$): δ 6.63 (dt, *J* = 17.9 Hz, 1H, **H_1**), 6.28 (d, *J* = 2.7 Hz, 1H, **H_{30}**), 6.27 (d, *J* = 2.5 Hz, 1H, **H_{29}**), 5.42 (d, *J* = 18.0 Hz, 1H, **H_{15}**), 5.09 (d, *J* = 4.3 Hz, 1H, **H_{26}**), 4.20-4.13 (m, 2H, **H_{13}**), 4.07 (d, *J* = 4.2 Hz, 1H, **H_{28}**), 2.14 (td, *J* = 7.8, 1.3 Hz, 2H, **H_2**), 1.70-1.63 (m, 2H, **H_{12}**), 1.44-1.33 (m, 2H, **H_3**), 1.33-1.19 (m, 28H, **$H_{4\text{-}11}$**, **$_{21\text{-}24}$**) ppm.

^{13}C-NMR (151MHz, $CDCl_3$): δ 170.1 (**C_{25}**), 155.0 (**C_1**), 140.4 (**C_{30}**), 136.7 (**C_{29}**), 118.5 (**C_{15}**, *deduced from HSQC*), 83.1 (2C, **$C_{19,20}$**), 65.5 (**C_{13}**), 56.5 (**C_{26}**), 54.1 (**C_{28}**), 36.0 (**C_2**), 29.8 (**$C_{3\text{-}12}$**), 29.8 (**$C_{3\text{-}12}$**), 29.7 (**$C_{3\text{-}12}$**), 29.7 (**$C_{3\text{-}12}$**), 29.4 (**$C_{3\text{-}12}$**), 29.4 (**$C_{3\text{-}12}$**), 28.8 (**$C_{3\text{-}12}$**), 28.4 (**$C_{3\text{-}12}$**), 26.0 (**$C_{3\text{-}12}$**), 25.0 (**$C_{3\text{-}12}$**), 24.9 (4C, **$C_{21\text{-}24}$**) ppm.

HRMS (ESI+): exact mass calculated for $[M+Na]^+$ ($C_{25}H_{42}BClO_4Na^+$) requiv.uired *m/z* 475.2762; found *m/z* 475.2744.

FT-IR (neat) ν_{max}: 2977, 2926, 2854, 1738, 1638, 1466, 1397, 1362, 1321, 1289, 1268, 1234, 1176, 1145, 1119, 1049, 998, 971, 915, 850, 773, 736 cm^{-1}.

2.8. Biological Experiments

2.8.1. EL4 T Cell Assay

EL4 T cell experiments were planned and conducted by Dr. Tuan-Anh Nguyen and Anna Koren. The procedure is included within this thesis for sake of completeness of information.

EL4 T cells (ATCC® TIB-39™) were cultured in Dulbecco's Modified Eagle Medium (DMEM, Thermo Fisher Scientific, D5030-10L) supplemented with 10% heat inactivated fetal bovine serum (FBS, Thermo Fisher Scientific, 10500).

Compounds were dissolved in DMSO (16 mM) and were dispensed with a Labcyte Echo 550 to 96-well plates (Corning, CLS3904-100EA). For each compound multiple volumes were plated to achieve six final assay concentrations ranging from 20 µM to 6.4 nM in 5-fold dilutions. The volume of DMSO in each well was adjusted to 0.25 µL. Eight wells per plate were filled with DMSO only to serve as negative control. 2000 EL4 T cells in 100 µL of medium were plated per well and after 72 h of incubation, cell viability was measured using a CellTiter-Glo Luminescent Cell Viability Assay (Promega, G7572). After equilibration of the plates and the reagent to room temperature, the Cell-Titer-Glo reagent was added to the wells using a Multidrop™ Combi Reagent Dispenser (Thermo Fisher Scientific) and cells were lysed by shaking. The luminescence signal was read after 20 min incubation at room temperature using an EnVision™ Multilabel Plate Reader (PerkinElmer). Signals were normalised to negative control wells on each plate and dose-response curves and IC_{50} values were calculated using GraphPad Prism 7.

2.8.2. PBMC Assay

PBMC experiments were planned by Laura Marie Gail and Manuel Schupp and were carried out by Laura Marie Gail. The procedure is included within this thesis for sake of completeness of information.

Peripheral blood mononuclear cells (PBMC) were isolated from whole blood of healthy donors on a Ficoll gradient and resuspended in RPMI (Gibco, #52400-025). Subsequently, $2.5 \cdot 10^5$ cells were seeded per well in a 96-well U-bottom plate and treated with the corresponding compounds at the desired concentration.

DMSO (Sigma-Aldrich, #41639) was added to untreated wells as solvent control. Cells were incubated with the compounds for 30 min at 37°C under an atmosphere containing 5% CO_2. Following incubation, the cells were stimulated with 1X Cell Activation Cocktail (CAC) containing Brefeldin A (Biolegend, #423303) or 1X Brefeldin A (Biolegend, #420601) only. Cells were incubated at 37°C under an atmosphere containing 5% CO_2 for 3 h. Afterwards, the cells were harvested and stained following a procedure described by Stary *et al*.[317] In short, cells were stained for 15 min at 20°C in the dark with a fixable viability dye (eBioscience eFluor 780; ThermoFisher, #65-0865-14 or Biolegend, #423107) and subsequently stained for 30 min at 4°C with surface marker antibodies (Table S1). After fixation and permeabilisation (Fixation Buffer, Biolegend #420801; Intracellular Staining Permeabilization Wash Buffer (10X), Biolegend #421002) cells were stained for 25 min at 20°C with intracellular cytokine antibodies (Table S 1). Washing was performed between each staining step. Stained cells were acquired on a CYTEK Aurora spectral flow cytometer equipped with five lasers and data analysis was performed inside FlowJo v10.8.1 and GraphPad Prism 9.0. Cell subsets were identified by gating on live single cells expressing canonical immune cell markers, including CD45 for leukocytes, CD3 for T cells, CD56 for NK cells and HLA-DR for APCs. Statistical differences between groups were determined by one-way ANOVA with multiple comparison.

CD (cluster of differentiation) and HLA-DR are surface markers for different cell types; IFN-γ, IL-6 and TNF-α are intracellular cytokines. BV = Brilliant Violet; AF = AlexaFluor; FVD = Fixable viability dye.

Antigen (Purpose)	Antibody/Fluorophore	Supplier	Catalogue Nr.	Dilution
FVD	eFluor780	Thermo-Fisher	65-0865-14	1:2000
Zombie UV™ FVD	ZombieUV™	Biolegend	423107	1:2000
CD3 (all T cells)	mouse IgG1 κ / PerCP	Biolegend	344814	1:300
CD4 (T helper cells)	Mouse Anti-Human / BUV563	BD Biosciences	750979	1:200
CD8 (T killer cells)	mouse IgG1 κ / BV 510™	Biolegend	300934	1:200
CD14 (monocytes)	mouse IgG1 κ / PerCP-Cy5.5	Biolegend	325622	1:500
CD20 (B cells)	mouse IgG1 κ / AF 700	Biolegend	302322	1:300
CD45 (leukocytes)	mouse IgG1 κ / BV570	Biolegend	304033	1:100
CD56 (NK cells)	mouse IgG1 κ / PE-Cy5	Biolegend	362515	1:200
CD86 (APCs)	mouse IgG1 κ / BV605	Biolegend	374231	1:100
HLA-DR (APC)	mouse IgG1 κ / APC-Cy7	Biolegend	307618	1:200
IFN-γ	mouse IgG1 κ / BV785	Biolegend	502542	1:80
IL-6	rat IgG1 κ / PE-Dazzle™ 594	Biolegend	501122	1:100
TNF-α	mouse IgG1 κ / APC	Biolegend	502912	1:100

Table S 1: Antibodies and FVD used in the PBMC assay with supplier information and dilution.

References

[1] G.-B. Zhang, F.-X. Wang, J.-Y. Du, H. Qu, X.-Y. Ma, M.-X. Wei, C.-T. Wang, Q. Li, C.-A. Fan, *Org. Lett.* **2012**, *14*, 3696–3699.
[2] J. Clayden, N. Greeves, S. Warren, *Organic Chemistry*, OUP Oxford, **2012**.
[3] L. Kürti, B. Czako, *Strategic Applications of Named Reactions in Organic Synthesis*, Elsevier Science, **2005**.
[4] R. R. Jones, R. G. Bergman, *J. Am. Chem. Soc.* **1972**, *94*, 660–661.
[5] R. G. Bergman, *Acc. Chem. Res.* **1973**, *6*, 25–31.
[6] M. Konishi, H. Ohkuma, K. Matsumoto, T. Tsuno, H. Kamei, T. Miyaki, T. Oki, H. Kawaguchi, G. D. Vanduyne, J. Clardy, *J. Antibiot.* **1989**, *42*, 1449–1452.
[7] K. Edo, M. Mizugaki, Y. Koide, H. Seto, K. Furihata, N. Otake, N. Ishida, *Tetrahedron Lett.* **1985**, *26*, 331–334.
[8] H. Meerwein, *Liebigs Ann. Chem.* **1914**, *405*, 129–175.
[9] D. Seyferth, R. S. Marmor, *Tetrahedron Lett.* **1970**, *11*, 2493–2496.
[10] J. C. Gilbert, U. Weerasooriya, *J. Org. Chem.* **1979**, *44*, 4997–4998.
[11] L. A. Paquette, *Organic Reactions* **1977**, 1–71.
[12] S. W. Kantor, C. R. Hauser, *J. Am. Chem. Soc.* **1951**, *73*, 4122–4131.
[13] L. Claisen, *Ber. Dtsch. Chem. Ges.* **1912**, *45*, 3157–3166.
[14] F. A. Carey, R. J. Sundberg, *Advanced Organic Chemistry: Part A: Structure and Mechanisms*, Springer, New York, NY, **2007**.
[15] F. A. Carey, R. J. Sundberg, *Advanced Organic Chemistry: Part B: Reaction and Synthesis*, Springer, New York, NY, **2007**.
[16] S. Poplata, A. Tröster, Y.-Q. Zou, T. Bach, *Chem. Rev.* **2016**, *116*, 9748–9815.
[17] R. K. Boeckman Jr, S. K. Yoon, D. K. Heckendorn, *J. Am. Chem. Soc.* **1991**, *113*, 9682–9684.
[18] W. Oppolzer, V. Snieckus, *Angew. Chem. Int. Ed.* **1978**, *17*, 476–486.
[19] R. B. Woodward, R. Hoffmann, *J. Am. Chem. Soc.* **1965**, *87*, 2511–2513.
[20] R. B. Woodward, R. Hoffmann, *Angew. Chem. Int. Ed.* **1969**, *8*, 781–853.
[21] R. A. J. Ditzler, A. V. Zhukhovitskiy, *J. Am. Chem. Soc.* **2021**, *143*, 20326–20331.
[22] A. Tena, S. Rangou, S. Shishatskiy, V. Filiz, V. Abetz, *Sci. Adv.* **2016**, *2*, e1501859.
[23] W. Wang, X. Qi, Y. Guan, F. Zhang, J. Zhang, C. Yan, Y. Zhu, X. Wan, *J. Polym. Sci. A Polym. Chem.* **2016**, *54*, 2050–2059.
[24] M. R. de la Viuda, A. Tena, S. Neumann, S. Willruth, V. Filiz, V. Abetz, *Polym. Chem.* **2018**, *9*, 4007–4016.
[25] D. Meis, A. Tena, S. Neumann, P. Georgopanos, T. Emmler, S. Shishatskiy, S. Rangou, V. Filiz, V. Abetz, *Polym. Chem.* **2018**, *9*, 3987–3999.
[26] M. Lemmerer, M. Schupp, D. Kaiser, N. Maulide, *Nat. Synth.* **2022**, *1*, 923–935.
[27] D. Kaldre, I. Klose, N. Maulide, *Science* **2018**, *361*, 664–667.
[28] W. Zhou, A. Voituriez, *Org. Lett.* **2021**, *23*, 247–252.
[29] W. Zhou, A. Voituriez, *J. Am. Chem. Soc.* **2021**, *143*, 17348–17353.
[30] A. C. Cope, E. M. Hardy, *J. Am. Chem. Soc.* **1940**, *62*, 441–444.
[31] Y. Kawamoto, N. Noguchi, T. Kobayashi, H. Ito, *Angew. Chem. Int. Ed.* **2023**, *62*, e202304132.
[32] M. F. Carroll, *J. Chem. Soc.* **1940**, 704–706.
[33] M. F. Carroll, *J. Chem. Soc.* **1941**, 507–511.
[34] W. Kimel, A. C. Cope, *J. Am. Chem. Soc.* **1943**, *65*, 1992–1998.
[35] S. R. Wilson, M. F. Price, *J. Org. Chem.* **1984**, *49*, 722–725.
[36] A. E. Wick, D. Felix, K. Steen, A. Eschenmoser, *Helv. Chim. Acta* **1964**, *47*, 2425–2429.
[37] W. S. Johnson, L. Werthemann, W. R. Bartlett, T. J. Brocksom, T.-T. Li, D. J. Faulkner, M. R. Petersen, *J. Am. Chem. Soc.* **1970**, *92*, 741–743.

[38] R. E. Ireland, R. H. Mueller, *J. Am. Chem. Soc.* **1972**, *94*, 5897–5898.
[39] R. E. Ireland, A. K. Willard, *Tetrahedron Lett.* **1975**, *16*, 3975–3978.
[40] R. E. Ireland, R. H. Mueller, A. K. Willard, *J. Am. Chem. Soc.* **1976**, *98*, 2868–2877.
[41] A. M. Martín Castro, *Chem. Rev.* **2004**, *104*, 2939–3002.
[42] A. M. Echavarren, J. de Mendoz, P. Prados, A. Zapata, *Tetrahedron Lett.* **1991**, *32*, 6421–6424.
[43] I. Shimizu, T. Yamada, J. Tsuji, *Tetrahedron Lett.* **1980**, *21*, 3199–3202.
[44] H. Meerwein, W. Florian, N. Schön, G. Stopp, *Liebigs Ann. Chem.* **1961**, *641*, 1–39.
[45] H. Takahashi, K. Oshima, H. Yamamoto, H. Nozaki, *J. Am. Chem. Soc.* **1973**, *95*, 5803–5804.
[46] K. Oshima, H. Takahashi, H. Yamamoto, H. Nozaki, *J. Am. Chem. Soc.* **1973**, *95*, 2963–2694.
[47] H. Kwart, C. M. Hackett, *J. Am. Chem. Soc.* **1962**, *84*, 1754–1755.
[48] H. Kwart, J. L. Schwartz, *J. Org. Chem.* **1974**, *39*, 1575–1583.
[49] T. Murai, T. Ezaka, S. Kato, *Synthesis* **2012**, *44*, 3197–3201.
[50] D. Kaldre, B. Maryasin, D. Kaiser, O. Gajsek, L. González, N. Maulide, *Angew. Chem. Int. Ed.* **2017**, *56*, 2212–2215.
[51] D. A. Evans, G. C. Andrews, *Acc. Chem. Res.* **1974**, *7*, 147–155.
[52] I. Colomer, M. Velado, R. Fernández de la Pradilla, A. Viso, *Chem. Rev.* **2017**, *117*, 14201–14243.
[53] D. Kaiser, I. Klose, R. Oost, J. Neuhaus, N. Maulide, *Chem. Rev.* **2019**, *119*, 8701–8780.
[54] C. M. Rojas, *Molecular Rearrangements in Organic Synthesis*, John Wiley & Sons, Nashville, TN, **2015**.
[55] K. B. Sharpless, R. F. Lauer, *J. Am. Chem. Soc.* **1973**, *95*, 2697–2699.
[56] T. Wirth, *Organoselenium Chemistry: Synthesis and Reactions*, John Wiley & Sons, **2011**.
[57] E. Vedejs, J. P. Hagen, B. L. Roach, K. L. Spear, *J. Org. Chem.* **1978**, *43*, 1185–1190.
[58] T. H. West, D. S. B. Daniels, A. M. Z. Slawin, A. D. Smith, *J. Am. Chem. Soc.* **2014**, *136*, 4476–4479.
[59] E. Tayama, S. Sotome, *Org. Biomol. Chem.* **2018**, *16*, 4833–4839.
[60] S. Xi, Y. Jiang, J. Yang, J. Yang, D. Miao, B. Chen, W. Huang, L. He, H. Qiu, M. Zhang, *Org. Lett.* **2022**, *24*, 6957–6961.
[61] Z. Zhang, Z. Sheng, W. Yu, G. Wu, R. Zhang, W.-D. Chu, Y. Zhang, J. Wang, *Nat. Chem.* **2017**, *9*, 970–976.
[62] F.-Y. Yang, T.-J. Han, S.-K. Jia, M.-C. Wang, G.-J. Mei, *Chem. Commun.* **2023**, *59*, 3107–3110.
[63] M. Sommelet, *CR Hebd. Seances Acad. Sci.* **1937**, *205*, 56–58.
[64] A. Sakuragi, N. Shirai, Y. Sato, Y. Kurono, K. Hatano, *J. Org. Chem.* **1994**, *59*, 148–153.
[65] X. Lin, W. Yang, W. Yang, X. Liu, X. Feng, *Angew. Chem. Int. Ed.* **2019**, *58*, 13492–13498.
[66] P. Bickart, F. W. Carson, J. Jacobus, E. G. Miller, K. Mislow, *J. Am. Chem. Soc.* **1968**, *90*, 4869–4876.
[67] R. Tang, K. Mislow, *J. Am. Chem. Soc.* **1970**, *92*, 2100–2104.
[68] D. A. Evans, G. C. Andrews, C. L. Sims, *J. Am. Chem. Soc.* **1971**, *93*, 4956–4957.
[69] R. W. Hoffmann, *Angew. Chem. Int. Ed.* **1979**, *18*, 563–572.
[70] M. G. Charest, C. D. Lerner, J. D. Brubaker, D. R. Siegel, A. G. Myers, *Science* **2005**, *308*, 395–398.
[71] K. B. Sharpless, R. F. Lauer, *J. Am. Chem. Soc.* **1972**, *94*, 7154–7155.
[72] H. J. Reich, *J. Org. Chem.* **1975**, *40*, 2570–2572.
[73] H. J. Reich, *Acc. Chem. Res.* **1979**, *12*, 22–30.
[74] P. A. Grieco, S. Gilman, M. Nishizawa, *J. Org. Chem.* **1976**, *41*, 1485–1486.
[75] K. B. Sharpless, M. W. Young, *J. Org. Chem.* **1975**, *40*, 947–949.
[76] T. Wirth, *Angew. Chem. Int. Ed.* **2000**, *39*, 3740–3749.
[77] T. Ohyoshi, S. Funakubo, Y. Miyazawa, K. Niida, I. Hayakawa, H. Kigoshi, *Angew. Chem. Int. Ed.* **2012**, *51*, 4972–4975.
[78] F. A. Davis, R. T. Reddy, *J. Org. Chem.* **1992**, *57*, 2599–2606.
[79] S. Uemura, S.-I. Fukuzawa, K. Ohe, *Tetrahedron Lett.* **1985**, *26*, 921–924.
[80] D. Yan, G. Wang, F. Xiong, W.-Y. Sun, Z. Shi, Y. Lu, S. Li, J. Zhao, *Nat. Commun.* **2018**, *9*, 4293.
[81] E. Bamberger, *Ber. Dtsch. Chem. Ges.* **1894**, *27*, 1548–1557.
[82] E. Bamberger, *Ber. Dtsch. Chem. Ges.* **1894**, *27*, 1347–1350.
[83] M. J. Vaidya, S. M. Kulkarni, R. V. Chaudhari, *Org. Process Res. Dev.* **2003**, *7*, 202–208.
[84] Y. Kikugawa, M. Shimada, *J. Chem. Soc. Chem. Commun.* **1989**, 1450–1451.
[85] Y. Kikugawa, K. Mitsui, *Chem. Lett.* **1993**, *22*, 1369–1372.
[86] K. N. Hojczyk, P. Feng, C. Zhan, M. Y. Ngai, *Angew. Chem. Int. Ed.* **2014**, *53*, 14559–14563.
[87] I. Nakamura, M. Owada, T. Jo, M. Terada, *Org. Lett.* **2017**, *19*, 2194–2196.
[88] I. Nakamura, T. Jo, Y. Ishida, H. Tashiro, M. Terada, *Org. Lett.* **2017**, *19*, 3059–3062.

[89] S. Oae, T. Sakurai, H. Kimura, S. Kozuka, *Chem. Lett.* **1974**, *3*, 671–674.
[90] H.-Y. Chuang, M. Schupp, R. Meyrelles, B. Maryasin, N. Maulide, *Angew. Chem. Int. Ed.* **2021**, *60*, 13778–13782.
[91] R. Meyrelles, M. Schupp, B. Maryasin, *Chem. Eur. J.* **2023**, e202302386.
[92] D. Dunlop, R. G. Shanks, *Br. J. Pharmacol. Chemother.* **1968**, *32*, 201–218.
[93] J. C. Danilewicz, J. E. Kemp, *J. Med. Chem.* **1973**, *16*, 168–169.
[94] K. Leftheris, M. Goodman, *J. Med. Chem.* **1990**, *33*, 216–223.
[95] A. Kamal, Y. Damayanthi, M. V. Rao, *Tetrahedron Asymmetry* **1992**, *3*, 1361–1364.
[96] "eEML - Electronic Essential Medicines List Diloxanide," can be found under https://list.essentialmeds.org/recommendations/771, **accessed 09.08.2023**.
[97] M. C. D. Xavier, E. M. A. Sandagorda, J. S. S. Neto, R. F. Schumacher, M. S. Silva, *RSC Adv.* **2020**, *10*, 13975–13983.
[98] M. J. Dabdoub, P. G. Guerrero, C. C. Silveira, *J. Organomet. Chem.* **1993**, *460*, 31–37.
[99] T. Frejd, K. B. Sharpless, *Tetrahedron Lett.* **1978**, *19*, 2239–2242.
[100] H. J. Reich, S. Wollowitz, *J. Am. Chem. Soc.* **1982**, *104*, 7051–7059.
[101] H. J. Reich, K. E. Yelm, S. Wollowitz, *J. Am. Chem. Soc.* **1983**, *105*, 2503–2504.
[102] D. R. Lide, *CRC Handbook of Chemistry and Physics, 86th Edition*, Taylor & Francis, **2005**.
[103] W. P. Teh, D. C. Obenschain, B. M. Black, F. E. Michael, *J. Am. Chem. Soc.* **2020**, *142*, 16716–16722.
[104] J. Wen, A. Wu, P. Chen, J. Zhu, *Tetrahedron Lett.* **2015**, *56*, 5282–5286.
[105] F. T. Wong, P. K. Patra, J. Seayad, Y. Zhang, J. Y. Ying, *Org. Lett.* **2008**, *10*, 2333–2336.
[106] K. Matsumoto, M. Kato, T. Sakamoto, Y. Kikugawa, *J. Chem. Res.* **1995**, *1*, 34–35.
[107] A. Bosum, S. Blechert, *Angew. Chem.* **1988**, *100*, 596–597.
[108] N. Böge, S. Krüger, M. Schröder, C. Meier, *Synthesis* **2007**, *2007*, 3907–3914.
[109] S. Shaaban, V. Tona, B. Peng, N. Maulide, *Angew. Chem. Int. Ed.* **2017**, *56*, 10938–10941.
[110] SANTEN PHARMACEUTICAL CO. LTD., *EP2119703 - NOVEL INDOLE DERIVATIVE HAVING INHIBITORY ACTIVITY ON I B KINASE*, **2008**, 2119703.
[111] R. Samanta, J. O. Bauer, C. Strohmann, A. P. Antonchick, *Org. Lett.* **2012**, *14*, 5518–5521.
[112] S. M. Mali, R. D. Bhaisare, H. N. Gopi, *J. Org. Chem.* **2013**, *78*, 5550–5555.
[113] P. Pracht, F. Bohle, S. Grimme, *Phys. Chem. Chem. Phys.* **2020**, *22*, 7169–7192.
[114] S. Grimme, *J. Chem. Theory Comput.* **2019**, *15*, 2847–2862.
[115] J. P. Perdew, K. Burke, M. Ernzerhof, *Phys. Rev. Lett.* **1996**, *77*, 3865–3868.
[116] J. P. Perdew, K. Burke, M. Ernzerhof, *Phys. Rev. Lett.* **1997**, *78*, 1396–1396.
[117] C. Adamo, V. Barone, *J. Chem. Phys.* **1999**, *110*, 6158–6170.
[118] S. Grimme, J. Antony, S. Ehrlich, H. Krieg, *J. Chem. Phys.* **2010**, *132*, 154104.
[119] S. Grimme, S. Ehrlich, L. Goerigk, *J. Comput. Chem.* **2011**, *32*, 1456–1465.
[120] E. Cancès, B. Mennucci, J. Tomasi, *J. Chem. Phys.* **1997**, *107*, 3032–3041.
[121] A. V. Marenich, C. J. Cramer, D. G. Truhlar, *J. Phys. Chem. B* **2009**, *113*, 6378–6396.
[122] "A Brief History of Vaccination," can be found under https://www.who.int/news-room/spotlight/history-of-vaccination/a-brief-history-of-vaccination, **accessed 02.08.2023**.
[123] M. Best, D. Neuhauser, *BMJ Qual. Saf.* **2004**, *13*, 233–234.
[124] K. Doi, *Phys. Med. Biol.* **2006**, *51*, R5-27.
[125] A. Fleming, *Br. J. Exp. Pathol.* **1929**, *10*, 226.
[126] P. M. Wright, I. B. Seiple, A. G. Myers, *Angew. Chem. Int. Ed.* **2014**, *53*, 8840–8869.
[127] M. I. Hutchings, A. W. Truman, B. Wilkinson, *Curr. Opin. Microbiol.* **2019**, *51*, 72–80.
[128] A. K. Abbas, A. H. Lichtman, S. Pillai, *Cellular and Molecular Immunology*, Elsevier, Philadelphia, **2012**.
[129] A. C. Allison, *Immunopharmacology* **2000**, *47*, 63–83.
[130] B. D. Kahan, *Nat. Rev. Immunol.* **2003**, *3*, 831–838.
[131] WHO Rapid Evidence Appraisal for COVID-19 Therapies (REACT) Working Group, J. A. C. Sterne, S. Murthy, J. V. Diaz, A. S. Slutsky, J. Villar, D. C. Angus, D. Annane, L. C. P. Azevedo, O. Berwanger, A. B. Cavalcanti, P.-F. Dequin, B. Du, J. Emberson, D. Fisher, B. Giraudeau, A. C. Gordon, A. Granholm, C. Green, R. Haynes, N. Heming, J. P. T. Higgins, P. Horby, P. Jüni, M. J. Landray, A. Le Gouge, M. Leclerc, W. S. Lim, F. R. Machado, C. McArthur, F. Meziani, M. H. Møller, A. Perner, M. W. Petersen, J. Savovic, B. Tomazini, V. C. Veiga, S. Webb, J. C. Marshall, *JAMA* **2020**, *324*, 1330–1341.

[132] H. C. Prescott, T. W. Rice, *JAMA* **2020**, *324*, 1292–1295.
[133] N. A. Pilch, L. J. Bowman, D. J. Taber, *Pharmacotherapy* **2021**, *41*, 119–131.
[134] T. E. Starzl, G. B. G. Klintmalm, K. A. Porter, S. Iwatsuki, G. P. J. Schröter, *N. Engl. J. Med.* **1981**, *305*, 266–269.
[135] T. R. Hakala, T. E. Starzl, J. T. Rosenthal, B. Shaw, S. Iwatsuki, *Transplant. Proc.* **1983**, *15*, 465–470.
[136] B. D. Kahan, *Transplant. Proc.* **2009**, *41*, 1423–1437.
[137] J. Chinen, R. H. Buckley, *J. Allergy Clin. Immunol.* **2010**, *125*, S324-35.
[138] T. Kino, H. Hatanaka, M. Hashimoto, M. Nishiyama, T. Goto, M. Okuhara, M. Kohsaka, H. Aoki, H. Imanaka, *J. Antibiot.* **1987**, *40*, 1249–1255.
[139] T. Kino, H. Hatanaka, S. Miyata, N. Inamura, M. Nishiyama, T. Yajima, T. Goto, M. Okuhara, M. Kohsaka, H. Aoki, T. Ochiai, *J. Antibiot.* **1987**, *40*, 1256–1265.
[140] H. Tanaka, A. Kuroda, H. Marusawa, H. Hatanaka, T. Kino, T. Goto, M. Hashimoto, T. Taga, *J. Am. Chem. Soc.* **1987**, *109*, 5031–5033.
[141] T. E. Starzl, S. Todo, J. Fung, A. J. Demetris, R. Venkataramman, A. Jain, *Lancet* **1989**, *2*, 1000–1004.
[142] M. Nakatsuka, J. A. Ragan, T. Sammakia, D. B. Smith, D. E. Uehling, S. L. Schreiber, *J. Am. Chem. Soc.* **1990**, *112*, 5583–5601.
[143] A. B. Jones, A. Villalobos, R. G. Linde, S. J. Danishefsky, *J. Org. Chem.* **1990**, *55*, 2786–2797.
[144] T. K. Jones, S. G. Mills, R. A. Reamer, D. Askin, R. Desmond, R. P. Volante, I. Shinkai, *J. Am. Chem. Soc.* **1989**, *111*, 1157–1159.
[145] R. E. Ireland, J. L. Gleason, L. D. Gegnas, T. K. Highsmith, *J. Org. Chem.* **1996**, *61*, 6856–6872.
[146] J. Liu, J. D. Farmer, W. S. Lane, J. Friedman, I. Weissman, S. L. Schreiber, *Cell* **1991**, *66*, 807–815.
[147] J. J. Siekierka, S. H. Hung, M. Poe, C. S. Lin, N. H. Sigal, *Nature* **1989**, *341*, 755–757.
[148] S. Ho, N. Clipstone, L. Timmermann, J. Northrop, I. Graef, D. Fiorentino, J. Nourse, G. R. Crabtree, *Clin. Immunol. Immunopathol.* **1996**, *80*, 40–45.
[149] C. Vézina, A. Kudelski, *J. Antibiot.* **1975**, *28*, 721–726.
[150] S. N. Sehgal, H. Baker, C. Vézina, *J. Antibiot.* **1975**, *28*, 727–732.
[151] R. R. Martel, J. Klicius, S. Galet, *Can. J. Physiol. Pharmacol.* **1977**, *55*, 48–51.
[152] E. J. Brown, M. W. Albers, T. Bum Shin, K. Ichikawa, C. T. Keith, W. S. Lane, S. L. Schreiber, *Nature* **1994**, *369*, 756–758.
[153] S. L. Schreiber, M. W. Albers, E. J. Brown, *Acc. Chem. Res.* **1993**, *26*, 412–420.
[154] D. Romo, S. D. Meyer, D. D. Johnson, S. L. Schreiber, *J. Am. Chem. Soc.* **1993**, *115*, 7906–7907.
[155] K. C. Nicolaou, T. K. Chakraborty, A. D. Piscopio, N. Minowa, P. Bertinato, *J. Am. Chem. Soc.* **1993**, *115*, 4419–4420.
[156] C. M. Hayward, D. Yohannes, S. J. Danishefsky, *J. Am. Chem. Soc.* **1993**, *115*, 9345–9346.
[157] A. B. Smith III, S. M. Condon, J. A. McCauley, J. L. Leazer Jr, J. W. Leahy, R. E. Maleczka Jr, *J. Am. Chem. Soc.* **1995**, *117*, 5407–5408.
[158] A. B. Smith III, S. M. Condon, J. A. McCauley, J. L. Leazer, J. W. Leahy, R. E. Maleczka, *J. Am. Chem. Soc.* **1997**, *119*, 962–973.
[159] M. L. Maddess, M. N. Tackett, H. Watanabe, P. E. Brennan, C. D. Spilling, J. S. Scott, D. P. Osborn, S. V. Ley, *Angew. Chem. Int. Ed.* **2007**, *46*, 591–597.
[160] S. V. Ley, M. N. Tackett, M. L. Maddess, J. C. Anderson, P. E. Brennan, M. W. Cappi, J. P. Heer, C. Helgen, M. Kori, C. Kouklovsky, S. P. Marsden, J. Norman, D. P. Osborn, M. Á. Palomero, J. B. J. Pavey, C. Pinel, L. A. Robinson, J. Schnaubelt, J. S. Scott, C. D. Spilling, H. Watanabe, K. E. Wesson, M. C. Willis, *Chem. Eur. J.* **2009**, *15*, 2874–2914.
[161] M. Schupp, I. Saridakis, D. Kaiser, N. Maulide, *Nature Synthesis* **2023**, DOI 10.1038/s44160-023-00423-2.
[162] B. Magnuson, B. Ekim, D. C. Fingar, *Biochem. J* **2012**, *441*, 1–21.
[163] S. L. Schreiber, *Cell* **2021**, *184*, 3–9.
[164] Robin C. E. Deutscher, C. Meyners, S. C. Schäfer, M. L. Repity, W. O. Sugiarto, J. Kolos, T. Heymann, T. M. Geiger, S. Knapp, F. Hausch, *ChemRxiv* **2023**, DOI 10.26434/chemrxiv-2023-4vb0m.
[165] P. T. Northcote, J. W. Blunt, M. H. G. Munro, *Tetrahedron Lett.* **1991**, *32*, 6411–6414.
[166] R. M. Rzasa, H. A. Shea, D. Romo, *J. Am. Chem. Soc.* **1998**, *120*, 591–592.

[167] R. M. Rzasa, D. Romo, D. J. Stirling, J. W. Blunt, M. H. G. Munro, *Tetrahedron Lett.* **1995**, *36*, 5307–5310.
[168] Y. Dang, W.-K. Low, J. Xu, N. H. Gehring, H. C. Dietz, D. Romo, J. O. Liu, *J. Biol. Chem.* **2009**, *284*, 23613–23621.
[169] W.-K. Low, J. Li, M. Zhu, S. S. Kommaraju, J. Shah-Mittal, K. Hull, J. O. Liu, D. Romo, *Bioorg. Med. Chem.* **2014**, *22*, 116–125.
[170] C.-X. Zhuo, A. Fürstner, *J. Am. Chem. Soc.* **2018**, *140*, 10514–10523.
[171] J.-J. Sanglier, V. Quesniaux, T. Fehr, H. Hofmann, M. Mahnke, K. Memmert, W. Schuler, G. Zenke, L. Gschwind, C. Maurer, W. Schilling, *J. Antibiot.* **1999**, *52*, 466–473.
[172] L. H. Zhang, J. O. Liu, *J. Immunol.* **2001**, *166*, 5611–5618.
[173] K. C. Nicolaou, F. Murphy, S. Barluenga, T. Ohshima, H. Wei, J. Xu, D. L. F. Gray, O. Baudoin, *J. Am. Chem. Soc.* **2000**, *122*, 3830–3838.
[174] B.-C. Yan, M. Zhou, J. Li, X.-N. Li, S.-J. He, J.-P. Zuo, H.-D. Sun, A. Li, P.-T. Puno, *Angew. Chem. Int. Ed.* **2021**, *60*, 12859–12867.
[175] R. B. Woodward, R. Hoffmann, *J. Am. Chem. Soc.* **1964**, *87*, 395–397.
[176] W. R. Dolbier, H. Koroniak, K. N. Houk, C. Sheu, *Acc. Chem. Res.* **1996**, *29*, 471–477.
[177] J. I. Brauman, W. C. Archie Jr, *J. Am. Chem. Soc.* **1972**, *94*, 4262–4265.
[178] H. M. Frey, *Trans. Faraday Soc.* **1962**, *58*, 957–960.
[179] H. M. Frey, R. K. Solly, *Trans. Faraday Soc.* **1969**, *65*, 448–452.
[180] W. Kirmse, N. G. Rondan, K. N. Houk, *J. Am. Chem. Soc.* **1984**, *106*, 7989–7991.
[181] N. G. Rondan, K. N. Houk, *J. Am. Chem. Soc.* **1985**, *107*, 2099–2111.
[182] C. W. Jefford, G. Bernardinelli, Y. Wang, D. C. Spellmeyer, A. Buda, K. N. Houk, *J. Am. Chem. Soc.* **1992**, *114*, 1157–1165.
[183] D. C. Spellmeyer, K. N. Houk, *J. Am. Chem. Soc.* **1988**, *110*, 3412–3416.
[184] K. Rudolf, D. C. Spellmeyer, K. N. Houk, *J. Org. Chem.* **1987**, *52*, 3708–3710.
[185] K. N. Houk, D. C. Spellmeyer, C. W. Jefford, C. G. Rimbault, Y. Wang, R. D. Miller, *J. Org. Chem.* **1988**, *53*, 2125–2127.
[186] E. J. Corey, J. Streith, *J. Am. Chem. Soc.* **1964**, *86*, 950–951.
[187] J. D. Williams, Y. Otake, G. Coussanes, I. Saridakis, N. Maulide, C. O. Kappe, *ChemPhotoChem* **2019**, *3*, 229–232.
[188] M. Luparia, D. Audisio, N. Maulide, *Synlett* **2011**, *2011*, 735–740.
[189] J. Tsuji, H. Takahashi, M. Morikawa, *Tetrahedron Lett.* **1965**, *6*, 4387–4388.
[190] B. M. Trost, T. J. Fullerton, *J. Am. Chem. Soc.* **1973**, *95*, 292–294.
[191] B. M. Trost, D. L. Van Vranken, *Chem. Rev.* **1996**, *96*, 395–422.
[192] B. M. Trost, M. L. Crawley, *Chem. Rev.* **2003**, *103*, 2921–2943.
[193] M. Luparia, M. T. Oliveira, D. Audisio, F. Frébault, R. Goddard, N. Maulide, *Angew. Chem. Int. Ed.* **2011**, *50*, 12631–12635.
[194] C. Souris, M. Luparia, F. Frébault, D. Audisio, C. Farès, R. Goddard, N. Maulide, *Chem. Eur. J.* **2013**, *19*, 6566–6570.
[195] C. Souris, F. Frébault, D. Audisio, C. Farès, N. Maulide, *Synlett* **2013**, *24*, 1286–1290.
[196] C. Souris, F. Frébault, A. Patel, D. Audisio, K. N. Houk, N. Maulide, *Org. Lett.* **2013**, *15*, 3242–3245.
[197] C. Souris, A. Misale, Y. Chen, M. Luparia, N. Maulide, *Org. Lett.* **2015**, *17*, 4486–4489.
[198] A. Misale, S. Niyomchon, N. Maulide, *Acc. Chem. Res.* **2016**, *49*, 2444.
[199] S. Niyomchon, D. Audisio, M. Luparia, N. Maulide, *Org. Lett.* **2013**, *15*, 2318–2321.
[200] M. Berger, Y. Chen, K. Bampali, M. Ernst, N. Maulide, *Chem. Commun.* **2018**, *54*, 2008–2011.
[201] R. G. Pearson, *J. Am. Chem. Soc.* **1963**, *85*, 3533–3539.
[202] R. G. Parr, R. G. Pearson, *J. Am. Chem. Soc.* **1983**, *105*, 7512–7516.
[203] H. L. Tran, K. W. Lexa, O. Julien, T. S. Young, C. T. Walsh, M. P. Jacobson, J. A. Wells, *J. Am. Chem. Soc.* **2017**, *139*, 2541–2544.
[204] A. Parenty, X. Moreau, J.-M. Campagne, *Chem. Rev.* **2006**, *106*, 911–939.
[205] Y. Li, X. Yin, M. Dai, *Nat. Prod. Rep.* **2017**, *34*, 1185–1192.
[206] R. K. Boeckman Jr, J. R. Pruitt, *J. Am. Chem. Soc.* **1989**, *111*, 8286–8288.
[207] I. B. Seiple, Z. Zhang, P. Jakubec, A. Langlois-Mercier, P. M. Wright, D. T. Hog, K. Yabu, S. R. Allu, T. Fukuzaki, P. N. Carlsen, Y. Kitamura, X. Zhou, M. L. Condakes, F. T. Szczypiński, W. D. Green, A. G. Myers, *Nature* **2016**, *533*, 338–345.

[208] J. W. Bode, E. M. Carreira, *J. Am. Chem. Soc.* **2001**, *123*, 3611–3612.
[209] J. S. Davies, *J. Pept. Sci.* **2003**, *9*, 471–501.
[210] C. A. G. N. Montalbetti, V. Falque, *Tetrahedron* **2005**, *61*, 10827–10852.
[211] X. Wu, J. L. Stockdill, P. Wang, S. J. Danishefsky, *J. Am. Chem. Soc.* **2010**, *132*, 4098–4100.
[212] R. H. Grubbs, S. J. Miller, G. C. Fu, *Acc. Chem. Res.* **1995**, *28*, 446–452.
[213] A. Fürstner, *Angew. Chem. Int. Ed.* **2000**, *39*, 3012–3043.
[214] A. Fürstner, P. W. Davies, *Chem. Commun.* **2005**, 2307–2320.
[215] A. Gradillas, J. Pérez-Castells, *Angew. Chem. Int. Ed.* **2006**, *45*, 6086–6101.
[216] A. H. Hoveyda, A. R. Zhugralin, *Nature* **2007**, *450*, 243–251.
[217] A. Fürstner, *Science* **2013**, *341*, 1229713.
[218] A. Fürstner, *Angew. Chem. Int. Ed.* **2013**, *52*, 2794–2819.
[219] A. Fürstner, *Acc. Chem. Res.* **2021**, *54*, 861–874.
[220] K. C. Nicolaou, P. G. Bulger, D. Sarlah, *Angew. Chem. Int. Ed.* **2005**, *44*, 4490–4527.
[221] J. Inanaga, K. Hirata, H. Saeki, T. Katsuki, M. Yamaguchi, *BCSJ* **1979**, *52*, 1989–1993.
[222] K. Narasaka, K. Maruyama, T. Mukaiyama, *Chem. Lett.* **1978**, *7*, 885–888.
[223] I. Shiina, T. Mukaiyama, *Chem. Lett.* **1994**, *23*, 677–680.
[224] I. Shiina, M. Kubota, R. Ibuka, *Tetrahedron Lett.* **2002**, *43*, 7535–7539.
[225] R. C. Larock, E. K. Yum, *J. Am. Chem. Soc.* **1991**, *113*, 6689–6690.
[226] M. Nesic, D. B. Ryffel, J. Maturano, M. Shevlin, S. R. Pollack, D. R. Gauthier, P. Trigo-Mouriño, L.-K. Zhang, D. M. Schultz, J. M. McCabe Dunn, L.-C. Campeau, N. R. Patel, D. A. Petrone, D. Sarlah, *J. Am. Chem. Soc.* **2022**, *144*, 14026–14030.
[227] Y.-C. Lin, F. Schneider, K. J. Eberle, D. Chiodi, H. Nakamura, S. H. Reisberg, J. Chen, M. Saito, P. S. Baran, *J. Am. Chem. Soc.* **2022**, *144*, 14458–14462.
[228] Y. Imai, K. J. Meyer, A. Iinishi, Q. Favre-Godal, R. Green, S. Manuse, M. Caboni, M. Mori, S. Niles, M. Ghiglieri, C. Honrao, X. Ma, J. J. Guo, A. Makriyannis, L. Linares-Otoya, N. Böhringer, Z. G. Wuisan, H. Kaur, R. Wu, A. Mateus, A. Typas, M. M. Savitski, J. L. Espinoza, A. O'Rourke, K. E. Nelson, S. Hiller, N. Noinaj, T. F. Schäberle, A. D'Onofrio, K. Lewis, *Nature* **2019**, *576*, 459–464.
[229] T. Fehr, J. Kallen, L. Oberer, J. J. Sanglier, W. Schilling, *J. Antibiot.* **1999**, *52*, 474–479.
[230] K. C. Nicolaou, O. Takashi, F. Murphy, S. Barluenga, J. Xu, N. Winssinger, *Chem. Commun.* **1999**, 809–810.
[231] K. C. Nicolaou, J. Xu, F. Murphy, S. Barluenga, O. Baudoin, H. X. Wei, D. L. F. Gray, T. Ohshima, *Angew. Chem. Int. Ed.* **1999**, *38*, 2447–2451.
[232] M. Duan, L. A. Paquette, *Tetrahedron Lett.* **2000**, *41*, 3789–3792.
[233] L. A. Paquette, I. Konetzki, M. Duan, *Tetrahedron Lett.* **1999**, *40*, 7441–7444.
[234] L. A. Paquette, M. Duan, I. Konetzki, C. Kempmann, *J. Am. Chem. Soc.* **2002**, *124*, 4257–4270.
[235] C.-F. Chang, H. A. Flaxman, C. M. Woo, *Angew. Chem. Int. Ed.* **2021**, *60*, 17045–17052.
[236] L. H. Zhang, H. D. Youn, J. O. Liu, *J. Biol. Chem.* **2001**, *276*, 43534–43540.
[237] G. Zenke, U. Strittmatter, S. Fuchs, V. F. Quesniaux, V. Brinkmann, W. Schuler, M. Zurini, A. Enz, A. Billich, J. J. Sanglier, T. Fehr, *J. Immunol.* **2001**, *166*, 7165–7171.
[238] C. Steinschulte, T. Taner, A. W. Thomson, G. Bein, H. Hackstein, *J. Immunol.* **2003**, *171*, 542–546.
[239] K. Fujine, M. Tanaka, K. Ohsumi, M. Hashimoto, S. Takase, H. Ueda, M. Hino, F. Takashi, *J. Antibiot.* **2003**, *56*, 55–61.
[240] K. Fujine, F. Abe, N. Seki, H. Ueda, M. Hino, T. Fujii, *J. Antibiot.* **2003**, *56*, 62–67.
[241] K. Fujine, F. Abe, N. Seki, H. Ueda, M. Hino, T. Fujii, *J. Antibiot.* **2003**, *56*, 68–71.
[242] J. R. Falck, A. He, H. Fukui, H. Tsutsui, A. Radha, *Angew. Chem. Int. Ed.* **2007**, *46*, 4527–4529.
[243] D. Amans, V. Bellosta, J. Cossy, *Org. Lett.* **2007**, *9*, 4761–4764.
[244] D. Amans, V. Bellosta, J. Cossy, *Chem. Eur. J.* **2009**, *15*, 3457–3473.
[245] A. Pohanka, A. Broberg, M. Johansson, L. Kenne, J. Levenfors, *J. Nat. Prod.* **2005**, *68*, 1380–1385.
[246] A. K. Ghosh, S. Rodriguez, *Tetrahedron Lett.* **2016**, *57*, 2884–2887.
[247] S. Yu, F. Liu, D. Ma, *Tetrahedron Lett.* **2006**, *47*, 9155–9157.
[248] J. S. Yadav, S. Sengupta, *European J. Org. Chem.* **2013**, *2013*, 376–388.
[249] D. H. Dethe, V. Kumar, N. C. Beeralingappa, K. B. Mishra, A. K. Nirpal, *Org. Lett.* **2022**, *24*, 2203–2207.
[250] N. Miyaura, K. Yamada, A. Suzuki, *Tetrahedron Lett.* **1979**, *20*, 3437–3440.
[251] N. Miyaura, A. Suzuki, *J. Chem. Soc. Chem. Commun.* **1979**, 866–867.

[252] N. Miyaura, A. Suzuki, *Chem. Rev.* **1995**, *95*, 2457–2483.
[253] Y. Chen, G. Coussanes, C. Souris, P. Aillard, D. Kaldre, K. Runggatscher, S. Kubicek, G. Di Mauro, B. Maryasin, N. Maulide, *J. Am. Chem. Soc.* **2019**, *141*, 13772.
[254] G. Fráter, U. Müller, W. Günther, *Tetrahedron* **1984**, *40*, 1269–1277.
[255] D. Seebach, D. Wasmuth, *Helv. Chim. Acta* **1980**, *63*, 197–200.
[256] A. R. Hooper, A. Oštrek, A. Milian-Lopez, D. Sarlah, *Angew. Chem. Int. Ed.* **2022**, e202212299.
[257] M. Lang, U. S. Ganapathy, L. Mann, R. Abdelaziz, R. W. Seidel, R. Goddard, I. Sequenzia, S. Hoenke, P. Schulze, W. W. Aragaw, R. Csuk, T. Dick, A. Richter, *J. Med. Chem.* **2023**, *66*, 5079–5098.
[258] E. Riedel, C. Janiak, *Anorganische Chemie*, Walter De Gruyter, **2011**.
[259] L. Horner, H. Hoffmann, H. G. Wippel, *Chem. Ber.* **1958**, *91*, 61–63.
[260] W. S. Wadsworth, W. D. Emmons, *J. Am. Chem. Soc.* **1961**, *83*, 1733–1738.
[261] G. Wittig, U. Schöllkopf, *Chem. Ber.* **1954**, *87*, 1318–1330.
[262] M. T. Crimmins, B. W. King, E. A. Tabet, *J. Am. Chem. Soc.* **1997**, *119*, 7883–7884.
[263] A. G. Myers, J. Liang, M. Hammond, P. M. Harrington, Y. Wu, E. Y. Kuo, *J. Am. Chem. Soc.* **1998**, *120*, 5319–5320.
[264] U. Galm, M. H. Hager, S. G. Van Lanen, J. Ju, J. S. Thorson, B. Shen, *Chem. Rev.* **2005**, *105*, 739–758.
[265] F. Giordanetto, J. Kihlberg, *J. Med. Chem.* **2014**, *57*, 278–295.
[266] D. Garcia Jimenez, V. Poongavanam, J. Kihlberg, *J. Med. Chem.* **2023**, *66*, 5377–5396.
[267] D. M. Bollag, P. A. McQueney, J. Zhu, O. Hensens, L. Koupal, J. Liesch, M. Goetz, E. Lazarides, C. M. Woods, *Cancer Res.* **1995**, *55*, 2325–2333.
[268] D. M. Bollag, *Expert Opin. Investig. Drugs* **1997**, *6*, 867–873.
[269] R. M. Borzilleri, X. Zheng, R. J. Schmidt, J. A. Johnson, S.-H. Kim, J. D. DiMarco, C. R. Fairchild, J. Z. Gougoutas, F. Y. F. Lee, B. H. Long, G. D. Vite, *J. Am. Chem. Soc.* **2000**, *122*, 8890–8897.
[270] N. Denduluri, S. M. Swain, *Expert Opin. Investig. Drugs* **2008**, *17*, 423–435.
[271] E. S. Thomas, H. L. Gomez, R. K. Li, H.-C. Chung, L. E. Fein, V. F. Chan, J. Jassem, X. B. Pivot, J. V. Klimovsky, F. H. de Mendoza, B. Xu, M. Campone, G. L. Lerzo, R. A. Peck, P. Mukhopadhyay, L. T. Vahdat, H. H. Roché, *J. Clin. Oncol.* **2007**, *25*, 5210–5217.
[272] C. Aghajanian, H. A. Burris III, S. Jones, D. R. Spriggs, M. B. Cohen, R. Peck, P. Sabbatini, M. L. Hensley, F. A. Greco, J. Dupont, O. A. O'Connor, *J. Clin. Oncol.* **2007**, *25*, 1082–1088.
[273] S. Kanemasa, M. Nishiuchi, A. Kamimura, K. Hori, *J. Am. Chem. Soc.* **1994**, *116*, 2324–2339.
[274] J. W. Bode, N. Fraefel, D. Muri, E. M. Carreira, *Angew. Chem. Int. Ed.* **2001**, *40*, 2082–2085.
[275] J. W. Bode, E. M. Carreira, *Org. Lett.* **2001**, *3*, 1587–1590.
[276] D. Muri, N. Lohse-Fraefel, E. M. Carreira, *Angew. Chem. Int. Ed.* **2005**, *44*, 4036–4038.
[277] N. Lohse-Fraefel, E. M. Carreira, *Chem. Eur. J.* **2009**, *15*, 12065–12081.
[278] A. A. Fuller, B. Chen, A. R. Minter, A. K. Mapp, *J. Am. Chem. Soc.* **2005**, *127*, 5376–5383.
[279] X. Long, Y. Ding, J. Deng, *Angew. Chem. Int. Ed.* **2018**, *57*, 14221–14224.
[280] D. Roman, M. Sauer, C. Beemelmanns, *Synthesis* **2021**, *53*, 2713–2739.
[281] O. Geiseler, J. Podlech, *Tetrahedron* **2012**, *68*, 7280–7287.
[282] I. Heilbron, E. R. H. Jones, F. Sondheimer, *J. Chem. Soc.* **1949**, 604–607.
[283] B. S. Bal, W. E. Childers, H. W. Pinnick, *Tetrahedron* **1981**, *37*, 2091–2096.
[284] B. O. Lindgren, T. Nilsson, *Acta Chem. Scand.* **1973**, *27*, 888–890.
[285] G. A. Kraus, M. J. Taschner, *J. Org. Chem.* **1980**, *45*, 1175–1176.
[286] G. A. Kraus, B. Roth, *J. Org. Chem.* **1980**, *45*, 4825–4830.
[287] M. Zhao, J. Li, E. Mano, Z. Song, D. M. Tschaen, E. J. J. Grabowski, P. J. Reider, *J. Org. Chem.* **1999**, *64*, 2564–2566.
[288] W.-Y. Tan, Y. Lu, J.-F. Zhao, W. Chen, H. Zhang, *Org. Lett.* **2021**, *23*, 6648–6653.
[289] K. C. Nicolaou, A. A. Estrada, M. Zak, S. H. Lee, B. S. Safina, *Angew. Chem. Int. Ed.* **2005**, *44*, 1378–1382.
[290] S. Kumari, A. V. Carmona, A. K. Tiwari, P. C. Trippier, *J. Med. Chem.* **2020**, *63*, 12290–12358.
[291] D. Seyferth, R. S. Marmor, P. Hilbert, *J. Org. Chem.* **1971**, *36*, 1379–1386.
[292] S. Müller, B. Liepold, G. J. Roth, H. J. Bestmann, *Synlett* **1996**, *6*, 521–522.
[293] C. W. Tornøe, C. Christensen, M. Meldal, *J. Org. Chem.* **2002**, *67*, 3057–3064.
[294] V. V. Rostovtsev, L. G. Green, V. V. Fokin, K. B. Sharpless, *Angew. Chem. Int. Ed.* **2002**, *41*, 2596–2599.

[295] L. Zhang, X. Chen, P. Xue, H. H. Y. Sun, I. D. Williams, K. B. Sharpless, V. V. Fokin, G. Jia, *J. Am. Chem. Soc.* **2005**, *127*, 15998–15999.
[296] M. Vig, J.-P. Kinet, *Nat. Immunol.* **2009**, *10*, 21–27.
[297] C. Thirsk, A. Whiting, *J. Chem. Soc. Perkin 1* **2002**, 999–1023.
[298] I. Saridakis, D. Kaiser, N. Maulide, *ACS Cent. Sci.* **2020**, *6*, 1869–1889.
[299] C. A. Brown, A. Yamashita, *J. Am. Chem. Soc.* **1975**, *97*, 891–892.
[300] S. R. Abrams, A. C. Shaw, *Org. Synth.* **1988**, *66*, 127.
[301] X. Qiu, J. G. Pierce, *J. Am. Chem. Soc.* **2022**, *144*, 12638–12641.
[302] S. Pereira, M. Srebnik, *Organometallics* **1995**, *14*, 3127–3128.
[303] W. Mechlinski, C. P. Schaffner, P. Ganis, G. Avitabile, *Tetrahedron Lett.* **1970**, *11*, 3873–3876.
[304] I. Umezawa, H. Takeshima, K. Komiyama, Y. Koh, H. Yamamoto, M. Kawaguchi, *J. Antibiot.* **1981**, *34*, 259–265.
[305] J. J. Primozic, J. Ilgen, P. Maibach, M. Brauser, J. Kind, C. M. Thiele, *J. Am. Chem. Soc.* **2023**, *145*, 15912–15923.
[306] L. Dubinsky, B. P. Krom, M. M. Meijler, *Bioorg. Med. Chem.* **2012**, *20*, 554–570.
[307] A. V. West, Y. Amako, C. M. Woo, *J. Am. Chem. Soc.* **2022**, *144*, 21174–21183.
[308] M. P. Wiesenfeldt, J. A. Rossi-Ashton, I. B. Perry, J. Diesel, O. L. Garry, F. Bartels, S. C. Coote, X. Ma, C. S. Yeung, D. J. Bennett, D. W. C. MacMillan, *Nature* **2023**, *618*, 513–518.
[309] M. A. M. Subbaiah, N. A. Meanwell, *J. Med. Chem.* **2021**, *64*, 14046–14128.
[310] S. K. Nistanaki, L. A. Boralsky, R. D. Pan, H. M. Nelson, *Angew. Chem. Int. Ed.* **2019**, *58*, 1724–1726.
[311] P. R. Skaanderup, T. Jensen, *Org. Lett.* **2008**, *10*, 2821–2824.
[312] B. DeBoef, W. R. Counts, S. R. Gilbertson, *J. Org. Chem.* **2007**, *72*, 799–804.
[313] B. A. Patel, J.-I. I. Kim, D. D. Bender, L.-C. Kao, R. F. Heck, *J. Org. Chem.* **1981**, *46*, 1061–1067.
[314] J. W. Bode, E. M. Carreira, *J. Org. Chem.* **2001**, *66*, 6410–6424.
[315] D. Jacoby, J. P. Célérier, H. Petit, G. Lhommet, *Synthesis* **1990**, *1990*, 301–304.
[316] B. T. Kelley, M. M. Joullié, *Org. Lett.* **2010**, *12*, 4244–4247.
[317] J. Strobl, R. V. Pandey, T. Krausgruber, L. Kleissl, B. Reininger, M. Herac, N. Bayer, C. Krall, P. Wohlfarth, M. Mitterbauer, P. Kalhs, W. Rabitsch, C. Bock, G. Hopfinger, G. Stary, *J. Invest. Dermatol.* **2020**, *140*, 2188–2198.